UNDERSTANDING THE RAL GTPASES: THE REGULATION BY PROTEIN LYSINE FATTY ACYLATION, SIRT2, AND INTERACTING PROTEINS

A Dissertation

Presented to the Faculty of the Graduate School

of Cornell University

In Partial Fulfillment of the Requirements for the Degree of

Doctor of Philosophy

by

Nicole Alexis Spiegelman

December 2018

UNDERSTANDING THE RAL GTPASES: THE REGULATION BY PROTEIN LYSINE FATTY ACYLATION, SIRT2, AND INTERACTING PROTEINS

Nicole Alexis Spiegelman, Ph. D.

Cornell University 2018

The RAS superfamily of small GTPases are molecular switches that control a wide range of cellular processes. Detailed understanding of these small GTPases is important for elucidating cell signaling mechanisms and identifying new disease treatment strategies. My thesis is centered on understanding two highly similar small GTPases, RalA and RalB. They are the two members of the Ras-like (Ral) GTPases in the Ras subfamily. Despite their similar biochemical and structurally properties, the Ral GTPases can exhibit diverging roles. My thesis work provides important insights into the differential regulation and function of RalA and RalB.

In one study (Chapter 2), I discovered that RalA and RalB are differentially regulated by lysine fatty acylation. Lipidation, such as cysteine palmitoylation and prenylation, is a key regulatory mechanism for small GTPases. Recently it has been reported that lysine fatty acylation also regulates several small GTPases. My graduate work shows that RalB, but not RalA, is regulated by lysine fatty acylation. RalB lysine fatty acylation is reversible and can be removed by SIRT2. Lysine fatty acylation promotes RalB GTP binding and cell migration.

To further understand the differential functions of RalA and RalB, in a second study (Chapter 3), we used a quantitative proteomic approach (stable isotope labeling of amino acids in cell culture or SILAC) to identify the interacting proteins of RalA and RalB. This study revealed many interacting proteins that can bind to RalA, RalB, or both in a nucleotide dependent manner. These interacting proteins provide important insights that will guide future studies. For example, among these interacting proteins identified, we confirmed that RalB

selectively interacts with ERK2 and can decrease its nuclear localization. This may explain why RalB could suppress anchorage-independent growth while RalA does not.

As protein lysine fatty acylation is becoming a more abundant protein post translational modification, we wanted to identify tools that could help us better understand the roles of lysine fatty acylation in signaling and cancer. Histone Deacetylases (HDACs), such as SIRT2, can act as protein lysine defatty-acylases (have the ability to hydrolyze long chain fatty acyl groups from lysine residues). Thus, SIRT2 inhibitors could be useful tools to study lysine fatty acylation. However, most reported SIRT2 inhibitors were not tested against its defatty-acylation activity. Through an in-depth comparison of four SIRT2 inhibitors (AGK2, SirReal2, Tenovin-6 and TM), we found that TM was the most potent and selective SIRT2 inhibitor (Chapter 4). However, TM could not efficiently inhibit defatty-acylation. In an attempt to find a tool compound that could be used to study sirtuin regulated de-fatty acylation, we identified a TM analogue, JH-T4 (Chapter 5). JH-T4 can more potently inhibit the defatty-acylation activity of SIRT2, although it can also inhibit SIRT1 and SIRT3.

I was interested in developing chemical proteomic tools to identify lysine fatty-acylated proteins. Through our proteomic studies aimed at identifying HDAC lysine fatty acylation substrates, we found that JAM-C has DHHC7-regulated cysteine palmitoylation (Chapter 6). However, current proteomic methods cannot provide site identification. This makes profiling lysine fatty acylated proteins challenging. To overcome this, I attempted to develop a chemical proteomic platform that would allow direct site detection of protein lipidation, including lysine fatty acylation with limited success (Chapter 7).

BIOGRAPHICAL SKETCH

Nicole Alexis Spiegelman was born in Miami, Florida. She attended Ransom Everglades High School in Coconut Grove, Florida. She continued her education at Wellesley College where she graduated with honors in Chemistry, and obtained a minor in psychology. At Wellesley College, she was awarded the Beck Sophomore Research Fellowship in 2011, as well as the Jean V. Crawford Prize in Chemistry in 2013. In the fall of 2013, she joined the department of Chemistry & Chemical Biology at Cornell University and from the fall of 2014 has since been working under the guidance of Hening Lin.

I dedicate my dissertation to my mom, dad, and sister--

none of this would have been possible without their continuous

love, guidance and support.

ACKNOWLEDGMENTS

First and foremost, I would like to thank my advisor Professor Hening Lin. I am extremely grateful for his continued guidance, mentorship and support since he gave me the amazing opportunity to join his lab. He has afforded me the opportunity to learn, discover and take my projects where I wanted to, but provide guidance and support when needed.

I would also like to thank my committee members Professor Yimon Aye and Professor Richard Cerione for their guidance and support. I am also grateful to have had the opportunity to collaborate Okwang Kwon, He Huang and Sunjoo Kim from Professor Yingming Zhao's lab.

I am extremely thankful to many previous and current Lin lab members, without them I would not have been able to accomplish all that I have over the past few years. First, I would like to thank Dr. Pornpun (Polly) Aramsangtienchai and Dr. Hui Jing for their friendship, mentorship and support, even from their new positions. I learned so much about science and more importantly life from you, and I cannot thank you both enough. I am also grateful for the friendship and support of Patricia Tolbert.

I would like to thank Dr. Xiaoyu Zhang and Dr. Ji Cao for their continuous support and help and for always being willing to discuss projects and problem solve. Their willingness to step in and help whenever I needed it is most appreciated. I am extremely grateful to have had the opportunity to work with Miao Wang as we have worked on studying the function of SIRT2, your help, suggestions and encouragement have been invaluable. I would also like to thank Dr. Min Yang, Dr. Ian Price, Jun Young Hong, Dr. Sushabhan Sadhukhan and Dr. Jing Hu for their help with the SIRT2 inhibitor

studies, and Dr. Zhi Li, Dr. Zhewang Lin, Dr. Zhen Tong, Dr. Yingling Chiang, and Xiao Chen for teaching me how to do things ranging from synthesis to cell culture. I would also like to thank Yugang Zhang, Lu Zhang, Dr. Shuai Zhang for always being willing to discuss science and life. Finally, I would like to thank Xuan Lu who always makes sure that the lab is organized and that we have everything we need to get our experiments done, and being there to help when we need it.

I have also had the amazing opportunity to work with three undergraduate students over my time in graduate school. I want to thank Ilana Kotlier for her endless help and being a great mentee—even though I was supposed to be teaching you I learned a lot from you. I would also like to thank Monica Moore and Kelly Rosch for their help on the RalB lysine fatty acylation project.

Lastly, I would like to thank all my family and friends. They have always been there to support me, even through the challenging times. I am grateful to my parents and sister who have always encouraged me and given me the confidence to go beyond what I think is possible. Without them, none of this would be possible.

TABLE OF CONTENTS

LIST OF FIGURES

LIST OF TABLES

CHAPTER 1

THE REGULATION AND FUNCTION OF THE RAL GTPASES AND TOOLS TO STUDY PROTEIN LIPIDATION

1. The Ras Related Proteins: RalA and RalB

1.1 The Ras Superfamily of Small GTPases

Small GTPases are responsible for regulating a wide range of cellular functions and are involved in numerous signaling pathways.[1] Over 150 proteins have been classified as a member of the Ras superfamily. Initially there were four Ras oncogene proteins from three genes: HRAS, NRAS, KRas4a and KRAS4b. With the discovery of other similar proteins, there are now five subfamilies: Ras, Rho, Rab, Ran and Arf. The Ras subfamily has 36 members and includes the Rap, R-Ras, Ral and Rheb proteins.[2,3]

Small GTPases are guanosine diphosphate (GDP)/ guanosine triphosphate (GTP) regulatory switches that can modulate many key biological processes. These proteins are typically around 20 kilo-Dalton (kDa), and are monomeric G proteins.[4] Small GTPases bind tightly to both GTP and GDP, but possess low GTP hydrolysis or GDP/GTP exchange activities.[3] There are several enzymes that catalyze the exchange and hydrolysis process, they are classified as Guanine nucleotide exchange factors (GEFs) or GTPase activating proteins (GAPs). GEFs activate GTPases by interacting with the switch I and II regions leading to a conformational change that weakens the nucleotide binding, causing the release of GDP and the binding to GTP.[2,3,5] Once the GTPase is bound to GTP, the GEF no longer binds leaving the GTPase in its active state. When active, the GTPase is able to bind to effector proteins due to conformational changes in the effector binding domain. Much of the current understanding of the GTPases cycle and the activation of GTPases comes from the initial studies of the small GTPase Rac1 and its association with its effector Pak1 (p21-activated kinase 1).[2,3,5,6] The

intrinsic hydrolysis activity of small GTPases tends to be fairly weak and GAPs help catalyze the hydrolysis by inserting an arginine finger. The arginine finger stabilizes the transition state for the GTPase reaction. Some GTPases also interact with guanine nucleotide dissociation inhibitors (GDIs) which prevent the proteins from interacting with GEFs.[6]

The Ras genes are some of the most frequently mutated genes in cancer. In fact, they are mutated in approximately 15% of all cancers.[5,7,8] They exert their function through several downstream effector pathways (Figure 1.1). The three most well established axis are the Raf kinases (Raf1, B-raf and A-raf), the phosphatidylinositol 3-kinases (PI3Ks) (p85-p110) and the RalGEF family (RalGDS, Rlf and Rgl) (Figure 1.1).[7,9]

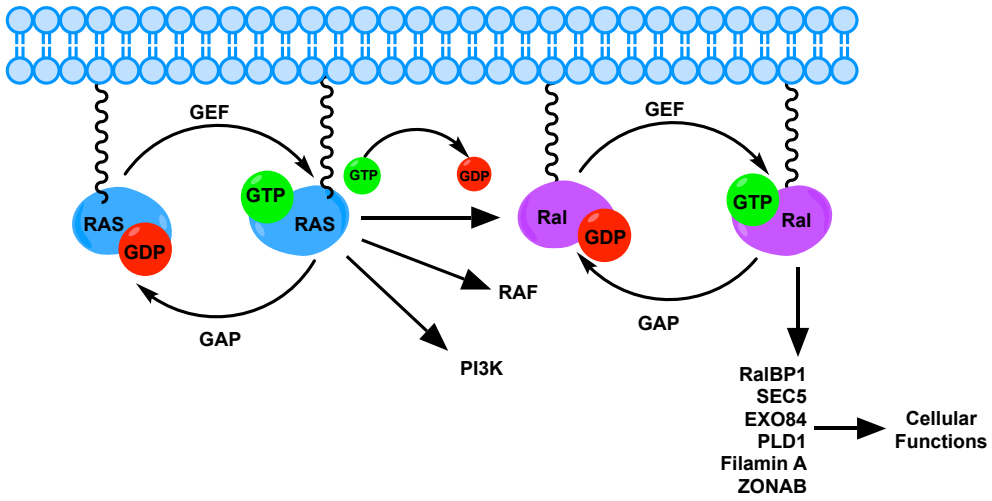

Figure 1.1. The interplay between the Ras and Ral GTPases. The canonical Ras GTPases (H-Ras, N-Ras, K-Ras4a and K-Ras4b) can cycle between their GTP(active) and GDP(inactive states). The intrinsic ability for Ras proteins to exchange GDP to GTP, and hydrolyze GTP to GDP is weak and is thereby regulated by two classes of enzymes guanine nucleotide exchange factors (GEFs) and GTPase activating proteins (GAPs). When bound to GTP the Ras proteins can interact with its known effectors PI3K, Raf and RalGDS. When Ras is bound to RalGDS, Ras can activate either of the Ral GTPases. The Ral GTPases also cycle between being bound to GDP and GTP. When bound to GTP, Ral can interact with one of its effector proteins and lead to a wide range of cellular effects.

As targeting Ras is considered a promising strategy for treating cancer, understanding its downstream effectors axis is critically important. The Raf and PI3K pathways are extremely well studied, and over 40 inhibitors have been developed which target Ras-driven cancers through Raf-MEF-ERK and PI3K-AKT-mTOR signaling pathways. However, even when these

pathways are successfully inhibited, Ras can still have a profound effect in promoting cancer through the Ral GEF pathway.[10]

1.2 The Ral Subfamily of GTPases

RalA and RalB are the sole members of the Ral subfamily in the Ras superfamily of GTPases. The Ral GTPases have been implicated in several biological processes including transcription, translation, cytoskeletal organization, membrane trafficking, cytokinesis, cell migration, cell proliferation, cell survival, autophagy, and endocytosis.[11-15] These two proteins share 85% sequence identify with each other, and about 50% identity with HRas, NRas and KRas.[16] The majority of the Ral sequence divergence comes from their C-terminal hypervariable region (Figure 1.2).[9] A lot of interest was placed on elucidating the role of the Ral GTPases in signaling and cancer as they are responsible for several Ras promoted cellular processes.[9]

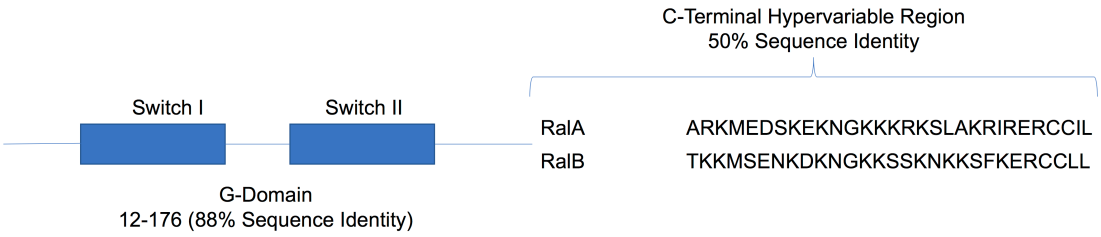

Figure 1.2. The structure of the Ral GTPases. The N-terminal of the Ral GTPases contains its G-Domain where the switch I and switch II regions are located. These regions are important for regulating the GDP/ GTP binding. The last twenty amino acids of the Ral GTPases comprise the hypervariable region (HVR) which is comprised of several poly basic lysine residues, phosphorylated serine residues, as well as prenylated and palmitoylated cysteine residues.

RalA was first identified through a screening with oligonucleotide probes aimed to identify Ras related genes from immortalized simian B-lymphocytes in 1986.[16] When initially identified, RalA was called v-ral simian leukemia viral oncogene homolog, because of its isolation from simian lymphocyte cDNA.[17] A few years later, RalB was identified using a RalA based probe from human cDNA library, during an attempt to isolate human RalA.[17]

The two Ral GTPases share 88% sequence identity in their G-domain. Their switch I

and II regions which are affected by the GTP-GDP cycle and are the domains responsible for both regulating and recognizing effector proteins are completely identical.[9,18] The largest difference in the two isoforms is in their C-terminal hypervariable region, where the two proteins only share 50% sequence identity.[9] Both isoforms have C-terminal cysteine prenylation their CAAX (cysteine-aliphatic amino acid-aliphatic amino acid-any amino acid) motif, and *S*-palmitoylation and phosphorylation. [9,19,20] The Ral proteins, like the Ras proteins, cycle between GTP- and GDP-bound states. Like the Ras proteins, there are several enzymes (guanine nucleotide exchange factors (GEFs) and GTPase activating proteins (GAPs)) that regulate this process. The RalGEFs are RalGDS, Rgl, Rgl2/Rif and Rgl3, RalGPS1, RalGPS2, and Rgl4. The Ral specific GAPs are RalGAPα1, RalGAPα2, and RalGAPβ.[9]

1.3 Regulation of Ral Activity

The first Ral GEF identified was Ral guanine nucleotide dissociation stimulator (RalGDS). RalGDS was identified through a PCR-based screening aimed at identifying genes with sequences similar to RasGEFs from yeast.[21] Despite its sequence similarity to other Ras GEFs, RalGDS was only able to exhibit GDP/GTP exchange activity for RalA and RalB.[21] Through a series of yeast two hybrid studies, the same method that was used to identify Raf as a Ras effector, RalGDS was identified as binding partners in screens for several Ras proteins including H-Ras, R-Ras, and R-Ras2.[21-24] The other Ral GEFs have been identified through similar yeast two hybrid experiments.[10]

RalGAPs have the ability to promote hydrolysis of GTP to GDP, making the Ral GTPases inactive. The first RalGAPs were called RalGAP1 and RalGAP2 and are heterodimeric complexes that contain either an α1 or α2 catalytic subunit and a conserved β subunit. RalGAP1 enhanced the RalA GTP hydrolysis by 280,000-fold. Interestingly, the Ral GAPs are similar to the tuberous sclerosis tumor suppressor complex (TSC) which is the GAP for the Rheb GTPases.[25] Soon after the identification of RalGAP1/2, the Ral GAP complex that regulates Ral

activity downstream of the PI3K-AKT pathway was identified. This complex is composed of a regulatory and catalytic subunit, RGC1 and RGC2, respectively. It was also found that insulin was able to inhibit the GAP activity, due to hyper-phosphorylation of RGC2, keeping Ral in its activated state.[26]

Several external stimuli have been found to modulate Ral activity. As noted above, insulin can activate Ral.[26] Complete starvation of all nutrients and serum by treatment of cells with an Earl's Based Salt Solution (EBSS) led to selective activation of RalB.[11] RalA GTP binding was enhanced by Ca^{2+}-Calmodulin.[27] Growth factors such as PDGF, TPA, EGF, LPA, α-thrombin, and forskolin, as well as reactive oxygen species (ROS), also have the ability to activate Ral.[28,29]

In addition to being activated by external stimuli, the Ral GTPases have been found to be hyper activated in several cancers, such as pancreatic cancer. This was found in human pancreatic tumor samples as well as in cancer cells. Despite the enhanced status of the Ral GTPases, AKT and ERK1/2 were not hyper-phosphorylated.[30] Ral GTPases were also found to be hyper activated in colorectal cancer tissue and cell lines. Interestingly, it was also found that depleting one of the Ral GTPases actually enhanced the GTP binding of the other isoform.[31] This suggests that the RalA and RalB are dependent on each other and can be key players in Ras-driven and other cancers.

1.4 Ral Effector Proteins

As expected, when bound to GTP, the Ral GTPases are active and can bind to a unique set of effector proteins and promote a wide range of cellular functions (Figure 1.1). The most well established Ral effector proteins are Ral binding protein 1 (RalBP1), and the exocyst components Sec5 and Exo84.[32-35] Other Ral effector proteins include Filamin, and phospholipase D1 (PLD1) (Figure 1.1).[9,36,37] The transcription factor zonula occludens 1-associated nucleic acid binding protein (Zonab), has been identified as a RalA specific

effector.[38] Interestingly, while both Ral isoforms can interact with the same effector proteins they can exhibit opposing roles in some cancer types, and promote different cellular functions.[3,9,10,20,35,36,38-41]

RALBP1 (Ral Binding Protein 1), or RLIP76 (76 kDa Ral-interacting protein), was the first Ral effector that was identified through a yeast 2-hybrid screen using RalA.[32,42,43] RalBP1 is interesting as it also serves as a regulatory protein for two other small GTPases Rac1 and Cdc42 because of its RhoGAP catalytic domain.[43] Interestingly, the Ral-RalBP1 interaction can affect the subcellular localization of Rac1 but cannot control its RhoGAP activity.[43] The Ral-RalBP1 interaction has also been shown to be important for the role of Ral in regulating endocytosis through interactions with the plasma membrane-associated AP-2 tetrameric complex and activin receptor interacting protein 2 (ARIP2).[12,44]

The two most well characterized, and studied, Ral effectors are two components of the exocyst complex Sec5 and Exo84.[10] The exocyst is a complex composed of eight components: EXOC1(Sec3), EXOC2(Sec5), EXOC3(Sec6), EXOC4(Sec8), EXOC5(Sec10), EXOC6(Sec15), EXOC7(Exo70) and EXOC8(Exo84), which has been implicated in cellular processes such as migration and exocytosis.[45] RalA and RalB have been shown to interact with Sec5 and Exo84, and the Ral-exocyst interaction is important for trafficking and exocytosis. Ral GTPases have been shown to modulate the assembly of the exocyst as well as control subcellular localization. The RalB-Sec5 interaction has been shown to be important for the innate immune response by promoting the TBK1-Sec5 interaction.[46] Under nutrient deprived conditions, RalB can interact with Exo84 and promote autophagasome formation by helping bring together the autophagasome machinery such as Beclin1 and ULK1.[11]

1.5 Ral GTPases in Cellular Functions and Cancer

Initial studies did not suggest that there was a role for the Ral GTPases in regulating vesicle sorting. However, localization studies show that in addition to plasma membrane

association, the Ral GTPases are located on many different endomembranes. Consistent with their different roles in different cancer types, Ral localization can be cell line dependent.[9] More recent studies have shown that RalB can regulate autophagy, in epithelial cells Ral proteins are important for basolateral delivery of membrane components, and the Ral proteins regulate protein secretion as well as receptor mediate endocytosis.[13]

Like its localization, the role the Ral GTPases play in cancer appears to be cancer type specific. In bladder cancer cells RalA suppresses and RalB promotes cell motility, and the two proteins similarly regulate tumor growth.[47] The Ral GTPases also play opposing roles in colorectal cancer. Studies show that in colorectal cancer cells, stable RalA depletion decreased anchorage intendent growth, while stable RalB depletion promoted it.[31] Interestingly, in lung cancer cells RalA and RalB show redundant functions, knock down of both proteins inhibited cell proliferation and anchorage independent growth.[39] In pancreatic cancer cells, through RNAi knockdown studies, RalA has been shown to be important for anchorage independent growth and tumorigenic growth, where RalB was important for invasion and metastatic growth.[30] Furthermore, in pancreatic ductal adenocarcinoma (PDAC) cells only RalB can promote invadopodia formation through its interaction with RalBP1.[48] For pancreatic cancer, it is believe that RalA is important for Ras-driven tumorigenesis, or the early stages of cancer progression, where RalB is important for malignant growth or the later stages of cancer development.[30] This highlights that the role of Ral GTPases is cancer cell type specific, and that the Ral GTPases can have redundant, dependent, or diverging roles.

1.6 The C-terminal Hypervariable Region of Ras Family GTPases

Difference in cellular functions and localization are often attributed to the divergent hypervariable regions of the two isoforms, and protein post-translational modifications. The C-terminal hypervariable region (HVR) of small GTPases is often important for protein localization. For example, the Rac1 HVR contains its nuclear localization signal.[49] The HVR

region tends to be a polybasic region, due to several lysine residues. The last four amino acids of the HVR tend to be the CAAX motif. The first cysteine of the CAAX motif is prenylated, except for two Rho GTPases Wrch1 and Wrch2. Often small GTPases also have a palmitoylated cysteine close to the prenylated cysteine.[50]

Prenylation is important for the proper processing of small GTPases. After being prenylated, the proteins are recruited to the endoplasmic reticulum (ER), where CAAX processing occurs. After anchoring to the ER the GTPases interact with Ras converting enzyme 1 (Rce1) a prenyl-CAAX-specific protease. This leads to the cleavage of the -AAX amino acids. The prenylated cysteine at the C-terminal of the protein is then methylated by isoprenylcysteine-directed carboxyl methyltransferase (Icmt). After capping of the free cysteine residue, the proteins are then recruited to the plasma membrane where they can be activated. However, CAAX processing is not the only requirement for membrane localization. It is now widely recognized that either several lysine residues (a poly basic region) or a palmitoylated cysteine are also necessary.[51]

1.7 The Ral C-terminal Hyper Variable Region

The Ral C-terminal HVR is important for the differential functions of RalA and RalB. Both Ral GTPases have prenylation on their C-terminal domain.[52,53] Additionally, both proteins are reported to have *S*-palmitoylation.[19,20] Recently, it was shown that there is an alternative processing mechanism for the CAAX motif through a study of Cdc42, for which the first A in CAAX is a cysteine. When a protein undergoes this alternative processing mechanism, the AAX motif is not cleaved by Rce1. Instead the cysteine residue next to the prenylated cysteine is palmitoylated. The dual lipidation promotes plasma membrane localization.[19] Since both RalA and RalB have the CCAX motif and exhibit *S*-palmitoylation, it is believed that they can also undergo this alternative processing mechanism. However, it was found that Rce1 was necessary for both RalA and RalB to associate with the plasma membrane. RalB also requires ICMT for

membrane localization where RalA does not. However, RalA does require ICMT for localizing to the recycling endosomes. Furthermore, RalB *S*-palmitoylation is also necessary for its plasma membrane localization, but RalA does not require *S*-palmitoylation for membrane localization.[20] In addition to C-terminal prenylation and *S*-palmitoylation, RalA and RalB both have c-terminal phosphorylation. While RalA and RalB have similar modifications, different proteins can regulate the modifications leading to distinct effects. As an example, protein kinase C regulates phosphorylation on RalB, while protein kinase A regulates phosphorylation on RalA. This differential regulation can partially explain the different functions of the Ral isoforms in bladder cancer cells, suggesting that the differences in the Ral C-terminal HVR can potentially explain the diverging function of these two highly similar small GTPases.[54]

2. Tools for Protein Lipidation: Small Molecule Inhibitors and Chemical Proteomic Platforms

2.1 Protein Lipidation

Proteins, such as small GTPases, control various biological processes and therefore, the regulation of proteins is crucial to maintain cellular homeostasis. As highlighted above, one way proteins are regulated is through protein post translation modifications (PTMs), or the covalent attachment of different functional groups onto amino acid residues after a protein is translated.[55] In a broader context, PTMs can be as small as a methyl group, or as large as a small protein such as ubiquitin. To date over three hundred PTMs have been identified, with lipidation being just one class.[56]

Protein lipidation typically refers to N-terminal glycine myristoylation, cysteine palmitoylation (*S*-palmitoylation), cysteine prenylation or modifications by GPI anchors (Table 1.1). N-terminal glycine myristoylation is the irreversible attachment of myristic acid via an amide linkage on a glycine residue on the N-terminal of a protein. Cysteine prenylation is also an irreversible lipid modification, where isoprenoids such as farnesyl or geranylgeranyl groups

are attached to cysteine residues via a thioether bond. *S*-palmitoylation is the attachment of palmitic acid to a cysteine residue via a thioester linkage, this lipid modification is reversible.

Table 1.1. Protein Lipidation. The structure, linkage, dynamic status and regulating enzymes are presented.

Modification	Linkage	Regulating Enzymes
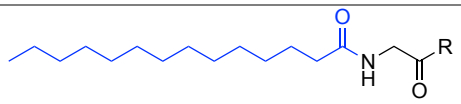 **N-Terminal Glycine Myristoylation**	Amide	NMT1, NMT2
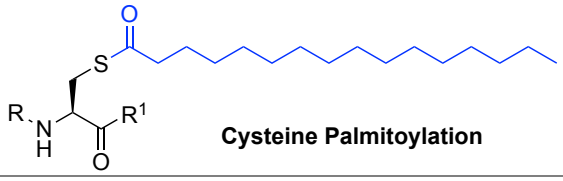 **Cysteine Palmitoylation**	Thioester	DHHC1-23, APT1/APT2, ABHD17
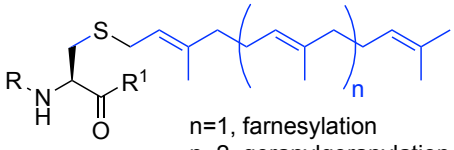 n=1, farnesylation n=2, geranylgeranylation **Cysteine Prenylation**	Thioether	FTase, GGTase
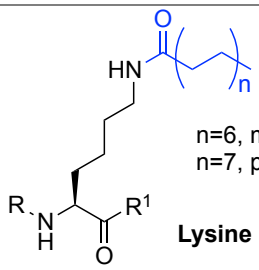 n=6, myristoylation n=7, palmitoylation **Lysine Fatty Acylation**	Amide	SIRT1,2,3,6,7 HDAC8, HDAC11
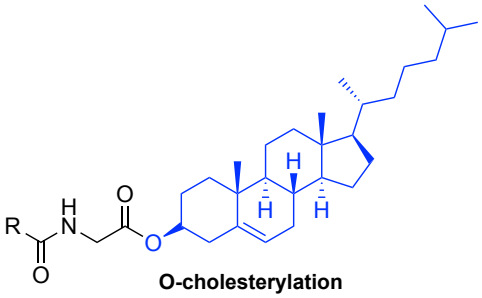 **O-cholesterylation**	Carboxlyate group of a carboxy-terminal glycine	Autocatalytic
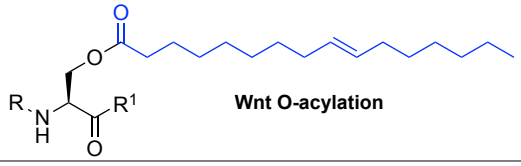 **Wnt O-acylation**	Ester bond on Serine	Porcupine

There are several other lipidation PTMs, and they include lysine fatty acylation, Wnt

O-acylation, Hedgehog N-terminal cysteine palmitoylation and Hedgehog O-cholesterylation (Table 1.1). Lysine fatty acylation, like S-palmitoylation, is a reversible PTM and is the addition of myristic or palmitic acid onto the branched chain of lysine residues by an amide bond. [57-60]

2.2 Protein Lipidation of Small GTPases

Lipidation, particularly cysteine prenylation and palmitoylation, is a key regulatory mechanism for many small GTPases. Only the Ran small GTPase does not require lipidation, as membrane anchoring is not required for its downstream signals.[6] The Arf family is unique as they have N-terminal lipidation, primarily N-terminal glycine myristoylation.[6] The Ras, Rho and Rab GTPases tend to have C-terminal lipidation. Ras subfamily members have farnesylation, while Rho and Rab GTPases are geranylgeranylated. The Ras subfamily members also tend to have palmitoylated cysteine residues either as part of the CAAX motif or upstream of it.[2,3,6,9,50,59,60] More recently, it has been found that several Ras subfamily GTPases also have lysine fatty acylation. Lipidation has been shown to be important for the proper protein processing, localization, activity, and transforming ability of GTPases.[19,20,58,59]

2.3 Protein Fatty Acylation: N-terminal Glycine Myristoylation, S-palmitoylation and Lysine Fatty Acylation

Protein lipidation has been shown to be important for myriad of biological processes, such as cancer, and many important proteins have been shown to be regulated by protein lipidation. Lipidation regulates the function of proteins by modulating the stability, protein-protein interactions, localization, activity, and numerous other properties of modified proteins. Below I will focus on protein fatty acylation, including N-terminal glycine myristoylation, *S*-palmitoylation, and lysine fatty acylation because of their similarities and their established roles in regulating small GTPases.[59-61] Numerous proteins have been reported to have these modifications as shown by the representative list of proteins in Table 1.2. This list highlights the diversity of proteins that have fatty acylation, and shows that fatty acylation is a general

regulatory mechanism that can influence numerous cellular functions.

N- terminal glycine myristoylation is important for membrane anchoring and cellular localization, as well as regulating protein-protein interactions, protein stability and enzymatic activity.[59] N-terminal glycine myristoylation can easily be predicted, as proteins with this modification have a consensus motif.[86] N-terminal glycine myristoylation is also unique as it can be either a co-translational or post-translation protein modification.[86]

Table 1.2. Proteins with N-terminal glycine myristoylation, s-palmitoylation and lysine fatty acylation.

Modification	Representative Proteins with the Modification
N-Terminal Glycine Myristoylation	Actin[62] ADP Ribosylation factor (ARF), ARF-like (ARL)[63,64] G-protein alpha subunit[65,66] MARCKS[67,68] Src Family Kinases (Fyn, Blk, Fgr, Hck, Lck, Lyn, Src, Yes)[69]
S-Palmitoylation	RalA[19,20], RalB[19,20], R-Ras[70], HRas[71], NRas[71], KRas4a[71] LCK[72] Fyn[73] Syntaxin-7[74] IFITM3[75,76] FasL[77] IFNAR1[78] PLM[79]
Lysine Fatty Acylation	TNF-α[80] IL-1α[81] aquaporin-0[82] R-Ras2[83] KRas4a[84] Rac1, Rac3, Cdc42[85]

In humans, there are two proteins that are responsible for adding the myristoyl group, NMT1 and NMT2. As N-terminal glycine myristoylation is important for regulating the function of several important proteins, small molecules have been developed to regulate the activity of NMT1 and NMT2 which have helped in elucidating the physiological role of N-terminal glycine myristoylation.[87-89]

S-palmitoylation, like N-terminal glycine myristoylation is also an important and

abundant protein post-translational modification that can regulate the function, localization and activity of several important proteins (Table 1.2). [59,60] Unlike N-terminal glycine myristoylation, *S*-palmitoylation is reversible as it can be hydrolyzed both enzymatically and non-enzymatically. Furthermore, *S*-palmitoylation cannot be easily predicted as there is no consensus sequence motif to be recognized by acyl transferases. However, many proteins that have *S*-palmitoylation also have other lipid modifications such as N-terminal glycine myristoylation and cysteine prenylation. Several proteins require N-terminal glycine myristoylation to anchor a protein to the membrane, where specific membrane bound acyl transferases can palmitoylate cysteine residues.[90-92] For example, Src family kinases have both N-terminal glycine myristoylation and *S*-palmitoylation. Alternatively, several Ras superfamily GTPases, such as bCdc42, RalA, and RalB have S-palmitoylation and cysteine prenylation at their C-terminal regions.[19]

The first human *S*-palmitoyl transferases that were identified are the zinc finger DHHC (aspartic acid-histidine-histidine-cysteine) enzymes. There are 23 mammalian DHHCs. The substrate selectivity of each is still not fully understood, and some proteins are substrates for multiple DHHCs. One reason there are still questions regarding substrate specificity is lack of methods to efficiently and accurately profile DHHC substrates.[59] APT1 and APT2, also known as LYPLA1 and 2, were the first known cysteine depalmitoylases.[93] More recently, the α/β-hydrolase domain 17 (ABHD17) family of proteins have also been found to be protein depalmitoylases.[94,95]

Recently, protein lysine fatty acylation is being recognized as a more abundant and important PTM than initial studies suggested. Despite being discovered in the early 1990s, until last year only three proteins were reported to have lysine fatty acylation: TNF-α, IL-1α and aquaporin-0.[80-82] The functional relevance of this PTM remained unstudied until 2013 when it was reported that lysine fatty acylation on TNF-α regulates its secretion. Further studies also

showed that lysine fatty acylation promotes the lysosomal sorting of TNF-α.[96,97] These two studies highlighted that protein lysine fatty acylation is a physiologically relevant, and important PTM. However, a more comprehensive understanding of the function of this PTM was lacking due to the limited scope of proteins reported to have lysine fatty acylation.

In the past year, several small GTPases, including R-Ras2, KRas4a, HRas, and Rac1, were reported to be regulated by protein lysine fatty acylation.[83-85] These studies have highlighted the importance of lysine fatty acylation. Lysine fatty acylation on R-Ras2 to promotes its activity and cell proliferation, while lysine fatty acylation on KRAS4a suppresses its interaction with A-Raf and its transforming activity in NIH 3T3 cells.[83,84] Lysine fatty acylation on Rac1, catalyzed by bacterial secreted factors, regulates it GTP binding or activity.[85]

The recent identification of several more proteins with lysine fatty acylation suggest that this modification is likely abundant and have important biological functions. Lysine fatty acylation is similar to *S*-palmitoylation in the sense that there is no known sequence motifs to predict the modification. Thus, to fully understand the scope of lysine fatty acylation, more proteins with this PTM need to be identified.

As PTMs regulate a proteins function by modulating its interacting partners, activity or localization, understanding how the modifications themselves are regulated is of great importance. There are various enzymes which regulate protein lipidation (Table 1.1). This chapter will specifically focus on our knowledge of the NAD dependent HDACs, Sirtuin 2 (SIRT2) and of one of the twenty-three DHHCs, DHHC7. The mechanism, known substrates, and physiological functions will be summarized. Understanding the enzymes that regulate protein lipidation will allow us to use them as tools to study these modifications.

2.4 Sirtuins

The NAD dependent class of histone deacetylases, known as Sirtuins have attracted a lot of research interest due to their connection to many biological processes including

metabolism, transcription, cancer and, aging. There are seven mammalian Sirtuins, SIRT1-7. They all share a common core catalytic domain with a NAD^+ binding site, but have varying N and C-terminal extensions, as well as different subcellular localizations.[98] (Table 1.4)

Table 1.3. Sirtuins, their subcellular localization and enzymatic activities.

Sirtuin	Subcellular Localization[99,100]	Enzymatic Activity on Which Acyl Groups
SIRT1	Nucleus, cytosol	Acetyl[101], Fatty-acyl[102]
SIRT2	Cytosol, Nucleus	Acetyl[103], Fatty-acyl[102,104], 4-Oxononoyl[105,106]
SIRT3	Mitochondria	Acetyl[107], Fatty-acyl[102]
SIRT4	Mitochondria	3-methylglutaonyl[108], Biotinyl[109], Hydroxymethylglutaryl[108], Lipoyl[109], methylglutaryl[108]
SIRT5	Mitochondria	Acetyl[110], Glutaryl[111], Malonyl[112], Succinyl[112]
SIRT6	Nucleus	Acetyl[113], Fatty-acyl[96,102]
SIRT7	Nucleolus	Acetyl[114], Fatty-acyl[115]

The physiological functions of Sirtuins is dependent on their enzymatic activity. Sirtuins were initially identified as NAD-dependent protein lysine deacetylases. Through several biochemical and structural studies, much progress has been made on elucidating the mechanism of Sirtuin deacylation. It is thought that the acylated substrate binds to the protein, followed by NAD binding to form the tertiary complex. Once the complex is formed, the oxygen from the carbonyl group from the acyl modification attacks the C1' position of NAD. This leads to the release of nicotinamide and formation of an alkylamidate intermediate. A histidine residue, which is conserved through all seven Sirtuins, acts a general base and deprotonates the ribose group forming a 1',2'-cyclic intermediate. The intermediate undergoes hydrolysis to form the 2'-O-acyl-ADP-ribose product (Figure 1.3).[116,117] Initially, it was thought that sirtuins only

catalyzed the removal of acetyl groups from substrates; however, it is now well established that Sirtuins possess various enzymatic activities, and can remove a wide variety of acyl groups from lysine residues (Table 1.3).

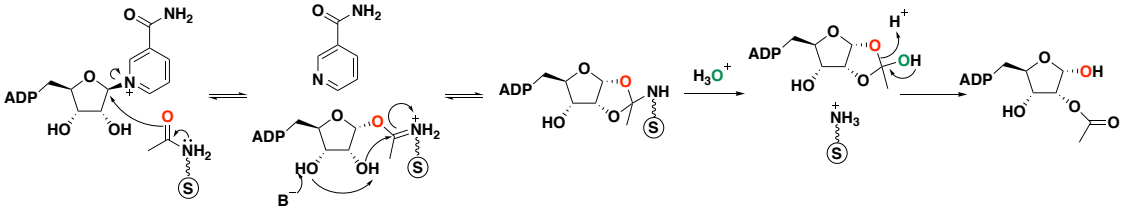

Figure 1.3. Catalytic Mechanism of Sirtuin deacylation.

2.5 The Physiological Function of SIRT2

Sirtuin 2, or SIRT2, is the only cytosolic sirtuin and has the ability to hydrolyze acetyl, long chain fatty acyl and 4-oxononanoyl groups from lysine residues.[103-106] Despite initial reports that presented conflicting roles of SIRT2 as a tumor promoter or tumor suppressor, it is now well established that SIRT2 is a promising cancer target.[118-121] In addition to its role in cancer, SIRT2 has been shown to play a role in several other biological processes including: cell cycle progression, oxidative stress response, cell growth, chromatin condensation regulation, microtubule dynamics, aging, differentiation, autophagy, apoptosis, transcription, and metabolism.[98,103,122-133] SIRT2 can deacylate a wide range of substrates (Table 1.4). However, only one SIRT2 defatty acylation substrate has been reported.[84]

Table 1.4. SIRT2 deacetylation substrates and the physiological function of deacylation.

Substrate	Modification and Modification Site	Physiological Function of SIRT2 Regulated Acylation
c-Jun kinase (JNK)	KAc (153)	Deacetylation promotes ATP binding and the enzymatic activity of JNK on c-Jun, promotes oxidative stress induced cell death[134]
NFATc2 transcription factor	KAc (site not identified)	Regulates the activity of the transcription factor NFATc2[135]
Glucokinase regulatory protein (GKRP)	KAc(126)	Promotes glucose dependent hepatic glucose uptake[136]

H3K18	KAc(18)	Suggests SIRT2 is a tumor suppressor, is important for infection[137]
nuclear factor-kappa B (NF-ϰB) p65	KAc	Alleviates neuropathic pain, inhibits neuroinflammation[138,139]
Prx1	KAc(27)	Resvestrol activates SIRT2 leading to deacetylation of Prx1 to promotes it ability to reduce H_2O_2[140]
BubR1	KAc(243) KAc(250)	BubR1 deacetylation protects oocytes from maternal age-associate meiotic defects[129] Deacetylation at K250 regulates spindle assembly checkpoint timing[128]
Rho guanine nucleotide dissociation inhibitor (RhoGDI)	KAc(52)	Lysine acetylation regulates the Rho bidning to RhoGDI and can modulate Rho signaling[141]
Tubulin	KAc(40)	Unknown[103]
p300	KAc	Inhibition of transcription[131]
H4K16	KAc(16)	Lysine acetylation regulates chromatin structure[142]
H4 K20 Methyl Transferase PR-Set7	KAc(90)	Lysine acetylation regulates chromatin structure[120]
CDK9	KAc(48)	Deacetylation promotes CDK9 kinase activity[143]
Hypoxia-inducible factor 1alpha (HIF1α)	KAc(709)	Deacetylation promotes hydroxylation on HIF1α leading to its degradation[144]
KRas	KAc(147) and KAc(104)	Lysine acetylation regulates cancer cell growth[145]
ATP-citrate lyase (ACLY)	KAc(540, 546, 554)	ACLY acetylation promotes protein stability and tumor growth, deacetylation destabilizes ACLY[146]
Pyruvate kinase 2 (PKM2)	KAc(305)	Acetylation reduced PKM2 activity by inhibiting the tetramerization of the enzyme (which is its active form) [147]
FoxO1	KAc	Deacetylation of FOXO1 decreases activity and increases cell death by promoting autophagy, also regulated

		adipocyte differentiate by regulating the phosphorylation of FOXO1[122,148]
Slug	KAc(116)	Acetylation regulates the proteolytic turnover of Slug, and deacetylation stabilizes slug[149]
Lactate dehydrogenase A (LDH-A)	KAc(5)	Deacetylation promotes LDH-A activity, When acetylated LDH-A is recognized by HSC70 and is degraded[119]
ENO1	KAc	Deacetylation downregulates activity[150]
LKB1	KAc(48)	Deacetylation promotes LKB1 phosphprylation and activates LKB1-AMPK signaling[151]
PRDX1	KAc(197)	SIRT2 deacetylation leads to a reduction in PRDX1 antioxidant peroxidase activity[152]
Phosphoglycerate mutase (PGAM)	KAc(100/106/113/138)	Acetylation promotes cancer cell growth[153]
Glucose-6-phosphate dehydrogenase (G6PD)	KAc(403)	Deacetylation promotes G6PD activity[126]
Aldolase (AldoA)	KAc(322)	Deacetylation downregulates AldoA activity[150]
GAPDH	KAc	Deacetylation downregulates activity[150]
PGK1	KAc	Deacetylation downregulates activity[150]
S6K1	KAc(484/485)	S6K1 acetylation can regulate mTORC1 phosphorylation and activity[154]

Recently, it was identified that SIRT2 can defatty-acylate one of the Ras oncogenes K-Ras4a. It was found that SIRT2 and lysine fatty acylation could regulate the transforming ability of K-Ras4a.[84] This suggested that the defatty-acylation activity of SIRT2 could also be important for its role in cancer. However, there are still several unanswered questions about the physiological function of SIRT2 that can possibly be explained through identification of additional substrates.

2.6 Small Molecule SIRT2 Inhibitors

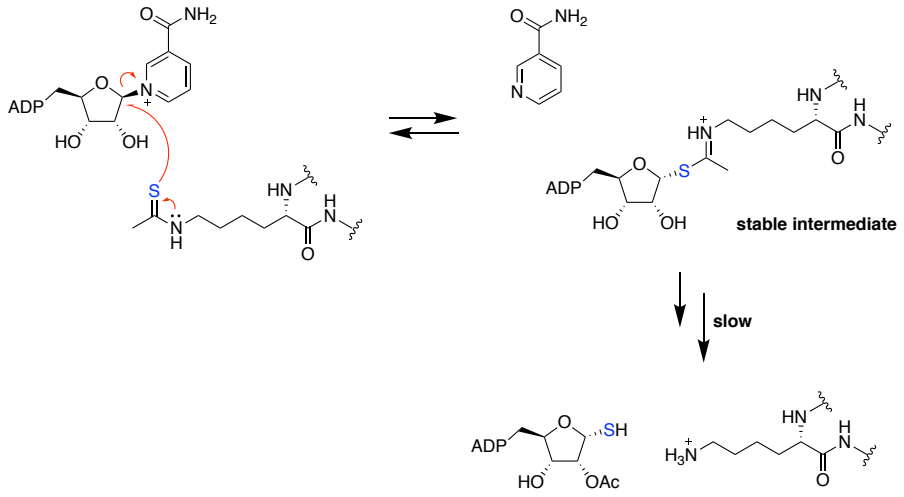

Figure 1.4. Mechanism based SIRT2 inhibitors form a stable intermediate.

Small molecule inhibitors are powerful tools that can be used to perturb the function of an enzyme to study the functional outcomes. Additionally, SIRT2 is a potential therapeutic target. Several different SIRT2 inhibitors have been developed.[155-158] There are two main classes of sirtuin inhibitors, mechanism-based and non-mechanism-based. The non-mechanism-based inhibitors bind to the sirtuin active site and compete with substrate (NAD or peptide) binding. Mechanism based SIRT2 inhibitors take advantage of the sirtuin catalytic mechanism and inhibit the enzyme by forming a stalled covalent intermediate[118] (Figure 1.4). The four most noteworthy SIRT2 inhibitors are AGK2, SirReal2, Tenovin-6, and TM (Figure 1.5).[118,159-161] These four compounds have been useful tools to identify SIRT2 as a promising therapeutic target for c-Myc driven cancers and for studying the function of SIRT2 in cells.[118,125,133,156,157,159,160,162,163] However, these inhibitors have not be compared side-by-side, and thus no information is available regarding which inhibitor is the best to use for inhibiting SIRT2.

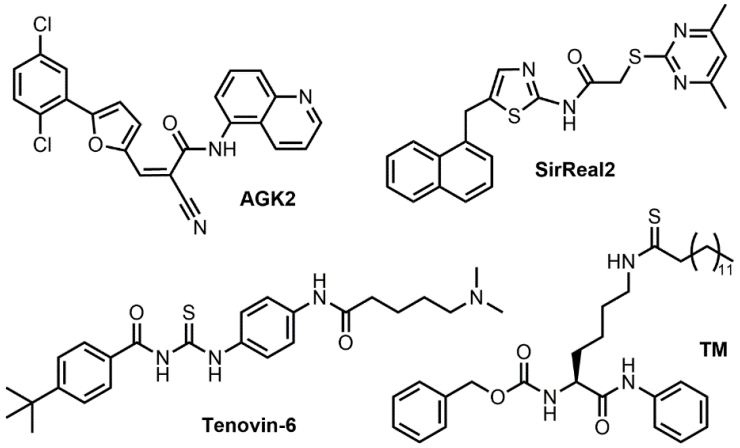

Figure 1.5. Structures of four well established SIRT2 inhibitors. AGK2, SirReal2, Tenovin-6 and TM.

As these inhibitors are being used as tools to identify the role of SIRT2 in signaling and cancer, it is important to know which enzymatic activity these inhibitors target. However, these compounds have only been evaluated regarding SIRT2 deacetylation activity. To better understand the role of lysine fatty acylation acylation, inhibitors that modulate this activity need to be identified. This could allow for deciphering between the enzymatic activities of SIRT2 and its physiological functions.

2.7 DHHC Enzymes

The class of enzymes that are responsible for catalyzing S-palmitoylation are known as the DHHC enzymes. These enzymes were first discovered in yeast through genetic studies.[164] It was found that Erf2p and Erf4p were essential for the complex that lead to S-palmitoylation of Ras. Erf2p which is found on the ER-membrane of yeast contained a conserved Asp-His-His-Cys (DHHC) Cys-rich domain (CRD). It has since been discovered that any mutations to the DHHC domain leads to abolition of the catalytic activity.[165] Concurrently, the acyl transferase for YCK2 *S*-palmitoylation was identified to be Akr1. This protein also contained a DHHC-CRD motif that was necessary for the enzymatic activity. The first mammalian DHHC that identified was DHHC3, or GODZ.[166]

Since the discovery of mammalian DHHC3, 22 other mammalian DHHC proteins

encoded by the zDHHC genes have been identified. All of the DHHCs contain the conserved DHHC-CRD which is essential for their enzymatic activity.[165,167] DHHC enzymes have four to six transmembrane domains, and both their N and C terminal domains are cytosolic.[168] Acylation by DHHC enzymes is thought to occur through a two-step mechanism. The DHHC is first autoacylated forming a transient acyl-intermediate. The palmitate group is then transferred to the substrate from the acyl intermediate.[169]

2.8 The Physiological Function of DHHC7

As more proteins with *S*-palmitoylation are being identified, more substrates for the DHHCs have been identified. DHHC substrate specificity is difficult to study as. it is not uncommon for a protein to be a substrate for multiple DHHC enzymes.[59,169,170] To better understand substrate specificity, comprehensive substrate profiling will be helpful. Of the DHHCs, DHHC7 tends to be promiscuous and numerous proteins have been identified as DHHC7 substrates (Table 1.5). DHHC7 is known to localize to the Golgi, and is found in multiple tissues. It has been reported that DHHC7 knock out (KO) mice developed hyperglycemia and glucose intolerance.[171] DHHC7 has also been reported to be a tumor suppressor. However many questions remain about its role in signaling and cancer.[172]

Table 1.5. DHHC7 Substrates and the physiological function of S-palmitoylation.

Protein	**Physiological Function of S-palmitoylation**
Scribble (SCRIB)	Regulation of cell polarity[172]
Fas	Protein stability[173]
Cystic fibrosis transmembrane regulator (CFTR)	Protein stability[174]
Endothelial nitric oxide synthase (eNOS)	Regulation of localization and activity[175]
Palmitoyl-protein thioesterase 1 (PPT1)	Protein activity[176]

Synaptosomal-associated protein 25 (SNAP25) (and SNAP23)	Plasma membrane localization[177]
Stress axis-regulated exon (STREX)	Plasma membrane localization[178]
Phosphatidylinositol 4-kinase type liα (PI4KIIα)	Golgi targeting[179]
SYDE-1	unknown[180]
TARPγ-2/ TARPγ-8	unknown[180]
Cornichon-2	unknown [180]
CaMKIIα	unknown[180]
NCDN/Norbin	Early endosome localization[180]
Zyxin	unknown [180]
TRPM8	unknown [180]
TRPC1	unknown [180]
Orexin 2 receptor	unknown[180]
Cysteine String Protein (CSP)	Plasma membrane localization[181]
RGS4	Protein stability[182]
Galpha(q), Galpha(s), and Galpha(i2)	Plasma membrane localization[183]
Glucose Transporter 4 (Glut4)	Plasma membrane localization[171,184]
Sex Steroid Receptors	Regulate localization and function[185]

To better understand the role of DHHC7, additional substrates need to be identified. While several methods have been developed to profile these modifications,[61] direct detection of

lipid modifications during proteomic studies has proven to be challenging. This is likely because the lipid modifications are hydrophobic and difficult to elute during LC-MS and often present in low abundance.[186]

2.9 Proteomic Profiling of Fatty Acylation

Due to the low abundance of the modification or the protein being modified, detection of lipidation (and PTMs in general), often requires enrichment.[66] For PTMs such as lysine acetylation, antibodies that recognize the PTM can be used for enrichment. However, there are no antibodies that can efficiently and effectively enrich *S*-palmitoylation or lysine fatty acylation.

The acyl biotin exchange method, or other closely related cysteine centric approaches, have been used to indirectly detect the site of palmitoylation (Figure 1.6). In this method, free cysteine residues are capped using N-ethylmaleimide, and the site of fatty acylation is then indirectly detected by cleaving the endogenous modification with hydroxylamine and then reacting with a biotin-HPDP probe which can form a disulfide bond with the free cysteine residues. While this method allows identification of the modification sites, it still has several drawbacks. First, N-ethylmaleimide may not block all free cysteine residues. This can lead to false positive results. Furthermore, the thioester cleavage by hydroxylamine may not be efficient and can be influenced by numerous factors, such as accessibility. However, the main drawback of this method is that the indirect identification method cannot be used to identify lysine fatty acylation site since the amide bond from lysine fatty acylation is resistant to hydroxylamine.[61]

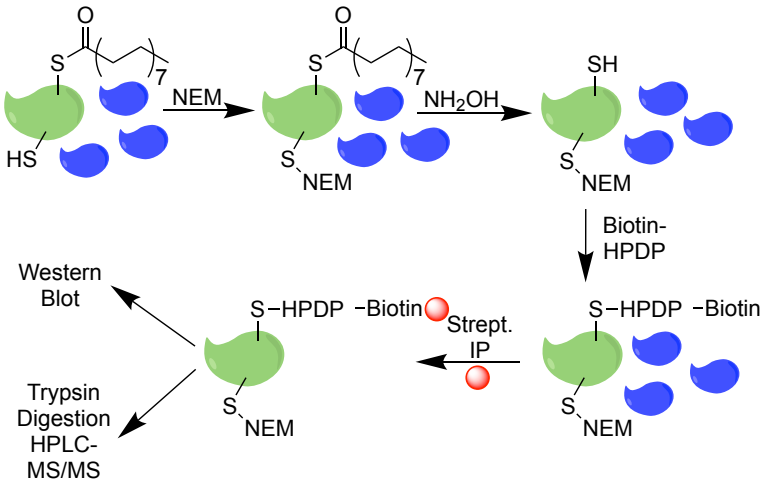

Figure 1.6. Acyl-Biotin Exchange method used to indirectly detect S-palmitoylation.

To overcome the challenges and drawbacks of the acyl biotin exchange method, biorthogonal probes such as Alkyne 14 (Alk14) have been used (Figure 1.7). For this method, palmitic acid mimics such as Alk14 are metabolically incorporated onto the fatty acylation sites of proteins. Click chemistry can then be used to attach biotin to the fatty acylation sites. Streptavidin immunoprecipitation (IP) can then be used to enrich all the fatty acylated proteins (Figure 1.7). [61,187]

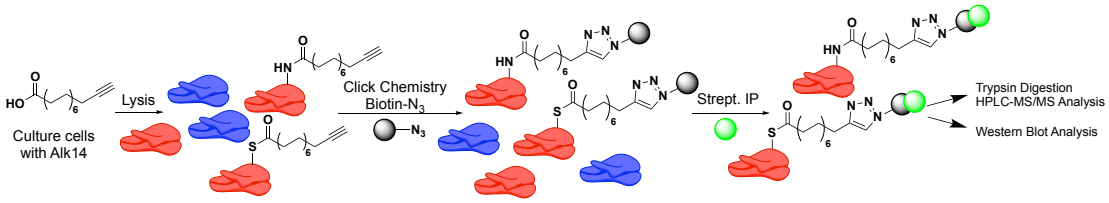

Figure 1.7. Metabolic labeling and affinity purification of lysine and cysteine palmitoylation.

However, because the biotin-streptavidin affinity is so strong, modification site information is typically lost. Furthermore, these probes are not specific for cysteine, lysine, or glycine fatty acylation and thus, all diferent protein fatty acylation would be identified. This method has been used to identify SIRT6 lysine defatty-acylation substrates. Because there was no site confirmation, of the false positive rate is very high.[83]

2.10 Cleavable Biotin-Azide Probes for Proteomic Studies

To help identify the modification site using Alk14 metabolic labeling, efforts have been placed on developing cleavable biotin probes.[188] Cleavable biotin probes typically have biotin attached to an azide reactive group with a cleavable spacer (Figure 1.8). The reactive group is often used in bioorthoganal reactions. There are four classes of cleavable biotin probes: (1) protease labile (2) pH (acid/base) labile (3) reduction oxidation sensitive (4) photo cleavable.[188] Several representative linkers are presented in Table 1.6. The cleavable probes make use of the well-established and efficient streptavidin IP, but they allow for site identification. Furthermore, they allow for elution without requiring on- bead trypsin digestion. However, these probes also have some disadvantages. The main one being the efficiency of the cleavage step in complex mixtures. While these probes have allowed for significant progress in profiling protein lipidation, there still has not been significant progress at direct detection of N-terminal glycine myristoylation or s-palmitoylation with high quality MS/MS spectra, and they have not been used to identify proteins with lysine fatty acylation.[56,61,188-190]

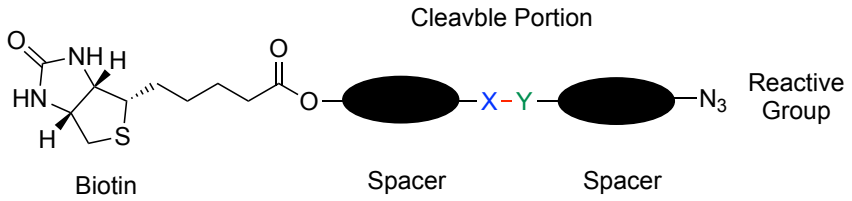

Figure 1.8. General Structure of Cleavable Linkers. Cleavable probes often include a biotin moiety for enrichment connected to the cleavable portion of the linker with a spacer often a PEG chain. A reactive group is linked to the cleavable portion also with a spacer.

Table 1.6. A Representation of several cleavable biotin azide probes that have been used to study biochemical processes.

Cleavable Linker	Class of Linker	Cleavage Conditions
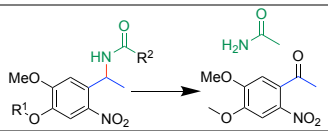	Photocleavable	365 nm light[191]
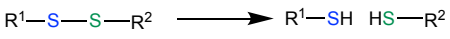	Redox-sensitive	1,4-Dithioreitol, Tris(2-carboxyethyl) phophine hydrochloride (TCEP), 2-Mercaptoethanol[191,192]
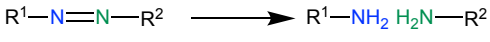	Redox-sensitive	Sodium Dithionite[193]
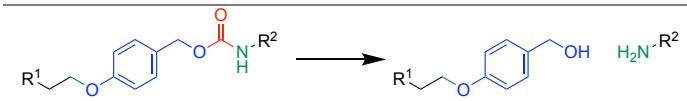	pH Sensitive	Trifluoroacetic Acid[194]
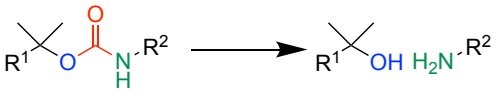	pH Sensitive	Trifluoroacetic Acid[191]
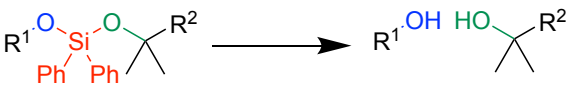	pH Sensitive	Formic Acid[191]
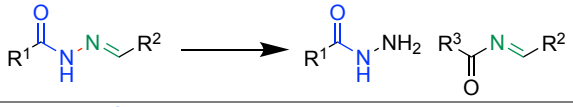	pH Sensitive	Acyl hydrazine[195]
	Photocleavable	254 nm light[196]
ENLYFQG → ENLYFQ-OH NH₂-G	Protease	TEV protease[197,198]

3. Dissertation Statement

Despite being identified in the early 1990s, protein lysine fatty acylation as remained an understudied PTM. However, with the recent identification of several lysine defatty acylases and the finding that several Ras GTPases have lysine fatty acylation, we hypothesized that this PTM is more abundant and important than initial studies suggested. We initially screened several Ras superfamily GTPases, presented in chapter 2, and found that several other small GTPases may have this PTM. We decided to further study protein lysine fatty acylation on RalB. We show that RalB lysine fatty acylation is regulated by SIRT2 and promotes RalB-GTP binding and cell migration.

We were intrigued by the fact that only RalB, and not RalA had lysine fatty acylation. As the Ral GTPases can exhibit opposing functions in some situations, we decided to further explore the similarities and differences between these two highly related proteins by identifying their interactomes using SILAC. In chapter 3, we identified many known and unknown interaction proteins of RalA and RalB. Furthermore, we show that RalB selectively interacts with ERK2, and can decrease ERK2 nuclear localization. The RalB-ERK2 interaction is dependent on the C-terminal HVR of RalB. This study highlighted utility of the interactome approach in studying the differences and similarities between the two Ral GTPases.

The study showing that RalB is a SIRT2 defatty acylation target highlighted the role of lysine fatty acylation in cell signaling and cancer. We were interested in developing tools that would allow us further understand the role of this not well studied PTM. Given that SIRT2 can remove lysine fatty acylation on several proteins, we hypothesized that SIRT2 inhibitors could be a way to regulate the levels of lysine fatty acylation and allow us to identify additional SIRT2 defatty acylation substrates. However, in most cases SIRT2 inhibitors have only been evaluated with respect to inhibiting SIRT2 deacetylation activity. We therefore carried out an in-depth comparison of four well established SIRT2 inhibitors (AGK2, SirReal2, Tenovin-6 and TM) in

Chapter 4. We found that TM was the most potent and selective SIRT2 inhibitor, however it could not efficiently inhibit SIRT2 defatty acylation activity. Since we were interested in identifying a compound that could modulate the fatty acylation activity of SIRT2, we developed other compounds as more potent SIRT2 inhibitors. We were excited to find that a TM analogue JH-T4 could modulate the lysine defatty acylation activity on K-Ras4a in cells (Chapter 5).

In another direction, I used a chemical proteomics approach to identify fatty acylated proteins. Through our efforts to identify HDAC defatty acylation substrates we found that JAM-C has *S*-palmitoylation as presented in Chapter 6. JAM-C is S-palmitoylated by DHHC7 S-palmitoylation regulates tight junction localization of JAM-C and cell migration.

Our JAM-C study highlighted that proteomic profiling of lysine fatty acylation would be challenging without direct site identification due to high false positives rates caused by the identification of proteins with N-terminal glycine myristoylation or S-palmitoylation. To overcome this challenge I attempted to use a cleavable biotin azide probe to directly identify protein lipidation from proteomic samples as shown in Chapter 7.

REFERENCES

(1) Rajalingam, K.; Schreck, R.; Rapp, U. R.; Albert, S. Ras oncogenes and their downstream targets. *Biochim Biophys Acta* **2007,** *1773* (8), 1177.

(2) Colicelli, J. Human RAS superfamily proteins and related GTPases. *Sci STKE* **2004,** *2004* (250), RE13.

(3) Wennerberg, K.; Rossman, K. L.; Der, C. J. The Ras superfamily at a glance. *J Cell Sci* **2005,** *118* (Pt 5), 843.

(4) Parmar, N.; Tamanoi, F. Rheb G-Proteins and the Activation of mTORC1. *Enzymes* **2010,** *27*, 39.

(5) Bos, J. L.; Rehmann, H.; Wittinghofer, A. GEFs and GAPs: critical elements in the control of small G proteins. *Cell* **2007,** *129* (5), 865.

(6) ten Klooster, J. P.; Hordijk, P. L. Targeting and localized signalling by small GTPases. *Biol Cell* **2007,** *99* (1), 1.

(7) Bos, J. L. All in the family? New insights and questions regarding interconnectivity of Ras, Rap1 and Ral. *EMBO J* **1998,** *17* (23), 6776.

(8) Bos, J. L. ras oncogenes in human cancer: a review. *Cancer Res* **1989,** *49* (17), 4682.

(9) Gentry, L. R.; Martin, T. D.; Reiner, D. J.; Der, C. J. Ral small GTPase signaling and oncogenesis: More than just 15minutes of fame. *Biochim Biophys Acta* **2014,** *1843* (12), 2976.

(10) Neel, N. F.; Martin, T. D.; Stratford, J. K.; Zand, T. P.; Reiner, D. J.; Der, C. J. The RalGEF-Ral Effector Signaling Network: The Road Less Traveled for Anti-Ras Drug Discovery. *Genes Cancer* **2011,** *2* (3), 275.

(11) Bodemann, B. O.; Orvedahl, A.; Cheng, T.; Ram, R. R.; Ou, Y. H.; Formstecher, E.; Maiti, M.; Hazelett, C. C.; Wauson, E. M.; Balakireva, M.et al. RalB and the exocyst mediate the cellular starvation response by direct activation of autophagosome assembly. *Cell* **2011,** *144* (2), 253.

(12) Matsuzaki, T.; Hanai, S.; Kishi, H.; Liu, Z.; Bao, Y.; Kikuchi, A.; Tsuchida, K.; Sugino, H. Regulation of endocytosis of activin type II receptors by a novel PDZ protein through Ral/Ral-binding protein 1-dependent pathway. *J Biol Chem* **2002,** *277* (21), 19008.

(13) Feig, L. A. Ral-GTPases: approaching their 15 minutes of fame. *Trends Cell Biol* **2003,** *13* (8), 419.

(14) Camonis, J. H.; White, M. A. Ral GTPases: corrupting the exocyst in cancer cells. *Trends Cell Biol* **2005,** *15* (6), 327.

(15) Bodemann, B. O.; White, M. A. Ral GTPases and cancer: linchpin support of the tumorigenic platform. *Nat Rev Cancer* **2008,** *8* (2), 133.

(16) Chardin, P.; Tavitian, A. The ral gene: a new ras related gene isolated by the use of a synthetic probe. *EMBO J* **1986,** *5* (9), 2203.

(17) Chardin, P.; Tavitian, A. Coding sequences of human ralA and ralB cDNAs. *Nucleic Acids Res* **1989,** *17* (11), 4380.

(18) Nicely, N. I.; Kosak, J.; de Serrano, V.; Mattos, C. Crystal structures of Ral-GppNHp and Ral-GDP reveal two binding sites that are also present in Ras and Rap. *Structure* **2004,** *12* (11), 2025.

(19) Nishimura, A.; Linder, M. E. Identification of a novel prenyl and palmitoyl modification at the CaaX motif of Cdc42 that regulates RhoGDI binding. *Mol Cell Biol* **2013,** *33* (7), 1417.

(20) Gentry, L. R.; Nishimura, A.; Cox, A. D.; Martin, T. D.; Tsygankov, D.; Nishida, M.; Elston, T. C.; Der, C. J. Divergent roles of CAAX motif-signaled posttranslational modifications in the regulation and subcellular localization of Ral GTPases. *J Biol Chem* **2015,**

290 (37), 22851.
(21) Albright, C. F.; Giddings, B. W.; Liu, J.; Vito, M.; Weinberg, R. A. Characterization of a guanine nucleotide dissociation stimulator for a ras-related GTPase. *EMBO J* **1993,** *12* (1), 339.
(22) Hofer, F.; Fields, S.; Schneider, C.; Martin, G. S. Activated Ras interacts with the Ral guanine nucleotide dissociation stimulator. *Proc Natl Acad Sci U S A* **1994,** *91* (23), 11089.
(23) Spaargaren, M.; Bischoff, J. R. Identification of the guanine nucleotide dissociation stimulator for Ral as a putative effector molecule of R-ras, H-ras, K-ras, and Rap. *Proc Natl Acad Sci U S A* **1994,** *91* (26), 12609.
(24) Lopez-Barahona, M.; Bustelo, X. R.; Barbacid, M. The TC21 oncoprotein interacts with the Ral guanosine nucleotide dissociation factor. *Oncogene* **1996,** *12* (3), 463.
(25) Shirakawa, R.; Fukai, S.; Kawato, M.; Higashi, T.; Kondo, H.; Ikeda, T.; Nakayama, E.; Okawa, K.; Nureki, O.; Kimura, T.et al. Tuberous sclerosis tumor suppressor complex-like complexes act as GTPase-activating proteins for Ral GTPases. *J Biol Chem* **2009,** *284* (32), 21580.
(26) Chen, X. W.; Leto, D.; Xiong, T.; Yu, G.; Cheng, A.; Decker, S.; Saltiel, A. R. A Ral GAP complex links PI 3-kinase/Akt signaling to RalA activation in insulin action. *Mol Biol Cell* **2011,** *22* (1), 141.
(27) Wang, K. L.; Roufogalis, B. D. Ca2+/calmodulin stimulates GTP binding to the ras-related protein ral-A. *J Biol Chem* **1999,** *274* (21), 14525.
(28) Wolthuis, R. M.; Zwartkruis, F.; Moen, T. C.; Bos, J. L. Ras-dependent activation of the small GTPase Ral. *Curr Biol* **1998,** *8* (8), 471.
(29) van den Berg, M. C.; van Gogh, I. J.; Smits, A. M.; van Triest, M.; Dansen, T. B.; Visscher, M.; Polderman, P. E.; Vliem, M. J.; Rehmann, H.; Burgering, B. M. The small GTPase RALA controls c-Jun N-terminal kinase-mediated FOXO activation by regulation of a JIP1 scaffold complex. *J Biol Chem* **2016,** *291* (3), 1200.
(30) Lim, K. H.; O'Hayer, K.; Adam, S. J.; Kendall, S. D.; Campbell, P. M.; Der, C. J.; Counter, C. M. Divergent roles for RalA and RalB in malignant growth of human pancreatic carcinoma cells. *Curr Biol* **2006,** *16* (24), 2385.
(31) Martin, T. D.; Samuel, J. C.; Routh, E. D.; Der, C. J.; Yeh, J. J. Activation and involvement of Ral GTPases in colorectal cancer. *Cancer Res* **2011,** *71* (1), 206.
(32) Cantor, S. B.; Urano, T.; Feig, L. A. Identification and characterization of Ral-binding protein 1, a potential downstream target of Ral GTPases. *Mol Cell Biol* **1995,** *15* (8), 4578.
(33) Ikeda, M.; Ishida, O.; Hinoi, T.; Kishida, S.; Kikuchi, A. Identification and characterization of a novel protein interacting with Ral-binding protein 1, a putative effector protein of Ral. *J Biol Chem* **1998,** *273* (2), 814.
(34) Moskalenko, S.; Henry, D. O.; Rosse, C.; Mirey, G.; Camonis, J. H.; White, M. A. The exocyst is a Ral effector complex. *Nat Cell Biol* **2002,** *4* (1), 66.
(35) Moskalenko, S.; Tong, C.; Rosse, C.; Mirey, G.; Formstecher, E.; Daviet, L.; Camonis, J.; White, M. A. Ral GTPases regulate exocyst assembly through dual subunit interactions. *J Biol Chem* **2003,** *278* (51), 51743.
(36) Yan, C.; Theodorescu, D. RAL GTPases: Biology and Potential as Therapeutic Targets in Cancer. *Pharmacol Rev* **2018,** *70* (1), 1.
(37) Kim, J. H.; Lee, S. D.; Han, J. M.; Lee, T. G.; Kim, Y.; Park, J. B.; Lambeth, J. D.; Suh, P. G.; Ryu, S. H. Activation of phospholipase D1 by direct interaction with ADP-ribosylation factor 1 and RalA. *FEBS Lett* **1998,** *430* (3), 231.
(38) Frankel, P.; Aronheim, A.; Kavanagh, E.; Balda, M. S.; Matter, K.; Bunney, T. D.; Marshall, C. J. RalA interacts with ZONAB in a cell density-dependent manner and regulates its transcriptional activity. *EMBO J* **2005,** *24* (1), 54.

(39) Guin, S.; Ru, Y.; Wynes, M. W.; Mishra, R.; Lu, X.; Owens, C.; Barn, A. E.; Vasu, V. T.; Hirsch, F. R.; Kern, J. A.et al. Contributions of KRAS and RAL in non-small-cell lung cancer growth and progression. *J Thorac Oncol* **2013,** *8* (12), 1492.
(40) Tecleab, A.; Zhang, X.; Sebti, S. M. Ral GTPase down-regulation stabilizes and reactivates p53 to inhibit malignant transformation. *J Biol Chem* **2014,** *289* (45), 31296.
(41) Shirakawa, R.; Horiuchi, H. Ral GTPases: crucial mediators of exocytosis and tumourigenesis. *J Biochem* **2015,** *157* (5), 285.
(42) Park, S. H.; Weinberg, R. A. A putative effector of Ral has homology to Rho/Rac GTPase activating proteins. *Oncogene* **1995,** *11* (11), 2349.
(43) Fenwick, R. B.; Campbell, L. J.; Rajasekar, K.; Prasannan, S.; Nietlispach, D.; Camonis, J.; Owen, D.; Mott, H. R. The RalB-RLIP76 complex reveals a novel mode of ral-effector interaction. *Structure* **2010,** *18* (8), 985.
(44) Jullien-Flores, V.; Mahe, Y.; Mirey, G.; Leprince, C.; Meunier-Bisceuil, B.; Sorkin, A.; Camonis, J. H. RLIP76, an effector of the GTPase Ral, interacts with the AP2 complex: involvement of the Ral pathway in receptor endocytosis. *J Cell Sci* **2000,** *113 (Pt 16)*, 2837.
(45) Liu, J.; Guo, W. The exocyst complex in exocytosis and cell migration. *Protoplasma* **2012,** *249* (3), 587.
(46) Chien, Y.; Kim, S.; Bumeister, R.; Loo, Y. M.; Kwon, S. W.; Johnson, C. L.; Balakireva, M. G.; Romeo, Y.; Kopelovich, L.; Gale, M., Jr.et al. RalB GTPase-mediated activation of the IkappaB family kinase TBK1 couples innate immune signaling to tumor cell survival. *Cell* **2006,** *127* (1), 157.
(47) Oxford, G.; Owens, C. R.; Titus, B. J.; Foreman, T. L.; Herlevsen, M. C.; Smith, S. C.; Theodorescu, D. RalA and RalB: antagonistic relatives in cancer cell migration. *Cancer Res* **2005,** *65* (16), 7111.
(48) Neel, N. F.; Rossman, K. L.; Martin, T. D.; Hayes, T. K.; Yeh, J. J.; Der, C. J. The RalB small GTPase mediates formation of invadopodia through a GTPase-activating protein-independent function of the RalBP1/RLIP76 effector. *Mol Cell Biol* **2012,** *32* (8), 1374.
(49) Lam, B. D.; Hordijk, P. L. The Rac1 hypervariable region in targeting and signaling: a tail of many stories. *Small GTPases* **2013,** *4* (2), 78.
(50) Aicart-Ramos, C.; Valero, R. A.; Rodriguez-Crespo, I. Protein palmitoylation and subcellular trafficking. *Biochim Biophys Acta* **2011,** *1808* (12), 2981.
(51) Michaelson, D.; Ali, W.; Chiu, V. K.; Bergo, M.; Silletti, J.; Wright, L.; Young, S. G.; Philips, M. Postprenylation CAAX processing is required for proper localization of Ras but not Rho GTPases. *Mol Biol Cell* **2005,** *16* (4), 1606.
(52) Shipitsin, M.; Feig, L. A. RalA but not RalB enhances polarized delivery of membrane proteins to the basolateral surface of epithelial cells. *Mol Cell Biol* **2004,** *24* (13), 5746.
(53) Lim, K. H.; Baines, A. T.; Fiordalisi, J. J.; Shipitsin, M.; Feig, L. A.; Cox, A. D.; Der, C. J.; Counter, C. M. Activation of RalA is critical for Ras-induced tumorigenesis of human cells. *Cancer Cell* **2005,** *7* (6), 533.
(54) Atala, A. Phosphorylation of RalB is Important for Bladder Cancer Cell Growth and Metastasis Editorial Comment. *J Urology* **2011,** *185* (6), 2423.
(55) Walsh, C. T.; Garneau-Tsodikova, S.; Gatto, G. J., Jr. Protein posttranslational modifications: the chemistry of proteome diversifications. *Angew Chem Int Ed Engl* **2005,** *44* (45), 7342.
(56) Heal, W. P.; Tate, E. W. Getting a chemical handle on protein post-translational modification. *Org Biomol Chem* **2010,** *8* (4), 731.
(57) Yeste-Velasco, M.; Linder, M. E.; Lu, Y. J. Protein S-palmitoylation and cancer. *Biochim Biophys Acta* **2015,** *1856* (1), 107.
(58) Resh, M. D. Covalent lipid modifications of proteins. *Curr Biol* **2013,** *23* (10), R431.

(59) Jiang, H.; Zhang, X.; Chen, X.; Aramsangtienchai, P.; Tong, Z.; Lin, H. Protein Lipidation: Occurrence, Mechanisms, Biological Functions, and Enabling Technologies. *Chem Rev* **2018,** *118* (3), 919.
(60) Nadolski, M. J.; Linder, M. E. Protein lipidation. *FEBS J* **2007,** *274* (20), 5202.
(61) Tate, E. W.; Kalesh, K. A.; Lanyon-Hogg, T.; Storck, E. M.; Thinon, E. Global profiling of protein lipidation using chemical proteomic technologies. *Curr Opin Chem Biol* **2015,** *24*, 48.
(62) Utsumi, T.; Sakurai, N.; Nakano, K.; Ishisaka, R. C-terminal 15 kDa fragment of cytoskeletal actin is posttranslationally N-myristoylated upon caspase-mediated cleavage and targeted to mitochondria. *FEBS Lett* **2003,** *539* (1-3), 37.
(63) D'Souza-Schorey, C.; Stahl, P. D. Myristoylation is required for the intracellular localization and endocytic function of ARF6. *Exp Cell Res* **1995,** *221* (1), 153.
(64) Lin, C. Y.; Li, C. C.; Huang, P. H.; Lee, F. J. A developmentally regulated ARF-like 5 protein (ARL5), localized to nuclei and nucleoli, interacts with heterochromatin protein 1. *J Cell Sci* **2002,** *115* (Pt 23), 4433.
(65) Chen, C. A.; Manning, D. R. Regulation of G proteins by covalent modification. *Oncogene* **2001,** *20* (13), 1643.
(66) Zhao, Y.; Jensen, O. N. Modification-specific proteomics: strategies for characterization of post-translational modifications using enrichment techniques. *Proteomics* **2009,** *9* (20), 4632.
(67) Taniguchi, H.; Manenti, S. Interaction of myristoylated alanine-rich protein kinase C substrate (MARCKS) with membrane phospholipids. *J Biol Chem* **1993,** *268* (14), 9960.
(68) Arbuzova, A.; Schmitz, A. A.; Vergeres, G. Cross-talk unfolded: MARCKS proteins. *Biochem J* **2002,** *362* (Pt 1), 1.
(69) Resh, M. D. Myristylation and palmitylation of Src family members: the fats of the matter. *Cell* **1994,** *76* (3), 411.
(70) Lowe, D. G.; Goeddel, D. V. Heterologous expression and characterization of the human R-ras gene product. *Mol Cell Biol* **1987,** *7* (8), 2845.
(71) Hancock, J. F.; Magee, A. I.; Childs, J. E.; Marshall, C. J. All ras proteins are polyisoprenylated but only some are palmitoylated. *Cell* **1989,** *57* (7), 1167.
(72) Yurchak, L. K.; Sefton, B. M. Palmitoylation of either Cys-3 or Cys-5 is required for the biological activity of the Lck tyrosine protein kinase. *Mol Cell Biol* **1995,** *15* (12), 6914.
(73) Sato, I.; Obata, Y.; Kasahara, K.; Nakayama, Y.; Fukumoto, Y.; Yamasaki, T.; Yokoyama, K. K.; Saito, T.; Yamaguchi, N. Differential trafficking of Src, Lyn, Yes and Fyn is specified by the state of palmitoylation in the SH4 domain. *J Cell Sci* **2009,** *122* (Pt 7), 965.
(74) He, Y.; Linder, M. E. Differential palmitoylation of the endosomal SNAREs syntaxin 7 and syntaxin 8. *J Lipid Res* **2009,** *50* (3), 398.
(75) Yount, J. S.; Moltedo, B.; Yang, Y. Y.; Charron, G.; Moran, T. M.; Lopez, C. B.; Hang, H. C. Palmitoylome profiling reveals S-palmitoylation-dependent antiviral activity of IFITM3. *Nat Chem Biol* **2010,** *6* (8), 610.
(76) Yount, J. S.; Karssemeijer, R. A.; Hang, H. C. S-palmitoylation and ubiquitination differentially regulate interferon-induced transmembrane protein 3 (IFITM3)-mediated resistance to influenza virus. *J Biol Chem* **2012,** *287* (23), 19631.
(77) Guardiola-Serrano, F.; Rossin, A.; Cahuzac, N.; Luckerath, K.; Melzer, I.; Mailfert, S.; Marguet, D.; Zornig, M.; Hueber, A. O. Palmitoylation of human FasL modulates its cell death-inducing function. *Cell Death Dis* **2010,** *1*, e88.
(78) Claudinon, J.; Gonnord, P.; Beslard, E.; Marchetti, M.; Mitchell, K.; Boularan, C.; Johannes, L.; Eid, P.; Lamaze, C. Palmitoylation of interferon-alpha (IFN-alpha) receptor subunit IFNAR1 is required for the activation of Stat1 and Stat2 by IFN-alpha. *J Biol Chem*

2009, *284* (36), 24328.
(79) Tulloch, L. B.; Howie, J.; Wypijewski, K. J.; Wilson, C. R.; Bernard, W. G.; Shattock, M. J.; Fuller, W. The inhibitory effect of phospholemman on the sodium pump requires its palmitoylation. *J Biol Chem* **2011,** *286* (41), 36020.
(80) Stevenson, F. T.; Bursten, S. L.; Locksley, R. M.; Lovett, D. H. Myristyl acylation of the tumor necrosis factor alpha precursor on specific lysine residues. *J Exp Med* **1992,** *176* (4), 1053.
(81) Stevenson, F. T.; Bursten, S. L.; Fanton, C.; Locksley, R. M.; Lovett, D. H. The 31-kDa precursor of interleukin 1 alpha is myristoylated on specific lysines within the 16-kDa N-terminal propiece. *Proc Natl Acad Sci U S A* **1993,** *90* (15), 7245.
(82) Schey, K. L.; Gutierrez, D. B.; Wang, Z.; Wei, J.; Grey, A. C. Novel fatty acid acylation of lens integral membrane protein aquaporin-0. *Biochemistry* **2010,** *49* (45), 9858.
(83) Zhang, X.; Spiegelman, N. A.; Nelson, O. D.; Jing, H.; Lin, H. SIRT6 regulates Ras-related protein R-Ras2 by lysine defatty-acylation. *Elife* **2017,** *6*.
(84) Jing, H.; Zhang, X.; Wisner, S. A.; Chen, X.; Spiegelman, N. A.; Linder, M. E.; Lin, H. SIRT2 and lysine fatty acylation regulate the transforming activity of K-Ras4a. *Elife* **2017,** *6*.
(85) Zhou, Y.; Huang, C.; Yin, L.; Wan, M.; Wang, X.; Li, L.; Liu, Y.; Wang, Z.; Fu, P.; Zhang, N.et al. N(epsilon)-Fatty acylation of Rho GTPases by a MARTX toxin effector. *Science* **2017,** *358* (6362), 528.
(86) Johnson, D. R.; Bhatnagar, R. S.; Knoll, L. J.; Gordon, J. I. Genetic and biochemical studies of protein N-myristoylation. *Annu Rev Biochem* **1994,** *63*, 869.
(87) Thinon, E.; Morales-Sanfrutos, J.; Mann, D. J.; Tate, E. W. N-Myristoyltransferase Inhibition Induces ER-Stress, Cell Cycle Arrest, and Apoptosis in Cancer Cells. *ACS Chem Biol* **2016,** *11* (8), 2165.
(88) Thinon, E.; Serwa, R. A.; Broncel, M.; Brannigan, J. A.; Brassat, U.; Wright, M. H.; Heal, W. P.; Wilkinson, A. J.; Mann, D. J.; Tate, E. W. Global profiling of co- and post-translationally N-myristoylated proteomes in human cells. *Nat Commun* **2014,** *5*, 4919.
(89) Sulejmani, E.; Cai, H. Targeting protein myristoylation for the treatment of prostate cancer. *Oncoscience* **2018,** *5* (1-2), 3.
(90) Korycka, J.; Lach, A.; Heger, E.; Boguslawska, D. M.; Wolny, M.; Toporkiewicz, M.; Augoff, K.; Korzeniewski, J.; Sikorski, A. F. Human DHHC proteins: a spotlight on the hidden player of palmitoylation. *Eur J Cell Biol* **2012,** *91* (2), 107.
(91) Resh, M. D. Trafficking and signaling by fatty-acylated and prenylated proteins. *Nat Chem Biol* **2006,** *2* (11), 584.
(92) Varner, A. S.; Ducker, C. E.; Xia, Z.; Zhuang, Y.; De Vos, M. L.; Smith, C. D. Characterization of human palmitoyl-acyl transferase activity using peptides that mimic distinct palmitoylation motifs. *Biochem J* **2003,** *373* (Pt 1), 91.
(93) Kong, E.; Peng, S.; Chandra, G.; Sarkar, C.; Zhang, Z.; Bagh, M. B.; Mukherjee, A. B. Dynamic palmitoylation links cytosol-membrane shuttling of acyl-protein thioesterase-1 and acyl-protein thioesterase-2 with that of proto-oncogene H-ras product and growth-associated protein-43. *J Biol Chem* **2013,** *288* (13), 9112.
(94) Lin, D. T.; Conibear, E. ABHD17 proteins are novel protein depalmitoylases that regulate N-Ras palmitate turnover and subcellular localization. *Elife* **2015,** *4*, e11306.
(95) Yokoi, N.; Fukata, Y.; Sekiya, A.; Murakami, T.; Kobayashi, K.; Fukata, M. Identification of PSD-95 Depalmitoylating Enzymes. *J Neurosci* **2016,** *36* (24), 6431.
(96) Jiang, H.; Khan, S.; Wang, Y.; Charron, G.; He, B.; Sebastian, C.; Du, J.; Kim, R.; Ge, E.; Mostoslavsky, R.et al. SIRT6 regulates TNF-alpha secretion through hydrolysis of long-chain fatty acyl lysine. *Nature* **2013,** *496* (7443), 110.
(97) Jiang, H.; Zhang, X.; Lin, H. Lysine fatty acylation promotes lysosomal targeting of

TNF-alpha. *Sci Rep* **2016,** *6*, 24371.
(98) Haigis, M. C.; Sinclair, D. A. Mammalian Sirtuins: Biological Insights and Disease Relevance. *Annu Rev Pathol* **2010,** *5*, 253.
(99) Frye, R. A. Phylogenetic classification of prokaryotic and eukaryotic Sir2-like proteins. *Biochem Biophys Res Commun* **2000,** *273* (2), 793.
(100) Herskovits, A. Z.; Guarente, L. Sirtuin deacetylases in neurodegenerative diseases of aging. *Cell Res* **2013,** *23* (6), 746.
(101) Vaziri, H.; Dessain, S. K.; Ng Eaton, E.; Imai, S. I.; Frye, R. A.; Pandita, T. K.; Guarente, L.; Weinberg, R. A. hSIR2(SIRT1) functions as an NAD-dependent p53 deacetylase. *Cell* **2001,** *107* (2), 149.
(102) Feldman, J. L.; Baeza, J.; Denu, J. M. Activation of the protein deacetylase SIRT6 by long-chain fatty acids and widespread deacylation by mammalian sirtuins. *J Biol Chem* **2013,** *288* (43), 31350.
(103) North, B. J.; Marshall, B. L.; Borra, M. T.; Denu, J. M.; Verdin, E. The human Sir2 ortholog, SIRT2, is an NAD+-dependent tubulin deacetylase. *Mol Cell* **2003,** *11* (2), 437.
(104) Teng, Y. B.; Jing, H.; Aramsangtienchai, P.; He, B.; Khan, S.; Hu, J.; Lin, H.; Hao, Q. Efficient demyristoylase activity of SIRT2 revealed by kinetic and structural studies. *Sci Rep* **2015,** *5*, 8529.
(105) Jin, J.; He, B.; Zhang, X.; Lin, H.; Wang, Y. SIRT2 Reverses 4-Oxononanoyl Lysine Modification on Histones. *J Am Chem Soc* **2016,** *138* (38), 12304.
(106) Cui, Y.; Li, X.; Lin, J.; Hao, Q.; Li, X. D. Histone Ketoamide Adduction by 4-Oxo-2-nonenal Is a Reversible Posttranslational Modification Regulated by Sirt2. *ACS Chem Biol* **2017,** *12* (1), 47.
(107) Schwer, B.; North, B. J.; Frye, R. A.; Ott, M.; Verdin, E. The human silent information regulator (Sir)2 homologue hSIRT3 is a mitochondrial nicotinamide adenine dinucleotide-dependent deacetylase. *J Cell Biol* **2002,** *158* (4), 647.
(108) Anderson, K. A.; Huynh, F. K.; Fisher-Wellman, K.; Stuart, J. D.; Peterson, B. S.; Douros, J. D.; Wagner, G. R.; Thompson, J. W.; Madsen, A. S.; Green, M. F.et al. SIRT4 Is a Lysine Deacylase that Controls Leucine Metabolism and Insulin Secretion. *Cell Metab* **2017,** *25* (4), 838.
(109) Mathias, R. A.; Greco, T. M.; Oberstein, A.; Budayeva, H. G.; Chakrabarti, R.; Rowland, E. A.; Kang, Y.; Shenk, T.; Cristea, I. M. Sirtuin 4 is a lipoamidase regulating pyruvate dehydrogenase complex activity. *Cell* **2014,** *159* (7), 1615.
(110) Schuetz, A.; Min, J.; Antoshenko, T.; Wang, C. L.; Allali-Hassani, A.; Dong, A.; Loppnau, P.; Vedadi, M.; Bochkarev, A.; Sternglanz, R.et al. Structural basis of inhibition of the human NAD+-dependent deacetylase SIRT5 by suramin. *Structure* **2007,** *15* (3), 377.
(111) Tan, M.; Peng, C.; Anderson, K. A.; Chhoy, P.; Xie, Z.; Dai, L.; Park, J.; Chen, Y.; Huang, H.; Zhang, Y.et al. Lysine glutarylation is a protein posttranslational modification regulated by SIRT5. *Cell Metab* **2014,** *19* (4), 605.
(112) Jintang Du, Y. Z., Xiaoyang Su, Jiu Jiu Yu, Saba Khan, Hong Jiang, Jungwoo Kim, Jimin Woo, Jun Huyn Kim, Brian Hyun Choi, Bin He, Wei Chen, Sheng Zhang, Richard A. Cerione, Johan Auwerx, Quan Hao, Hening Lin. Sirt5 Is a NAD-Dependent Protein Lysine Demalonylase and Desuccinylase. *Science* **2011,** *334* (6057), 806.
(113) Michishita, E.; McCord, R. A.; Berber, E.; Kioi, M.; Padilla-Nash, H.; Damian, M.; Cheung, P.; Kusumoto, R.; Kawahara, T. L.; Barrett, J. C.et al. SIRT6 is a histone H3 lysine 9 deacetylase that modulates telomeric chromatin. *Nature* **2008,** *452* (7186), 492.
(114) Tong, Z.; Wang, Y.; Zhang, X.; Kim, D. D.; Sadhukhan, S.; Hao, Q.; Lin, H. SIRT7 Is Activated by DNA and Deacetylates Histone H3 in the Chromatin Context. *ACS Chem Biol* **2016,** *11* (3), 742.

(115) Tong, Z.; Wang, M.; Wang, Y.; Kim, D. D.; Grenier, J. K.; Cao, J.; Sadhukhan, S.; Hao, Q.; Lin, H. SIRT7 Is an RNA-Activated Protein Lysine Deacylase. *ACS Chem Biol* **2017,** *12* (1), 300.
(116) Sauve, A. A.; Wolberger, C.; Schramm, V. L.; Boeke, J. D. The biochemistry of sirtuins. *Annu Rev Biochem* **2006,** *75*, 435.
(117) Sauve, A. A. Sirtuin chemical mechanisms. *Biochim Biophys Acta* **2010,** *1804* (8), 1591.
(118) Jing, H.; Hu, J.; He, B.; Negron Abril, Y. L.; Stupinski, J.; Weiser, K.; Carbonaro, M.; Chiang, Y. L.; Southard, T.; Giannakakou, P.et al. A SIRT2-Selective Inhibitor Promotes c-Myc Oncoprotein Degradation and Exhibits Broad Anticancer Activity. *Cancer Cell* **2016,** *29* (5), 767.
(119) Zhao, D.; Zou, S. W.; Liu, Y.; Zhou, X.; Mo, Y.; Wang, P.; Xu, Y. H.; Dong, B.; Xiong, Y.; Lei, Q. Y.et al. Lysine-5 acetylation negatively regulates lactate dehydrogenase A and is decreased in pancreatic cancer. *Cancer Cell* **2013,** *23* (4), 464.
(120) Serrano, L.; Martinez-Redondo, P.; Marazuela-Duque, A.; Vazquez, B. N.; Dooley, S. J.; Voigt, P.; Beck, D. B.; Kane-Goldsmith, N.; Tong, Q.; Rabanal, R. M.et al. The tumor suppressor SirT2 regulates cell cycle progression and genome stability by modulating the mitotic deposition of H4K20 methylation. *Genes Dev* **2013,** *27* (6), 639.
(121) Liu, P. Y.; Xu, N.; Malyukova, A.; Scarlett, C. J.; Sun, Y. T.; Zhang, X. D.; Ling, D.; Su, S. P.; Nelson, C.; Chang, D. K.et al. The histone deacetylase SIRT2 stabilizes Myc oncoproteins. *Cell Death Differ* **2013,** *20* (3), 503.
(122) Zhao, Y.; Yang, J.; Liao, W.; Liu, X.; Zhang, H.; Wang, S.; Wang, D.; Feng, J.; Yu, L.; Zhu, W. G. Cytosolic FoxO1 is essential for the induction of autophagy and tumour suppressor activity. *Nat Cell Biol* **2010,** *12* (7), 665.
(123) Inoue, T.; Nakayama, Y.; Li, Y.; Matsumori, H.; Takahashi, H.; Kojima, H.; Wanibuchi, H.; Katoh, M.; Oshimura, M. SIRT2 knockdown increases basal autophagy and prevents postslippage death by abnormally prolonging the mitotic arrest that is induced by microtubule inhibitors. *FEBS J* **2014,** *281* (11), 2623.
(124) North, B. J.; Rosenberg, M. A.; Jeganathan, K. B.; Hafner, A. V.; Michan, S.; Dai, J.; Baker, D. J.; Cen, Y.; Wu, L. E.; Sauve, A. A.et al. SIRT2 induces the checkpoint kinase BubR1 to increase lifespan. *EMBO J* **2014,** *33* (13), 1438.
(125) Chopra, V.; Quinti, L.; Kim, J.; Vollor, L.; Narayanan, K. L.; Edgerly, C.; Cipicchio, P. M.; Lauver, M. A.; Choi, S. H.; Silverman, R. B.et al. The sirtuin 2 inhibitor AK-7 is neuroprotective in Huntington's disease mouse models. *Cell Rep* **2012,** *2* (6), 1492.
(126) Wang, Y. P.; Zhou, L. S.; Zhao, Y. Z.; Wang, S. W.; Chen, L. L.; Liu, L. X.; Ling, Z. Q.; Hu, F. J.; Sun, Y. P.; Zhang, J. Y.et al. Regulation of G6PD acetylation by SIRT2 and KAT9 modulates NADPH homeostasis and cell survival during oxidative stress. *EMBO J* **2014,** *33* (12), 1304.
(127) Wang, F.; Nguyen, M.; Qin, F. X.; Tong, Q. SIRT2 deacetylates FOXO3a in response to oxidative stress and caloric restriction. *Aging Cell* **2007,** *6* (4), 505.
(128) Suematsu, T.; Li, Y.; Kojima, H.; Nakajima, K.; Oshimura, M.; Inoue, T. Deacetylation of the mitotic checkpoint protein BubR1 at lysine 250 by SIRT2 and subsequent effects on BubR1 degradation during the prometaphase/anaphase transition. *Biochem Biophys Res Commun* **2014,** *453* (3), 588.
(129) Qiu, D.; Hou, X.; Han, L.; Li, X.; Ge, J.; Wang, Q. Sirt2-BubR1 acetylation pathway mediates the effects of advanced maternal age on oocyte quality. *Aging Cell* **2018,** *17* (1).
(130) Li, W.; Zhang, B.; Tang, J.; Cao, Q.; Wu, Y.; Wu, C.; Guo, J.; Ling, E. A.; Liang, F. Sirtuin 2, a mammalian homolog of yeast silent information regulator-2 longevity regulator, is an oligodendroglial protein that decelerates cell differentiation through deacetylating alpha-

tubulin. *J Neurosci* **2007,** *27* (10), 2606.
(131) Li, Y.; Matsumori, H.; Nakayama, Y.; Osaki, M.; Kojima, H.; Kurimasa, A.; Ito, H.; Mori, S.; Katoh, M.; Oshimura, M.et al. SIRT2 down-regulation in HeLa can induce p53 accumulation via p38 MAPK activation-dependent p300 decrease, eventually leading to apoptosis. *Genes Cells* **2011,** *16* (1), 34.
(132) Jiang, W.; Wang, S.; Xiao, M.; Lin, Y.; Zhou, L.; Lei, Q.; Xiong, Y.; Guan, K. L.; Zhao, S. Acetylation regulates gluconeogenesis by promoting PEPCK1 degradation via recruiting the UBR5 ubiquitin ligase. *Mol Cell* **2011,** *43* (1), 33.
(133) Dryden, S. C.; Nahhas, F. A.; Nowak, J. E.; Goustin, A. S.; Tainsky, M. A. Role for human SIRT2 NAD-dependent deacetylase activity in control of mitotic exit in the cell cycle. *Mol Cell Biol* **2003,** *23* (9), 3173.
(134) Sarikhani, M.; Mishra, S.; Desingu, P. A.; Kotyada, C.; Wolfgeher, D.; Gupta, M. P.; Singh, M.; Sundaresan, N. R. SIRT2 regulates oxidative stress-induced cell death through deacetylation of c-Jun NH2-terminal kinase. *Cell Death Differ* **2018**, DOI:10.1038/s41418-018-0069-8 10.1038/s41418-018-0069-8.
(135) Sarikhani, M.; Maity, S.; Mishra, S.; Jain, A.; Tamta, A. K.; Ravi, V.; Kondapalli, M. S.; Desingu, P. A.; Khan, D.; Kumar, S.et al. SIRT2 deacetylase represses NFAT transcription factor to maintain cardiac homeostasis. *J Biol Chem* **2018,** *293* (14), 5281.
(136) Watanabe, H.; Inaba, Y.; Kimura, K.; Matsumoto, M.; Kaneko, S.; Kasuga, M.; Inoue, H. Sirt2 facilitates hepatic glucose uptake by deacetylating glucokinase regulatory protein. *Nat Commun* **2018,** *9* (1), 30.
(137) Eskandarian, H. A.; Impens, F.; Nahori, M. A.; Soubigou, G.; Coppee, J. Y.; Cossart, P.; Hamon, M. A. A role for SIRT2-dependent histone H3K18 deacetylation in bacterial infection. *Science* **2013,** *341* (6145), 1238858.
(138) Zhang, Y.; Chi, D. Overexpression of SIRT2 Alleviates Neuropathic Pain and Neuroinflammation Through Deacetylation of Transcription Factor Nuclear Factor-Kappa B. *Inflammation* **2018,** *41* (2), 569.
(139) Rothgiesser, K. M.; Erener, S.; Waibel, S.; Luscher, B.; Hottiger, M. O. SIRT2 regulates NF-kappaB dependent gene expression through deacetylation of p65 Lys310. *J Cell Sci* **2010,** *123* (Pt 24), 4251.
(140) Pan, Y.; Zhang, H.; Zheng, Y.; Zhou, J.; Yuan, J.; Yu, Y.; Wang, J. Resveratrol Exerts Antioxidant Effects by Activating SIRT2 To Deacetylate Prx1. *Biochemistry* **2017,** *56* (48), 6325.
(141) Kuhlmann, N.; Wroblowski, S.; Knyphausen, P.; de Boor, S.; Brenig, J.; Zienert, A. Y.; Meyer-Teschendorf, K.; Praefcke, G. J.; Nolte, H.; Kruger, M.et al. Structural and Mechanistic Insights into the Regulation of the Fundamental Rho Regulator RhoGDIalpha by Lysine Acetylation. *J Biol Chem* **2016,** *291* (11), 5484.
(142) Vaquero, A.; Scher, M. B.; Lee, D. H.; Sutton, A.; Cheng, H. L.; Alt, F. W.; Serrano, L.; Sternglanz, R.; Reinberg, D. SirT2 is a histone deacetylase with preference for histone H4 Lys 16 during mitosis. *Genes Dev* **2006,** *20* (10), 1256.
(143) Zhang, H.; Park, S. H.; Pantazides, B. G.; Karpiuk, O.; Warren, M. D.; Hardy, C. W.; Duong, D. M.; Park, S. J.; Kim, H. S.; Vassilopoulos, A.et al. SIRT2 directs the replication stress response through CDK9 deacetylation. *Proc Natl Acad Sci U S A* **2013,** *110* (33), 13546.
(144) Seo, K. S.; Park, J. H.; Heo, J. Y.; Jing, K.; Han, J.; Min, K. N.; Kim, C.; Koh, G. Y.; Lim, K.; Kang, G. Y.et al. SIRT2 regulates tumour hypoxia response by promoting HIF-1alpha hydroxylation. *Oncogene* **2015,** *34* (11), 1354.
(145) Song, H. Y.; Biancucci, M.; Kang, H. J.; O'Callaghan, C.; Park, S. H.; Principe, D. R.; Jiang, H.; Yan, Y.; Satchell, K. F.; Raparia, K.et al. SIRT2 deletion enhances KRAS-induced tumorigenesis in vivo by regulating K147 acetylation status. *Oncotarget* **2016,** *7* (49), 80336.

(146) Lin, R.; Tao, R.; Gao, X.; Li, T.; Zhou, X.; Guan, K. L.; Xiong, Y.; Lei, Q. Y. Acetylation stabilizes ATP-citrate lyase to promote lipid biosynthesis and tumor growth. *Mol Cell* **2013,** *51* (4), 506.
(147) Park, S. H.; Ozden, O.; Liu, G.; Song, H. Y.; Zhu, Y.; Yan, Y.; Zou, X.; Kang, H. J.; Jiang, H.; Principe, D. R.et al. SIRT2-Mediated Deacetylation and Tetramerization of Pyruvate Kinase Directs Glycolysis and Tumor Growth. *Cancer Res* **2016,** *76* (13), 3802.
(148) Jing, E.; Gesta, S.; Kahn, C. R. SIRT2 regulates adipocyte differentiation through FoxO1 acetylation/deacetylation. *Cell Metab* **2007,** *6* (2), 105.
(149) Zhou, W.; Ni, T. K.; Wronski, A.; Glass, B.; Skibinski, A.; Beck, A.; Kuperwasser, C. The SIRT2 Deacetylase Stabilizes Slug to Control Malignancy of Basal-like Breast Cancer. *Cell Rep* **2016,** *17* (5), 1302.
(150) Cha, Y.; Han, M. J.; Cha, H. J.; Zoldan, J.; Burkart, A.; Jung, J. H.; Jang, Y.; Kim, C. H.; Jeong, H. C.; Kim, B. G.et al. Metabolic control of primed human pluripotent stem cell fate and function by the miR-200c-SIRT2 axis. *Nat Cell Biol* **2017,** *19* (5), 445.
(151) Tang, X.; Chen, X. F.; Wang, N. Y.; Wang, X. M.; Liang, S. T.; Zheng, W.; Lu, Y. B.; Zhao, X.; Hao, D. L.; Zhang, Z. Q.et al. SIRT2 Acts as a Cardioprotective Deacetylase in Pathological Cardiac Hypertrophy. *Circulation* **2017,** *136* (21), 2051.
(152) Fiskus, W.; Coothankandaswamy, V.; Chen, J.; Ma, H.; Ha, K.; Saenz, D. T.; Krieger, S. S.; Mill, C. P.; Sun, B.; Huang, P.et al. SIRT2 Deacetylates and Inhibits the Peroxidase Activity of Peroxiredoxin-1 to Sensitize Breast Cancer Cells to Oxidant Stress-Inducing Agents. *Cancer Res* **2016,** *76* (18), 5467.
(153) Tsusaka, T.; Guo, T.; Yagura, T.; Inoue, T.; Yokode, M.; Inagaki, N.; Kondoh, H. Deacetylation of phosphoglycerate mutase in its distinct central region by SIRT2 down-regulates its enzymatic activity. *Genes Cells* **2014,** *19* (10), 766.
(154) Hong, S.; Zhao, B.; Lombard, D. B.; Fingar, D. C.; Inoki, K. Cross-talk between sirtuin and mammalian target of rapamycin complex 1 (mTORC1) signaling in the regulation of S6 kinase 1 (S6K1) phosphorylation. *J Biol Chem* **2014,** *289* (19), 13132.
(155) Villalba, J. M.; Alcain, F. J. Sirtuin activators and inhibitors. *Biofactors* **2012,** *38* (5), 349.
(156) Hu, J.; Jing, H.; Lin, H. Sirtuin inhibitors as anticancer agents. *Future Med Chem* **2014,** *6* (8), 945.
(157) Yoon, Y. K.; Oon, C. E. Sirtuin Inhibitors: An Overview from Medicinal Chemistry Perspective. *Anticancer Agents Med Chem* **2016,** *16* (8), 1003.
(158) Rotili, D.; Tarantino, D.; Nebbioso, A.; Paolini, C.; Huidobro, C.; Lara, E.; Mellini, P.; Lenoci, A.; Pezzi, R.; Botta, G.et al. Discovery of salermide-related sirtuin inhibitors: binding mode studies and antiproliferative effects in cancer cells including cancer stem cells. *J Med Chem* **2012,** *55* (24), 10937.
(159) Tiago Fleming Outeiro, E. K., Stephen M. Altmann, Irina Kufareva, Katherine E. Strathearn, Allison M. Amore, Catherine B. Volk, Michele M. Maxwell, Jean-Christophe Rochet, Pamela J. McLean, Anne B. Young, Ruben Abagyan,; Mel B. Feany, B. T. H., Aleksey G. Kazantsev. Sirtuin 2 Inhibitors Rescue a-Synuclein–Mediated Toxicity in
Models of Parkinson's Disease. *Science* **2007,** *317* (5837), 516.
(160) Lain, S.; Hollick, J. J.; Campbell, J.; Staples, O. D.; Higgins, M.; Aoubala, M.; McCarthy, A.; Appleyard, V.; Murray, K. E.; Baker, L.et al. Discovery, in vivo activity, and mechanism of action of a small-molecule p53 activator. *Cancer Cell* **2008,** *13* (5), 454.
(161) Rumpf, T.; Schiedel, M.; Karaman, B.; Roessler, C.; North, B. J.; Lehotzky, A.; Olah, J.; Ladwein, K. I.; Schmidtkunz, K.; Gajer, M.et al. Selective Sirt2 inhibition by ligand-induced rearrangement of the active site. *Nat Commun* **2015,** *6*, 6263.
(162) Kim, H. W.; Kim, S. A.; Ahn, S. G. Sirtuin inhibitors, EX527 and AGK2, suppress cell

migration by inhibiting HSF1 protein stability. *Oncol Rep* **2016,** *35* (1), 235.
(163) Dai, H.; Sinclair, D. A.; Ellis, J. L.; Steegborn, C. Sirtuin activators and inhibitors: Promises, achievements, and challenges. *Pharmacol Ther* **2018**, DOI:10.1016/j.pharmthera.2018.03.004 10.1016/j.pharmthera.2018.03.004.
(164) Lobo, S.; Greentree, W. K.; Linder, M. E.; Deschenes, R. J. Identification of a Ras palmitoyltransferase in Saccharomyces cerevisiae. *J Biol Chem* **2002,** *277* (43), 41268.
(165) Roth, A. F.; Feng, Y.; Chen, L.; Davis, N. G. The yeast DHHC cysteine-rich domain protein Akr1p is a palmitoyl transferase. *J Cell Biol* **2002,** *159* (1), 23.
(166) Keller, C. A.; Yuan, X.; Panzanelli, P.; Martin, M. L.; Alldred, M.; Sassoe-Pognetto, M.; Luscher, B. The gamma2 subunit of GABA(A) receptors is a substrate for palmitoylation by GODZ. *J Neurosci* **2004,** *24* (26), 5881.
(167) Fukata, M.; Fukata, Y.; Adesnik, H.; Nicoll, R. A.; Bredt, D. S. Identification of PSD-95 palmitoylating enzymes. *Neuron* **2004,** *44* (6), 987.
(168) Linder, M. E.; Deschenes, R. J. New insights into the mechanisms of protein palmitoylation. *Biochemistry* **2003,** *42* (15), 4311.
(169) De, I.; Sadhukhan, S. Emerging Roles of DHHC-mediated Protein S-palmitoylation in Physiological and Pathophysiological Context. *Eur J Cell Biol* **2018**, DOI:10.1016/j.ejcb.2018.03.005 10.1016/j.ejcb.2018.03.005.
(170) Aramsangtienchai, P.; Spiegelman, N. A.; Cao, J.; Lin, H. S-Palmitoylation of Junctional Adhesion Molecule C Regulates Its Tight Junction Localization and Cell Migration. *J Biol Chem* **2017,** *292* (13), 5325.
(171) Du, K.; Murakami, S.; Sun, Y.; Kilpatrick, C. L.; Luscher, B. DHHC7 Palmitoylates Glucose Transporter 4 (Glut4) and Regulates Glut4 Membrane Translocation. *J Biol Chem* **2017,** *292* (7), 2979.
(172) Chen, B.; Zheng, B.; DeRan, M.; Jarugumilli, G. K.; Fu, J.; Brooks, Y. S.; Wu, X. ZDHHC7-mediated S-palmitoylation of Scribble regulates cell polarity. *Nat Chem Biol* **2016,** *12* (9), 686.
(173) Rossin, A.; Durivault, J.; Chakhtoura-Feghali, T.; Lounnas, N.; Gagnoux-Palacios, L.; Hueber, A. O. Fas palmitoylation by the palmitoyl acyltransferase DHHC7 regulates Fas stability. *Cell Death Differ* **2015,** *22* (4), 643.
(174) McClure, M. L.; Barnes, S.; Brodsky, J. L.; Sorscher, E. J. Trafficking and function of the cystic fibrosis transmembrane conductance regulator: a complex network of posttranslational modifications. *Am J Physiol Lung Cell Mol Physiol* **2016,** *311* (4), L719.
(175) Fernandez-Hernando, C.; Fukata, M.; Bernatchez, P. N.; Fukata, Y.; Lin, M. I.; Bredt, D. S.; Sessa, W. C. Identification of Golgi-localized acyl transferases that palmitoylate and regulate endothelial nitric oxide synthase. *J Cell Biol* **2006,** *174* (3), 369.
(176) Segal-Salto, M.; Sapir, T.; Reiner, O. Reversible Cysteine Acylation Regulates the Activity of Human Palmitoyl-Protein Thioesterase 1 (PPT1). *PLoS One* **2016,** *11* (1), e0146466.
(177) Greaves, J.; Prescott, G. R.; Fukata, Y.; Fukata, M.; Salaun, C.; Chamberlain, L. H. The hydrophobic cysteine-rich domain of SNAP25 couples with downstream residues to mediate membrane interactions and recognition by DHHC palmitoyl transferases. *Mol Biol Cell* **2009,** *20* (6), 1845.
(178) Tian, L.; McClafferty, H.; Jeffries, O.; Shipston, M. J. Multiple palmitoyltransferases are required for palmitoylation-dependent regulation of large conductance calcium- and voltage-activated potassium channels. *J Biol Chem* **2010,** *285* (31), 23954.
(179) Lu, D.; Sun, H. Q.; Wang, H.; Barylko, B.; Fukata, Y.; Fukata, M.; Albanesi, J. P.; Yin, H. L. Phosphatidylinositol 4-kinase IIalpha is palmitoylated by Golgi-localized palmitoyltransferases in cholesterol-dependent manner. *J Biol Chem* **2012,** *287* (26), 21856.
(180) Oku, S.; Takahashi, N.; Fukata, Y.; Fukata, M. In silico screening for palmitoyl

substrates reveals a role for DHHC1/3/10 (zDHHC1/3/11)-mediated neurochondrin palmitoylation in its targeting to Rab5-positive endosomes. *J Biol Chem* **2013,** *288* (27), 19816.
(181) Greaves, J.; Salaun, C.; Fukata, Y.; Fukata, M.; Chamberlain, L. H. Palmitoylation and membrane interactions of the neuroprotective chaperone cysteine-string protein. *J Biol Chem* **2008,** *283* (36), 25014.
(182) Wang, J.; Xie, Y.; Wolff, D. W.; Abel, P. W.; Tu, Y. DHHC protein-dependent palmitoylation protects regulator of G-protein signaling 4 from proteasome degradation. *FEBS Lett* **2010,** *584* (22), 4570.
(183) Tsutsumi, R.; Fukata, Y.; Noritake, J.; Iwanaga, T.; Perez, F.; Fukata, M. Identification of G protein alpha subunit-palmitoylating enzyme. *Mol Cell Biol* **2009,** *29* (2), 435.
(184) Ren, W.; Sun, Y.; Du, K. Glut4 palmitoylation at Cys223 plays a critical role in Glut4 membrane trafficking. *Biochem Biophys Res Commun* **2015,** *460* (3), 709.
(185) Pedram, A.; Razandi, M.; Deschenes, R. J.; Levin, E. R. DHHC-7 and -21 are palmitoylacyltransferases for sex steroid receptors. *Mol Biol Cell* **2012,** *23* (1), 188.
(186) Ji, Y.; Leymarie, N.; Haeussler, D. J.; Bachschmid, M. M.; Costello, C. E.; Lin, C. Direct detection of S-palmitoylation by mass spectrometry. *Anal Chem* **2013,** *85* (24), 11952.
(187) Yount, J. S.; Zhang, M. M.; Hang, H. C. Emerging roles for protein S-palmitoylation in immunity from chemical proteomics. *Curr Opin Chem Biol* **2013,** *17* (1), 27.
(188) Yang, Y.; Fonovic, M.; Verhelst, S. H. Cleavable Linkers in Chemical Proteomics Applications. *Methods Mol Biol* **2017,** *1491*, 185.
(189) Broncel, M.; Serwa, R. A.; Ciepla, P.; Krause, E.; Dallman, M. J.; Magee, A. I.; Tate, E. W. Myristoylation profiling in human cells and zebrafish. *Data Brief* **2015,** *4*, 379.
(190) Yang, Y. Y.; Grammel, M.; Raghavan, A. S.; Charron, G.; Hang, H. C. Comparative analysis of cleavable azobenzene-based affinity tags for bioorthogonal chemical proteomics. *Chem Biol* **2010,** *17* (11), 1212.
(191) Szychowski, J.; Mahdavi, A.; Hodas, J. J.; Bagert, J. D.; Ngo, J. T.; Landgraf, P.; Dieterich, D. C.; Schuman, E. M.; Tirrell, D. A. Cleavable biotin probes for labeling of biomolecules via azide-alkyne cycloaddition. *J Am Chem Soc* **2010,** *132* (51), 18351.
(192) Yang, Y.; Verhelst, S. H. Cleavable trifunctional biotin reagents for protein labelling, capture and release. *Chem Commun (Camb)* **2013,** *49* (47), 5366.
(193) Verhelst, S. H.; Fonovic, M.; Bogyo, M. A mild chemically cleavable linker system for functional proteomic applications. *Angew Chem Int Ed Engl* **2007,** *46* (8), 1284.
(194) van der Veken, P.; Dirksen, E. H.; Ruijter, E.; Elgersma, R. C.; Heck, A. J.; Rijkers, D. T.; Slijper, M.; Liskamp, R. M. Development of a novel chemical probe for the selective enrichment of phosphorylated serine- and threonine-containing peptides. *Chembiochem* **2005,** *6* (12), 2271.
(195) Park, K. D.; Liu, R.; Kohn, H. Useful tools for biomolecule isolation, detection, and identification: acylhydrazone-based cleavable linkers. *Chem Biol* **2009,** *16* (7), 763.
(196) Orth, R.; Sieber, S. A. A photolabile linker for the mild and selective cleavage of enriched biomolecules from solid support. *J Org Chem* **2009,** *74* (21), 8476.
(197) Speers, A. E.; Cravatt, B. F. A tandem orthogonal proteolysis strategy for high-content chemical proteomics. *J Am Chem Soc* **2005,** *127* (28), 10018.
(198) Weerapana, E.; Speers, A. E.; Cravatt, B. F. Tandem orthogonal proteolysis-activity-based protein profiling (TOP-ABPP)--a general method for mapping sites of probe modification in proteomes. *Nat Protoc* **2007,** *2* (6), 1414.

CHAPTER 2

SIRT2 REGULATED LYSINE FATTY ACYLATION MODULATES THE ACTIVITY OF RALB[1]

Abstract

Protein lysine fatty acylation is increasingly recognized as a prevalent and important protein post-translation modification. Recently, it has been shown that K-Ras4a and R-Ras2 are regulated by lysine fatty acylation. Here we investigated whether other members of the Ras superfamily could also be regulated by lysine fatty acylation. Several other small GTPases exhibit hydroxylamine resistant fatty acylation, suggesting they may also have protein lysine fatty acylation. We further characterized one of these GTPases, RalB. We show that RalB has C-terminal lysine fatty acylation, with its predominate modification site being Lys200. The lysine acylation of RalB is regulated by SIRT2, a member of the sirtuin family of NAD-dependent protein lysine deacylases. Lysine fatty acylated RalB bound more to GTP, than the mutant deficient of protein lysine fatty acylation. Furthermore, lysine fatty acylated RalB exhibited enhanced co-localization with its known effector Sec5. The activation of RalB leads to SIRT2 dependent promotion of A549 cell migration.

1. Introduction:

Protein posttranslational modifications (PTMs) affect a wide range of biological functions, including transcription, cell signaling, metabolism, cell survival, and life span.[1]

---

[1]For this chapter, I (Nicole A. Spiegelman) designed and performed all the biochemical studies except those noted below. Xiaoyu Zhang helped with cloning, the RalB mass spectrometry and the ^{32}P NAD assay. Hui Jing validated the RalB labeling results and the ^{32}P NAD assay. Ji Cao repeated the cell migration assay. Xiao Chen validated the labeling of the various Ras GTPases. Miao Wang and Pornpun Aramsangtienchai assisted in cell line generation. Ilana B. Kotlier and Kelly Rosch helped generated the RalB mutants. Hening Lin directed and supervised the study. We would like thank Dr. Maurine Linder for providing several of the GTPase plasmids.

Protein lipidation is a well-established mechanism that regulates cellular homeostasis and cancer.[2,3] Lipidation has been shown to regulate membrane anchoring, protein stability and protein-protein interactions.[4] Much of our understanding of this class of modifications comes from the study of N-terminal myristoylation, cysteine palmitoylation (S-palmitoylation), cysteine prenylation, and modifications by GPI anchors.[2-4] A similar, but not well studied modification is protein lysine fatty acylation, the modification of lysine residues with long-chain fatty acyl groups such as myristoyl or palmitoyl. Until about a year ago, only three proteins were identified to undergo lysine fatty acylation: TNF-α, IL-1α and lens integral membrane protein aquaporin-0.[5-7] Recent work has started to point to the prevalence and importance of lysine fatty acylation.[8-14]

Sirtuins, the NAD dependent Class III of Histone Deacetylase (HDAC) proteins have attracted the interest of many researchers due to their connection to metabolism, cancer, and aging.[15] Sirtuins were initially identified as protein lysine deacetylases. However, recently it was identified that several histone deacetylases (HDACs), including Sirtuin (SIRT)1, SIRT2, SIRT3, SIRT6 and SIRT7, as well as HDAC8 and HDAC11 possess lysine defatty acylation activity.[8,12,14,16-18] These findings suggested that lysine fatty acylation is more prevalent than initially thought. Consistent with this hypothesis, it was recently identified that several Ras family GTPases had protein lysine fatty acylation, and two of these proteins K-Ras4a and R-Ras2, are SIRT2 and SIRT6 defatty acylation substrates, respectively.[9-11]

The Ras family of small GTPases are molecular switches; they are active when bound to guanosine triphosphate (GTP) and inactive when bound to guanosine-diphosphate (GDP).[19] Small GTPases have been implicated in playing important roles in regulating cancer, cellular senescence and apoptosis, cell growth, as well as autophagy.[20] It is well established that protein lipidation, such as cysteine prenylation and palmitoylation serve as regulatory mechanisms for several small GTPases.[9,10,21] Looking closely at small GTPases that were recently identified to

have lysine fatty acylation, we saw that they shared common structural components in their C-terminal hypervariable region (HVR).[9-11] They all have multiple lysine residues, palmitoylated and prenylated cysteine residues. We noticed that many other small GTPases also have these features. We hypothesized that protein lysine fatty acylation may be a regulatory mechanism for other small GTPases and investigated this possibility here.

2. Results:

2.1 Several members of the Ras superfamily exhibit hydroxylamine resistant fatty acylation

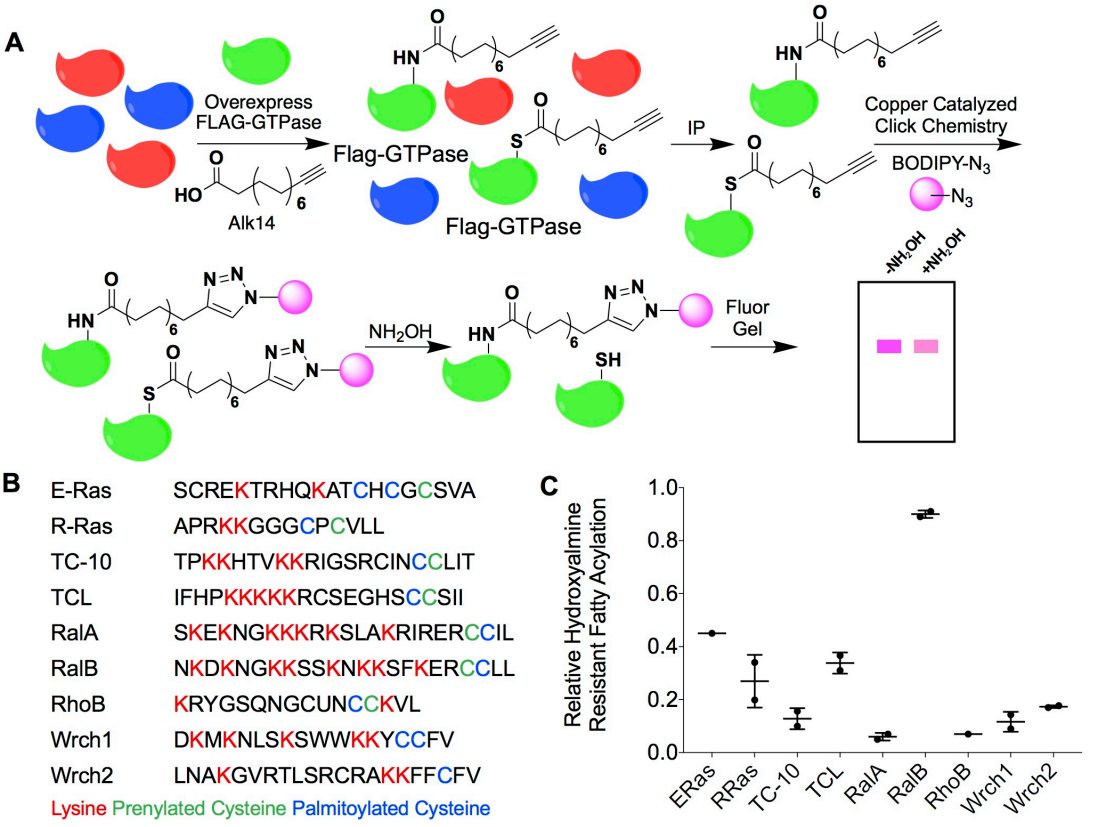

Figure 2.1. Several members of the Ras family small GTPases contain hydroxylamine-resistant fatty acylation. (A) The method used to detect lysine fatty acylation on proteins using the palmitic/myristic acid analogue, Alk14. N-terminal Flag-tagged small GTPases were overexpressed in HEK-239T cells. The cells were treated with 50μM Alk14 for 6 hours. After FLAG immunoprecipitation and on-bead click chemistry, fatty acylation levels were visualized using in-gel fluorescence with and without hydroxylamine treatment. (**B**) A list of related Ras family small GTPases and their respective c-terminal hypervariable region. Palmitoylated cysteine residues are highlighted in blue, prenylated cysteine residues are highlighted in green, and lysine residues that are potential sites for lysine fatty acylation are highlighted in purple. (**C**) Quantification of the relative amount of hydroxylamine resistant fatty acylation each small GTPase exhibits.

To visualize the level of lysine fatty acylation on a specific protein, we used a biorthogonal palmitic acid analogue Alkyne-14 (Alk14). This probe is metabolically incorporated and subsequently functionalizes fatty acylated proteins and allows in-gel fluorescence visualization of protein fatty acylation after click chemistry conjugation of a fluorescent dye with azide (Figure 2.1A). This method labels both cysteine and lysine fatty acylation, but hydroxylamine can be used to remove s-palmitoylation, and allows for visualization of lysine fatty acylation, which is resistant to hydroxylamine (Figure 2.1A).

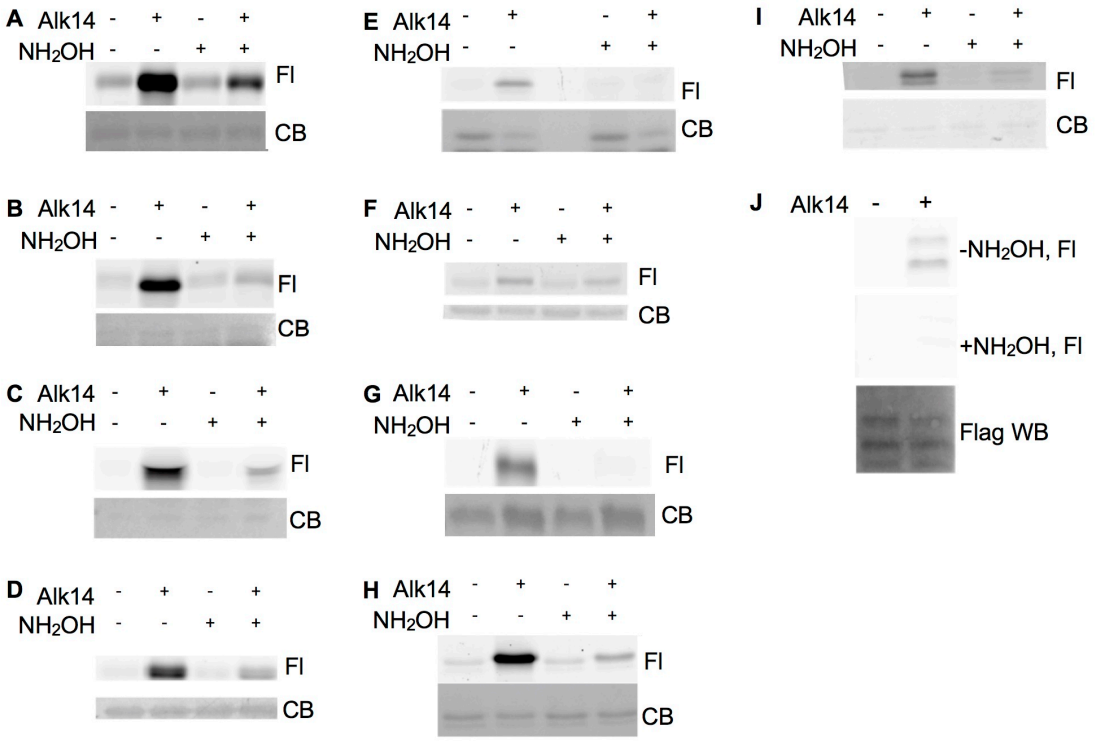

Figure 2.2. Several Ras family small GTPases has hydroxylamine-resistant fatty acylation as determined by Alk14 labeling. Labeling were done with and without 330μM hydroxylamine (NH_2OH) (pH=7.4) treatment (**A**) E-Ras; (**B**) R-Ras; (**C**) TC-10; (**D**) TCL; (**E**) RalA; (**F**) RalB; (**G**) RhoB; (**H**)Wrch1; (**I**) Wrch2. (**J**) Control TNF□ labeling to show hydroxylamine treatment is sufficient to remove all S- palmitoylation. Previously, TNFα was reported to have lysine fatty acylation. Mutation of the four lysine residues to generate the TNFα4KR mutant, which was deficient of lysine fatty acylation exhibited no hydroxylamine resistant signal. (Fl, fluorescence gel, CB Coomassie blue gel, WB western blot)

To test our hypothesis that other Ras superfamily GTPases also are regulated by lysine fatty acylation, we first generated a list of small GTPases that contain multiple lysine residues, a plamitoylated cysteine, and/or a prenylated cysteine (characteristics that were seen with KRas4a and R-Ras2) (Figure 2.1B).

We initially screened various small GTPases to determine how much of their fatty acylation was hydroxylamine resistant (Figure 2.1C, Figure 2.2A-J). Interestingly, almost all the GTPases we tested exhibited significant amount of hydroxylamine resistant fatty acylation. To ensure the hydroxylamine treatment was sufficient, we used a TNFα 4KR mutant as a positive control (Figure 2.2L). The TNFα 4KR mutant only has S-palmitoylation, and therefore should exhibit no hydroxylamine resistant signal, which was what we saw.[14] These results suggested lysine fatty acylation could be very general, similar to cysteine palmitoylation or prenylation.

2.2 RalB, but not RalA, has lysine fatty acylation

While many of the proteins exhibited hydroxylamine resistant fatty acylation, for further validation and functional studies, we decided to focus on the RAS like proto-oncogene A and B (RalA and RalB). RalA and RalB share 80% of their amino acid sequence, and most of their sequence divergence is found in their C-terminal hyper variable region (Figure 1A).[22] Despite their high sequence similarity, RalA and RalB often have different, or even opposing roles in cancer.[22-25] The screening results indicated that RalB shows high level of hydroxylamine resistant fatty acylation while RalA has very little. We therefore thought that lysine fatty acylation could be a factor to differentiate the function of these two small GTPases.

To determine if either of the Ral GTPases, RalA or RalB, had lysine fatty acylation we ectopically overexpressed N-terminally Flag-tagged RalA (Flag-RalA) and RalB (Flag-RalB) in HEK-293T cells, and labeled the proteins using the method described above. RalA had higher levels of palmitoylation, but almost of its fatty acylation signal could be removed by

hydroxylamine, while RalB had labeling that was ~90% retained after hydroxylamine treatment (Figure 2.3A, B).[9] This suggested that RalB, but not RalA, may have lysine fatty acylation.

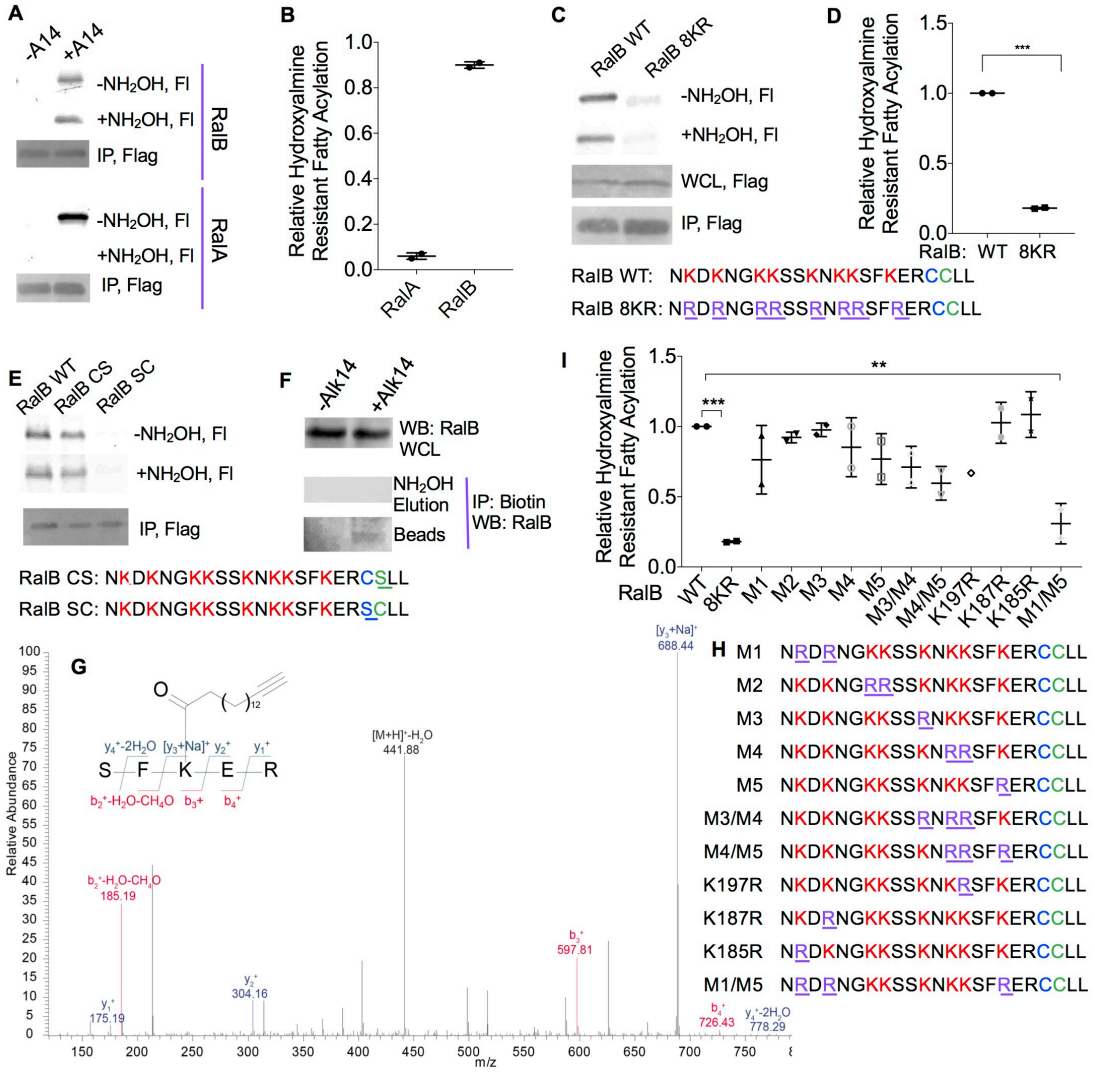

Figure 2.3. RalB contains Lysine Fatty Acylation. (**A**) Alk14 labeling of RalA and RalB with and without hydroxylamine treatment in HEK-239T Cells. (**B**) Quantification of the relative level of hydroxylamine resistant fatty acylation of RalA and RalB shown in A. (**C**) Alk14 labeling of RalB WT and the 8KR mutant in WT HEK-293T cells. (**D**) Quantification of fluorescence labeling of RalB WT and the 8KR mutant shown in (**C**). (**E**) Alk14 labeling before and after hydroxylamine treatment of RalB WT, the non-prenylated (RalB SC) and non-S-palmitoylated (RalB CS) RalB mutants in HEK-293T cells. (**F**) Endogenous fatty acylation of RalB in WT HEK-293T cells. (**G**) Tandem MS/MS spectra of a doubly charged Alk14 modified peptide on RalB. (**H**) C-terminal sequences of RalB lysine to arginine mutants generated. (**I**) Relative hydroxylamine-resistant fatty acylation levels of the various RalB lysine to arginine mutants in HEK-293T cells. For all quantification results, statistical significance was calculated using Prism 7 software using an unpaired student's t-test.

To further support that the hydroxylamine resistant signal on RalB comes from lysine-fatty acylation we mutated all eight lysine residues (K185, K187, K190, K191, K194, K196, K197, and K200) in the C-terminal hypervariable region of RalB to arginine to generate the RalB 8KR mutant. The RalB 8KR mutant showed approximately 20% of labeling compared to RalB WT, and exhibited essentially no hydroxylamine resistant signal (Figure 2.3C, 2.3D). This supports that the hydroxylamine resistant fluorescence signal we saw on RalB was from lysine fatty acylation. Additionally, to show that the hydroxylamine resistant signal was not a result of hydroxylamine resistant S-palmitoylation, we mutated the palmitoylated cysteine to serine to generate the RalB C205S mutant. This mutant still contained fatty acylation that was almost entirely hydroxylamine resistant. However, removal of the prenylated cysteine (the C204S mutant) prevented RalB from having any fatty acylation (Figure 2.3E). The lack of labeling on the non-prenylated construct was not surprising, as prenylation has been established to be important for the proper processing and S-palmitoylation of proteins.[26-28]

To show that endogenous RalB also has lysine fatty acylation, we treated cells with vehicle control or Alk14 and enriched Alk14-labeled proteins by attaching biotin-azide with click chemistry and subsequent streptavidin immunoprecipitation. S-palmitoylated proteins were removed from the streptavidin beads by hydroxylamine treatment, leaving proteins with lysine fatty acylation on the streptavidin beads, which were then detected by western blot. Indeed, we could detect RalB from the boiled streptavidin beads suggesting endogenous RalB, like overexpressed RalB, has lysine fatty acylation (Figure 2.3F). We previously showed that RalA does not have endogenous lysine fatty acylation using the same method.[9]

To further confirm RalB has lysine fatty acylation by HPLC-MS/MS. After immunoprecipitation of Alk14-labeled Flag-RalB and trypsin digestion, we detected by tandem MS/MS a doubly charged Alk14-modified peptide in which RalB Lys200 was modified by Alk-14 (Figure 2.3G). To confirm the mass spectrometry results, we generated several different RalB

lysine to arginine mutants (Figure 2.3H). We saw that the RalB M1 and M5 mutants both exhibited a slight decrease in fatty acylation levels. Further combinations suggested that the RalB M1M5 mutant exhibited a significant decrease in fatty acylation (Figure 2.3I, 2.4). The redundancy of the lysine fatty acylation is not surprising, as it is similar to what was observed for R-Ras2, KRas4a, and Rac1.[9-11] It is likely that if the predominate site of fatty acylation is mutated, other nearby lysine residues would have increased fatty acylation to compensate.

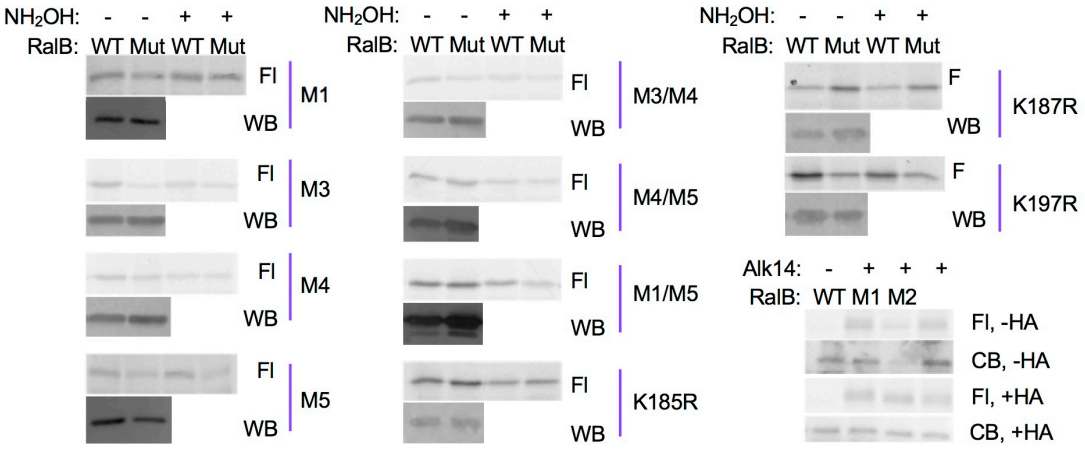

Figure 2.4. RalB has redundant C-terminal lysine fatty acylation. The gel images compare the Alk14 labeling of RalB WT and various mutants before and after 330μM hydroxylamine treatment (NH_2OH or HA) (pH=7.4). (Fl/F fluorescence gel, WB western blot, CB Coomassie blue protein gel)

2.3 SIRT2 Regulates RalB Lysine Fatty Acylation

We next wanted to identify a regulator for RalB lysine fatty acylation. Over the past few years, it has been established that several HDACs, particularly sirtuins, possess lysine defatty-acylation activity.[8,12,14,16] To see if RalB is a sirtuin target, we first treated purified Alk14 labeled RalB with PfSir2A, one of the two sirtuins from *Plasmodium falciparum* that was shown to exhibit lysine defatty acylation activity.[29] We saw that PfSir2A could remove the lysine fatty acylation of RalB in a NAD dependent manner (Figure 2.5A). This suggested RalB might be a sirtuin defatty-acylation target.

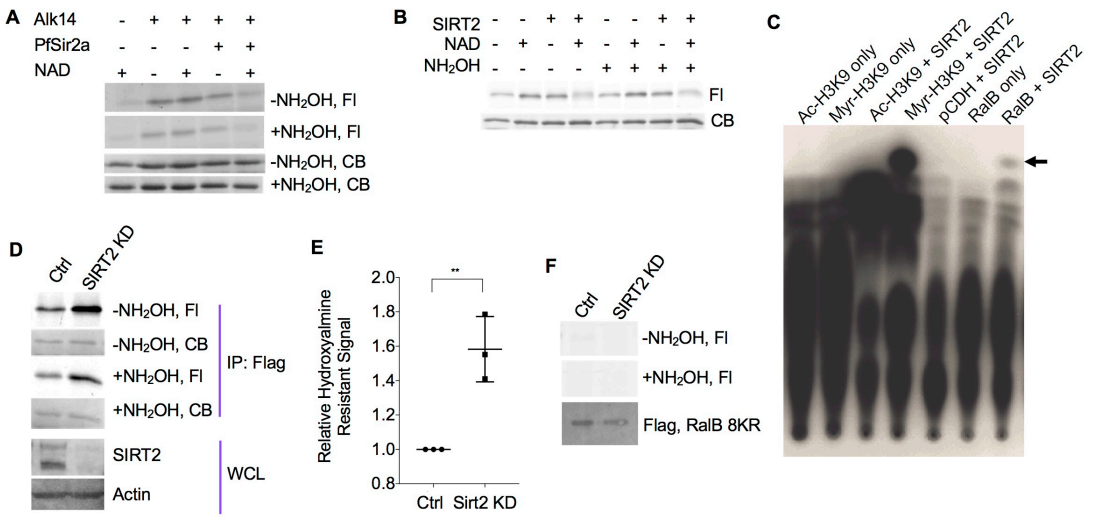

Figure 2.5. RalB is a SIRT2 defatty acylation substrate. (A) PfSIR2A decreased RalB hydroxylamine-resistant fatty acylation in vitro in an NAD-dependent manner. **(B)** SIRT2 decreased RalB hydroxylamine-resistant fatty acylation in vitro in an NAD-dependent manner. **(C)** ^{32}P-NAD assay with RalB and SIRT2. The formation of the ^{32}P-labeled fatty acyl-ADPR was detected, showing that RalB contained lysine fatty acylation. **(D)** Alk14 labeling of WT RalB in SIRT2 control and KD HEK-239T cells. **(E)** Quantification of the relative hydroxylamine-resistant fatty acylation levels in SIRT2 WT and KD HEK-293T cells. Fluorescence signal was normalized to the protein level based on blue staining. Statistical significance was calculated using Prism7 software using a student's t-test. **(F)** Alk14 labeling of the RalB 8KR mutant in SIRT2 control and KD HEK-239T cells.

To test if RalB is a mammalian HDAC target we next treated purified Alk14 labeled Flag-RalB from HEK-293T Cells, and examined the lysine fatty acylation levels of RalB after *in vitro* treatment with SIRT1, SIRT2, SIRT3, SIRT6, SIRT7, and HDAC8. (Figure 2.5B, Figure 2.6A-E). We saw that only SIRT2 was able to remove RalB lysine fatty acylation in an NAD-dependent manner. Using a previously established ^{32}P-NAD assay, we detected the 2'-O-fatty acyl ADPR product in the SIRT2-catalyzed deacylation reaction, further supporting that SIRT2 was removing fatty acyl groups from a lysine residue of RalB (Figure 2.5C).

We next wanted to see if RalB was a SIRT2 target in cells. To evaluate this, we looked at the fatty acylation levels of RalB in SIRT2 control and KD cells. In SIRT2 KD cells, RalB had significantly more hydroxylamine resistant fatty acylation (Figure 2.5D and 2.5E). In contrast, the RalB 8KR mutant did not have SIRT2-regulated lysine fatty acylation (Figure 2.5F).

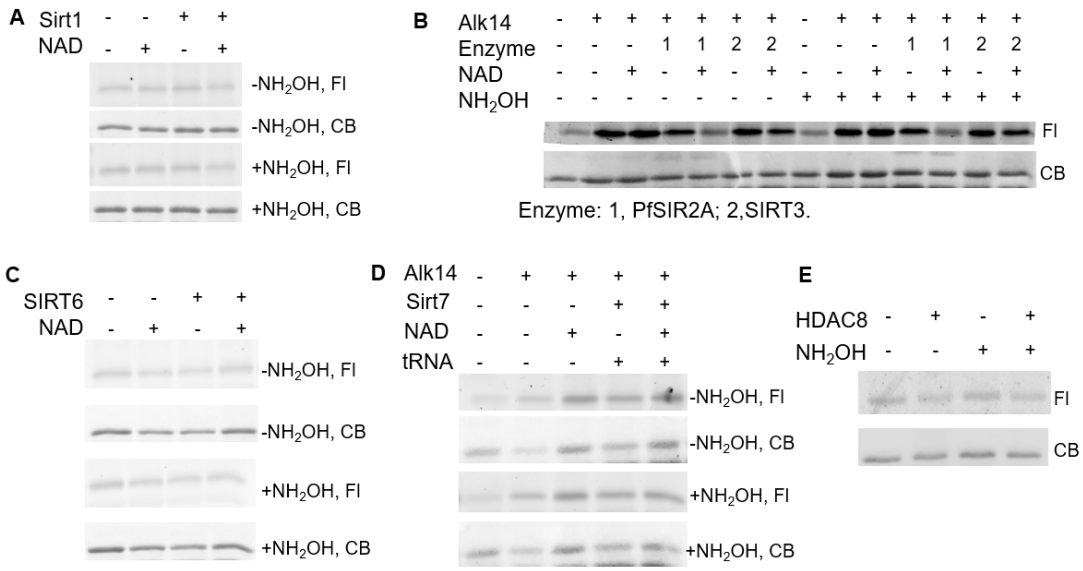

Figure 2.6. RalB is only a SIRT2 defatty-acylation substrate. *In vitro* treatment with SIRT1 (**A**), SIRT3 (**B**), SIRT6 (**C**), SIRT7 (**D**), HDAC8 (**E**) did not change RalB hydroxylamine resistant fatty acylation level.

2.4 RalB Lysine Fatty Acylation Promotes RalB GTP binding and Sec5 co-localization

Like other GTPases, RalB can be bound to either GTP or GDP. When bound to GTP, RalB can associate with its effector proteins such as Exo84, RalBP1, and Sec5.[25] We first evaluated if RalB fatty acylation affects its activation (GTP binding). We co-overexpressed GFP-tagged RalB WT or 8KR and mCherry-Sec5RBD (Ral binding domain). Activated GTP-bound RalB can bind to Sec5RBD, but inactive RalB cannot. Through live cell imaging, we observed that RalB-WT co-localized more with the Sec5RBD than the lysine fatty acylation deficient 8KR mutant (Figure 2.7A and 2.7B). We further confirmed this using a GTP binding assay with the Sec5RBD. RalB WT bound more GTP than the 8KR mutant, suggesting that fatty acylation affected the GTP binding of RalB (Figure 2.7C).

To make sure that the GTP binding and Sec5 interaction difference between WT and the 8KR mutant was due to lysine acylation, but not the intrinsic effect of the 8KR mutation, we also examined the co-localization of RalB with endogenous Sec5 under control or SIRT2 KD conditions Consistent with the idea that lysine fatty acylation of RalB promotes its GTP

binding and Sec5 interaction, SIRT2 KD promoted the co-localization of RalB and Sec5 (Figure 2.7D).

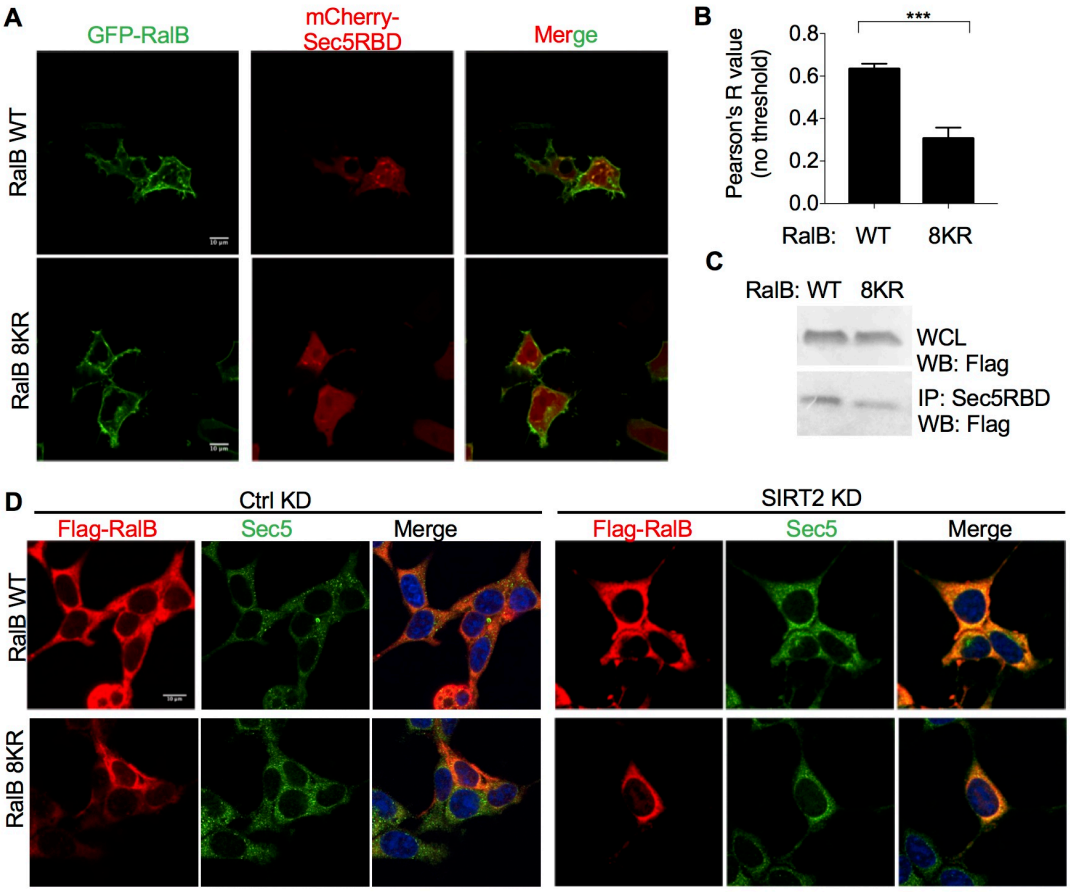

Figure 2.7. RalB lysine fatty acylation promotes RalB-GTP binding. (A) Live cell imaging of HEK-293T cells co-overexpressing GFP-RalB (WT and 8KR) with mCherry-Sec5RBD. **(B)** Colocalization quantification from Figure 4A. **(C)** GTP binding of RalB WT and RalB 8KR determined using the Sec5-RBD after 30min EBSS starvation. **(D)** Immunofluorescence to detect the RalB-Sec5 co-localization in stable SIRT2 KD HEK-293T cells.

2.5 SIRT2 Regulated RalB Lysine Fatty Acylation Promotes Cancer Cell Migration

RalB has been shown to play a role in cell proliferation, anchorage independent growth and cell migration.[30-32] We wanted to see if lysine fatty acylation was important for the role RalB plays in these physiological processes. We first investigated if lysine fatty acylation could promote cell proliferation. As it has previously been shown that RalB is important for A549 cell growth, to test if lysine fatty acylation was important for this, we transiently overexpressed

pCDH control vector, Flag-RalB WT, and Flag-RalB 8KR and subsequently transiently knocked down SIRT2 in A549 cells (Figure 2.8A). We monitored the cell proliferation for seven days, and saw that lysine fatty acylation did not promote A549 cell proliferation.

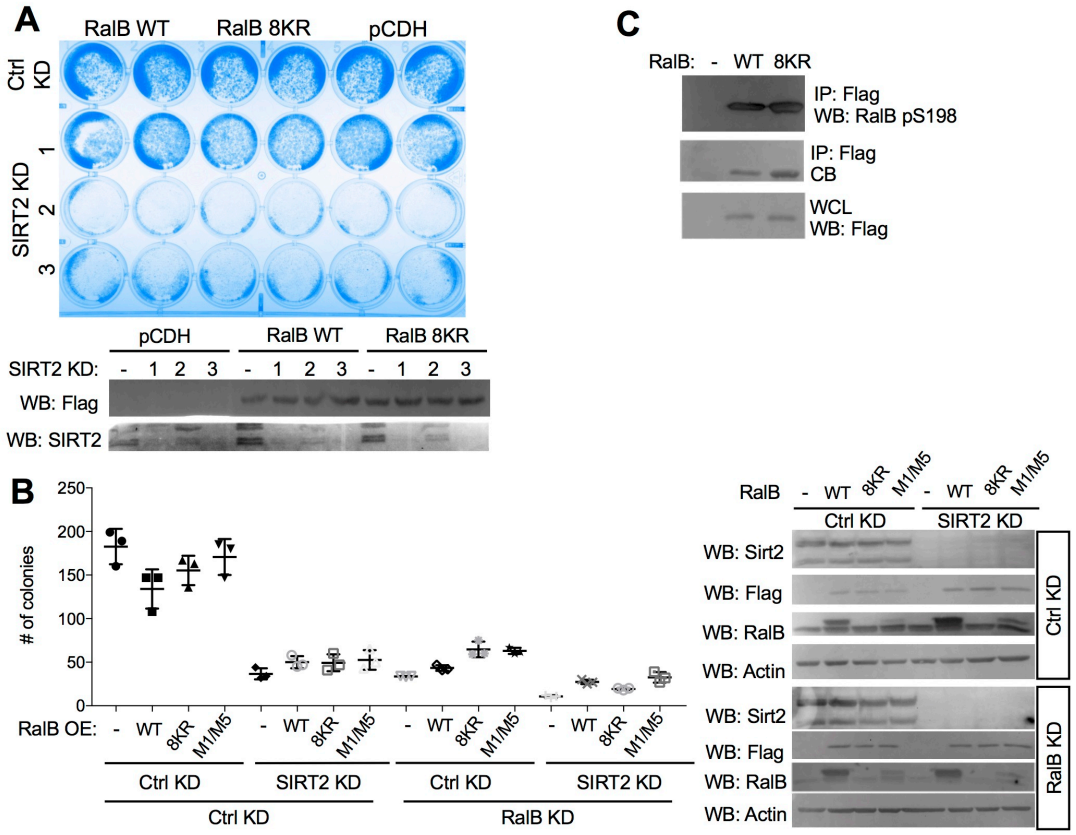

Figure 2.8. RalB lysine fatty acylation does not promote cell proliferation or anchorage independent growth. (A) Representative image of a crystal violet stained plate (Day 7) to monitory cell proliferation. RalB overexpression was confirmed by Flag western blot, and SIRT2 knock down was confirmed by a SIRT2 western blot. **(B)** lysine fatty acylation does not promote anchorage independent growth in HCT116 cells. RalB and SIRT2 knockdown was monitored using the respective antibodies, and overexpression was monitored by Flag western blot. The number of colonies were counted using ImageJ, and the quantified results are shown. **(C)** RalB S198 phosphorylation levels were detected using a specific antibody after flag immunoprecipitation.

While RalA more commonly is shown to be important for anchorage independent growth, as detected by a soft agar colony formation assay, RalB has been shown to modulate colony formation of HCT116 cells.[30,32] To evaluate if lysine fatty acylation was important for the role RalB plays in anchorage independent growth, we generated stable RalB KD HCT116 cells, and subsequently overexpressed RalB WT or 8KR with and without SIRT2 KD. Lysine

fatty acylation did not significantly affect anchorage independent growth (Figure 2.8B).

To evaluate if RalB lysine fatty acylation could promote cell migration, we generated stable pCDH (control), Flag-RalB WT, and Flag-RalB 8KR overexpressing A549 cells. SIRT2 was transiently knocked down, and we subsequently examined cell migration. Expression of RalB WT or 8KR had very little effect on cell migration, and knockdown of SIRT2 slightly increased cell migration. Interestingly, however, under SIRT2 knockdown, overexpression of RalB WT dramatically increased cell migration, but not the expression of RalB 8KR that cannot be lysine fatty acylated (Figure 2.9A and 2.9B). This result suggests that RalB lysine fatty acylation promotes cell migration in A549 cells in a SIRT2 dependent manner.

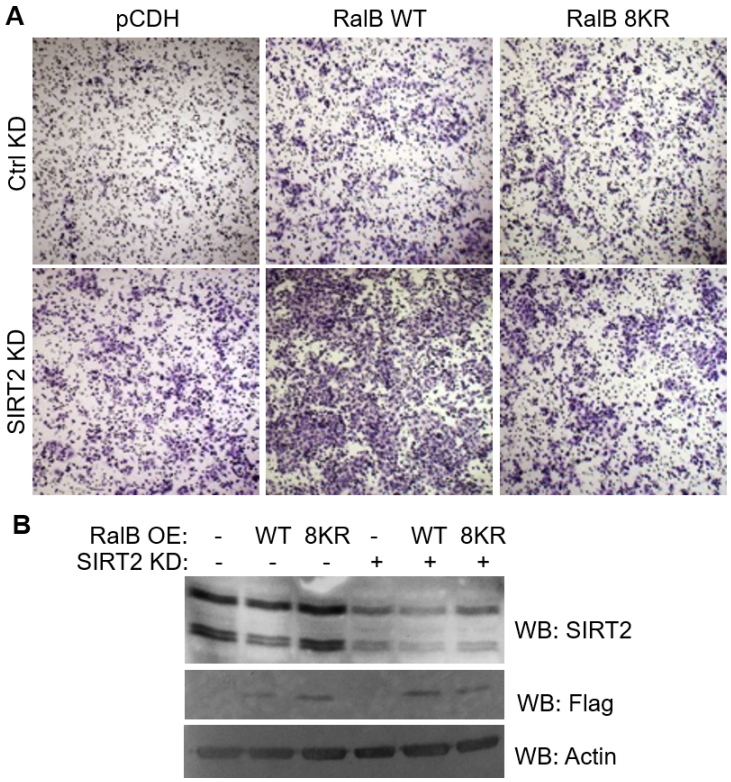

Figure 2.9. RalB lysine fatty acylation promotes A549 cell migration. (A) Images of the stained Boyden chambers after 24 hour cell migration. Images shown are from one of three representative experiments **(B)** Western blots to confirm SIRT2 KD, and Flag-RalB WT and Flag-RalB 8KR overexpression in A549 cells.

Previously, it has been shown that RalB phosphorylation on serine 198 is important for cell migration.[33] To confirm that the RalB 8KR mutation was not affecting RalB

phosphorylation, we compared the phosphorylation of RalB WT and RalB 8KR in HEK-293T cells (Figure 2.8C). The RalB 8KR mutant did not change RalB S198 phosphorylation level, suggesting that the effect of RalB lysine fatty acylation on cell migration was not a result of the 8KR mutant impairing RalB phosphorylation.

3. Discussion

Despite being identified in the early 1990s, protein lysine fatty acylation has remained an under-recognized protein post translation modification (PTM). This is largely due to the fact that only a few proteins have been identified to have this modification. Our studies here provide important support for the prevalence and importance of lysine fatty acylation. The screening of GTPases suggested that numerous members in the Ras superfamily are likely regulated by lysine fatty acylation. It is likely that the abundance and importance of lysine fatty acylation is similar to cysteine palmitoylation that has been well studied.

In this study, we further focused on the role lysine fatty acylation of RalB. RalB is predominately fatty acylated at Lys200. Interestingly only RalB, but not RalA, exhibited lysine fatty acylation despite their high sequence similarity. This observation highlights that there are specific requirements for lysine fatty acylation to occur. Understanding what determines this interesting specificity requires the identification of lysine fatty acyl transferases in the future.

RalB lysine fatty acylation is regulated by SIRT2, one of the sirtuin family of NAD-dependent lysine deacylases. SIRT2 has been reported to regulate many biological pathways via different substrate proteins, including metabolic enzymes, histones, signaling proteins, and transcription factors. However, to date, almost all the known substrates (except one) of SIRT2 are deacetylation substrates, not defatty-acylation substrates. Here, we have identified the second SIRT2 defatty-acylation substrate. These findings show that SIRT2 regulated lysine fatty acylation can affect KRAS4a-induced colony formation and RalB-mediated cancer cell migration. These findings highlight that there is still much to be learned about the roles that

SIRT2 plays in normal physiology and diseases. To further elucidate the role of SIRT2, we think it is important to further study its defatty-acylation activity.

Our study identified a novel regulatory mechanism for RalB, lysine fatty acylation. We found that lysine fatty acylation was important for the GTP binding of RalB. This is similar to what was recently seen for Rac1.[11] RalB has been known to regulate cell proliferation, anchorage-independent growth, cell migration, and cell adhesion. Interestingly, lysine fatty acylation does not significantly affect cell proliferation or anchorage-independent growth, but affects cell migration and cell adhesion. We were initially puzzled by this, but knowing that lysine fatty acylation of RalB promotes GTP-binding and Sec5 interaction, the effect on cell migration and adhesion can be explained. Sec5 is a component of the exocyst complex, the major role of which is to bring lipid vesicles to specific cellular locals where membrane needs to expand, such as the migrating cell front. Lysine fatty acylation and activated RalB is localized to the cell migration front and serves to recruit exocyst, thus promoting cell migration.

In conjunction with recent findings that several other small GTPases also exhibit hydroxylamine resistant fatty acylation, this suggests that lysine fatty acylation could be an additional mechanism which regulates many GTPases. As modulating Ras family of GTPases can affect various cancer phenotypes such as cell migration, proliferation or anchorage independent growth, elucidating the role of lysine fatty acylation as a regulatory mechanism may lead to new treatment strategies for human diseases.

4. Methods

Reagents and plasmids. Alk14 was synthesized as previously described.[34] Bodipy-N_3 (520) was purchased from Lumiprobe. Biotin-PEG-N_3 (762024), Tris[(1-benzyl-1H-1,2,3-triazol-4-yl)methyl]amine (TBTA) (678937), Tris(2-carboxyethyl)phosphine (TCEP) (75259), hydroxylamine (159417), Crystal Violet (C0775), low-melting point agarose (A0701), NAD

(NAD100-RO), anti-EXOC2 (*SAB2701511*), anti-Flag M2 antibody conjugated with horseradish peroxidase (A8592), and the anti-Flag M2 affinity gel (A2220) were purchased from Sigma-Aldrich. The pLKO.1-puro lentiviral shRNAs constructs for luciferase and human SIRT2 were also purchased from Sigma-Aldrich. Luciferase shRNA (SHC007), human SIRT2 shRNAs (TRCN0000040221) were used. Puromycin hydrochloride (P-600-100) was purchased from gold bio. ^{32}P-NAD^{+} was purchased from PerkinElmer. The antibodies to detect RalB (04-037) and phosphor-RalB (Serine 198) (ABS173) were purchased from Millipore. Corning™ Transwell™ Multiple Well Plate with Permeable Polyester Membrane Inserts (0.8μM) were purchased from Corning. FuGENE6 transfection reagent and sequencing grade modified trypsin (V5117) were purchased from Promega. Enzyme-linked chemiluminescence (ECL) plus (32132) western blotting detection reagent, Collagen I Rat Protein, Tail (A1048301), and the high capacity Streptavidin agarose (20357) were purchased from Thermo Fisher Scientific. The anti-SIRT2 (12650), Rabbit HRP(7074), mouse HRP (7076), RalB (90879), mouse anti-Flag (8146) antibodies were purchased from cell signaling technologies.

pCMV5-Flag-TC10, pCMV5-Flag-RalA, pCMV5-Flag-RalB, and pCMV5-Flag-Wrch1 were gifts from Dr. Maurine E. Linder (Department of Molecular Medicine, Cornell University). The pCMV4a- TNFα4KR mutant was previously reported.[14] pCMV5-Flag-ERas was obtained by cloning ERas into pCMV5 using the BglII and SalI restriction sites. ERas was amplified from FUW-CAGGS-ERAS (Addgene 52416) with the forward primer (CAATTATATAGATCTATGGAGCTGCCAACAAAGCC) and the reverse primer (ACGCACGCGTCGACTCAGGCCACAGAGCAGCC). pCMV5-Flag-RRas was obtained by ligating RRas into the ECORI and SalI restriction sites. R-Ras was amplified using CDNA template from transomic with the forward primer CAATTATATGAATTCATGGACTACAAAGACGATGACGACAAGATGAGCAGCGGG GCGGCGT and the reverse primer (ACGCACGCGTCGACTCAGGCCACAGAGCAGCC).

pCMV5-Flag-TCL was obtained by cloning TCL into the BglII and SalI restriction sites. TCL was amplified from the GFP-TCL plasmid (Addgene 23231) using the forward primer (CAATTATATAGATCTATGAACTGCAAAGAGGGAACT) and the reverse primer (ACGCACGCGTCGACTCAGATAATTGAACAGCAGCTG). pCMV5-Flag-RhoB was cloned from HEK-293T CDNA library using the forward primer (CAATTATATAGATCTATGGCGGCCATCCGCAAG) and the reverse primer (ACGCACGCGTCGACTCATAGCACCTTGCAGCAG) into the BglII and SalI restriction sites. pCMV5-Flag-Wrch2 was cloned by amplifying Wrch2 from CDNA template from transomic (171177) into the ECORI and SalI restriction sites with the forward primer (CAATTATATGAATTCATGGACTACAAAGACGATGACGACAAGATGCCGCCGCGG GAGCTG) and the reverse primer (ACGCACGCGTCGACTCAAACGAAGCAGAAGAACTTC). The RalB mutants were generated either by overlap PCR, or quick change mutagenesis using Pfx Platinum or Phusion respectively. The RalB constructs were ligated into the BglII and SalI restriction sites. For lentiviral expression Flag-RalB WT and Flag-RalB 8KR were cloned into pCDH-CMV-MCS-EF1-Puro vector between the NotI and SalI sites. To generate GFP-RalB, RalB WT and 8KR were cloned into the SalI and BamHI restriction sites of the pAcGFP1-C1 vector. GST-Sec5 RBD was cloned by amplifying the first 120 amino acids of Sec5 into the pGEX vector using the BamHI and SalI restriction sites.

Cell Culture. Cells were maintained at 37˚C with 5% CO_2. HEK-239T were cultured in DMEM supplemented with 10% FBS (Invitrogen). A549 cells were cultured in RPMI supplemented with 10% FBS (Invitrogen). HCT116 cells were cultured in McCoy's 5A supplemented with 10% FBS (Invitrogen). All cell culture media was purchased from Thermo.

Generation of lentivirus. To generate lentivirus, HEK-293T cells were thawed. After recovery, 1.5 million cells were seeded in a 10cm dish. After the cells were 60% confluent, transfected

with the packaging plasmids and constructs. For the transfection, 5 μg of empty pCDH-CMV-MCS-EF1-Puro or pCDH-CMV-MCS-EF1-Puro with Flag-RalB WT or Flag-RalB 8KR or the shRNA constructs from sigma were added to 5 μg of pCMV-ΔR8.2 and 1 μg of pM2D.G in 576uL of serum free DMEM with 36μL of FuGene6. After 15 minutes, the transfection mixture was added to cells with 8mL of fresh DMEM (supplemented with 10% FBS). After 12-16 hours, the media was changed to 8mL of fresh FBS supplemented media. After 24, 48 and 72 h the media was collected. Cell debris was pelleted by spinning down at 1,300 rpm for 8 minutes. The supernatant was filtered using a 0.45μ filter. The virus was stored at -80˚C until use.

Generation of Stable SIRT2 KD HEK-293T Cells. To generate stable SIRT2 KD HEK-293T cells, 100,000 cells were seeded per well of a 6 well dish. After 12 hours, the cells were infected with SIRT2 shRNA or Luciferase shRNA supplemented with 6μg/mL of polybrene for 6 hours. After infection, the media was changed. 72 hours later, the cells were treated with puromycin hydrochloride at a concentration of 2.5μg/mL. After 1 week, cells were collected to confirm SIRT2 KD, and the cells were allowed to recover.

Generation of Stable Overexpressing RalB A549 Cells. To generate the stable RalB overexpressing cells, the same method above was followed, except the cells were infected with empty PCDH, Flag-RalB WT or Flag-RalB 8KR virus. The cells were treated with puromycin-hydrochloride at a concentration of 2μg/mL.

Generation of Stable RalB KD HCT116 Cells. To generate stable RalB KD HCT116 cells, RalB shRNA was used. The cells were treated with with puromycin-hydrochloride at a concentration of 3μg/mL.

Western blots. The proteins were resolved by 12% SDS-PAGE, unless otherwise specified, and transferred to polyvinylidene fluoride (PVDF) membrane. The membrane was incubated with 5% bovine serum albumin (BSA) in TBST buffer (0.1% Tween-20, 25 mM Tris-HCl pH 7.6, 150 mM NaCl) at room temperature for 1 hour. Antibodies were subsequently diluted in

5% BSA in TBST incubated with the membranes. Antibody dilutions and incubation times were determined based on the manufactures suggestions. After incubating the membrane with the antibodies, the membrane was washed three times with TBST buffer, and the corresponding HRP conjugated secondary antibody was diluted in fresh 5% BSA in TBST buffer and incubated with the membrane for 1 hour at room temperature. Using ECL plus, the membranes were developed and the chemiluminescence signal was recorded using a Typhoon 9400 Variable Mode Imager.

Detection of Fatty Acylation Levels in cells. Flag-GTPase constructs were ectopically overexpressed in WT HEK-293T, or stable SIRT2 KD HEK-293T cells using FuGene 6 transfection reagent according to the manufactures protocol (a 3:1 ratio of FuGene6 reagent: μg of DNA was used). After 24 hours, the cells were treated with complete DMEM media with 10% FBS supplemented with either 50 μM of Alk14 or 50 μM of DMSO (sigma, biotechnology grade) for 6 hours. The cells were collected at 500x g for 5 min, and washed with PBS two times. Subsequently the cells were lysed in 1% Nonidet P-40 lysis buffer (25 mM Tris-HCl pH 8.0, 150 mM NaCl, 10% glycerol, and 1 % Nonidet P-40) with protease inhibitor cocktail (1:100 dilution). After mixing to a homogenous solution the cells were placed on a rocker at 4˚C. After 30 minutes, the lysate was cleared by centrifuging at 17,000xg for 20 minutes. The cleared lysate was incubated with anti-Flag affinity gel (0.2% NP40 washing buffer (25 mM Tris-HCl pH 8.0, 150 mM NaCl and 0.2% Nonidet P-40) for 2 hours at 4 ˚C with gentle rocking. After two hours, the anti-Flag affinity gel was washed three times with 0.2% NP40 washing buffer (25 mM Tris-HCl pH 8.0, 150 mM NaCl and 0.2% Nonidet P-40). After the third wash the gel was dried, and resuspended in 20μL of 0.2% NP40 wash buffer. After resuspending the gel, the click chemistry reaction was started by adding in sequential order 520-Bodipy azide (1μL of 3mM bodipy solution in DMF), TBTA (1μL of 10 mM solution in DMF), $CuSO_4$ (1μL of 40 mM solution in H_2O) and TCEP (1 μL of 40 mM solution in H_2O). After 30 minutes in the dark,

the click chemistry reaction was quenched by adding 10μL of 6X protein loading dye. The samples were heated at 95˚C for 7 minutes. The samples were centrifuged at 17,000xg for 1 min, and the supernatant was transferred to a new tube. Half of the sample was treated with 330μM of water, and the other half was treated with 330μM of hydroxylamine (pH=7.4) at 95˚C for 7 minutes. The samples were then resolved by a 12% SDS-PAGE gel. The gel was allowed to destain over night in destaining buffer (50% methanol, 40% water, 10% acetic acid), and subsequently washed with water. The in-gel fluorescence was detected using a Typhoon 9400 Variable Mode Imager (GE Healthcare Life Sciences). IMAGEJ was used to quantify fluorescence levels. Protein loading was confirmed by coomassie blue staining of the fluorescence gels.

Endogenous Labeling. WT HEK-293T cells were cultured in 50µM Alk14 for 6 hours. The cells were collected and washed with PBS two times and lysed with 4% SDS lysis buffer (4% SDS, 50mM trieathanolamine pH 7.4, 150 mM NaCl) lysis buffer supplemented with PIC and universal cell nuclease (Thermo). Protein concentration was quantified using the BCA assay (Thermo) following the manufactures protocol. 40mg of whole cell lysate per sample was aliquoted and diluted to a concentration of 2mg/mL in 4% SDS lysis buffer. The samples were then subjected to click chemistry using the same concentrations listed above, except biotin-N_3 was used instead of bodipy-N_3. After 2 hours, the proteins were precipitated using a standard methanol, water and chloroform precipitation procedure. Briefly, 13.3mL of ice cold methanol was added, followed by 5mL of ice-cold chloroform and 10mL of ice-cold water per 5mL (10mg) of lysate. The samples were vortexed and centrifuged at 4,500 xg for 1 hour. After 1 hour, the top layer was removed at the protein pellet was washed three times with 20mL of ice-cold methanol. (30 min spin at 4˚C (4,500 xg).After the last spin remove as much methanol as possible and let the pellet dry for 10 minutes at room temperature. The protein was then resolubilized in 4% SDS lysis buffer supplemented with EDTA (pH=8.0). The SDS

concentration was diluted with 1% Brij97 buffer (1% BRIJ 97, Sodium Chloride, Tris) so the final SDS concentration was less than 1%. High capacity streptavidin beads were washed three times with 1% Brij97 buffer, and subsequently added to the samples. The samples were incubated on a rocker for 90 minutes at room temperature. After washing the samples three times with 1mL of PBS, and three times with 1% SDS in PBS, the samples were then incubated with 1mL of 1M hydroxylamine (pH=7.4) diluted in 1% SDS in PBS at room temperature for 1 hour. The hydroxylamine supernatant was collected and concentrated with a 3KDa concentrator. The streptavidin beads were washed five times with 1mL of 1% SDS in PBS. The beads were boiled with 4% SDS lysis buffer, and the concentrated hydroxylamine supernatant and boiled beads were resolved by SDS page. Endogenous RalB was detected by western blot using the RalB CST antibody.

Detection of Fatty Acylated RalB Peptides by LC-MS/MS. Stable overexpressing Flag-RalB WT SIRT2 KD HEK-293T cells were cultured in 50μM Alk14 for 6 hours and were collected and lysed with 1% NP40 lysis buffer supplemented with PIC as described above. RalB-WT was purified by immunoprecipitation with anti-Flag affinity gel for 2 hours at 4 ˚C with gentle rocking. After two hours, the anti-Flag affinity gel was washed three times with 0.2% NP40 washing buffer (25 mM Tris-HCl pH 8.0, 150 mM NaCl and 0.2% Nonidet P-40). After the third wash, the affinity gel was dried and resuspended in a 1% SDS buffer (1% sodium dodecyl sulfate, 50mM Tris-HCL pH=8.0). To elute the purified RalB, the sample was then boiled for 10 minutes at 95˚C, and subsequently treated with 300μM hydroxylamine at 95˚C. The eluted RalB was then precipitated out of solution using a standard methanol/ chloroform protein precipitation method. The sample was resolubilized and treated with standard reagents for disulfide bond reduction and alkylation as previously described.[10] RalB was treated with 1.5μg of trypsin in glass vial at 37˚C for 2 hours and subsequently desalted using a Sep-Pak C18 cartridge. The peptides were processed as previously described, and data was acquired using

Xcalibur 2.2 operation software.[9,10]

***In Vitro* Sirtuin Assay.** Flag-RalB WT was ectopically overexpressed in WT HEK-293T cells using the standard FuGene6 protocol. After 16 hours, the cells were treated with 50μM Alk14 for 6 hours. The cells were harvested and subsequently washed two times with 1x PBS. After washing the pellet the cells were lysed with 1% NP40 (25 mM Tris-HCl pH 8.0, 150 mM NaCl, 10% glycerol, and 1 % Nonidet P-40) lysis buffer supplemented with PIC as previously described. Flag immunoprecipitation, as previously described, was used to isolate WT RalB. After the last wash with 0.2% NP40 buffer, the flag affinity gel was then washed three times with 50mM Tris buffer. The affinity gel was dried, and then resuspended in 20 μL of reaction buffer (50 mM Tris pH 8.0, 150 mM NaCl, 1 mM DTT). To each reaction 5 μM SIRT2 WT/ pfSir2A/ Sirt1/ Sirt3/ Sirt6/ Sirt7 (with tRNA) or enzyme buffer as well as NAD or water was added. The samples were placed on a rocker at 37˚C for two hours. After the enzymatic reaction, the affinity gel was washed three times with 0.2% NP40 buffer. After the last wash, the affinity gel was dried and the standard click chemistry methods described above were used to visualize the lysine fatty acylation levels on RalB after the enzymatic reaction.

^{32}P-NAD^{+} assay. WT HEK-239T cells with stable overexpression of either PCDH or Flag-RalB WT were treated with Alk14 for 6 hours. The cells were collected and lysed with 1% NP40 lysis buffer supplemented with PIC. The lysis buffer was added to the cell pellet and placed on a rocker at 4˚C for 30 minutes. The lysate was cleared by centrifuging at 17,000xg for 30 minutes. The cleared lysate was collected and the protein concentration was determined by Bradford Assay. The protein was purified by Flag immunoprecipitation as previously described. Purified RalB-WT was kept on the Flag affinity for the ^{32}P-NAD^{+} assay. To the on bead RalB or empty vector 10 μL of reaction buffer (50 mM Tris pH 8.0, 150 mM NaCl, 1 mM DTT, 5 μM SIRT2 WT, and 0.1 μCi of ^{32}P-NAD) was added. The samples were placed at 37 ˚C for 1 hour. After the reaction occurred, 2 μL of each reaction mixture was spotted onto a polyester-backed silica

plate for chromatography. The plate was developed in a 30:70 (v/v) mixture of 1 M ammonium bicarbonate:95% ethanol. The plate was exposed in the phosphor imaging screen (GE Healthcare) overnight. The signal was detected using Typhoon 9400 Variable Mode Imager. As standards, H3K9 myristoyl and H3K9 acetyl peptides were incubated with SIRT2 using the same reaction conditions mentioned above. The standard peptides were synthesized as previously described. [8,29]

Live Cell Imaging to Detect the SEC5 RBD/ RalB Co-Localization. 100,000 WT HEK-293T cells were seeded in a glass bottom dish from MaTEK. After 12 hours, mCherry-Sec5 RBD and GFP-RalB were co-overexpressed (1µg of each construct) using FuGene6 following the protocol described above. After 24 hours, the cells were placed in live cell imaging solution (Thermo) and visualized using an inverted Zeiss 880 confocal microscope in a chamber set at 37˚C with 5% CO_2. Images were processed using FIJI software. Statistical significance was determined using an unpaired two-tailed student's t-test. (*** = $p < 0.001$)

RalB and mCherry-SECRBD Colocalization. 100,000 WT HEK-293T cells were seeded in a glass bottom dish from MaTEK. After 12 hours, mCHERRY-SEC5RBD and GFP-RalBWT or GFP-RalB 8KR were co-overexpressed (1µg of each construct) using FuGene6 following the protocol described above. After 24 hours, the cells were placed in live cell imaging solution (Thermo) and visualized using an inverted Zeiss 880 confocal microscope in a chamber set at 37˚C with 5% CO_2. Images were processed using FIJI software. Colocalization was calculated in FIJI using the co-loc2 plugin.

SEC5-RBD GTP Binding Assay. The Sec5RBD (first 121 amino acids of Sec5) was cloned into a pGEX vector. GST-Sec5RBD was transformed into BL21 cells. A starter culture was allowed to grow for 8 hours, and was then transferred to a larger culture. The cells were allowed to grow until the OD reached 0.6-0.8. Once the cells reached this OD, they were placed on ice for 10 minutes. To induce protein expression, IPTG was added to a final concentration of

0.1mM. The culture was placed at 16˚C, and allowed to incubate overnight. The cells were harvest by centrifugation at top speed. The cell pellet was re-suspend lysis buffer (500mM NaCl, 1mM DTT, and 50mM Tris-HCl pH=8.0). Lysozyme (1mg, 0.4% w/v) and nuclease (0.1µL, 50U/mL of lysis buffer, Thermo) were added and sample was allowed to incubate at 25˚C for 1 hour. The mixture was then snapped freezed in liquid nitrogen, and subsequently thawed at 25˚C. The sample was centrifuged at 17,000xg for 30 minutes (at room temperature). The GST-Resin was prewashed three times with 1mL of the lysis buffer. The GST resin was added to the cleared lysate for 30 minutes at 4˚C. After incubating, wash the beads 5 times with lysis buffer. After drying the beads, re-suspend the beads in Ral GTP-binding lysis buffer (COMPONETS). While purifying the GST-Sec5 RBD, cells that were transfected with Flag-RalB WT/ 8KR were quickly collected and lysed on ice using the Ral-GTP binding lysis buffer described above. The cells were lysed by adding the buffer and incubating on ice for 20 minutes. The lysate was cleared by centrifugation at 17,000xg for 10 minutes. The protein concentration was determined using a Bradford assay. After normalizing input amounts, GST immobilized Sec5RBD was added to each sample. The samples were placed on the rocker at 4˚C for 30 minutes. The GST-resin was subsequently washed three times with lysis buffer and the samples were boiled. The boiled samples were resolved by SDS page and GTP bound RalB was detected by flag western blot.

Immunofluorescence to Detect RalB-Sec5 co-localization. 100,000 cells (SIRT2 WT and KD) were seeded in glass bottom dishes (MaTek) After 12 hours, 1µg of Flag-RalB WT and Flag-RalB 8KR were overexpressed using FuGene6, following the same protocol anove. After 30 hours, the cells were washed two times with 1x PBS, and then fixed with methanol. After fixing the cells, the membrane was permeabilized by adding 0.25% Triton-X to the samples for 10 minutes. The cells were then washed with PBS for 5 minutes, three times. After which blocking solution (1% BSA in TBST) was added to the samples for 1 hour. The Sec5 antibody

was added to cells at a concentration of 2.5μg /mL in 1% BSA in TBST and allowed to incubate overnight at 4˚C. The samples were washed three times for 5 minutes with TBST. After three washes, the Flag antibody was added (1:1000) for 1 hour at room temperature in 1% BSA in TBST. After 1 hour, the samples were washed three times for 5 minutes each with TBST. The secondary antibodies (1:1000) were subsequently added for 1 hour at room temperature in 1% BSA in TBST. After 1 hour, the samples were washed with TBST for 5 minutes, three times each. After the final wash, the DAPI was used to mount the samples. Samples were imaged on an inverted Zeiss 880 confocal microscope.

A549 Cell Migration Assay. 100,000 A549 were seeded in a 6 well dish. After 12 hours, the cells were infected with SIRT2 lentivirus for 6 hours supplemented with polybrene at a concentration of 6μg/ mL. After 60 hours, the cells were serum starved for 16 hours. Cells were trypsin digested, and subsequently washed with serum free media three times. Cells were counted. Cell solutions at a concentration of 250,000 cells/ mL of media were made by diluting a correct number of cells in serum free media. To control for cell seeding, 100μL of the cell solutions were added to two-three wells of a 96 well dish. 20μL of Cell-titer blue (Promega) was added. After three hours, the fluorescence was measured. For the assay, boyden chambers with a 0.8μm polycarbonate filter were placed in 600μL of complete media. To the top of the chamber, 200μL of the cell solutions were added. The assay was done in at least triplicate. After 24 hours, the chambers were washed with 1x PBS three times and then placed in methanol for 10 minutes. The inserts were stained with crystal violet (0.25% crystal violet in 25% methanol). The cells on the top of the chamber were removed with a cotton swab. The inserts were washed with water three times and then imaged with a microscope. Representative images are shown.

Cell Proliferation Assay. 10,000 A549 cells were seeded per well of a 24 well plate. After 12 hours, the cells were infected with PCDH/ Flag-RalB WT/ Flag-RalB 8KR virus supplemented

with polybrene (6μg/mL) for 6 hours The cells were then infected with SIRT2 shRNA virus supplemented with polybrene (6μg/mL) for an additional 6 hours. The cells were then placed in RPMI with 10% FBS. Cells were fixed each day by washing the cells with 1x PBS two times and then fixed with ice cold methanol for 10 minutes. The cells were stained with 0.25% crystal violet for 5 minutes. After 5 minutes, the plates were washed with water, and allowed to dry. Plates were fixed and stained every day for 5 days.

Anchorage Independent Growth Assay. 100,000 cells were seeded per well of a 6 well dish. The cells were infected with SIRT2 shRNA for 6 hours supplemented with 6μg/ mL of polybrene. After 48 hours, the cells were transfected with empty vector, pCMV5-Flag-RalB WT, 8KR or M1/M5 for 24 hours using the standed FuGene6 protocol. 2μg of DNA was used per well. After 24 hours, the cells were counted. For the soft agar assay first the bottom layer was made by adding 10mL of 3% low melting point agar to 40 mL of McCoy's 5A media to make 0.6% agar solution. 2mL of the solution was added to each well, and the plates were allowed to solidify at room temperature. Cell solutions with a concentration of 20,000 cells/ 1mL of media were made. Cell titer blue, as mentioned above, was used to control for cell seeding. 200μL of each cell solution was added to 4mL of 0.3% LMP agar. The 0.3% LMP agar was made by adding 5mL of 3% agar to 45mL of McCoy's 5A. The cells and agar were mixed well, and then 1mL of the solution was added to each well. The assay was done in triplicate. The plates were allowed to sit at room temperature for 30 minutes. Subsequently, 1mL of 0.3% LMP agar was then added. The plates were placed at 37˚C for 10-14 days. After 7 days, an additional 1mL of 0.3% LMP agar in McCoy's 5A media was added.

Detection of RalB phosphorylation. At 60% confluency, empty vector, Flag-RalB WT and Flag-RalB 8KR were transiently overexpressed using FuGene6 in HEK-293T Cells. After 24 hours, the cells were collected and washed twice with 1x PBS. Cells were lysed with 4% SDS lysis buffer supplemented with protease inhibitor cocktail, nuclease and phosphatase inhibitor

cocktail 3 (Sigma Aldrich P0044). After lysing the cells, protein concentrations were normalized using a standard BCA assay (Thermo). The SDS concentration was diluted to less than 0.1%, and the overexpressed proteins were enriched by Flag immunoprecipitation as described above. After washing the samples three times with 0.2% NP40 Flag IP wash buffer, the flag affinity agarose was dried and resuspended and boiled at 95˚C for 5 min in 2x protein loading dye as described above. The samples were resolved by SDS PAGE, and a RalB pS198 specific antibody (Millipore, ABS173) was used to detect phosphor-RalB (Ser198). The antibody was used at a 1:1000 dilution in 5% BSA in TBST overnight at 4˚C.

REFERENCES

(1) Prabakaran, S.; Lippens, G.; Steen, H.; Gunawardena, J. Post-translational modification: nature's escape from genetic imprisonment and the basis for dynamic information encoding. *Wiley Interdiscip Rev Syst Biol Med* **2012,** *4* (6), 565.
(2) Jiang, H.; Zhang, X.; Chen, X.; Aramsangtienchai, P.; Tong, Z.; Lin, H. Protein Lipidation: Occurrence, Mechanisms, Biological Functions, and Enabling Technologies. *Chem Rev* **2018,** *118* (3), 919.
(3) Nadolski, M. J.; Linder, M. E. Protein lipidation. *FEBS J* **2007,** *274* (20), 5202.
(4) Resh, M. D. Covalent lipid modifications of proteins. *Curr Biol* **2013,** *23* (10), R431.
(5) Schey, K. L.; Gutierrez, D. B.; Wang, Z.; Wei, J.; Grey, A. C. Novel fatty acid acylation of lens integral membrane protein aquaporin-0. *Biochemistry* **2010,** *49* (45), 9858.
(6) Stevenson, F. T.; Bursten, S. L.; Locksley, R. M.; Lovett, D. H. Myristyl acylation of the tumor necrosis factor alpha precursor on specific lysine residues. *J Exp Med* **1992,** *176* (4), 1053.
(7) Stevenson, F. T.; Bursten, S. L.; Fanton, C.; Locksley, R. M.; Lovett, D. H. The 31-kDa precursor of interleukin 1 alpha is myristoylated on specific lysines within the 16-kDa N-terminal propiece. *Proc Natl Acad Sci U S A* **1993,** *90* (15), 7245.
(8) Aramsangtienchai, P.; Spiegelman, N. A.; He, B.; Miller, S. P.; Dai, L.; Zhao, Y.; Lin, H. HDAC8 Catalyzes the Hydrolysis of Long Chain Fatty Acyl Lysine. *ACS Chem Biol* **2016,** *11* (10), 2685.
(9) Jing, H.; Zhang, X.; Wisner, S. A.; Chen, X.; Spiegelman, N. A.; Linder, M. E.; Lin, H. SIRT2 and lysine fatty acylation regulate the transforming activity of K-Ras4a. *Elife* **2017,** *6*.
(10) Zhang, X.; Spiegelman, N. A.; Nelson, O. D.; Jing, H.; Lin, H. SIRT6 regulates Ras-related protein R-Ras2 by lysine defatty-acylation. *Elife* **2017,** *6*.
(11) Zhou, Y.; Huang, C.; Yin, L.; Wan, M.; Wang, X.; Li, L.; Liu, Y.; Wang, Z.; Fu, P.; Zhang, N.et al. N(epsilon)-Fatty acylation of Rho GTPases by a MARTX toxin effector. *Science* **2017,** *358* (6362), 528.
(12) Tong, Z.; Wang, M.; Wang, Y.; Kim, D. D.; Grenier, J. K.; Cao, J.; Sadhukhan, S.; Hao, Q.; Lin, H. SIRT7 Is an RNA-Activated Protein Lysine Deacylase. *ACS Chem Biol* **2017,** *12* (1), 300.
(13) Jiang, H.; Zhang, X.; Lin, H. Lysine fatty acylation promotes lysosomal targeting of TNF-alpha. *Sci Rep* **2016,** *6*, 24371.
(14) Jiang, H.; Khan, S.; Wang, Y.; Charron, G.; He, B.; Sebastian, C.; Du, J.; Kim, R.; Ge, E.; Mostoslavsky, R.et al. SIRT6 regulates TNF-alpha secretion through hydrolysis of long-chain fatty acyl lysine. *Nature* **2013,** *496* (7443), 110.
(15) Haigis, M. C.; Sinclair, D. A. Mammalian sirtuins: biological insights and disease relevance. *Annu Rev Pathol* **2010,** *5*, 253.
(16) Teng, Y. B.; Jing, H.; Aramsangtienchai, P.; He, B.; Khan, S.; Hu, J.; Lin, H.; Hao, Q. Efficient demyristoylase activity of SIRT2 revealed by kinetic and structural studies. *Sci Rep* **2015,** *5*, 8529.
(17) Moreno-Yruela, C.; Galleano, I.; Madsen, A. S.; Olsen, C. A. Histone Deacetylase 11 Is an epsilon-N-Myristoyllysine Hydrolase. *Cell Chem Biol* **2018**, DOI:10.1016/j.chembiol.2018.04.007 10.1016/j.chembiol.2018.04.007.
(18) Kutil, Z.; Novakova, Z.; Meleshin, M.; Mikesova, J.; Schutkowski, M.; Barinka, C. Histone Deacetylase 11 Is a Fatty-Acid Deacylase. *ACS Chem Biol* **2018,** *13* (3), 685.
(19) ten Klooster, J. P.; Hordijk, P. L. Targeting and localized signalling by small GTPases. *Biol Cell* **2007,** *99* (1), 1.
(20) Colicelli, J. Human RAS superfamily proteins and related GTPases. *Sci STKE* **2004,**

2004 (250), RE13.
(21) Aicart-Ramos, C.; Valero, R. A.; Rodriguez-Crespo, I. Protein palmitoylation and subcellular trafficking. *Biochim Biophys Acta* **2011,** *1808* (12), 2981.
(22) Gentry, L. R.; Martin, T. D.; Reiner, D. J.; Der, C. J. Ral small GTPase signaling and oncogenesis: More than just 15minutes of fame. *Biochim Biophys Acta* **2014,** *1843* (12), 2976.
(23) Yan, C.; Theodorescu, D. RAL GTPases: Biology and Potential as Therapeutic Targets in Cancer. *Pharmacol Rev* **2018,** *70* (1), 1.
(24) Shirakawa, R.; Horiuchi, H. Ral GTPases: crucial mediators of exocytosis and tumourigenesis. *J Biochem* **2015,** *157* (5), 285.
(25) Neel, N. F.; Martin, T. D.; Stratford, J. K.; Zand, T. P.; Reiner, D. J.; Der, C. J. The RalGEF-Ral Effector Signaling Network: The Road Less Traveled for Anti-Ras Drug Discovery. *Genes Cancer* **2011,** *2* (3), 275.
(26) Falsetti, S. C.; Wang, D. A.; Peng, H.; Carrico, D.; Cox, A. D.; Der, C. J.; Hamilton, A. D.; Sebti, S. M. Geranylgeranyltransferase I inhibitors target RalB to inhibit anchorage-dependent growth and induce apoptosis and RalA to inhibit anchorage-independent growth. *Mol Cell Biol* **2007,** *27* (22), 8003.
(27) Nishimura, A.; Linder, M. E. Identification of a novel prenyl and palmitoyl modification at the CaaX motif of Cdc42 that regulates RhoGDI binding. *Mol Cell Biol* **2013,** *33* (7), 1417.
(28) Gentry, L. R.; Nishimura, A.; Cox, A. D.; Martin, T. D.; Tsygankov, D.; Nishida, M.; Elston, T. C.; Der, C. J. Divergent roles of CAAX motif-signaled posttranslational modifications in the regulation and subcellular localization of Ral GTPases. *J Biol Chem* **2015,** *290* (37), 22851.
(29) Zhu, A. Y.; Zhou, Y.; Khan, S.; Deitsch, K. W.; Hao, Q.; Lin, H. Plasmodium falciparum Sir2A preferentially hydrolyzes medium and long chain fatty acyl lysine. *ACS Chem Biol* **2012,** *7* (1), 155.
(30) Martin, T. D.; Samuel, J. C.; Routh, E. D.; Der, C. J.; Yeh, J. J. Activation and involvement of Ral GTPases in colorectal cancer. *Cancer Res* **2011,** *71* (1), 206.
(31) Guin, S.; Ru, Y.; Wynes, M. W.; Mishra, R.; Lu, X.; Owens, C.; Barn, A. E.; Vasu, V. T.; Hirsch, F. R.; Kern, J. A.et al. Contributions of KRAS and RAL in non-small-cell lung cancer growth and progression. *J Thorac Oncol* **2013,** *8* (12), 1492.
(32) Tecleab, A.; Zhang, X.; Sebti, S. M. Ral GTPase down-regulation stabilizes and reactivates p53 to inhibit malignant transformation. *J Biol Chem* **2014,** *289* (45), 31296.
(33) Atala, A. Phosphorylation of RalB is Important for Bladder Cancer Cell Growth and Metastasis Editorial Comment. *J Urology* **2011,** *185* (6), 2423.
(34) Charron, G.; Zhang, M. M.; Yount, J. S.; Wilson, J.; Raghavan, A. S.; Shamir, E.; Hang, H. C. Robust fluorescent detection of protein fatty-acylation with chemical reporters. *J Am Chem Soc* **2009,** *131* (13), 4967.

CHAPTER 3

NUCLEOTIDE-DEPENDENT INTERACTOME ANALYSIS INDENTIFIED SHARED AND UNIQUE FUNCTIONS OF RALA AND RALB[2]

Abstract

Despite their high sequence identity and many shared functions, the Ral GTPases, RalA and RalB, often have opposing roles in cancer and tumorigenesis. Here, we aim to gain molecular understandings of the shared and unique properties of RalA and RalB through a nucleotide dependent interactome analysis using stable isotope labeling of amino acids in cell culture (SILAC). The interactome study identified several well-known Ral effector proteins, such as components of the exocyst complex, suggesting that the results are reliable. Several proteins that were not previously known to interact with Ral were identified, such as the eIF2□ kinase activator, GCN1, transferrin receptor (TfR1), and ERK2. While many of the effectors are shared by RalA and RalB, ERK2 interacts with only RalB and not RalA. The RalB-ERK2 interaction decreases the ERK2 nuclear localization, and thus suppresses the nuclear activity of ERK2, potentially leading to suppression of tumorigenesis. As the Ral GTPases plays important roles in regulating signaling and cancer, this study provides new insights into the functions these two highly similar but functionally different small GTPases.

1. Introduction

Small GTPases are molecular switches that can regulate many cellular functions, and are therefore important for physiology and diseases. These monomeric 20-25kDa G-proteins have the ability to bind to GTP and subsequently hydrolyze GTP to GDP with the help of

[2] For this chapter, I (Nicole A. Spiegelman) designed and performed all the biochemical studies except those noted below. Xiaoyu Zhang assisted in preparing the mass spectrometry samples. Ilana B. Kotlier helped generated the Ral mutants. Hening Lin directed and supervised the study. I would like to thank Mike Smith for continuing this project.

regulator proteins. When bound to GTP, small GTPases are active and can bind to effector proteins to promote signaling. They are inactive when bound to GDP. Over 150 proteins comprise the Ras superfamily of small GTPases.[1] The superfamily can be further separated into six subfamilies, the Ras, Rho, Rab, Ran, Arf, and Rad subfamilies. The Ras subfamily has 36 members and includes the Rap, R-Ras, Ral, and Rheb proteins.[1,2] The three most common Ras genes are HRas, KRas and NRas, the original proteins of the Ras superfamily. These genes are the most highly mutated genes in tumors and cancers. The Ras proteins can signal to and control many downstream effectors including to the RalGEFs which controls the Ras like (Ral) GTPases.[2-4] The Ral GTPases share approximately 50% identity with HRas, NRas and KRas. In humans, there are two proteins in the Ral subfamily: RalA and RalB. Not surprisingly, the Ral GTPases have been shown to modulate cell proliferation, survival and metastasis.[3,5-7]

The Ral GTPases have been reported to regulate the exocyst, transcription, endocytosis, and autophagy. The physiological function of the Ral GTPases is mediated by their interactions with different effector proteins. The most well established Ral effectors are Ral binding protein 1 (RALBP1 or RLIP76), Sec5 and exocyst complex 84 (Exo84). Other effectors include tank binding kinase 1 (Tbk1), Zonab, Filamin and phospholipase C delta 1 and phospholipase D1.[5,7-11] RalA and RalB share over 80% of their sequence identity with the majority of their divergence being in their C-terminal hypervariable domain, where they only show 50% sequence identity.[5-7] Despite their high sequence identity and shared functions, RalA and RalB have been shown to exhibit different or even opposing roles in cancer. As an example RalA was found to be important for anchorage independent growth, where RalB inhibited it.[12] In addition, there are also reported differences in their regulation and cellular functions. [5,6,10-25]

Small GTPases are regulated by several protein post-translational modifications. Like the Ras GTPases, the Ral GTPases have a C-terminal CaaX (C: cysteine; a: aliphatic amino acid; X: any amino acid) motif. Both RalA and RalB have a CCaX and are prenylated on the

first cysteine and palmitoylated on the second cysteine residue.[26] These lipidation events are important for the subcellular localization and activity of Ral proteins. Additionally, both RalA and RalB have C-terminal phosphorylation, RalA being modified on serine 194 and RalB on serine 198. For both proteins phosphorylation was important for endomembrane localization and is important for RalA-mediated anchorage independent growth and RalB's role in migration and metastasis.[5,25] More recently, we found that RalB has Sirtuin 2 (SIRT2)- regulated lysine fatty acylation at the C-terminal hypervariable region, while RalA does not have lysine fatty acylation (Chapter 2).

Our recent finding about the difference in lysine fatty acylation, and the often opposing and divergent roles of the two Ral GTPases prompted us to ask if there are Ral isoform-specific effectors or interacting proteins. Recently, our lab used a quantitative proteomic approach to identify the interactomes of two Ras isforms: KRas4a and KRas4b.[27] The method produced reliable results and provided important insights into the functions of KRas4a and KRas4b. Therefore, here we decided to employ the same method to investigate interactome of the Ral isoforms.

2. Results

2.1 Identification of RalA and RalB Interacting Proteins Using SILAC and AP-MS

To identify interacting partners and effectors of the Ral proteins we used stable isotope labeling of amino acids in cell cultures and affinity purification mass spectrometry (AP-MS). Since we were interested in identifying novel effectors, we utilized both the Ral active (Q72L) and inactive (S28N) mutants. The RalQ72L mutant is constitutively bound to GTP while the

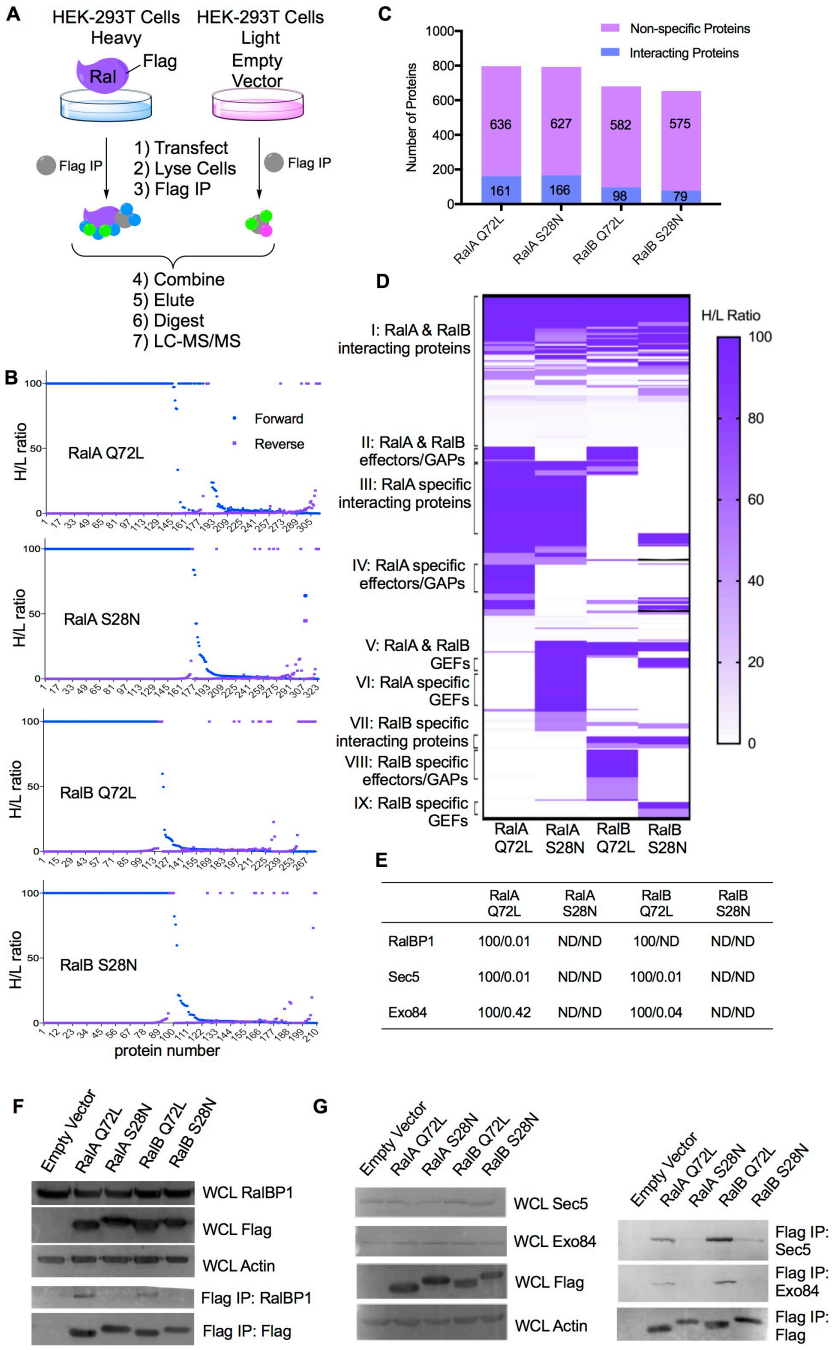

	RalA Q72L	RalA S28N	RalB Q72L	RalB S28N
RalBP1	100/0.01	ND/ND	100/ND	ND/ND
Sec5	100/0.01	ND/ND	100/0.01	ND/ND
Exo84	100/0.42	ND/ND	100/0.04	ND/ND

Figure 3.1. Nucleotide Dependent Ral GTPase Interactome Identifies Several Ral Effector Proteins **(A)** SILAC based affinity purification method used to identify the Ral interactome **(B)** Plots showing the H/L ratio in the forward and reverse SILAC experiments for proteins with more than two unique peptides identified and H/L ratios that suggest they are possible interacting proteins not proteins that were non-specifically pulled down **(C)** classification of all of the proteins identified either as non-specific or interacting **(D)** a heat map based on the average H/L ratio of the forward and inverse reverse H/L ratios of all of the proteins identified **(E)** Known effector proteins and localization markers that were identified **(F)** Validation of the Ral-RalBP1 interaction **(G)** validation of the Ral-Exo84/ Sec5 interaction**.**

S28N mutant is always bound to GDP. Effector proteins would typically only bind to the active mutant, but not the inactive mutant.

To minimize false positives, we employed both the forward and reverse SILAC AP-MS experiments as presented in Figure 1A. In the forward SILAC experiment, we transfected Flag-tagged RalA/RalB Q72L or S28N mutants in "heavy" HEK-293T cells and empty vector in "light" HEK-293T cells. We lysed the cells and carried out Flag affinity purification separately. We then mixed the flag resin from the heavy and light samples and boiled the flag beads. After protein purification and trypsin digestion, the samples were subjected to MS analysis (Figure 3.1A). In the reverse SILAC experiment, Ral proteins was expressed in "light" HEK-293T cells and the empty vector was used in "heavy" HEK-293T cells while the rest was the same as the forward SILAC.

In Figure 3.1B, we plotted the heavy/ light ratio for each protein identified for each Ral protein. For proteins identified to be considered as potential interacting proteins of RalA/RalB, the heavy/ light (H/L) ratio for the forward SILAC needed to be >1.5, with at least two unique peptides. At the same time, the proteins should also be identified in the reverse SILAC with a H/L ratio <0.67 and at least two unique peptides. Using these criteria, we filtered the proteomic results to obtain the interactomes for RalA Q72L, RalA S28N, RalB Q72L, and RalB S28N. After applying these criteria, about 17% of the identified proteins were considered possible interacting proteins (Figure 3.1C). We identified 161 RalA Q72L, 166 RalA S28N, 98 RalB Q72L, and 79 RalB S28N potential interacting proteins (Figure 3.1C).

To further analyze the results to extract useful information, we generated a heat map to help classify the identified interacting proteins into the following groups (Figure 3.1D):

(I) Proteins that interact with all four bait proteins (RalA & RalB interacting proteins);

(II) Proteins that interact with only RalA Q72L and RalB Q72L (RalA & RalB shared effectors/GAPs candidates);

(III) Proteins that interact with only RalA Q72L and S28N (RalA-specific interacting proteins);

(IV) Proteins that interact with only RalA Q72L (RalA-specific interacting proteins);

(V) Proteins that interact with only RalA S28N and RalB S28N (RalA & RalB shared GEFs candidates);

(VI) Proteins that only interact with RalA S28N (RalA-specific GEFs candidates);

(VII) Proteins that interact with RalB Q72L and S28N (RalB-specific interacting proteins);

(VIII) Proteins that interact with RalB Q72L only (RalB-specific effectors/GAPs candidates);

(IX) Proteins that only interact with RalB S28N (RalB-specific GEFs candidates).

This classification would give us a more holistic view of the similarities and differences between the Ral isoforms.

To determine if the results we obtained were reliable, we looked at the H/L ratio and peptide scores for known Ral effectors and interacting proteins (Figure 3.1E). A known Ral effector, RalBP1, was identified in RalA and RalB Q72L interactomes, but not the S28N interactomes. The interaction between RalBP1 and RalA/B Q72L was further confirmed by co-immunoprecipitation (Co-IP) (Figure 3.1A). Two components of the exocyst complex, Sec5, and Exo84, are knonw Ral effectors. In our interactome data, they both interact with the active RalA Q72L and RalB Q72L mutants, but not with the inactive mutants. Co-IP results further confirmed this (Figure 3.1F, G). These findings suggested that the SILAC AP-MS results we obtained were reliable.

2.2 The Interactome Data Highlights Different Cellular Functions of RalA and RalB

RalA and RalB often exhibit different, even opposing cellular functions. We were therefore interested in further exploring the difference and similarities between the two proteins.

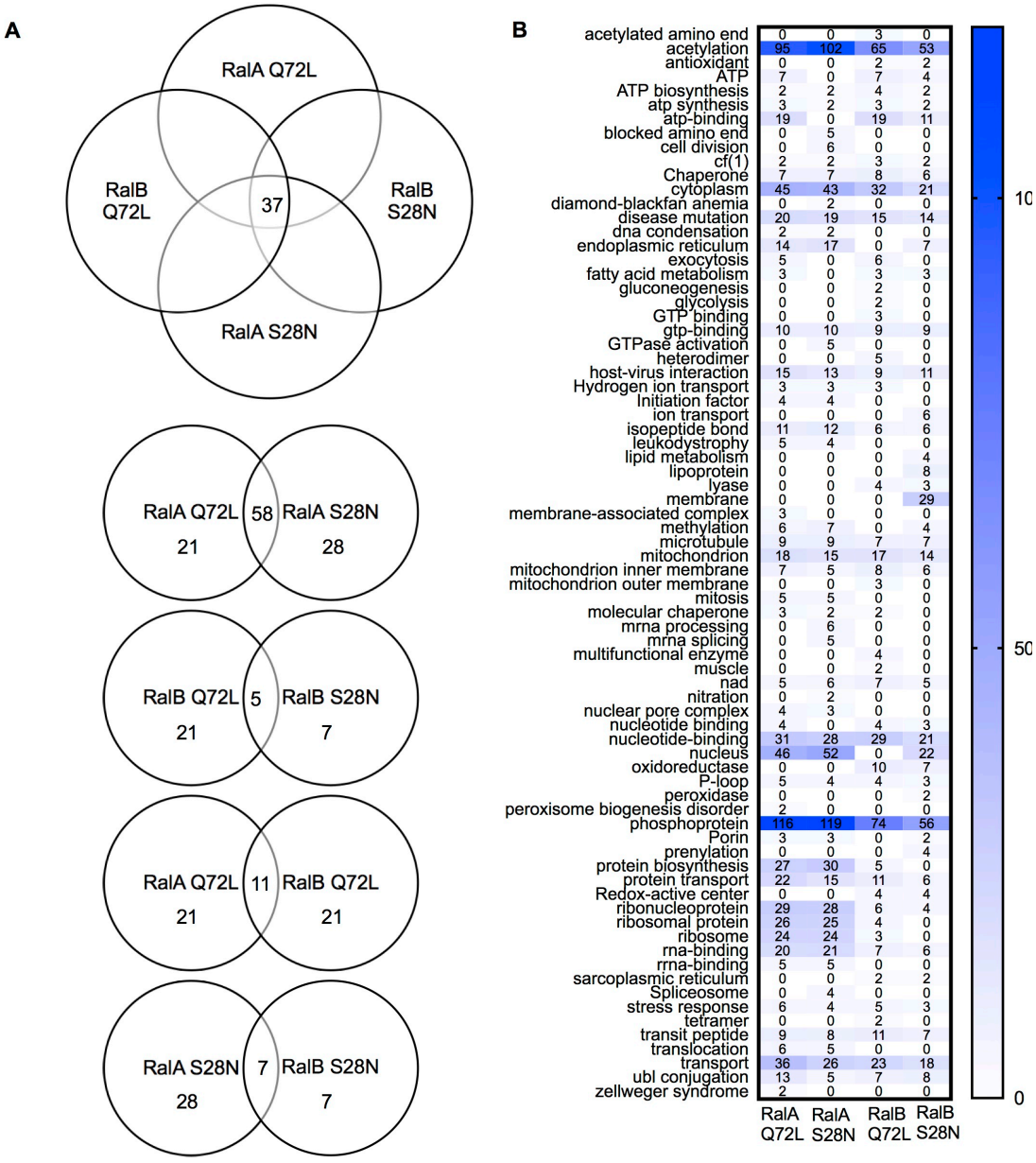

Figure 3.2. **The proteomics results highlight there are many similarities and differences between the Ral GTPases** (**A**) Venn Diagrams showing the number of overlapping and distinct proteins between the Ral GTPases accounting for the nucleotide status (**B**) Heat map showing the results from analyzing the data using a DAVID analysis with UP_KEYWORDS.

To do this we analyzed the results to determine how many proteins identified were specific for RalA or RalB. Again, we only looked at proteins that appeared in both the forward and reverse SILAC experiments with cutoffs mentioned above.

We identified 37 proteins as Ral interacting partners as they interacted with both RalA

and RalB independent of the nucleotide status (Figure 3.2A). There were 11 proteins that interacted with both the active forms of RalA and RalB (Figure 3.2A), several of which were components of the exocyts including Exo84 and Sec5. These proteins could be potential shared effectors or GAPs of RalA and RalB. RalA Q72L and RalB Q72L each selectively interacted with 21 proteins. These proteins could potentially be RalA-specific or RalB-specific effectors or GAPs. Interestingly, there were seven proteins (one of them being transferrin receptor 1, TfR1) that specifically interacted with the inactive RalA S28N and RalB S28N mutants. These proteins could potentially be shared GEFs of RalA and RalB.

We further analyzed the results using DAVID analysis, specifically looking at the UP_KEYWORDS (Figure 3.2B).[28,29] The DAVID analysis highlights that RalA and RalB are functionally different, although there are many similarities. RalA interacting proteins are enriched in proteins associated with the endoplasmic reticulum (ER) and the nucleus. Furthermore, RalA interacting proteins were enriched in ribonucleoproteins, ribosomal proteins, ribosome, RNA binding proteins, or rRNA binding proteins. This suggests RalA may play a role in regulating translation. Interestingly, RalB Q72L interacting proteins were enriched in proteins associated with fatty acid metabolism, gluconeogenesis, and glycolysis. Both RalA Q72L and RalB Q72L pulled out proteins associated with exocytosis, which was not surprising as two of the most well established Ral effectors are Sec5 and Exo84, two components of the exocyst. This analysis highlights that there are a lot of similarities but also several differences between the two Ral proteins.

2.3 Consistent with Membrane Localization Ral Interact with Na(+)/K(+) ATPase α-1

As RalA and RalB both are localized on the plasma membrane (Figure 3A) it was not surprising that Na(+)/K(+) ATPase α-1 subunit was identified from all of the proteomics samples (Figure 3.3B). the Na(+)/K(+) ATPase α-1 subunit is responsible for helping maintain the transmembrane gradients of Na^+ and K^+, and is ubiquitously expressed as an integral plasma

membrane protein.[30] To further confirm these findings, we looked at the co-localization of RalB Q72L and RalB S28N with Na(+)/K(+) ATPase α-1 subunit. As expected we were able to detect the co-localization of these two proteins at the plasma membrane (Figure 3.3C). This further supported that the data set we obtained was reliable and could provide insight into the Ral GTPases.

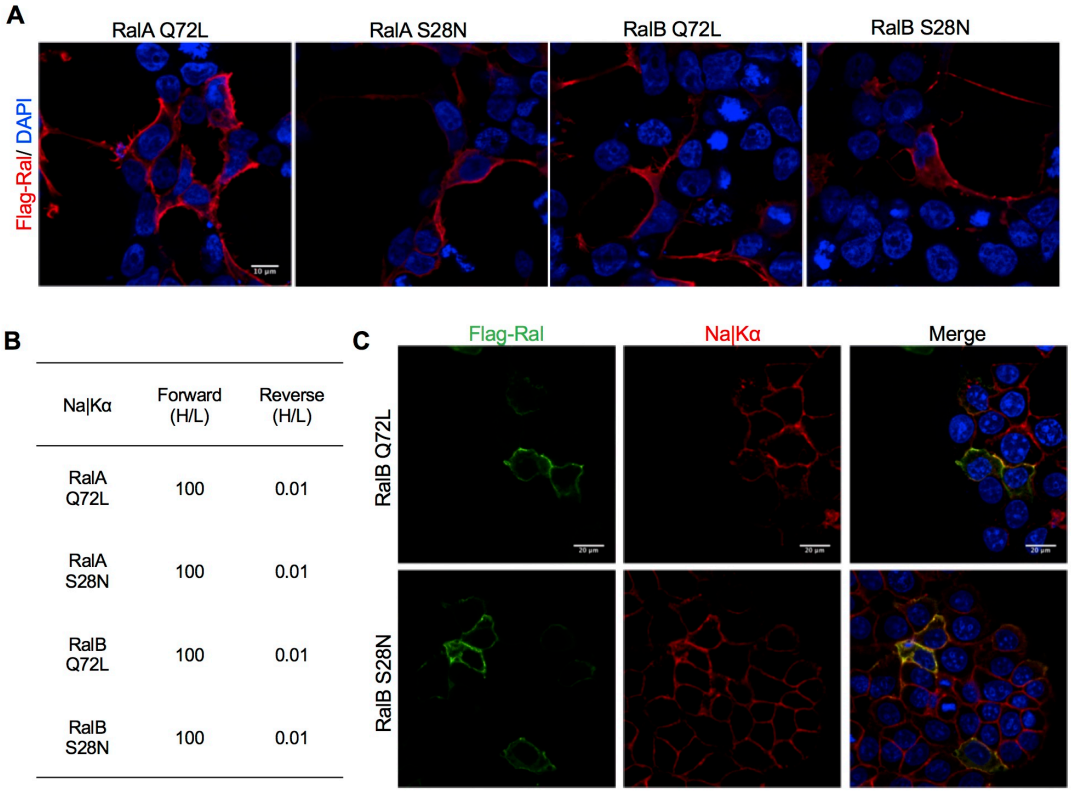

Na|Kα	Forward (H/L)	Reverse (H/L)
RalA Q72L	100	0.01
RalA S28N	100	0.01
RalB Q72L	100	0.01
RalB S28N	100	0.01

Figure 3.3. **Ral proteins co-localize with NaKα on the plasma membrane. (A)** Immunofluorescecne showing the Ral GTPases are localized on the membrane **(B)** The AP-MS results suggesting Ral and NaKα co-localize **(C)** Co-localization of RalBQ72L and RalB S28N with NaKα in MCF-7 cells.

2.4 The Ral GTPases interact with eIF2α Kinase Activator GCN1

Our proteomic data indicated that GCN1 is a potential interacting protein for RalA and RalB (Figure 3.4A). The Ral GTPases have previously been implicated to play a role in stress response, such as viral infection or amino acid depletion. RalB has also been shown to play a role in regulating mTOR activity, especially under serum depletion. We were therefore

interested in confirming the Ral-GCN1 interaction. Consistent with the proteomics data, all of the Ral GTPases co-IP with GCN1 (Figure 3.4B) GCN1 is well established to be upstream of the GCN2 and modulate eIF2α phosphorylation levels. To see if the Ral-GCN1 interaction modulated a change in GCN1 activity, we overexpressed both the active and inactive forms of RalA and RalB in HCT116 cells and looked at ATF4 and IF2α phosphorylation levels (Figure 3.4C). Interestingly, it seems that over expression of RalA and RalB Q72L, but not the S28N mutant, could slightly increase ATF4 protein level and eIF2a phosphorylation. Thus, our interactome analysis suggests that the Ral GTPases may play a role in regulating GCN1 activity.

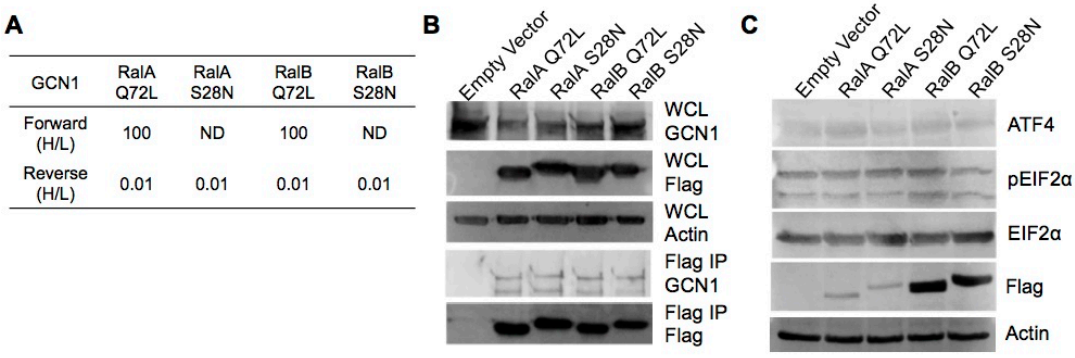

GCN1	RalA Q72L	RalA S28N	RalB Q72L	RalB S28N
Forward (H/L)	100	ND	100	ND
Reverse (H/L)	0.01	0.01	0.01	0.01

Figure 3.4. **Ral proteins interact with GCN1 (A)** The interactome results suggest that the Ral GTPases would interact with GCN1 **(B)** Validation of the Ral-GCN1 interaction by co-immunoprecipitation in HEK-293T cells **(C)** Ral overexpression does not modulate GCN1 activity as evaluated by ATF4 transcription factor, and pEIF2α levels in HCT116 cells

2.5 ERK-2 is a RalB Specific Interacting Protein

As Ral has not previously been liked to ERK signaling, we were surprised to see that ERK2 was identified as a RalB Q72L interacting protein in our SILAC experiment (Figure 3.5A). Using co-IP, we confirmed that RalB selectively interacted with ERK2 (Figure 3.5B). Since much of the divergence of the two Ral isoforms comes from the variation in their C-terminal hyper-variable region (HVR), we wanted to see if the interaction selectivity was also dependent on the HVR. To test this, we used Ral chimera that contained RalB Q72L N-terminal and RalA HVR. This chimera did not interact with ERK2 (Figure 3.5C), suggesting that RalB-

ERK2 interaction is dependent on the C-terminal HVR.

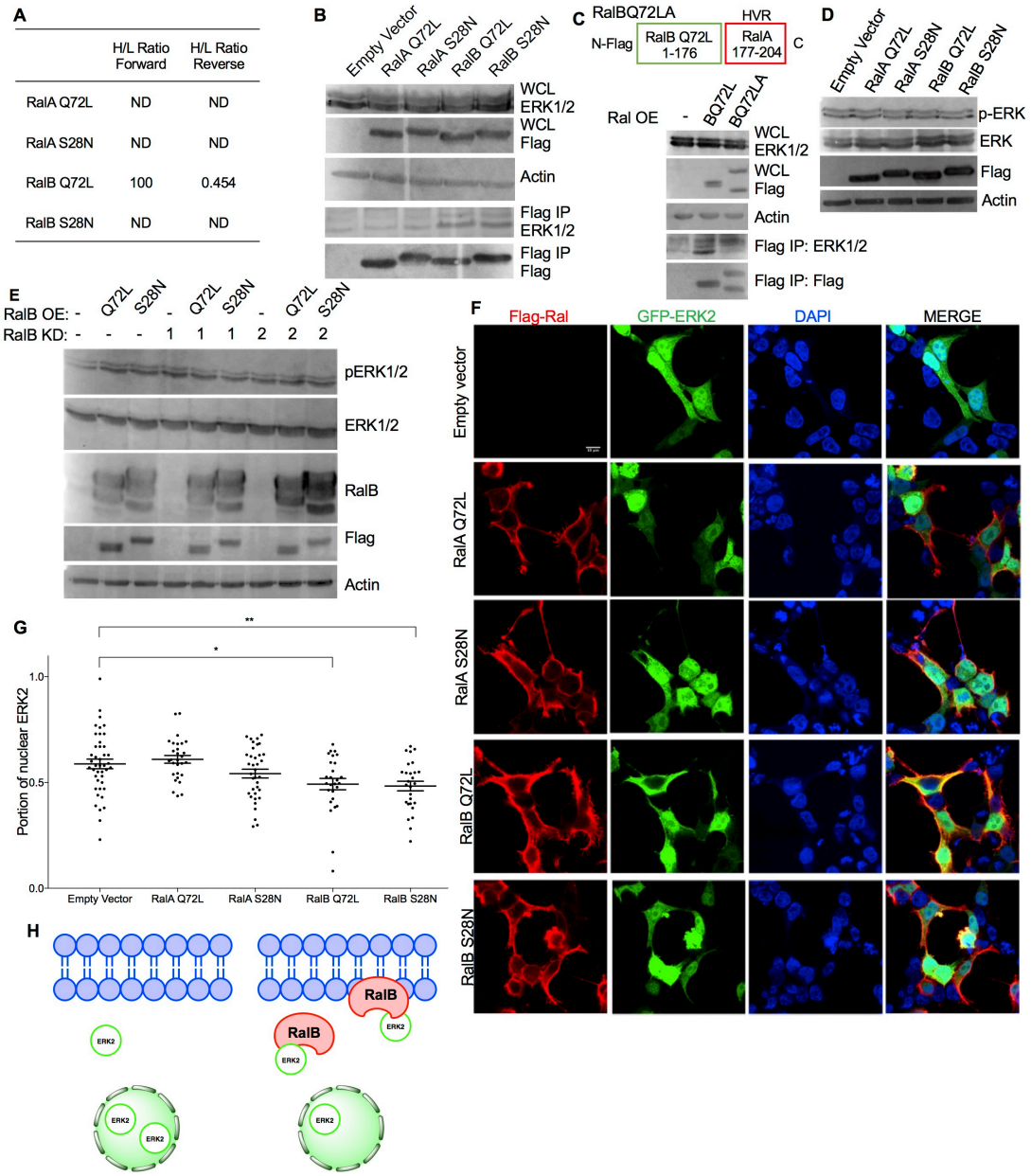

Figure 3.5. RalB selectively interacts with ERK2. **(A)** The Ral interactome results suggesting that RalB selectively would interact with ERK2. **(B)** Validation of the RalB-ERK2 interaction by co-immunoprecipitation in HEK-293T cells **(C)** Co-immunoprecipiation of the RalBQ72LA chimera with ERK2 in HEK-293T Cells. Overexpression of Ral constructs does not modulate phosphorylation of ERK in (**D**) HEK-293T cells and (**E**) HCT116 cells. **(F)** RalB overexpression decreases the ERK2 nuclear/ whole cell ratio. **(G)** Quantification of the signal of ERK2 in the nucleus/ whole cell. The nucleus was determined by DAPI staining. Statistical analysis was done using multiple unpaired students t-tests in Prism 7 software. (**H**) proposed model that shows the RalB-ERK2 interaction leads to decreased ERK2 in the nucleus.

We next wanted to investigate the physiological function of this interaction. We first checked whether expression of RalA/B Q72L or S28N mutant in HEK 293T cells would affect the phosphorylation of ERK. No ERK phosphorylation difference was observed (Figure 3.5D). We also stably knocked down RalB in HCT116 cells and then introduced back RalB. Again, no difference in ERK phosphorylation was observed.

We next investigated if RalB could regulate ERK2 localization. We used a GFP-tagged ERK2 to monitor ERK2 subcellular localization. ERK2 was located in the cytosol and nucleus (Figure 3.5F). We saw that only RalB co-localized with ERK2, and it looked as if the majority of the co-localization occurred on the cell perimeter, possibly the plasma membrane. We then hypothesized that RalB was preventing the nuclear translocation of ERK2. To evaluate this, we compared the amount of nuclear ERK2 signal to the total ERK2 signal for each cell by looking at the ratio of the Raw integrated density for the fluorescence signal in the nucleus (as determined by DAPI staining) compared to the total GFP signal through the entire cell. We found that in RalB overexpressing cells, there was a statistically significant decrease in the ratio of nuclear ERK2 to whole cell ERK2. This suggest that RalB can potentially prevent ERK2 nuclear translocation.

2.6 Inactive RalA and RalB interact with Transferrin Receptor

RalA/B has previously been reported to play a role in receptor promoted endocytosis.[31] It is established that active RalA/B (RalA G23V and RalB G23V) inhibit transferrin internalization. We were therefore intrigued by the proteomic results showing that TfR1 only interacts with the inactive RalA and RalB (Figure 3.6A). Co-IP experiments indeed confirmed that TfR1 only interacts with inactive RalA and RalB (Figure 3.6B).

We next wanted to see if this interaction was dependent on transferrin or iron. To evaluate this, we investigated whether the interaction between ectopically expressed Ral mutants and endogenous TfR1 was affected by 16-hour serum starvation (depletion of

transferrin). There was no difference in the interaction before and after serum starvation suggesting that transferrin is not important for the interaction.

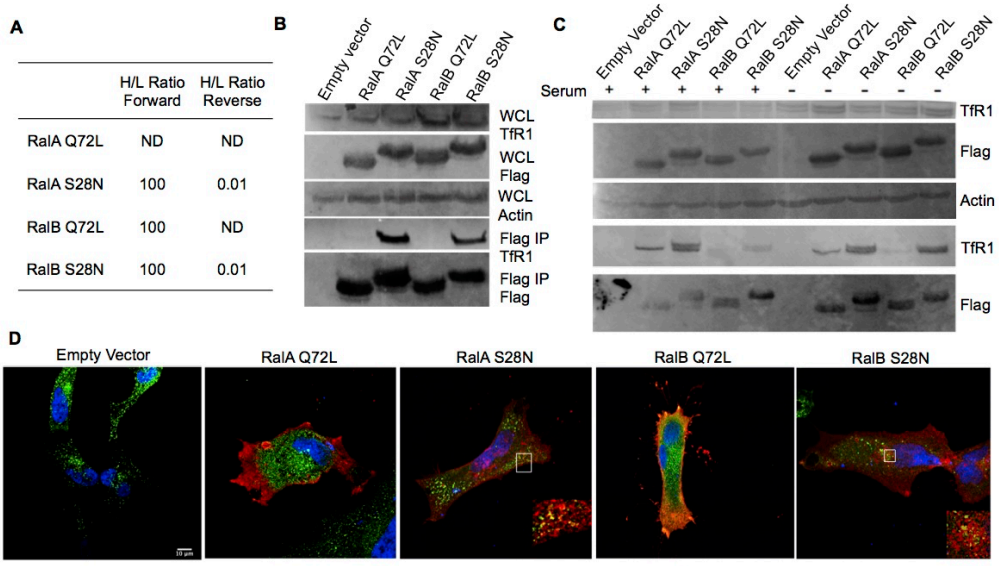

Figure 3.6. Inactive RalA and RalB interact with Transferrin Receptor 1 (TfR1) (A) The Ral interactome results suggesting that inactive RalA and RalB interact with TfR1 **(B)** Validation of the interactome results by co-immunoprecipitation in HEK-293T cells. **(D)** Co-immunoprecipitation of the Ral constructs with endogenous TfR1 after 16hrs of serum starvation in HEK-293T Cells. (**E)** confocal imaging looking at the co-localization of Ral and TfR1 in HeLa cells.

We then hypothesized that maybe the interaction could explain the difference in TfR1 internalization that was previously been reported. It previously was shown that overexpression of active Ral (the Ral G23V mutants) could prevent internalization of 488-transferrin, due to the ability of active Ral to interact with RalBP1 (RLIP76) and modulate the interaction of RalBP1 with machinery that controls endocytosis such as the AP2 complex.[31] We examined the co-localization of Ral mutants and TfR1 in HeLa cells. Cells expressing RalA or RalB Q72L mutants had fewer big TfR1 puncta, but had more diffusive TfR1 signal in the cytosol. Cells expressing the inactive Ral mutants had more large TfR1 puncta but very little diffusive TfR1 signal. Furthermore, RalA S28N and RalB S28N in many cases colocalized with the large TfR1 puncta while the active Ral mutants had very little such co-localization. Our data thus support a model in which inactive RalA and RalB bind TfR and help promote TfR1 trafficking to the

large puncta.

3. Discussion

Here, we have performed a Ral interactome analysis to help identify and understand the differences and similarities between these two highly related small GTPases. We identified ~160 highly confident RalA interacting proteins, and ~80-90 highly confident RalB interacting proteins. The interactome analysis highlights that there are potentially more Ral isoform-specific effector proteins or binding proteins.

We show that Ral, in a nucleotide independent manner, interacts with GCN1. Overexpression of active Ral slightly increases pEIF2α and ATF4 levels suggesting that the interaction maybe important for regulating GCN1 in stress response. Based on localization, it is possible that Ral serves to either bring GCN1 to the ER, or translocate it from the ER, but more studies are needed to confirm this. It is also possible, that there are additional cellular functions of GCN1 that have yet to be explored that the Ral GTPases may be more important for. Our findings, however, show a novel connection of the Ral GTPases and GCN1.

We also found that RalB selectively interacts with ERK2, which was not previously known. By binding to ERK2, Ral decreases ERK2 nuclear localization and thus likely its activity on certain transcription factors. Alternatively, it is possible that RalB recruits ERK2 to the cell membrane to phosphorylate a membrane bound or cytosolic substrate. However, there are still several questions about which ERK substrates are ERK2 selective. Furthermore, it was interesting that RalB only interacted with ERK2, and not EKR1. While some people argue for functional redundancy of the two ERK isoforms, this finding suggests that there may be more differences between these two kinases and that not all functions are redundant.[32] The decreased ERK2 nuclear localization could also play a role in regulating tumorigenesis. Future studies should investigative if RalB could be used as a therapeutic target to regulate ERK2 driven tumorigenesis.

Two well established effectors of the Ral GTPases are Exo84 and Sec5, components of the exocyst complex. It has previously been reported that active RalB is able to promote autophagy.[14] Furthermore, overexpression of active RalA has also been shown to promote exocytosis.[9,31] It has been reported that active RalB inhibits the internalization of transferrin while the inactive RalB does not.[31] This is largely consistent with our observation here. One possible explanation for this could be that inactive RalA/B bind TfR1 and help to traffick TfR1 to the large puncta, while active RalA/B could not because they do not bind to TfR1 Alternatively it is possible that active Ral promotes exocytosis to counter the promotion of endocytosis by inactive Ral, and that the Ral GTPase cycle is important to balance these two cellular processes and maintain cellular homeostasis. Future studies are needed to differentiate these two possibilities and to investigate whether TfR1 could serve as GEF for RalA and RalB.

The Ral GTPases are key players in cancer cell regulation and tumorigenesis. This study highlights that there are many similarities and differences between the two highly related small GTPases. Targeting the Ral proteins is becoming a promising therapeutic option for Ras driven cancers, as Ras induced activation of Ral is necessary for tumorigenesis..[6] Further studying the differences between these GTPases could help elucidate when which isoform should be targeted. Our interactome data thus represents a rich resource that will significantly facilitate further understanding the Ral and other small GTPases.

4. Methods

Reagents. Antibodies to detect ERK (#4696), p-ERK Thr202, Tyr204 (#4370), ATF4 (#11815), pEIF2α(Ser51)(#3398), EIF2α(#5324), RalBP1(#5739), Rabbit-HRP(#7074), Mouse-HRP(#7076), and Flag-Mouse(#8146) were purchased from Cell Signaling Technology. The β-actin (sc-4777) antibody was purchased Santa Cruz Biotechnology. The EXOC2 (Sec5)(# 12751-1-AP) and EXOC8 (Exo84)(# LS-C116539) antibodies were purchased from ProteinTech and LSBio respectively. Anti- FLAG affinity gels (#A2220) and FLAG antibody

(#A8592) were purchased from Sigma. The antibodies to detect TfR1(#84036) and GCN1 (#86139) were purchased from Abcam.

Human RalB shRNAs, (sh1 TRCN0000072953 and sh2, TRCN00002999771), protease inhibitor cocktail, phosphatase inhibitor cocktail and polybrene were purchased from Sigma Aldrich. Puromycin hydrochloride was from GoldBio. FuGENE6 transfection reagent and sequencing grade modified trypsin were purchased from Promega. ECL plus Western blotting detection reagent was purchased from Thermo. The Sep-Pak C18 cartridge was purchased from Waters. The GFP-ERK2 construct was a gift from Dustin Maly (Addgene Plasmid #40777).[33] The mCherry-Sec61 plasmid was a gift from Gia Voeltz (Addgene plasmid #49155). [34]

The pCMV5-Flag-RalA and pCMV5-Flag-RalB constructs were generous gifts from Dr. Maurine Linder. The Q72L and S28N constructs were generated by quick change mutagenesis. The RalBQ72LA chimera was cloned using the pBabepuro-myc-RalB Q72L/A plasmid as CDNA template which was a gift from Christopher Counter (Addgene Plasmid #11121).[19]

C18 seppack cartridges for peptide purification were purchased from Waters.

Cell Culture. All cells were maintained at 37˚C with 5% CO_2. HEK-293T and HeLa cells were cultured in DMEM wih 10% FBS (Invitrogen). HCT116 Cells were culture in McCoy's 5A with 10% FBS (Invitrogen). SILAC DMEM was also purchased from Thermo and supplemented with L-lysine and L-arginine or [$^{13}C_6$,$^{15}N_2$]-L-Lysine and [$^{13}C_6$,$^{15}N_4$]-L-arginine purchased from Sigma and 10% Dialyzed FBS that was already heat inactivated from Thermo.

Generation of Stable Cells. To generate lentivirus, the 5µg of the shRNA constructs purchased from Sigma were co-transfected with 5 μg of pCMV-ΔR8.2 and 1 μg of pM2D.G with FuGene6 in WT-HEK-293T cells. After 12 hours, the media was changed and 24 hours later the virus was collected and cleared of cell debirs by centrifugation (1300 rpm for 5 min) and filtered with

a 0.455 μm filter. To infect, cells were treated with the lentivirus supplemented with 6μg/ mL of polybrene. After 72 hours, cells were treated with 2mg/mL of puromycin. After 1 week, cells were collected and RalB KD efficiency was determined by western blot.

Western Blots. For detection of phosphorylated proteins, the samples were lysed with 4% SDS lysis buffer supplemented with universal cell nuclease (Thermo), protease inhibitor cocktail and phosphatase inhibitor cocktail. For all western blots and experiments, protein concentration was determined using either a Bradford (Thermo) or BCA Assay (Thermo). After denaturing the samples, proteins were resolved by SDS PAGE gels (12% unless otherwise specified). The gel was run at 200V for 50 min. Proteins were transferred to PVDF membrane at 330mA for 2hrs in ice cold transfer buffer. Membranes were blocked with 5% BSA in TBST (0.1% Tween-20, 25 mM Tris-HCl pH 7.6, 150 mM NaCl) for 1 hours. Antibodies were added following the manufactures protocol.

Ral Interactome. The Ral interactome was preformed using the published protocol.[27] Briefly, HEK-239T cells were cultured in heavy and light supplemented DMEM with 10% FBS. At 60% confluency, cells were transfected either with empty vector or the Ral constructs. After 30 hours, the samples were collected and washed with PBS three times. The samples were lysed with 1% NP40 lysis buffer (25 mM Tris-HCl pH 8.0, 150 mM NaCl, 10% glycerol, and 1 % Nonidet P-40) supplemented with protease inhibitor cocktail. After normalizing protein concentration, flag-affinity gel was added to the samples for 2 hours at 4˚C. The samples were washed with 0.2% NP40 IP wash buffer (25 mM Tris-HCl pH 8.0, 150 mM NaCl, 0.2% NP40) with 1mL of buffer three times. After the third wash, the heavy and light samples were mixed and washed two additional times. The Flag tagged proteins and their interacting proteins were eluted by boiling the samples at 95˚C for 10 minutes in 1% SDS elution buffer (1% SDS, 25mM Tris-HCL pH=7.4, and 150mM NaCl2l). After boiling the samples, the proteins were precipitated using water, methanol and chloroform. The resulting pellet was resuspended and denatured in

6M Urea with 10mM DTT, and 50mM Tris-HCl pH=8.0 at room temperature for 1 hour. The samples were incubated with 40mM iodoacetomide at room temperature for 1 hour to alkylate the proteins. DTT was then added for 1 hour at room temperature to stop the alkylation. The samples were then diluted with 50mM Tris-HCl pH=8.0 and 1mM $CaCl_2$. 1μg of trypsin was added, and the samples were placed at 37˚C for 18 hours. To quench the trypsin, trifluoroacetic acid (0.1% diluted in water) was added. The peptides were desalted using a Sep-pak C18 catride. The peptides were dried using a lyophilizer, an analyzed by LC-MS/MS analysis (LTQ-Orbitrap Elite mass spectrometry coupled with nanoLC). The peptides were reconstituted in 2% acetonitrile with 0.5% formic acid and subjected to LC-MS/MS analysis using the same method previously repored.[27]

Co-Immunoprecipitation. The same method was used as previously reported.[27] Briefly, constructs were overexpressed in HEK-293T cells using the standard FuGENE 6 protocol (1:3 ratio of DNA: FuGENE6. After 24-30 hours, cells were collected and washed with PBS two times. The cells were lysed with 1% NP40 lysis buffer (25 mM Tris-HCl pH 8.0, 150 mM NaCl, 10% glycerol, and 1 % Nonidet P-40) supplemented with protease inhibitor cocktail. Protein concentration was determined using a standard Bradford assay. After normalizing the input, anti-flag affinity gel was pre-washed with 0.2% IP wash buffer (25 mM Tris-HCl pH 8.0, 150 mM NaCl, 0.2% NP-40). The samples were placed on a rocker at 4˚C for 2 hours. After which they were washed three times with 1mL of 0.2% IP wash buffer. The samples were boiled at 95˚C for 5-7 minutes and analyzed by western blots.

Immunofluorescence and Live Cell Imaging. Between 100,000-300,000 cells were seeded in glass bottom dishes (MaTak). The next day, respective constructs were transfected (1-2μg of plasmid per plate) using FuGENE6. After 24-30 hours, cells were either serum starved for 12-16 hours or fixed with methanol or 4% paraformaldehyde (dependent on the manufactures protocols for different antibodies). The membrane was pearmabilized with 0.25% Triton-X in

PBS for 10 minutes. The samples were then washed three times with PBS. After the last wash, the samples were blocked in 1% BSA in TBST for 1 hour at room temperature. The antibodies (except for Flag) were added at the recommended dilution overnight at 4˚C. The next day, the samples were washed three times, for 5 minutes each, with TBST. Flag antibody was added (1:800) in 1% BSA in TBST at room temperature for 1 hour. After an additional three washes, the samples were again washed with TBST and then incubated with the respective secondary antibodies (1:1000) for 1 hour at room temperature in 1% BSA in TBST. The samples were washed three additional times with TBST for 5 minutes each time, and subsequently mounted with DAPI Fluoromount, or Fluoromount G. Data was analyzed using FIJI software.[35]

REFERENCES

(1) Colicelli, J. Human RAS superfamily proteins and related GTPases. *Sci STKE* **2004,** *2004* (250), RE13.

(2) Wennerberg, K.; Rossman, K. L.; Der, C. J. The Ras superfamily at a glance. *J Cell Sci* **2005,** *118* (Pt 5), 843.

(3) Bos, J. L. All in the family? New insights and questions regarding interconnectivity of Ras, Rap1 and Ral. *EMBO J* **1998,** *17* (23), 6776.

(4) Bos, J. L. ras oncogenes in human cancer: a review. *Cancer Res* **1989,** *49* (17), 4682.

(5) Yan, C.; Theodorescu, D. RAL GTPases: Biology and Potential as Therapeutic Targets in Cancer. *Pharmacol Rev* **2018,** *70* (1), 1.

(6) Shirakawa, R.; Horiuchi, H. Ral GTPases: crucial mediators of exocytosis and tumourigenesis. *J Biochem* **2015,** *157* (5), 285.

(7) Gentry, L. R.; Martin, T. D.; Reiner, D. J.; Der, C. J. Ral small GTPase signaling and oncogenesis: More than just 15minutes of fame. *Biochim Biophys Acta* **2014,** *1843* (12), 2976.

(8) Ikeda, M.; Ishida, O.; Hinoi, T.; Kishida, S.; Kikuchi, A. Identification and characterization of a novel protein interacting with Ral-binding protein 1, a putative effector protein of Ral. *J Biol Chem* **1998,** *273* (2), 814.

(9) Moskalenko, S.; Henry, D. O.; Rosse, C.; Mirey, G.; Camonis, J. H.; White, M. A. The exocyst is a Ral effector complex. *Nat Cell Biol* **2002,** *4* (1), 66.

(10) Moskalenko, S.; Tong, C.; Rosse, C.; Mirey, G.; Formstecher, E.; Daviet, L.; Camonis, J.; White, M. A. Ral GTPases regulate exocyst assembly through dual subunit interactions. *J Biol Chem* **2003,** *278* (51), 51743.

(11) Neel, N. F.; Martin, T. D.; Stratford, J. K.; Zand, T. P.; Reiner, D. J.; Der, C. J. The RalGEF-Ral Effector Signaling Network: The Road Less Traveled for Anti-Ras Drug Discovery. *Genes Cancer* **2011,** *2* (3), 275.

(12) Martin, T. D.; Samuel, J. C.; Routh, E. D.; Der, C. J.; Yeh, J. J. Activation and involvement of Ral GTPases in colorectal cancer. *Cancer Res* **2011,** *71* (1), 206.

(13) Atala, A. Phosphorylation of RalB is Important for Bladder Cancer Cell Growth and Metastasis Editorial Comment. *J Urology* **2011,** *185* (6), 2423.

(14) Bodemann, B. O.; Orvedahl, A.; Cheng, T.; Ram, R. R.; Ou, Y. H.; Formstecher, E.; Maiti, M.; Hazelett, C. C.; Wauson, E. M.; Balakireva, M.et al. RalB and the exocyst mediate the cellular starvation response by direct activation of autophagosome assembly. *Cell* **2011,** *144* (2), 253.

(15) Camonis, J. H.; White, M. A. Ral GTPases: corrupting the exocyst in cancer cells. *Trends Cell Biol* **2005,** *15* (6), 327.

(16) Chien, Y.; Kim, S.; Bumeister, R.; Loo, Y. M.; Kwon, S. W.; Johnson, C. L.; Balakireva, M. G.; Romeo, Y.; Kopelovich, L.; Gale, M., Jr.et al. RalB GTPase-mediated activation of the IkappaB family kinase TBK1 couples innate immune signaling to tumor cell survival. *Cell* **2006,** *127* (1), 157.

(17) Feig, L. A. Ral-GTPases: approaching their 15 minutes of fame. *Trends Cell Biol* **2003,** *13* (8), 419.

(18) Frankel, P.; Aronheim, A.; Kavanagh, E.; Balda, M. S.; Matter, K.; Bunney, T. D.; Marshall, C. J. RalA interacts with ZONAB in a cell density-dependent manner and regulates its transcriptional activity. *EMBO J* **2005,** *24* (1), 54.

(19) Lim, K. H.; Baines, A. T.; Fiordalisi, J. J.; Shipitsin, M.; Feig, L. A.; Cox, A. D.; Der, C. J.; Counter, C. M. Activation of RalA is critical for Ras-induced tumorigenesis of human cells. *Cancer Cell* **2005,** *7* (6), 533.

(20) Lim, K. H.; O'Hayer, K.; Adam, S. J.; Kendall, S. D.; Campbell, P. M.; Der, C. J.;

Counter, C. M. Divergent roles for RalA and RalB in malignant growth of human pancreatic carcinoma cells. *Curr Biol* **2006,** *16* (24), 2385.
(21) Neel, N. F.; Rossman, K. L.; Martin, T. D.; Hayes, T. K.; Yeh, J. J.; Der, C. J. The RalB small GTPase mediates formation of invadopodia through a GTPase-activating protein-independent function of the RalBP1/RLIP76 effector. *Mol Cell Biol* **2012,** *32* (8), 1374.
(22) Oxford, G.; Owens, C. R.; Titus, B. J.; Foreman, T. L.; Herlevsen, M. C.; Smith, S. C.; Theodorescu, D. RalA and RalB: antagonistic relatives in cancer cell migration. *Cancer Res* **2005,** *65* (16), 7111.
(23) Shipitsin, M.; Feig, L. A. RalA but not RalB enhances polarized delivery of membrane proteins to the basolateral surface of epithelial cells. *Mol Cell Biol* **2004,** *24* (13), 5746.
(24) Tecleab, A.; Zhang, X.; Sebti, S. M. Ral GTPase down-regulation stabilizes and reactivates p53 to inhibit malignant transformation. *J Biol Chem* **2014,** *289* (45), 31296.
(25) Wang, H.; Owens, C.; Chandra, N.; Conaway, M. R.; Brautigan, D. L.; Theodorescu, D. Phosphorylation of RalB is important for bladder cancer cell growth and metastasis. *Cancer Res* **2010,** *70* (21), 8760.
(26) Gentry, L. R.; Nishimura, A.; Cox, A. D.; Martin, T. D.; Tsygankov, D.; Nishida, M.; Elston, T. C.; Der, C. J. Divergent roles of CAAX motif-signaled posttranslational modifications in the regulation and subcellular localization of Ral GTPases. *J Biol Chem* **2015,** *290* (37), 22851.
(27) Zhang, X.; Cao, J.; Miller, S. P.; Jing, H.; Lin, H. Comparative Nucleotide-Dependent Interactome Analysis Reveals Shared and Differential Properties of KRas4a and KRas4b. *ACS Cent Sci* **2018,** *4* (1), 71.
(28) Huang da, W.; Sherman, B. T.; Lempicki, R. A. Systematic and integrative analysis of large gene lists using DAVID bioinformatics resources. *Nat Protoc* **2009,** *4* (1), 44.
(29) Huang, D. W.; Sherman, B. T.; Tan, Q.; Kir, J.; Liu, D.; Bryant, D.; Guo, Y.; Stephens, R.; Baseler, M. W.; Lane, H. C.et al. DAVID Bioinformatics Resources: expanded annotation database and novel algorithms to better extract biology from large gene lists. *Nucleic Acids Res* **2007,** *35* (Web Server issue), W169.
(30) Mobasheri, A.; Pestov, N. B.; Papanicolaou, S.; Kajee, R.; Cozar-Castellano, I.; Avila, J.; Martin-Vasallo, P.; Foster, C. S.; Modyanov, N. N.; Djamgoz, M. B. Expression and cellular localization of Na,K-ATPase isoforms in the rat ventral prostate. *BJU Int* **2003,** *92* (7), 793.
(31) Jullien-Flores, V.; Mahe, Y.; Mirey, G.; Leprince, C.; Meunier-Bisceuil, B.; Sorkin, A.; Camonis, J. H. RLIP76, an effector of the GTPase Ral, interacts with the AP2 complex: involvement of the Ral pathway in receptor endocytosis. *J Cell Sci* **2000,** *113 (Pt 16)*, 2837.
(32) Busca, R.; Pouyssegur, J.; Lenormand, P. ERK1 and ERK2 Map Kinases: Specific Roles or Functional Redundancy? *Front Cell Dev Biol* **2016,** *4*, 53.
(33) Hari, S. B.; Merritt, E. A.; Maly, D. J. Conformation-selective ATP-competitive inhibitors control regulatory interactions and noncatalytic functions of mitogen-activated protein kinases. *Chem Biol* **2014,** *21* (5), 628.
(34) Zurek, N.; Sparks, L.; Voeltz, G. Reticulon short hairpin transmembrane domains are used to shape ER tubules. *Traffic* **2011,** *12* (1), 28.
(35) Schindelin, J.; Arganda-Carreras, I.; Frise, E.; Kaynig, V.; Longair, M.; Pietzsch, T.; Preibisch, S.; Rueden, C.; Saalfeld, S.; Schmid, B.et al. Fiji: an open-source platform for biological-image analysis. *Nat Methods* **2012,** *9* (7), 676.

CHAPTER 4

DIRECT COMPARISON OF SIRT2 INHIBITORS: POTENCY, SPECIFICTY, ACTIVITY-DEPENDENT INHIBITION, AND ON-TARGET ANTICANCER ACTIVITIES[3]

Abstract

Sirtuin inhibitors have attracted much interest due to the involvement of sirtuins in various biological processes. Several SIRT2-selective inhibitors have been developed, and some exhibit anticancer activities. To facilitate the choice of inhibitors in future studies and the development of better inhibitors, we directly compared several reported SIRT2-selective inhibitors: AGK2, SirReal2, Tenovin-6, and TM. In vitro, TM is the most potent and selective inhibitor, and only TM could inhibit the demyristoylation activity of SIRT2. SirReal2, Tenovin-6, and TM all showed cytotoxicity in cancer cell lines, with Tenovin-6 being the most potent, but only TM showed cancer cell-specific toxicity. All four compounds inhibited the anchorage-independent growth of HCT116 cells, but the effect of TM was most significantly affected by SIRT2 overexpression, suggesting that the anticancer effect of TM depends more on SIRT2 inhibition. These results not only provide useful guidance about choosing the right SIRT2 inhibitor in future studies, but also suggest general practices that should be followed for small molecule inhibitor development activities.

---

[3]This is a revised version of the published paper: Spiegelman, N.A., Price, I.R., Jing, H., Wang, M., Yang, M., Cao, J., Hong, J.Y., Zhang, X., Aramsangtienchai, P., Sadhukhan, S., Lin, H. Direct Comparison of SIRT2 Inhibitors: Potency, Specificity, Activity-Dependent Inhibition, and On-Target Anticancer Activitys . *ChemMedChem,* 13, 1890-1894 (2018).
For this paper, I (NAS) designed and performed all the biochemical studies except those noted below, and synthesized some of the TM. I.R.P and X.Z. purified Sirtuin enzymes. H.J. and J.Y.H obtained preliminary *in vitro* results, and H.J. obtained preliminary in cell data. M.W. generated the stable overexpressing SIRT2 HCT-116 cell line. J.C. assisted with the in-cell inhibition assays. M.Y. synthesized TM. P.A. and S.S. synthesized and purified substrate peptides. H.L. supervised and directed the study. N.A.S. and H.L. wrote the manuscript, all authors approved of the final manuscript.

1. Introduction

The nicotinamide adenine dinucleotide (NAD)-dependent protein lysine deacylases, or sirtuins, have attracted a lot of attention as potential targets to treat cancer and various other diseases such as neurodegeneration.[1] There are seven mammalian sirtuins, SIRT1-SIRT7, which have been shown to play important roles in vivo by regulating processes such as DNA repair, transcription, cell cycle, and metabolism.[2]

The physiological function of sirtuins is a result of their enzymatic activity on different substrate proteins. Sirtuins can remove various acyl modifications from lysine residues on histone and non-histone proteins. SIRT1, SIRT2 and SIRT3 can efficiently deacetylate proteins, while SIRT5 preferentially hydrolyzes succinyl and malonyl groups, and SIRT1, SIRT2, SIRT3, SIRT6, and SIRT7 can all hydrolyze long-chain fatty acyl groups. [3-5]

Among the mammalian seven sirtuins, inhibition of SIRT2 has been reported to have beneficial effects in cancer and neurodegenerative diseases.[1,2] SIRT2 plays an important role in regulating the cell cycle, oxidative stress response, metabolism, apoptosis, autophagy, differentiation, and aging.[1,2,6-15] Initial studies presented conflicting results that suggested SIRT2 has both tumor suppressing and promoting roles.[16-20] More recently, it has been shown that SIRT2 depletion, or inhibition, has anticancer effects.[16,21] However, the full potential of inhibiting SIRT2 as a therapeutic option requires the development of potent and selective SIRT2 inhibitors. In the past decade, several SIRT2 inhibitors have been reported. Several of them, AGK2, SirReal2, Tenovin-6, and a thiomyristoyl lysine compound TM (Figure 4.1) are commercially available.

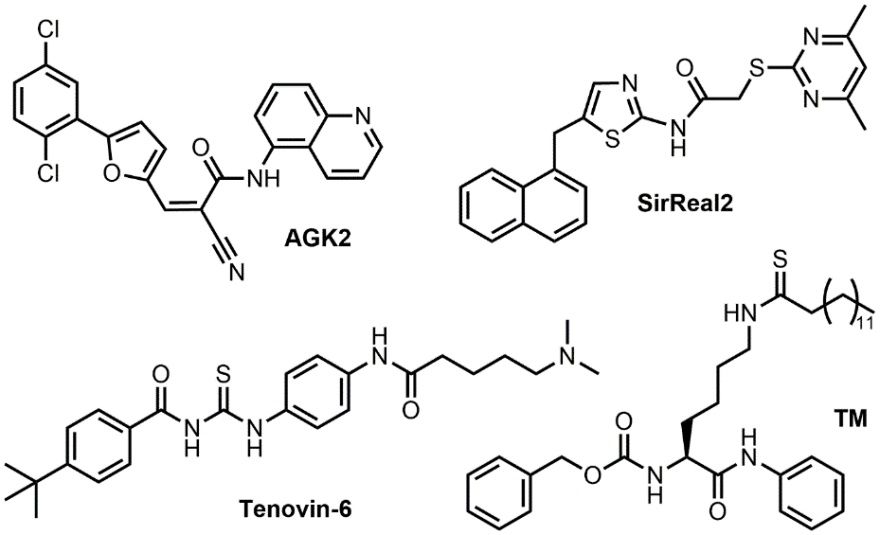

Figure 4.1. Structures of SIRT2 inhibitors AGK2, SirReal2, Tenovin-6, and TM.

AGK2 was identified from a screening of 200 compounds as a potent SIRT2 inhibitor that could rescue α-synuclein-mediated toxicity.[22] It has also been reported to exhibit an anticancer effect in a few cancer cells.[23] SirReal2 was also identified through a compound screening that was aimed at identifying more potent and selective sirtuin inhibitors.[24] However, there have not been any studies reported regarding its effect on cancer cells. Tenovin-6 was identified when screening compounds that could activate the tumor suppressor p53.[25] Tenovin-6 has been shown to effectively inhibit SIRT1 and SIRT2 in cells, and shows promising anticancer activity. Recently, our lab developed TM, a mechanism-based selective SIRT2 inhibitor. TM exhibits broad anticancer effects and promotes the degradation of the c-Myc oncoprotein in several cancer cell lines.[16] TM exhibits broad anticancer effects and promotes the degradation of the c-Myc oncoprotein in several cancer cell lines. Given the availability of different SIRT2 inhibitors, we reasoned that a direct comparison would be useful to help users choose the right compounds for the proper applications. This is especially true because in most studies, only in vitro IC_{50} values (concentrations that lead to 50% of SIRT2 inhibition) were reported, which is known to be dependent on the exact experimental conditions used. Thus, it is still ambiguous as to which inhibitor is the most potent, selective, and exhibits the best

anticancer effect. Furthermore, it is also unclear which enzymatic activity (deacetylation or defatty-acylation) these inhibitors are potent against. Here, we directly compare the potency and selectivity of these compounds to help identify which inhibitor should be used to study the function of SIRT2, and explore its therapeutic potential.

2. Results and Discussion

The SIRT2 inhibition potency and selectivity of the four inhibitors was determined using a high-performance liquid chromatography (HPLC)-based assay. In this assay, we first incubated the enzyme with the inhibitors for 15 min and then added the substrates to initiate the reactions. The activity of the enzymes was detected using two different substrates, histone H3

Table 4.1. In vitro IC_{50} Values (μM) of AGK2, SirReal2, Tenovin-6 and TM at inhibiting Sirtuin enzymatic activity. Values shown are an average and standard deviation from three independent experiments).

	AGK2	**SirReal2**	**Tenovin-6**	**TM**
SIRT1 H3K9Ac	42 ± 4	82 ± 14	26 ± 10	26 ± 15
SIRT2 H3K9Ac	8 ± 5	0.23 ± 0.08	9 ± 7	0.04 ± 0.02
SIRT2 H3K9Myr	>100	>100	>200	0.05 ± 0.03
SIRT3 H3K9Ac	>50	>50	>50	>50
SIRT6 H3K9Myr	>100	>200	>200	>200
Selectivity[a]	5	357	3	650

[a] (IC_{50} for SIRT1 on H3K9Ac) / (IC_{50} for SIRT2 on H3K9Ac)

lysine 9 (H3K9) acetyl (H3K9Ac) and myristoyl (H3K9Myr) peptides. We determined the IC_{50} values for inhibiting the deacetylation activity of SIRT1-3 and the demyristoylation activity of SIRT2 and SIRT6 (Table 4.1). We found TM was the most potent and selective SIRT2 inhibitor

among all the tested compounds. TM was able to inhibit both the deacetylation (IC_{50} 0.038 μM) and demyristoylation (IC_{50} 0.049 μM) activity of SIRT2. Furthermore, TM is the most selective inhibitor as it inhibited SIRT2 activity 650-fold more efficiently than it could inhibit SIRT1, and it essentially did not inhibit SIRT3 or SIRT6.

SirReal2 inhibits the deacetylation activity of SIRT2 with a relatively low IC50 value of 0.23 μM, however, consistent with a recent report it was unable to inhibit the demyristoylation activity of SIRT2 at the highest concentration tested.[26] AGK2 and Tenovin-6 inhibited both SIRT1 and SIRT2 deacetylation with similar IC50 values, suggesting that these two inhibitors are not very selective. Like SirReal2, these compounds did not inhibit the demyristoylation activity of SIRT2 at the highest concentration tested.

Table 4.2. In vitro IC_{50} (μM) values for inhibition of SIRT2 deacetylation and demyristoylation activity without pre-incubating SIRT2 with the inhibitors and NAD+.

	deacetylation	demyristoylation
AGK2	10 ± 8	>200
SirReal2	0.16 ± 0.01	>100
Tenovin-6	24 ± 9	>200
TM	0.04 ± 0.01	>100

Because competitive inhibitors do not require pre-incubating the enzyme and inhibitor, while the mechanism-based inhibitor TM requires pre-incubation to reach maximum SIRT2 inhibition, we also determined the IC50 values for the inhibitors without pre-incubation (Table 4.2). As expected, the IC50 values for the competitive inhibitors with and without pre-incubation were comparable. For TM, the IC50 values for inhibiting SIRT2 deacetylation were similar with and without pre-incubation, but TM did not inhibit SIRT2 demyristoylation activity without pre-incubation.

In the absence of pre-incubation, TM needs to compete with H3K9Ac or H3K9Myr for

binding to SIRT2. H3K9Myr likely binds much stronger than TM because of the extra hydrogen bonding provided by the peptide backbone, making TM ineffective at inhibiting demyristoylation. However, TM likely binds stronger than H3K9Ac to SIRT2 because the thiomyristoyl group contributes a lot to the binding free energy because of the strong hydrophobic interaction, rendering TM an efficient inhibitor for the deacetylation activity of SIRT2. However, with pre-incubation, TM will first form an ADP-ribosyl covalent intermediate, which binds to SIRT2 much more tightly than TM due to binding interactions from both the ADP-ribose and TM. This covalent intermediate can efficiently prevent both the H3K9Ac and H3K9Myr peptides from binding to SIRT2, rendering TM an effective inhibitor for both deacetylation and demyristoylation under pre-incubation conditions.

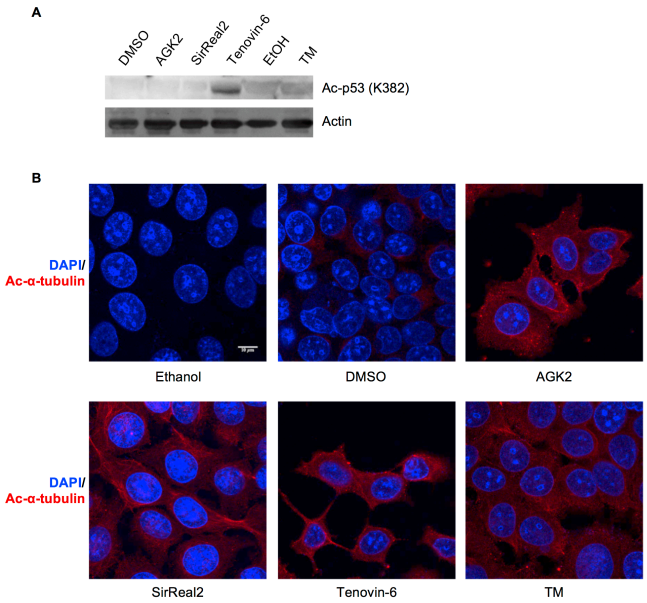

Figure 4.2. Evaluation of the inhibition of SIRT1 and SIRT2 by different inhibitors in cells. (A) Detection of acetyl p53 (Ac-p53) levels in MCF-7 cells after 6-hour treatment with indicated inhibitors and 200 nM of TSA, an HDAC inhibitor. **(B)** Detection of acetyl α-tubulin (Ac-α-tubulin) levels by immunofluorescence in MCF-7 cells after 6-hour treatment with indicated inhibitors.

For other inhibitors that are not mechanism-based, the inhibitors are competitive with the H3K9Ac or H3K9Myr peptides. Because H3K9Myr binds SIRT2 more tightly than H3K9Ac, the inhibitors cannot effectively compete with H3K9Myr, making them ineffective at

inhibiting the demyristoylation activity of SIRT2.

To further study the selectivity of these SIRT2 inhibitors, we next examined their effects on the acetylation levels of known SIRT1 and SIRT2 substrates. The tumor suppressor p53 is a well-established SIRT1 deacetylation target.[27] To determine if the compounds can efficiently inhibit SIRT1 in cells, we looked at the acetylation levels of p53 in MCF-7 cells after treating the cells with the inhibitors. Only Tenovin-6 increased p53 acetylation (Figure 4.2A), which is consistent with a previous report showing that Tenovin-6 can increase Ac-p53 levels through SIRT1 inhibition.[24] These results suggest that only Tenovin-6 inhibits the deacetylation activity of SIRT1 in cells.

To examine the inhibition of SIRT2 in cells, we detected acetylation levels on α-tubulin, a well-established SIRT2 substrate, using immunofluorescence after inhibitor treatment.[10] As expected, all the compounds increased the acetylation of α-tubulin in MCF-7 cells at 25μM (Figure 4.2B). Thus, it appears that all the compounds can inhibit SIRT2's tubulin deacetylation activity. Tenovin-6, with an in vitro IC_{50} value of 9 μM for SIRT2 deacetylation, was able to inhibit tubulin deacetylation in cells at 25 μM. TM and SirReal2, with much lower in vitro IC50 values for SIRT2 deacetylation, still require tens of μM concentrations to inhibit tubulin deacetylation. Differences in cellular uptake and solubility of the inhibitors may lead to this observation. The in vitro and in cell inhibition of SIRT1 is also consistent with this explanation. For example, both TM and Tenovin-6 inhibit SIRT1 in vitro with an IC_{50} values of ~26 μM, but in cells at 25 μM, only Tenovin-6 was able to inhibit SIRT1 (measured by p53 deacetylation). Thus, TM is the most potent and selective in vitro SIRT2 inhibitor and the SIRT2 selectivity is maintained in cells, while Tenovin-6 is not very selective for SIRT2, but it may have better solubility and cellular uptake.

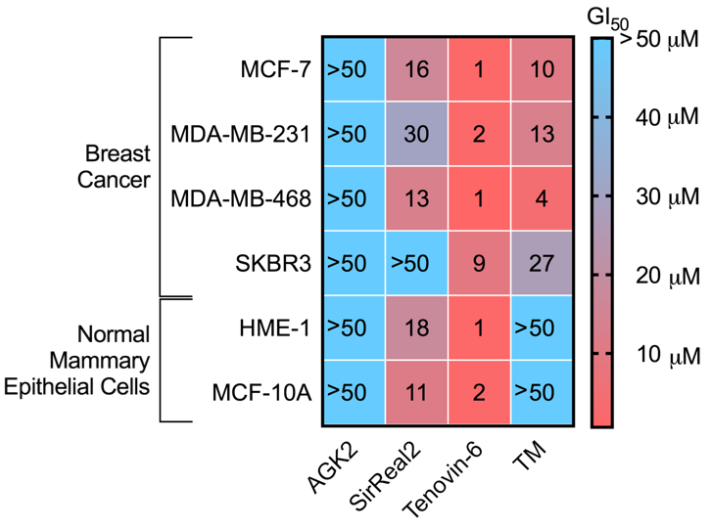

Figure 4.3. Heat map of GI_{50} (μM) values of different SIRT2 inhibitors in various breast cancer and normal breast cell lines. The values represent the average of three independent experiments done in duplicate.

To evaluate the anticancer effect of these four inhibitors, we first looked at cytotoxicity of these compounds in several breast cancer cell lines (MDA-MB-468, MDA-MB-231, MCF-7, SK-BR-3) and two normal mammary epithelial cell lines (MCF10A and HME-1 cells). (Figure 4.3, Table 4.3, Figure 4.4) To evaluate the cytotoxicity, we looked at the GI_{50} value, or the small molecule inhibitor concentration which inhibits 50% of cell growth. Tenovin-6 was

Table 4.3. GI_{50} values (in μM) of different SIRT2 inhibitors in various breast cancer and normal breast cell lines. The values are average of three independent experiments each done in duplicate.

	AGK2	SirReal2	Tenovin-6	TM
MCF-7	>50	16.3 ± 0.2	1.24 ± 0.05	10.3 ± 0.7
MDA-MB-231	>50	30 ± 10	1.6 ± 0.4	13 ± 4
MDA-MB-468	>50	13 ± 4	0.61 ± 0.05	4 ± 1
SK-BR-3	>50	>50	9.3 ± 1.7	27 ± 7
HME-1	>50	18 ± 2	1.4 ± 0.2	>50
MCF-10A	>50	11 ± 2	1.7 ± 0.3	>50

The most potent compound, exhibiting GI_{50} values of a few μM. The anticancer effect of SirReal2 had not previously been studied, it was interesting to note that it had a modest effect on several of the cell lines tested, including the normal mammary epithelial cell lines. TM was not as potent as Tenovin-6, but was more potent than SirReal2. More interestingly, TM was more potent in the cancer cell lines than in the normal mammary epithelial cell lines (GI_{50} >50 μM in MCF10A and HME-1 cells), suggesting it selectively targets cancer cells. AGK2 had very weak effects on the cell proliferation of the cell lines tested, with all the GI_{50} values >50 μM.

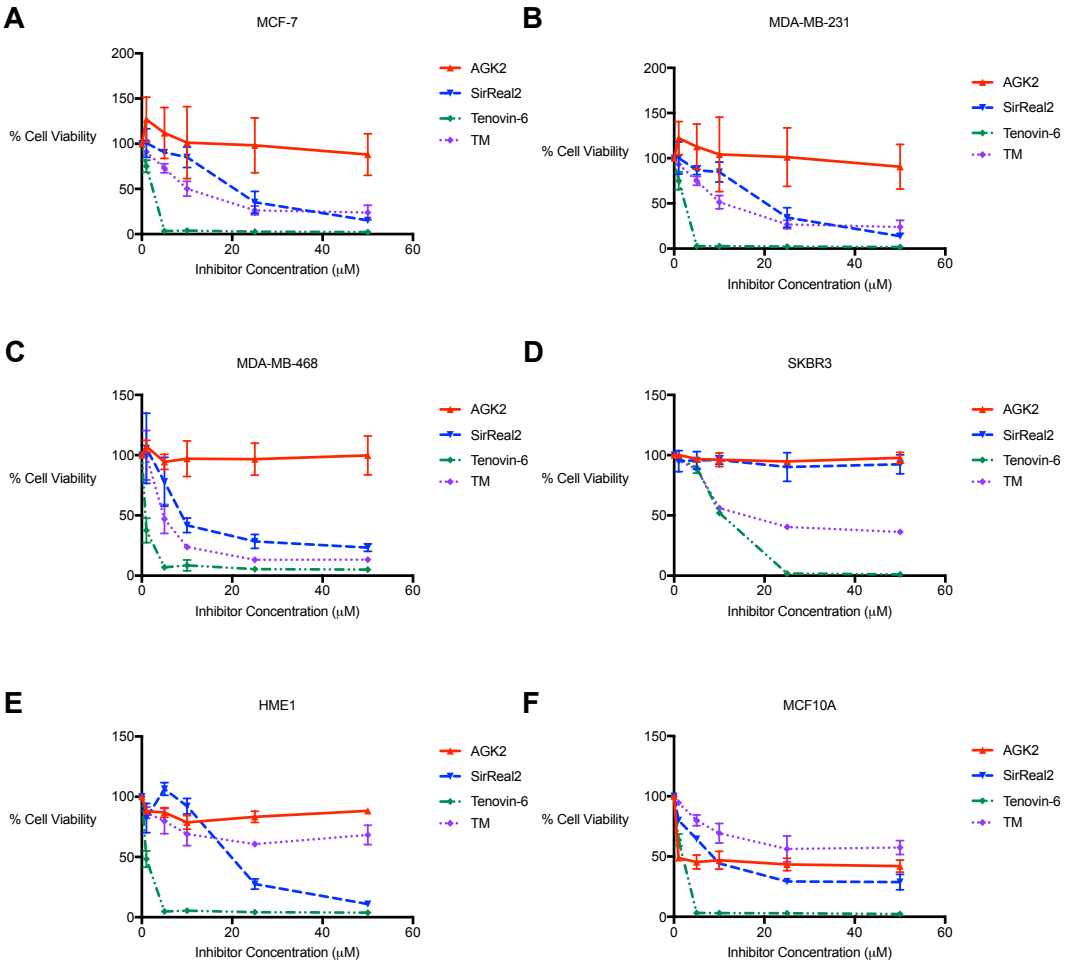

Figure 4.4. Inhibition of cell viability curves from one representative trial of at least three independent experiments. (A) MCF-7 cells, **(B)** MDA-MB-231 cells, **(C)** MDA-MB-468 cells, **(D)** SK-BR-3 cells, **(E)** HME-1 cells, **(F)** MCF-10A cells.

We next determined the GI_{50} values of these inhibitors in various other cancer cell lines, including colon cancer (HCT116, SW948, and HT29), lung cancer (A549 and H520), leukemia (K562), cervical cancer (HeLa), and pancreatic cancer (ASPC1 and CFPAC1) cell lines (Figure 4.5, Table 4.4, and Figure 4.6). Like the results obtained with breast cancer cell lines, Tenovin-6 was the most potent compound in almost every cell line tested. TM was the second most potent compound, followed by SirReal2 in almost all of the cell lines tested, while AGK2 was in general the least potent compound. As AGK2 efficiently inhibits the deacetylation

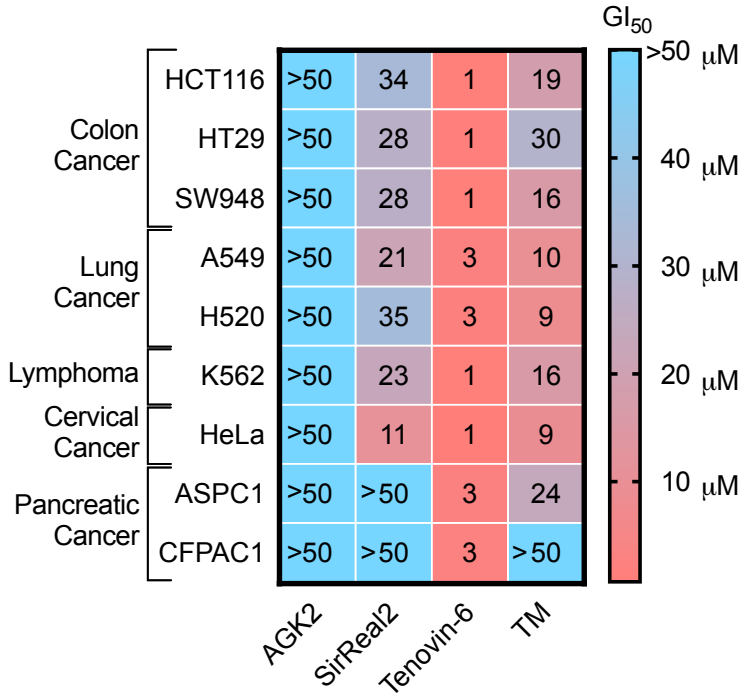

Figure 4.5. Heat map of GI_{50} values (μM) of different SIRT2 inhibitors in various cancer cell lines. The values represent an average of three independent experiments done in duplicate.

of α-tubulin, but it is not particularly toxic to cancer cells, our data suggests that inhibiting tubulin deacetylation does not contribute to the anticancer activity of these inhibitors.

Table 4.4 GI_{50} values (μM) of different SIRT2 inhibitors in various cancer cell lines. The values are average and standard deviation of three independent experiments (except those noted) each done in duplicate.

Cancer type	Cell Line	AGK2	SirReal2	Tenovin-6	TM
Colon	HCT116	>50	34 ± 1*	1.34 ± 0.05	19 ± 0.8
	HT29	>50	28 ± 2	1.4 ± 0.2	30 ± 3
	SW948	>50	27.6 ± 0.8*	1.05 ± 0.08	16 ± 2*
Lung	A549	>50	21 ± 3	3 ± 1	10 ± 5
	H520	>50	35 ± 1	2.6 ± 0.2	8.6 ± 1.2
Lukemia	K562	>50	23 ± 6	0.94 ± 0.09	16 ± 2
Cervical	HeLa	>50	11 ± 2	0.7 ± 0.1	9.1 ± 0.8
Pancreatic	ASPC1	>50	>50	3.0 ± 0.3	24 ± 5
	CFPAC1	>50	>50	3.2 ± 0.3	>50

*This value was determined by two independent experiments.

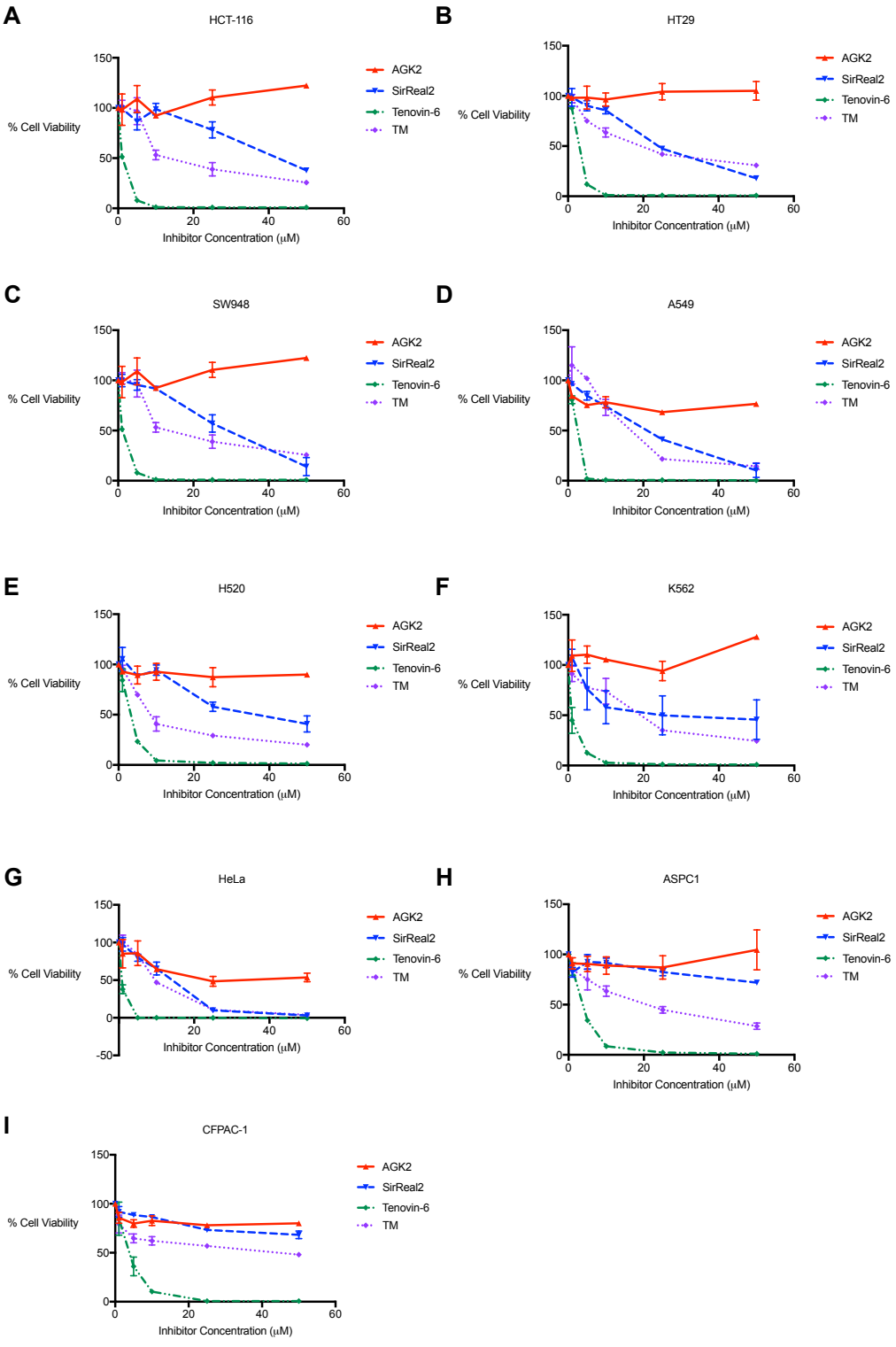

Figure 4.6. Cell proliferation curves from one representative trial of at least three independent experiments. (**A**) HCT-116 cells (**B**) HT-29 cells (**C**) SW948 cells (**D**) A549 cells (**E**) H520 cells (**F**) K-562 cells (**G**) HeLa cells (**H**) ASPC1 cells (**I**) CFPAC1 cells

Cancer cells have the ability to grow on soft agar without attaching to extracellular matrix, while normal cells cannot. Thus, a soft agar anchorage-independent growth assay is typically used to examine the transformed phenotype of cancer cells. We therefore examined the effect of SIRT2 inhibitors on anchorage-independent growth. Because this assay is more labor-intensive and time consuming, we limited our study to one cancer cell line, HCT116. Interestingly, we saw a different activity trend from the cytotoxicity assay. (Table 4.5, Figure 4.7A,B) Tenovin-6 is still the most potent compound with a GI_{50} value of 2.1 μM. TM is the second most potent compound with a GI_{50} value of 13.5 μM. SirReal2 was not very active in this assay, with a GI50 value of 55.8 μM. In contrast, AGK2, which was not active in the cytotoxicity assay, showed much better activity in the soft agar assay with an GI_{50} value of 24.1 μM.

Table 4.5. The GI_{50} (μM) values of different SIRT2 inhibitors on the anchorage-independent growth of HCT116 cells with and without SIRT2 overexpression. Results were obtained from all individual samples from at least three replicates, standard deviation are presented in supplemental information

	AGK2	SirReal2	Tenovin-6	TM
Control	24.1	55.8	2.1	13.5
SIRT2 expression	27.6	58.1	2.3	24.2
Fold Change[a]	1.2	1	1.1	1.8

[a] (GI_{50} for SIRT2 expression) / (GI_{50} for Control)

To study if the effect on anchorage-independent growth is a result of SIRT2 inhibition, we obtained the GI_{50} values of these inhibitors on the anchorage-independent growth of HCT116 cells with SIRT2 overexpression and compare to that on HCT116 cells without SIRT2

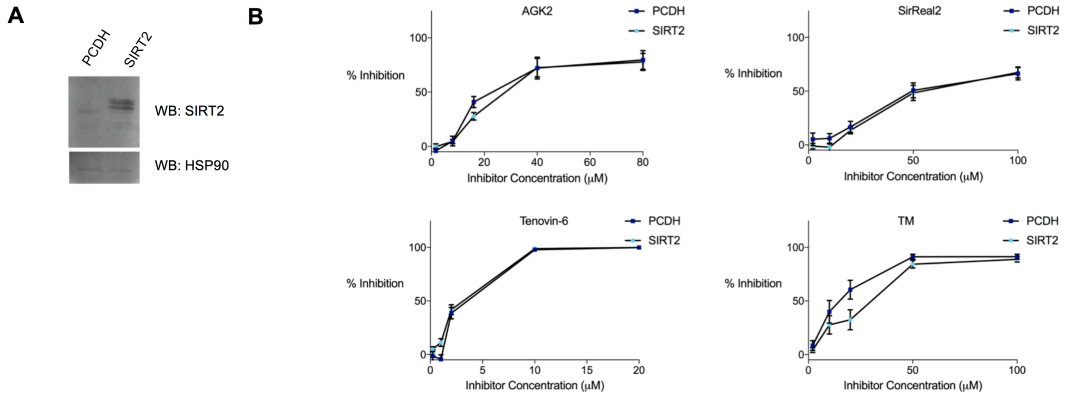

Figure 4.7. Soft Agar assay showed that SIRT2 overexpression desensitizes HCT116 cells to the effect of TM and to a smaller extent AGK2, but not SirReal2 or Tenovin-6 on anchorage independent growth. (A) Representative western blot confirming SIRT2 overexpression in the pCDH/ SIRT2 HCT116 cells. **(B)** Inhibition curves used to calculate the GI50 values (the mean and SEM (n=12 for AGK2, SirReal2, Tenovin-6 and n=9 for TM) from all individual values from all replicates are presented.

overexpression (Table 4.5, Figure 4.7). SIRT2 overexpression increased the GI_{50} value of TM by 1.8-fold, suggesting that the suppressive effect on anchorage-independent growth is

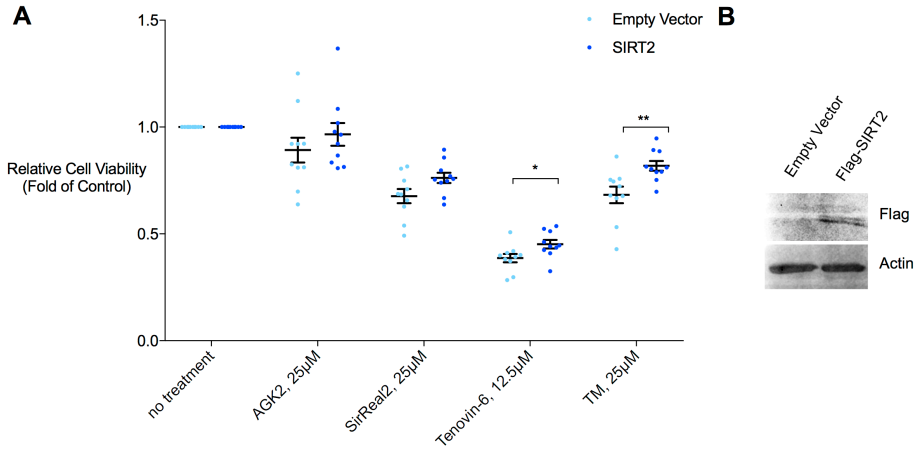

Figure 4.8. The inhibition effect from TM in MDA-MB-468 cells is most sensitive to SIRT2 overexpression. (A) Relative cell viability after 12-h inhibitor treatment in MDA-MB-468 cells overexpressing empty vector or SIRT2. Statistical significance was determined using an unpaired two-tailed student's t test in Excel. Error bars represent the SEM, and the center bar represents the mean. * $P < 0.05$, **= $P < 0.01$. (B) Representative western blot showing SIRT2 overexpression

dependent on SIRT2 inhibition. In contrast, SIRT2 overexpression had no or very little effect on the GI50 values of SirReal2, Tenovin-6, or AGK2, suggesting off-target effects. This is consistent with a recent report suggesting that Tenovin-6 impairs autophagy independent of

sirtuins.[28] We also examined the effect of SIRT2 overexpression on the cytotoxicity of these inhibitors in MDA-MB-468 (Figure 4.8) and HCT116 cells (Figure 4.9) and the results were similar to that on anchorage-independent growth.

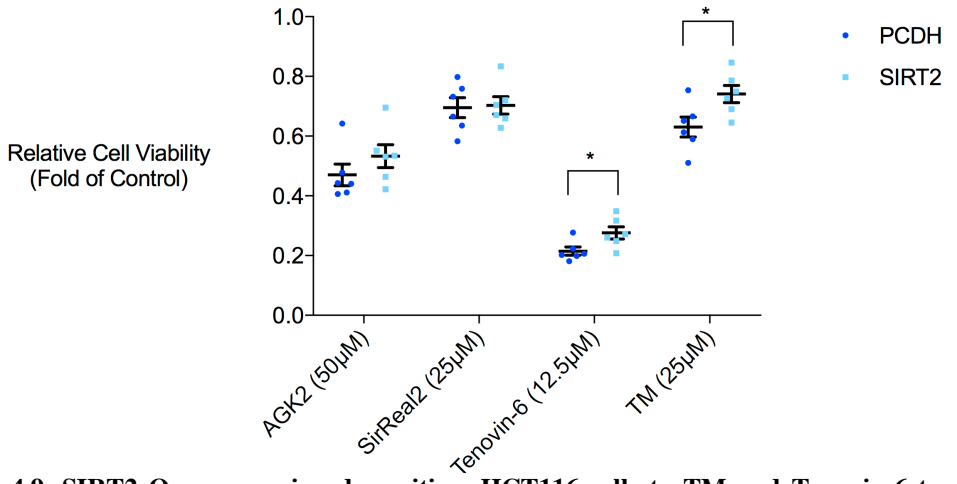

Figure 4.9. SIRT2 Overexpression desensitizes HCT116 cells to TM and Tenovin-6 treatment. Statistical significance was determined using a two-tailed student's t test in Excel. Error bars represent the SEM, and the center bar represents the mean. *= $P < 0.05$.

In summary, we have compared four established SIRT2 inhibitors: AGK2, SirReal2, Tenovin-6, and TM. This study will help people interested in using SIRT2 inhibitors to choose the proper compounds to elucidate the function of SIRT2 and to explore the therapeutic potential of inhibiting SIRT2. TM, while not the most potent inhibitor against cancer cells, is the most potent and selective SIRT2 inhibitor and its anticancer activity is dependent on SIRT2 inhibition. We suggest future studies to understand the physiological function of SIRT2 should use TM before better SIRT2 inhibitors are developed.

Our study also highlights a previously under-appreciated point regarding small molecule inhibitors for enzymes, which is the substrate or activity-dependent inhibition of enzymes. SIRT2 has been reported to have both deacetylation and demyristoylation activities. Interestingly, most of the inhibitors tested here only inhibited the deacetylation activity, but not the demyristoylation activity. TM is the only compound that can inhibit both activities, but the inhibition of demyristoylation is less potent. We think this is likely because myristoyl peptides

have much higher binding affinities (reflected by the much lower Km values) compared to acetyl peptides. Therefore, it is easier for the inhibitors to displace the acetyl peptide than to displace the myristoyl peptide from SIRT2 active site. It may be beneficial to inhibit the demyristoylation activity of SIRT2 in order to achieve anticancer activity, given the recent report that lysine fatty acylated KRas-4a is less effective at promoting anchorage-independent growth compared to the deacylated KRas-4a.[29]

Furthermore, our study underlies the importance of careful comparative and validation studies for the development of small molecule inhibitors. As we embrace the power of small molecule inhibitors to probe biology and treat human diseases, we must be careful as off-target effects are very common. Small molecule inhibitor development should be accompanied by detailed validation studies (such as target knockdown or overexpression) to make sure that the biological effects observed is due to target engagement. Similarly, because IC_{50} values are dependent on the experimental conditions (e.g. enzyme, substrate concentrations and specific activity of different batches of enzymes) used, it will be particularly informative if direct comparisons are performed. We therefore strongly recommend the chemical biology community to adopt these practices.

3. Methods

Reagents, antibodies and plasmids. AGK2 (Selleckchem, S7577), SirReal2 (Sigma Aldrich, SML1514), Tenovin-6 (Axon Medchem, 2249), and Trichostatin A or TSA (Apex Bio, A8183) were all purchased in the highest purity available. TM was synthesized as previously described.[16] Tenovin-6, AGK2, and SirReal2 were dissolved in dimethyl sulfoxide (DMSO), and TM was dissolved in ethanol (EtOH).

The acetyl-p53 (K382) (CST #2525) (used with 1:1000 dilution, overnight at 4˚C), SIRT2 (CST #12650) (used with a 1:1000 dilution, overnight at 4˚C or 3 hr at room temperature), HSP90 (CST #4877) (used with a 1:5000 dilution, 1 hr at room temperature) and

anti-rabbit conjugated to horseradish peroxidase (CST #2525) (used with 1:3000 dilution, 1 hr at room temperature) antibodies were purchased from cell signaling technologies. The anti-β-actin conjugated to horseradish peroxidase (sc-47778 HRP) (used with 1:5000 dilution, 1 hr at room temperature) was purchased from Santa Cruz Biotechnologies. Anti-Flag M2 conjugated to horseradish peroxidase (A8592) (used with 1:7500 dilution, 1 hr at room temperature), and the anti-acetyl-α-tubulin (6-11B-1) (MABT868) antibodies were from Sigma-Aldrich. Cy3 Goat-anti-mouse (A10521) was purchased from Life Technologies. Nitrotetrazolium Blue chloride (N6876) and low gelling temperature agarose (A0701) were purchased from Sigma Aldrich.

For ectopic overexpression of SIRT2, pCMV4a-Flag-SIRT2 was cloned as previously described.[16] For lentiviral overexpression of SIRT2, pCDH-Flag-SIRT2 was cloned by inserting SIRT2 into pCDH-CMV-MCS-EF1-Puro between the EcoRI and XhoI restriction sites with a C-terminal Flag tag.

Expression and Purification of Sirtuins. Human SIRT1, SIRT2, SIRT3 and SIRT6 were expressed and purified as previously described.[16,26]

Synthesis of H3K9Ac and Myr peptides. H3K9Ac, H3K9Myr, and H3K9 peptides were all synthesized as previously described using standard solid phase peptide synthesis.[27]

In vitro deacylation assay (with pre-incubation). Various concentrations of AGK2, SirReal2, Tenovin-6 (in DMSO) and TM (in EtOH) (0.0064, 0.032, 0.16, 0.8, 4.0, 20, 100, and 200 μM) were added to solutions containing 20 mM Tris-HCl (pH 8.0), 1 mM NAD, 1 mM dithiothreitol (DTT), and 0.1 μM of SIRT1, 0.2 μM of SIRT2, or 0.4 μM of SIRT3. The reaction mixtures were incubated at 37˚C for 15 min. Then 10 μM of H3K9Ac peptide or 0.10 μM of H3K9Myr was added to initiate the deacylation reactions. The reactions were incubated at 37°C (3 min reaction for SIRT1, 6 min reaction for SIRT2 with H3K9Ac, 5 min reaction for SIRT2 with H3K9Myr, 10 min reaction for SIRT3 with H3K9Ac, and 75 min reaction for SIRT6 with

H3K9Myr). The reaction times were determined to ensure a conversion of no more than 20% from the acylated to free peptide for the control samples. The reactions were stopped by adding an equal volume of acetonitrile. After quenching the reactions, the samples were centrifuged at 17,000 g for 20 min to remove any precipitated proteins. The cleared supernatant was analyzed by HPLC with a reverse phase C18 column (Kinetex XB-C18 100A, 100 mm × 4.60 mm, 2.6 μm, Phenomenex) using a gradient of two solvents (A: 0.1% trifluoroacetic acid in water; B: 0.1% trifluoroacetic acid in acetonitrile): starting with 0% B for 2 min, then 0% to 20% B in 2 min, 20% to 40% B in 13 min, and then 40% to 100% for 2 min at 0.5 mL/min. The peak areas of free H3K9 and either H3K9Ac or H3K9Myr were measured based on the absorbance monitored at 280 nm. The conversion rate was calculated from the peak areas as the fraction of the free H3K9 peptide from the total peptide. AGK2 and Tenovin-6 peaks overlapped with the H3K9Myr peptide peak, and thus the areas of these compounds were subtracted from the H3K9Myr peptide peak area. IC50 values were calculated using Prism 7 software.

In vitro deacylation assay (without pre-incubation): Various concentrations of AGK2, SirReal2, Tenovin-6 (in DMSO) and TM (in EtOH) (0.0064, 0.032, 0.16, 0.8, 4.0, 20, 100, and 200 μM) were added to solutions containing 20 mM Tris-HCl (pH 8.0), 1 mM NAD, 1 mM DTT, 10 μM H3K9Ac peptide or 0.10 μM H3K9Myr peptide, and 0.2 μM of SIRT2. The reactions were incubated at 37 °C for 15 min and then quenched and analyzed similarly as described above.

Cell culture and transfection. All cells were cultured in media supplemented with 10% (vol/vol) heat-inactivated fetal bovine serum (FBS; Invitrogen) and at 37˚C with 5% CO2 unless otherwise specified. MCF-7, MDA-MB-231, MDA-MB-468, HeLa, HME1, and HEK-293T cells were grown in DMEM media (Invitrogen). SK-BR-3, K562, SW948, A549, H520, and ASPC-1 cells were grown in RPMI-1640 media (Invitrogen). HCT116 and HT29 cells were cultured in McCoy's 5A medium, and CF-PAC1 cells were cultured in IMDM. The MCF-10A

cells were cultured in mammary epithelial cell growth medium (MEGM; Lonza) with supplements according to manufacturer's instruction.

To overexpress SIRT2 in MDA-MB-468 cells, the pCMV-tag-4a vector containing SIRT2 or empty pCMV-tag-4a (negative control) were transfected into cells using FuGene 6 (Promega, Madison, WI) according to manufacturer's protocol.

Cell viability assay. To determine the GI50 values of the compounds in cells, between 1,000-6,000 cells (depending on the cell line) were seeded per well in a 96 well plate in 100 μL of media. The next day, 100 μL of inhibitors in media were added to each well-- so the final concentrations of the inhibitors used were 50, 25, 10, 5, 1, and 0 μM. After 72 hours, CellTiter blue (Promega) was added to each well and the plates were placed at 37°C for 4 hours. After 4 hours, the cell viability was measured according to the manufactures protocol. The background was subtracted, and the IC50 values were calculated using Prism 7 software.

Western blot. Proteins were detected by western blot as previously described.[4] Briefly, proteins were resolved on a 12% SDS-PAGE gel and subsequently transferred to PVDF membranes. After incubation with HRP conjugated primary or secondary antibodies, the proteins of interest were detected using the ECL reagent (Pierce Biotechnology Inc.) and visualized on a Typhoon 9400 Imager (GE Healthcare). Western blots were processed using ImageJ software.[28]

Detection of Ac-p53 levels in cells. MCF-7 cells were treated with the 25 μM of the noted inhibitor and 200 nM of Trichostatin A (TSA) for 6 hours. After treatment, the cells were collected, and washed with ice cold PBS three times. The cell pellet was subsequently lysed with 4% SDS lysis buffer supplemented with protease inhibitor cocktail (Sigma) and universal cell nuclease (Thermo). The protein concentration was determined using the Pierce BCA assay kit (Thermo) following the manufactures protocol, and Ac-p53 and levels were detected by western blot.

Immunofluorescence to detect acetyl-α-tubulin levels in cells. To detect Ac-α-tubulin levels

in cells, slight modifications were made to previous protocols. Briefly, 2 x 105 MCF-7 cells were seeded in in 35-mm glass bottom dishes (MatTek). After 24 hours, the cells were treated with either the inhibitor at the noted concentration or the control for 6 hours. The cells were washed three times with PBS and fixed with ice cold methanol (10 minutes). To permeabilize the membrane, the cells were treated with 0.1% Triton-X in PBS. After 10 minutes, the cells were washed three times (5 minute each) with PBS. After the final wash, the cells were blocked with 1% BSA in TBST (25 mM Tris-HCl, pH 7.4, 150 mM NaCl, and 0.1% Tween-20) for 30 minutes and then incubated with the Ac-α-tubulin antibody (1:100) in 1% BSA overnight at 4˚C. After primary antibody incubation, the cells were washed with TBST three times (5 minute each). Subsequently the fluorophore conjugated antibody was added to the cells in 1% BSA in TBST (1:1000) and incubated for 1 hour at room temperature in the dark. After three 5-minute TBST washes, the cells were mounted and the nuclei was stained with DAPI Fluoromount-G® (Southern Biotech, 0100-01), and a coverslip was placed on top of the cells. The cells were imaged using a Zeiss LSM880 inverted confocal microscope set up with a 40x oil objective, using the same settings for all samples, and the images were processed using Fiji software.[28]

Generation of pCDH/ Flag-SIRT2 lentivirus. Approximately 1.5 to 2 million WT-HEK-239T cells in a 10cm dish were transfected with 5 μg of empty pCDH-CMV-MCS-EF1-Puro or pCDH-CMV-MCS-EF1-Puro with FLAG-SIRT2, 5 μg of pCMV-ΔR8.2 and 1 μg of pM2D.G. For the transfection, 36μL of FuGene6 was added to 576uL of serum free DMEM. After 5 minutes the plasmids were added and allowed to incubate. After 15 minutes, the transfection mixture was added to cells with 8mL of fresh DMEM (supplemented with 10% FBS). After 12 h, the media was changed to 8mL of fresh FBS supplemented media. After 24, 48 and 72 h the media was harvested, and spun down at 3000 rpm for 10 minutes. The virus was then filtered with a 0.45 μM filter. Virus was stored at -80˚C in the dark until use.

Generation of stable overexpressing SIRT2 HCT116 cells. HCT-116 cells overexpressing

SIRT2 or empty vector control were generated by infecting cells with viruses containing either pCDH-Flag-SIRT2 vector or empty pCDH vector. About 1 x 105 HCT116 cells were seeded in a 6-well dish. The next day, 1 mL of virus was added to the cells with polybrene at a concentration of 6 μg/mL. After 6 hours, the cells were placed in McCoy's 5A media with 10% FBS. After 72 hours the cells were treated with puromycin for 1 week. After puromycin selection, the cells were allowed to recover. SIRT2 overexpression was confirmed by SIRT2 and Flag western blots.

Soft agar colony formation assay. To each well in a 6-well dish, 2 mL of a 0.6% LMP agar solution was plated. After 30 minutes, 1,000 cells were plated in 1 mL 0.3% LMP agar solution supplemented with the noted inhibitor or vehicle control concentration. After 30 minutes, an additional 1 mL of 0.3% LMP agar solution supplemented with the noted inhibitor concentration was added. The plates were placed in the incubator at 37˚C supplemented with 5% CO2. An additional 1 mL of inhibitor-supplemented 0.3% LMP agar solution was added after 6 days. After 10-12 days, 200 μL of 1 mg/mL of Nitrotetrazolium Blue chloride in PBS was added to each well. After 12 hours, the plates were placed at 4˚C, and imaged using a chemi-doc imager with the Coomassie blue settings. Colonies were counted using FIJI software.[28]

Cytotoxicity assay with SIRT2 overexpression in MDA-MB-468 cells. MDA-MB-468 were seeded in a 12-well plate with 3 x 104 cells/well. After 12 hours, either pCMV4a-Flag-SIRT2 or empty pCMV4a was overexpressed (1 μg of DNA per well of a 12-well dish) using Fugene6 (Promega). After 24 hours, the cells were treated with either ethanol, DMSO or the indicated inhibitor at the noted concentrations. After 12 hours the media was removed, and the cells were washed two times with PBS. To fix the cells, ice cold methanol was added. After 10 minutes, the cells were stained with 0.25% crystal violet (m/v, in 25% methanol) (SIGMA) for 5 minutes. The stained cells were washed with water, and allowed to air dry. The stain was resolubilized in a solution of 0.2% SDS in 50% ethanol, and the absorbance of the solution was read at 550

nm. SIRT2 overexpression was confirmed by western blot. Statistical significance was determined using an unpaired, two tailed, student's t-test in Microsoft Excel.

Cytotoxicity assay with SIRT2 overexpression in stable SIRT2 overexpressing HCT116 cells. HCT116 cells stably over-expressing SIRT2 or empty pCDH vector were seeded in a 12-well plate with 3 x 104 cells/well. After 24 hours, the inhibitors were added for 24 hours. The rest of the procedure was the same that used for MDA-MB-468 cells described above.

REFERENCES

(1) Chopra, V.; Quinti, L.; Kim, J.; Vollor, L.; Narayanan, K. L.; Edgerly, C.; Cipicchio, P. M.; Lauver, M. A.; Choi, S. H.; Silverman, R. B.et al. The sirtuin 2 inhibitor AK-7 is neuroprotective in Huntington's disease mouse models. *Cell Rep* **2012,** *2* (6), 1492.

(2) Haigis, M. C.; Sinclair, D. A. Mammalian Sirtuins: Biological Insights and Disease Relevance. *Annu Rev Pathol* **2010,** *5*, 253.

(3) Teng, Y. B.; Jing, H.; Aramsangtienchai, P.; He, B.; Khan, S.; Hu, J.; Lin, H.; Hao, Q. Efficient demyristoylase activity of SIRT2 revealed by kinetic and structural studies. *Sci Rep* **2015,** *5*, 8529.

(4) Jiang, H.; Khan, S.; Wang, Y.; Charron, G.; He, B.; Sebastian, C.; Du, J.; Kim, R.; Ge, E.; Mostoslavsky, R.et al. SIRT6 regulates TNF-alpha secretion through hydrolysis of long-chain fatty acyl lysine. *Nature* **2013,** *496* (7443), 110.

(5) Jintang Du, Y. Z., Xiaoyang Su, Jiu Jiu Yu, Saba Khan, Hong Jiang, Jungwoo Kim, Jimin Woo, Jun Huyn Kim, Brian Hyun Choi, Bin He, Wei Chen, Sheng Zhang, Richard A. Cerione, Johan Auwerx, Quan Hao, Hening Lin. Sirt5 Is a NAD-Dependent Protein Lysine Demalonylase and Desuccinylase. *Science* **2011,** *334* (6057), 806.

(6) Zhao, Y.; Yang, J.; Liao, W.; Liu, X.; Zhang, H.; Wang, S.; Wang, D.; Feng, J.; Yu, L.; Zhu, W. G. Cytosolic FoxO1 is essential for the induction of autophagy and tumour suppressor activity. *Nat Cell Biol* **2010,** *12* (7), 665.

(7) Wang, Y. P.; Zhou, L. S.; Zhao, Y. Z.; Wang, S. W.; Chen, L. L.; Liu, L. X.; Ling, Z. Q.; Hu, F. J.; Sun, Y. P.; Zhang, J. Y.et al. Regulation of G6PD acetylation by SIRT2 and KAT9 modulates NADPH homeostasis and cell survival during oxidative stress. *EMBO J* **2014,** *33* (12), 1304.

(8) Wang, F.; Nguyen, M.; Qin, F. X.; Tong, Q. SIRT2 deacetylates FOXO3a in response to oxidative stress and caloric restriction. *Aging Cell* **2007,** *6* (4), 505.

(9) North, B. J.; Rosenberg, M. A.; Jeganathan, K. B.; Hafner, A. V.; Michan, S.; Dai, J.; Baker, D. J.; Cen, Y.; Wu, L. E.; Sauve, A. A.et al. SIRT2 induces the checkpoint kinase BubR1 to increase lifespan. *EMBO J* **2014,** *33* (13), 1438.

(10) North, B. J.; Marshall, B. L.; Borra, M. T.; Denu, J. M.; Verdin, E. The human Sir2 ortholog, SIRT2, is an NAD+-dependent tubulin deacetylase. *Mol Cell* **2003,** *11* (2), 437.

(11) Li, Y.; Matsumori, H.; Nakayama, Y.; Osaki, M.; Kojima, H.; Kurimasa, A.; Ito, H.; Mori, S.; Katoh, M.; Oshimura, M.et al. SIRT2 down-regulation in HeLa can induce p53 accumulation via p38 MAPK activation-dependent p300 decrease, eventually leading to apoptosis. *Genes Cells* **2011,** *16* (1), 34.

(12) Jing, E.; Gesta, S.; Kahn, C. R. SIRT2 regulates adipocyte differentiation through FoxO1 acetylation/deacetylation. *Cell Metab* **2007,** *6* (2), 105.

(13) Jiang, W.; Wang, S.; Xiao, M.; Lin, Y.; Zhou, L.; Lei, Q.; Xiong, Y.; Guan, K. L.; Zhao, S. Acetylation regulates gluconeogenesis by promoting PEPCK1 degradation via recruiting the UBR5 ubiquitin ligase. *Mol Cell* **2011,** *43* (1), 33.

(14) Inoue, T.; Nakayama, Y.; Li, Y.; Matsumori, H.; Takahashi, H.; Kojima, H.; Wanibuchi, H.; Katoh, M.; Oshimura, M. SIRT2 knockdown increases basal autophagy and prevents postslippage death by abnormally prolonging the mitotic arrest that is induced by microtubule inhibitors. *FEBS J* **2014,** *281* (11), 2623.

(15) Dryden, S. C.; Nahhas, F. A.; Nowak, J. E.; Goustin, A. S.; Tainsky, M. A. Role for human SIRT2 NAD-dependent deacetylase activity in control of mitotic exit in the cell cycle. *Mol Cell Biol* **2003,** *23* (9), 3173.

(16) Jing, H.; Hu, J.; He, B.; Negron Abril, Y. L.; Stupinski, J.; Weiser, K.; Carbonaro, M.; Chiang, Y. L.; Southard, T.; Giannakakou, P.et al. A SIRT2-Selective Inhibitor Promotes c-Myc Oncoprotein Degradation and Exhibits Broad Anticancer Activity. *Cancer Cell* **2016,** *29* (5), 767.

(17) Zhao, D.; Zou, S. W.; Liu, Y.; Zhou, X.; Mo, Y.; Wang, P.; Xu, Y. H.; Dong, B.; Xiong, Y.; Lei, Q. Y.et al. Lysine-5 acetylation negatively regulates lactate dehydrogenase A and is decreased in pancreatic cancer. *Cancer Cell* **2013,** *23* (4), 464.

(18) Serrano, L.; Martinez-Redondo, P.; Marazuela-Duque, A.; Vazquez, B. N.; Dooley, S. J.; Voigt, P.; Beck, D. B.; Kane-Goldsmith, N.; Tong, Q.; Rabanal, R. M.et al. The tumor suppressor SirT2 regulates cell cycle progression and genome stability by modulating the mitotic deposition of H4K20 methylation. *Genes Dev* **2013,** *27* (6), 639.

(19) Liu, P. Y.; Xu, N.; Malyukova, A.; Scarlett, C. J.; Sun, Y. T.; Zhang, X. D.; Ling, D.; Su, S. P.; Nelson, C.; Chang, D. K.et al. The histone deacetylase SIRT2 stabilizes Myc oncoproteins. *Cell Death Differ* **2013,** *20* (3), 503.

(20) Kim, H. S.; Vassilopoulos, A.; Wang, R. H.; Lahusen, T.; Xiao, Z.; Xu, X.; Li, C.; Veenstra, T. D.; Li, B.; Yu, H.et al. SIRT2 maintains genome integrity and suppresses tumorigenesis through regulating APC/C activity. *Cancer Cell* **2011,** *20* (4), 487.

(21) Mellini, P.; Itoh, Y.; Tsumoto, H.; Li, Y.; Suzuki, M.; Tokuda, N.; Kakizawa, T.; Miura, Y.; Takeuchi, J.; Lahtela-Kakkonen, M.et al. Potent mechanism-based sirtuin-2-selective inhibition by an in situ-generated occupant of the substrate-binding site, "selectivity pocket" and NAD(+)-binding site. *Chem Sci* **2017,** *8* (9), 6400.

(22) Tiago Fleming Outeiro, E. K., Stephen M. Altmann, Irina Kufareva, Katherine E. Strathearn, Allison M. Amore, Catherine B. Volk, Michele M. Maxwell, Jean-Christophe Rochet, Pamela J. McLean, Anne B. Young, Ruben Abagyan,; Mel B. Feany, B. T. H., Aleksey G. Kazantsev. Sirtuin 2 Inhibitors Rescue a-Synuclein–Mediated Toxicity in Models of Parkinson's Disease. *Science* **2007,** *317* (5837), 516.

(23) Rotili, D.; Tarantino, D.; Nebbioso, A.; Paolini, C.; Huidobro, C.; Lara, E.; Mellini, P.; Lenoci, A.; Pezzi, R.; Botta, G.et al. Discovery of salermide-related sirtuin inhibitors: binding mode studies and antiproliferative effects in cancer cells including cancer stem cells. *J Med Chem* **2012,** *55* (24), 10937.

(24) Rumpf, T.; Schiedel, M.; Karaman, B.; Roessler, C.; North, B. J.; Lehotzky, A.; Olah, J.; Ladwein, K. I.; Schmidtkunz, K.; Gajer, M.et al. Selective Sirt2 inhibition by ligand-induced rearrangement of the active site. *Nat Commun* **2015,** *6*, 6263.

(25) Lain, S.; Hollick, J. J.; Campbell, J.; Staples, O. D.; Higgins, M.; Aoubala, M.; McCarthy, A.; Appleyard, V.; Murray, K. E.; Baker, L.et al. Discovery, in vivo activity, and mechanism of action of a small-molecule p53 activator. *Cancer Cell* **2008,** *13* (5), 454.

(26) Kudo, N.; Ito, A.; Arata, M.; Nakata, A.; Yoshida, M. Identification of a novel small molecule that inhibits deacetylase but not defatty-acylase reaction catalysed by SIRT2. *Philos Trans R Soc Lond B Biol Sci* **2018,** *373* (1748).

(27) Vaziri, H.; Dessain, S. K.; Ng Eaton, E.; Imai, S. I.; Frye, R. A.; Pandita, T. K.; Guarente, L.; Weinberg, R. A. hSIR2(SIRT1) functions as an NAD-dependent p53 deacetylase. *Cell* **2001,** *107* (2), 149.

(28) Yuan, H.; Tan, B.; Gao, S. J. Tenovin-6 impairs autophagy by inhibiting autophagic flux. *Cell Death Dis* **2017,** *8* (2), e2608.

(29) Jing, H.; Zhang, X.; Wisner, S. A.; Chen, X.; Spiegelman, N. A.; Linder, M. E.; Lin, H. SIRT2 and lysine fatty acylation regulate the transforming activity of K-Ras4a. *Elife* **2017,** *6*.

CHAPTER 5

A SMALL MOLECULE SIRT2 INHIBITOR THAT PROMOTES K-RAS4A LYSINE FATTY ACYLATION [4]

Abstract

SIRT2 is a member of the sirtuin family of protein lysine deacylases. SIRT2 has been identified as a promising therapeutic target. In addition to catalyzing deacetylation, SIRT2 has recently been shown to remove fatty acyl groups from K-Ras4a and promote its transforming activity. Among the SIRT2 specific inhibitors, only the thiomyristoyl lysine compound, TM, can weakly inhibit the demyristoylation activity of SIRT2. Thus, more potent small molecule SIRT2 inhibitors are needed to further evaluate the therapeutic potential of SIRT2 inhibition, and to understand the function of protein lysine defatty-acylation. Here we report a SIRT2 inhibitor, JH-T4, which can increase K-Ras4a lysine fatty acylation. This is the first small molecule inhibitor that can modulate the lysine fatty acylation levels of K-Ras4a. JH-T4 also inhibits SIRT1 and SIRT3 *in vitro*. The increased potency of JH-T4 is likely due to the formation of hydrogen bonding between the hydroxyl group and SIRT1, SIRT2, and SIRT3. This is further supported by *in vitro* studies with another small molecule inhibitor, NH-TM. These studies provide useful insights for future SIRT2 inhibitor development.

---

[4]This is a revised version of the submitted paper: Spiegelman, N.A.*, Hong, J.Y.*, Hu, J.,* Jing, H.,* Wang, M., Price, I.R., Cao, J., Yang, M., Zhang, X., Lin, H. A Small Molecule SIRT2 Inhibitor that Promotes K-Ras4a Lysine Fatty-acylation.

For this paper, I (NAS) designed and performed all the biochemical studies except those noted below. N. A. S. carried out the in vitro assays and the cellular assays, synthesized Alk14 and TM, and wrote the manuscript. J. Y. H. synthesized JH-T4 and NH-TM, carried out in vitro assays with NH-TM. J. H. first developed JH-T4 and carried out preliminary in vitro assays. H. J. contributed to K-Ras4a fatty acylation determination and initial assays with JH-T4. M. W. generated the stable SIRT2 OE HCT116 Cells. J. C. helped optimizing the SIRT2 OE experiment and culturing of the cells for cytotoxicity studies. I. R. P. and X. Z. purified sirtuin enzymes. M. Y. synthesized TM. H.L. supervised and directed the study. N.A.S. and H.L. wrote the manuscript, all authors approved of the final manuscript.

We thank Dr. Pornpun Aramsangtienchai and Dr. Sushabhan Sadhukhan for providing the substrate peptides.

1. Introduction

Sirtuins, the NAD-dependent class of the histone deacetylase family, have attracted a lot of research interest due to their connection to many biological processes such as transcription, metabolism, cancer, and aging.[1] Among the seven mammalian sirtuins, SIRT2 is the only sirtuin predominately localized in the cytosol.[1] Despite early studies suggesting a tumor suppressor role for SIRT2, many recent reports show that inhibiting SIRT2 has a broad anti-cancer effect.[2-6] Thus, SIRT2 is a promising anticancer target. SIRT2 was initially identified as a protein lysine deacetylase. However, it can also efficiently hydrolyze long chain fatty acyl groups from lysine residues. [7-10] Most of the current understanding of SIRT2 comes from its deacetylation activity. SIRT2 deacetylates various substrates ranging from metabolic enzymes, such as ENO1, to transcription factors such as HIF1-α.[11,12] Meanwhile, not much is known about the defatty-acylation activity of SIRT2. Recently, the first defatty-acylation substrate of SIRT2, K-Ras4a, was identified.[13] SIRT2-mediated lysine defatty-acylation promotes the transforming activity of K-Ras4a.[13] Since K-Ras4a is an important oncoprotein, the defatty-acylation activity of SIRT2 could be significant for the role of SIRT2 in cancer.

Several SIRT2 inhibitors have been identified. [2,14-22] Recent studies suggest that among these compounds, only TM can weakly inhibit the demyristoylation activity of SIRT2.[23,24] TM is a thiomyristoyl lysine compound, and is a mechanism-based SIRT2 inhibitor.[2] TM has been shown to possess a broad anticancer effect.[2,23,25] In many cancer cell lines, TM inhibits SIRT2 and promotes c-Myc degradation.[2] TM efficiently inhibits the deacetylation activity of SIRT2 in cells, while only weakly inhibits the defatty-acylation activity of SIRT2.[2,23] Due to the promising potential of SIRT2 as a therapeutic target, we are interested in developing more potent SIRT2 inhibitors that can inhibit both the deacetylation and the defatty-acylation activity of SIRT2. Here we report JH-T4, a TM analogue, which is also a potent SIRT2 inhibitor, but unlike TM has the ability to inhibit the defatty-acylation of K-Ras4a by SIRT2 both *in vitro* and

in cells.

2. Results and Discussion

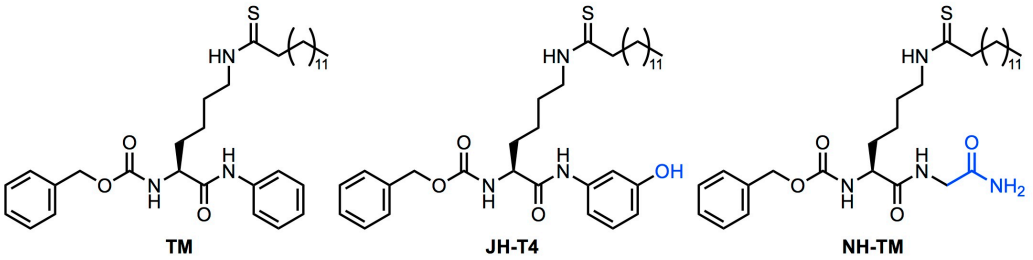

Figure 5.1. Small Molecule Sirtuin Inhibitors. Our previous studies reported the SIRT2 selective inhibitor TM. Here we identify two TM analogues, JH-T4 and NH-TM. The blue highlights the structural difference between the different small molecule inhibitors.

In our efforts to develop a more potent SIRT2 inhibitor, we developed a compound very similar to TM, JH-T4 (Figure 5.1). JH-T4 differs from TM by a single hydroxyl group on the aniline moiety attached to the carboxy termi of the thio-myristoyl lysine. We measured the *in vitro* IC_{50} values (Table 5.1) of JH-T4 toward SIRT1, SIRT2, SIRT3, and SIRT6 under pre-incubation conditions (enzymes, NAD, and inhibitors were first incubated for 15 min before substrates were added to start the enzymatic reaction) and compared them to the IC_{50} values of TM. For SIRT2, we determined the IC_{50} values for both deacetylation and demyritoylation activities.

Table 1. *In vitro* IC_{50} values (μM) of TM, JH-T4 and NH-TM for inhibiting sirtuin deacylation activity

	IC_{50} (μM)		
	TM	JH-T4	NH-TM
SIRT1 deacetylation	25±15	0.3±0.2	0.4±0.1
SIRT2 deacetylation	0.04±0.02	0.03±0.01	0.088±0.003
SIRT2 defatty-acylation	0.05±0.03	0.04±0.03	ND
SIRT3 deacetylation	>50	15±5	2.42±0.01
SIRT6 defatty-acylation	>200	>100	ND
Selectivity*	650	10	4.8

*(SIRT1 deacetylation IC_{50})/(SIRT2 deacetylation IC_{50}), N.D = not determined

Despite its similarity in structure to TM, JH-T4 showed a different sirtuin inhibition profile. TM is a SIRT2 selective inhibitor, exhibiting a 650-fold selectivity for inhibition of SIRT2 over SIRT1 deacetylation activity.[23] In contrast, JH-T4 exhibited only a 10-fold selectivity for SIRT2 as it inhibits SIRT1, SIRT2, and SIRT3 *in vitro* with IC_{50} values of 15 μM or lower. Interestingly, under the pre-incubation assay condition, TM and JH-T4 inhibited both the deacetylation and defatty-acylation activity of SIRT2 *in vitro* comparably (IC_{50} values in the 30-50 nM range) (Table 5.1).

To further compare the defatty-acylation inhibition by TM and JH-T4 we determined the IC_{50} value for inhibition of SIRT2 demyristoylation activity without pre-incubating the enzyme with NAD and inhibitor. Without preincubation, the *in vitro* IC_{50} value of TM was > 200 μM (42% inhibition at 200 □M), but the IC_{50} of JH-T4 was 110 μM. This suggests that JH-T4 is more efficient at inhibiting the defatty-acylation activity of SIRT2 than TM is.

We next wanted to compare the potency and selectivity of these compounds in cells. To evaluate the inhibition of SIRT1 deacetylation activity, we examined p53 acetylation levels, as Lys382 of p53 is a well-established SIRT1 substrate.[26] As expected, JH-T4, but not TM,

increased Ac-p53 level on Lys382 in MCF-7 cells (Figure 5.2A). We further tested if these compounds could inhibit the deacetylation activity of SIRT2 in cells based on acetyl α-tubulin immunofluorescence, as acetyl α-tubulin is a widely used cellular readout of SIRT2 activity.[7] Both the TM and JH-T4 treated samples showed a dramatic increase in acetyl α-tubulin levels compared to the sample treated with the vehicle control, ethanol. Thus, both compounds efficiently inhibit SIRT2 deacetylation activity in MCF-7 cells (Figure 5.2B).

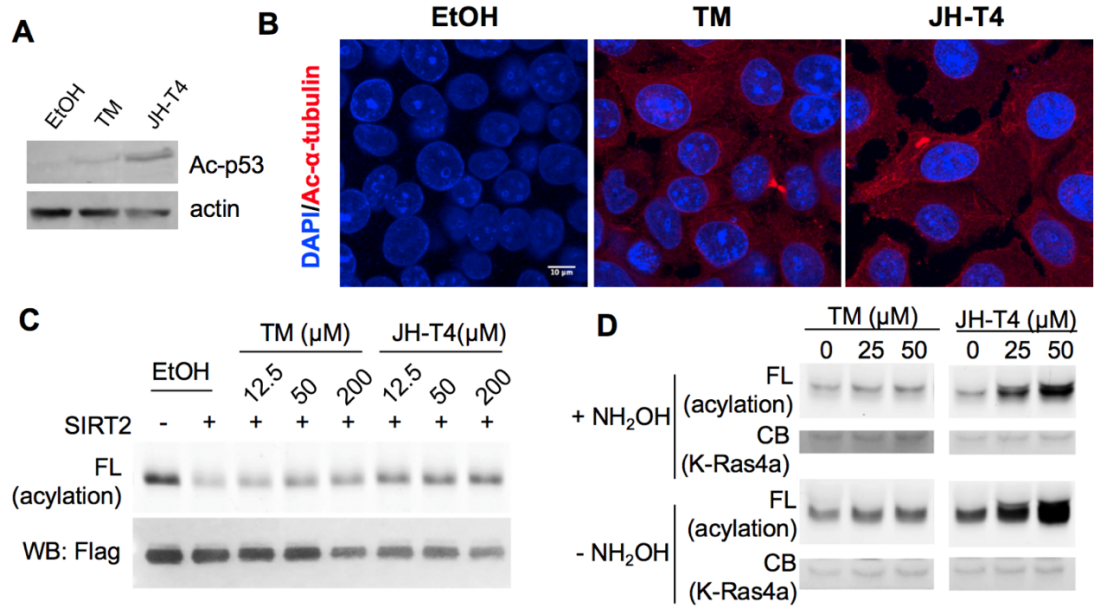

Figure 5.2. In-Cell Sirtuin Potency of TM and JH-T4. (**A**) Ac-p53 levels to evaluate the inhibition of SIRT1 in cells after 6 hr 25μM inhibitor and 200 nM trichostatin A (TSA) treatment in MCF-7 cells. (**B**) Ac-α-tubulin levels to detect inhibition of SIRT2 after 6 hr 25 μM inhibitor treatment in MCF-7 cells. (**C**) Inhibition of SIRT2 *in vitro* by TM and JH-T4 treatment by evaluating K-Ras4a lysine fatty acylation levels. (**D**) Detection of K-Ras4a lysine fatty acylation levels to evaluate in-cell inhibition of SIRT2 defatty-acylation activity. FL, fluorescence; CB, Coomassie blue staining.

We next investigated whether either of the two compounds could inhibit the defatty-acylation activity of SIRT2 by evaluating the lysine fatty acylation level of K-Ras4a, the only reported SIRT2 defatty-acylation target. We made use of the biorthogonal palmitic acid analogue Alk14 following the same methods previously described.[13] First, we looked at the ability of the compounds to inhibit SIRT2 defatty-acylation on K-Ras4a *in vitro*. Alk14 labeled

K-Ras4a was purified from HEK-293T cells, and subsequently treated with SIRT2, NAD, and either TM, JH-T4, or the vehicle control ethanol. Click chemistry was used to attach a fluorophore to read fatty acylation level of K-Ras4a from the in-gel fluorescence intensity. K-Ras4a samples treated with JH-T4 had higher lysine fatty-acylation levels (hydroxylamine resistant fatty acylation) than those treated with either the control, ethanol, or TM (Figure 5.2C, note that JH-T4 treated cells have lower protein loading but stronger fluorescence signal).

Next, we tested whether JH-T4 was able to inhibit SIRT2-catalyzed K-Ras4a defatty-acylation in cells. Consistent with the *in vitro* inhibition of SIRT2 defatty-acylation of K-Ras4a, JH-T4 could also increase the fatty acylation level on K-Ras4a efficiently in cells (Figure 5.2D). In contrast, TM had very little effect on the lysine fatty acylation of K-Ras4a. JH-T4 is therefore the first inhibitor to efficiently inhibit the defatty-acylation activity on K-Ras4a in cells.

Given that JH-T4 is a potent SIRT2 inhibitor that inhibits the defatty-acylation of K-Ras4a, we next evaluated the anti-cancer effect of these compounds in a wide range of cancer cells. We looked at their GI_{50} values in pancreatic cancer (ASPC1), colon cancer (HCT116), lung cancer (NCI-H23), and breast cancer (MDA-MB-231) cells, as well as in two normal mammary epithelial cells (HME1 and MCF10A). JH-T4 was more potent than TM in all the cell lines evaluated. However, unlike TM which exhibited cancer cell selectivity over normal cells, JH-T4 was also toxic to the normal cell lines HME1 and MCF10A. (Table 5.2)

Table 5.2. GI_{50} values (μM) of TM and JH-T4 in several cancer and normal cells. The values are an average of three independent experiments, each done in duplicate. WT = wild type

Cell Line	Cell Type	K-Ras Mutation	GI_{50} (μM)	
			TM	JH-T4
ASPC1	pancreatic cancer	G12D	24 ± 5	8.6 ± 0.9
HCT116	colon cancer	G13D	19 ± 1	6.2 ± 0.2
NCI-H23	lung cancer	G12C	29 ± 6	6.6 ± 0.3
MDA-MB-231	breast cancer	G13D	13 ± 4	6 ± 2
HME1	normal mammary epithelial cells	WT	>50	11 ± 4
MCF10A	normal mammary epithelial cells	WT	>50	3 ± 1.2

The cytotoxicity of JH-T4 to normal cell lines (Table 5.2) may come from the fact that JH-TM can inhibit several sirtuins. To evaluate if the anticancer effect of JH-T4 is through SIRT2 inhibition we evaluated the inhibition of anchorage independent growth in HCT116 cells overexpressing pCDH and Flag-SIRT2. While cells overexpressing SIRT2 were less sensitive to TM treatment, there was no difference in JH-T4 potency between the two cell lines (Table 5.3).[23] This suggests that the potency of JH-T4 is not primarily through SIRT2 inhibition. Thus, future SIRT2 inhibitor development should focus on regaining SIRT2 selectivity, while maintaining the potency of JH-T4.

Table 5.3. GI_{50} values (μM) of TM[23] and JH-T4 for inhibiting anchorage independent growth in pCDH and SIRT2 overexpressing HCT116 cells. Values are the average from three independent experiments done in triplicate.

Inhibitor	GI_{50} (μM)		Fold Change*
	Control	SIRT2 Expression	
TM	13.5	24.2	1.8
JH-T4	12.6	12.7	1

*GI_{50} for SIRT2 Expression/ GI_{50} Control

To facilitate future inhibitor development efforts, we became interested in understanding how the introduction of the hydroxyl group on JH-T4 leads to decreased SIRT2 selectivity and increased inhibition of the defatty-acylation activity of SIRT2. We hypothesized

that introduction of the hydroxyl group on TM allowed the compound to form hydrogen bonds with SIRT1, SIRT2 and SIRT3, making the compound a more efficient suicide substrate, which leads to the increased inhibition of SIRT1 and SIRT3, as well as better inhibition of the defatty-acylation activity of SIRT2.

To test this hypothesis, we synthesized another TM analogue, NH-TM (Figure 1), where the aniline moiety was replaced with glycine. NH-TM, like JH-T4, should be able to form more hydrogen bonds than TM with SIRT1, SIRT2 and SIRT3. If our hypothesis is correct, we expect NH-TM to behave similarly to JH-T4 at inhibiting SIRT1, SIRT2, and SIRT3 deacetylation activities. Indeed, NH-TM was potent against SIRT2, exhibiting an IC_{50} value of 0.088 μM (Table 5.1). NH-TM, like JH-T4, inhibits both SIRT1 and SIRT3 with IC_{50} values of 0.43 μM and 2.4 μM, respectively (Table 5.1).

Our study here not only provides the first SIRT2 inhibitor (JH-T4) that can inhibit the defatty-acylation of K-Ras4a in cells, but also highlights that a small change in structure can lead to a significant change in the potency and selectivity of a small molecule inhibitor. The introduction of a hydroxyl group on the selective SIRT2 inhibitor TM (JH-T4) decreased the selectivity, but increased the ability to inhibit the defatty-acylation activity of SIRT2. Our data suggest that this is due to the ability of the compound to form additional hydrogen bonds with SIRT1, SIRT2 and SIRT3.

Protein lysine fatty acylation is emerging as an important protein post-translational modification. Recently, several Ras family of small GTPases have been reported to be regulated by lysine fatty acylation and sirtuin-catalyzed defatty-acylation.[13,27,28] Small molecules that can inhibit the defatty-acylation activity of sirtuins would enable us and others to better understand the functions of protein lysine fatty acylation. Here, we identify JH-T4 as the first small molecule that can modulate the level of lysine fatty acylation on K-Ras4a. JH-T4 can be used as a tool to further study protein lysine fatty acylation, an understudied but important protein

post-translational modification.

Interestingly, JH-T4 is more cytotoxic than TM in several human cell lines, likely due to inhibition of other sirtuins as SIRT2 overexpression did not protect the cells from the effect of JH-T4. However, compared to TM, JH-T4 loses the selective toxicity to cancer cells. At this point, it is not clear whether the lack of cancer cell selectivity is due to ability of JH-T4 to inhibit other sirtuins or due to inhibition of the defatty-acylation activity of SIRT2. To address this question, future SIRT2 inhibitor development should focus on obtaining compounds that can inhibit the defatty-acylation activity and are SIRT2-selective.

3. Methods

Reagents, antibodies and plasmids. TM and JH-T4 were synthesized as previously described.[2] TM and JH-T4 were dissolved in ethanol (EtOH). For studies with NH-TM, all compounds were dissolved in dimethyl sulfoxide (DMSO). For western blots, the acetyl-p53 (CST #2525) (1:1000, o/n 4˚C) and anti-rabbit conjugated to horseradish peroxidase (CST #2525) were purchased from cell signaling technologies and used at the indicated dilutions and incubation time. Anti-Flag M2 conjugated to horseradish peroxidase (A8592) (1:7500, 1 hr, rt), and the anti-acetyl-α-tubulin (6-11B-1) (MABT868) antibodies were purchased from Sigma-Aldrich. The Anti-Flag M2 affinity agarose was from Sigma. For immunofluorescence, the secondary CY3 goat-anti-mouse (A10521) was purchased from Life Technologies and used at a 1:1000 dilution for 1 hour at room temperature. For ectopic overexpression of K-Ras4a, pCMV5-Flag-K-Ras4a was cloned as previously described.[13] Alk14 was synthesized as previously described.[27]

Cell Culture and Transfection. MCF-7, MDA-MB-231, MDA-MB-468 and HME-1 cells were cultured in DMEM supplemented with 10% FBS (Invitrogen). ASPC-1, and NCI-H23 cells were cultured in RPMI media supplemented with 10% FBS. HCT116 cells were cultured in McCoy's 5A media with 10% FBS. Mammary epithelial cell growth medium (MEGM; Lonza) supplemented according to manufacturer's instruction was used to culture MCF10A

cells. All cells were maintained at 37˚C with 5% CO_2.

Expression and Purification of Sirtuins. Human SIRT1, SIRT2, SIRT3 and SIRT6 were expressed and purified as previously described.[2,29]

***In vitro* deacylation assay (with and without pre-incubation).** *In vitro* IC_{50} values were determined using the same method previously reported.[2,23]

Western Blots. Western blots were performed as previously described. Briefly, protein samples were lysed in 4% SDS lysis buffer supplemented with protease inhibitor cocktail (Sigma) and universal cell nuclease (Thermo). After determining the protein concentration by BCA assay, the samples were normalized, denatured and resolved by 12% SDS PAGE at a constant voltage of 200 V for approximately 50 min. The proteins were then transferred to Polyvinylidene difluoride (PVDF) membrane at a constant current of 330 mA for 90 min to 120 min. After transferring, the membrane was blocked in 5% bovine serum albumin (BSA) in TBST buffer (0.1% Tween-20, 25 mM Tris-HCl pH 7.6, 150 mM NaCl) for 1 hr at room temperature. The antibodies were added according to the manufacture instructions. After primary antibody incubation, the membrane was washed three times with TBST buffer for 5 minutes each. The appropriate secondary antibody was added to the sample at a ratio of (1:3000) for 1 hr at room temperature in 5% BSA in TBST. After secondary antibody incubation, the membrane was washed 5 times with TBST buffer for 5 min each. After the final wash the membranes were developed using ECL Plus (Pierce).

Detection of Ac-α-Tubulin Levels by Immunofluorescence. The same method previously reported was used.[23] Briefly, 2×10^5 MCF-7 cells were seeded in 35mm glass bottom dishes from MatTek. After 24 hr cells were treated either with 25 μM of inhibitor or vehicle control for 6 hr. After 6 hr the cells were washed three times with 1× PBS and fixed by placing the cells in ice cold methanol for 10 min. Cells were treated with 0.1% Triton-X in PBS for 10 min to permeabilize the membrane. The cells were then washed with 1× PBS three times, for 5 min

each. After the last wash, the cells were placed in 1% BSA in TBST (25 mM Tris-HCl pH 7.4, 150 mM NaCl, and 0.1% Tween-20) for 30 min at room temperature. After blocking, the Ac-α-tubulin antibody was added to the samples at a 1:100 dilution in 1% BSA in TBST, and the samples were placed at 4°C overnight. The samples were washed three times with TBST (5 min per wash), and the secondary antibody (CY3) was added to the samples (1:1000, in 1% BSA in TBST) for 1 hr at room temperature. After 1 hr, the samples were washed three times with TBST for 5 min each and then mounted with DAPI-Fluoromount G (Southern Biotech). Samples were imaged using a Zeiss 880i confocal microscope. Fiji software was used for analysis.[30]

Detection of K-Ras4a Fatty Acylation after *in vitro* treatment with SIRT2. pCMV5-Flag-K-Ras4a was transfected into HEK-293T cells. After 24 hours, the cells were treated with 50 μM Alk14 for 6 hours. The cells were collected and lysed with 1% NP40 lysis buffer (50 mM Tris pH 8.0, 150 mM NaCl, 10% glycerol, and 1% NP40) supplemented with protease inhibitor cocktail. To isolate K-Ras4a, anti-Flag M2 affinity agarose was added to the samples. After 2 hours incubation at 4°C, the affinity agarose was washed three times with 1 mL of 0.2% NP40 wash buffer (50 mM Tris pH 8.0, 150 mM NaCl, 0.2% NP40). The affinity gel was then washed three times with 50 mM Tris pH 8.0, and aliquoted equally into 8 tubes. The affinity gel was then suspended in 25 μl of assay buffer (50 mM Tris-HCl pH 8.0, 100 mM NaCl, 2 mM $MgCl_2$, 1 mM DTT) with 5 μM SIRT2 with 1 mM NAD and the noted inhibitor at the indicated concentration and placed at 37 °C for 1 h. After the enzymatic reaction, the affinity gel was again washed three times with 1 mL of 0.2% NP40 wash buffer. After the last wash, the affinity gel was dried and resuspended in 20 μL of 0.2% NP40 wash buffer. To each tube, Rh-N_3 (3 μL of 1 mM solution in DMF, final concentration 200 μM), followed by TBTA (1 μL of 10 mM solution in DMF, final concentration 500 μM), $CuSO_4$ (1 μL of 40 mM solution in H_2O, final concentration 2 mM), and TCEP (1 μL of 40 mM solution in H_2O, final concentration 2 mM) were added, and the click chemistry reaction was allowed to proceed for 30 minutes at room

temperature in the dark. The reaction was quenched by adding 10 μL of 6 × protein loading buffer (60 mM Tris pH 6.8, 0.12 % SDS (w/v), 47% glycerol, 0.6 M DTT and 0.0006% bromophenol blue (w/v)) and heating the sample at 95 °C for 10 min. The sample was then treated with hydroxylamine (pH 8.0, final concentration 300 μM) at 95 °C for 7 min. To visualize the fatty acylation levels by in gel fluorescence, the samples were resolved by 12% SDS-PAGE. Fluorescence signal was detected using a Typhoon 9400 Variable Mode Imager (GE Healthcare Life Sciences, Piscataway, NJ) with the emission/excitation settings of Green (532 nm)/580BP30 with a PMT setting of 500 V (normal sensitivity). Fiji software was used for analysis.[30]

Detection of K-Ras4a Fatty Acylation after in cell treatment with different inhibitors. HEK-293T cells were transfected with pCMV5-Flag-K-Ras4a, cultured for 24 hours, and then were treated with the indicated concentration of inhibitor for 6 hours. The media was then changed with the indicated concentration of inhibitor and 50 μM of Alk14 for an additional 6 hours. The samples were collected and lysed with 1% NP40 lysis buffer supplemented with protease inhibitor cocktail. After determining the protein concentration using a Bradford assay, 0.5-1 mg of whole cell lysate was aliquoted out, and diluted to a protein concentration of 1mg/1mL. To the samples, 10 μL of pre-washed M2 affinity agarose was added to each. After incubation for 2 hours at 4˚C, the affinity agarose was washed three times with 1 mL of 0.2% NP40 wash buffer. The same click chemistry conditions described above were used to detect fatty acylation levels.

Cell Viability Assay. In cell GI_{50} values were determined using the method previously published.[23] Briefly, 2,000-6,000 cells/ well were seeded in a 96 well dish. After 24 hr, inhibitors were added. After 72 hr, Cell Titer Blue (Promega) was added following the manufactures protocol. GI_{50} values were determined using Prism7 software.

Anchorage-Independent Growth Assay. In cell GI_{50} values for anchorage-independent growth were determined using the method previously published.[23] Briefly, cells were counted and 1,000 cells per well were seeded in 0.3% low melting point agar supplemented with the appropriate amount of inhibitor (Sigma Aldrich) on top of a 0.6% low melting point agar layer. Additional agar was added after 7 days of culture. Colonies were stained with nitrotetrazolium blue chloride in PBS after 14 days of culture at 37˚C and 5% CO_2. Images were taken on a BioRad imager, and the number of colonies per well was quantified using FIJI/ ImageJ software.[30]

General Synthetic Methods and Materials. Reagents were obtained from ChemImpex, Alfa Aesar and Sigma-Aldrich. All ^{1}H-NMR were performed on Bruker 500 spectrometers. All LC-MS data were obtained by Shimadzu HPLC LC20-AD and Thermo Scientific LCQ Fleet. The column used was Kinetex 5u EVO C18 100A column (30 × 2.1 mm, 5 μm). The compounds were monitored at 215 and 260 nm with positive detection mode. Solvents used were water with 0.1 % HPLC-grade acetic acid and acetonitrile with 0.1% HPLC-grade acetic acid.

Synthesis of H3K9-Ac and Myr peptides. The peptides used for the *in vitro* activity assays were synthesized using solid phase peptide synthesis as previously reported.[31]

Synthesis of JH-T4. JH-T4 was synthesized following a procedure for TM described in the literature.[2] Briefly, to a solution of N^2-((benzyloxy)carbonyl)-N^6-tetradecanethioyllysine (10 mmol) and N-methylmorpholine (10 mmol) in dimethylformamide at 0˚C, isobutyl chloroformate was added dropwise. 3-Aminophenol was added subsequently added. After 30 min at 0˚C, the reaction was warmed to room temperature and stirred overnight. The reaction was concentrated, and the product was purified using silica gel flash chromatography (hexanes: ethyl acetate = 3:2) as a white solid. ^{1}H-NMR (400 MHz, $CDCl_3$): δ 8.53 (s, 1H), 7.68 (s, 1H), 7.39 (m, 1H), 7.32 (m, 6H), 7.12 (t, J = 8.1 Hz, 1H), 6.86 (d, J = 7.9 Hz, 1H), 6.61 (dd, J = 8.3, 2.3 Hz, 1H), 5.65 (d, J = 7.9 Hz, 1H), 5.28 – 4.89 (m, 2H), 4.35 (m, 1H), 3.61 (m, 2H), 2.57 (t, J= 7.5 Hz, 2H), 1.90 (m, 1H), 1.67 (m, 5H), 1.43 (m, 2H), 1.22 (m, 21H), 0.86 (t, J = 6.7 Hz,

3H). LCMS (ESI) calcd. for $C_{34}H_{52}N_3O_4S$ $[M+H]^+$ 598.36, observed. 598.25.

Synthesis of NH-TM. The synthesis of N^2-((benzyloxy)carbonyl)-N^6-tetradecanethioyllysine was done following the procedure in the literature[2]. To the solution of N^2-((benzyloxy)carbonyl)-N^6-tetradecanethioyllysine (.1006 g, .985 mmol), glycinamide (220 mg, 0.1985 mmol) and triethylamine (83 μL, 0.5956 mmol) in dimethylformamide (2 mL), 1-Ethyl-3-(3-dimethylaminopropyl)carbodiimide hydrochloride (419 mg, 0.2184 mmol) and hydroxybenzotriazole (365 mg, 0.2382 mmol) were added. The reaction mixture was stirred overnight at room temperature. Dimethylformamide was removed in vacuo at 70 °C. The mixture was re-dissolved in ethyl acetate, and washed by 5% sodium bicarbonate, 10% citric acid, water and brine. After washing, it was dried with sodium sulfate. The mixture was purified by column (dichloromethane: methanol) to afford the final compound (265 mg, 24% yield) as a white solid. ^{1}H NMR (500 MHz, Methanol-d4) δ 7.42 – 7.27 (m, 5H), 5.16 – 5.07 (m, 2H), 4.07 (dd, J = 8.6, 5.5 Hz, 1H), 3.82 (d, J = 16.9 Hz, 2H), 3.60 (t, J = 7.1 Hz, 2H), 2.62 – 2.57 (m, 2H), 1.85 (ddt, J = 13.7, 10.0, 6.0 Hz, 1H), 1.79 – 1.60 (m, 5H), 1.56 – 1.39 (m, 2H), 1.31 (m, J = 10.5 Hz, 20H), 0.92 (t, J = 6.9 Hz, 3H). ^{13}C NMR (125 MHz, Methanol-d4) δ 205.08, 174.01, 172.90, 157.41, 136.67, 128.09 (2C), 127.67, 127.52 (2C), 66.44, 55.43, 45.68, 45.13, 41.77, 31.68, 30.98, 29.44, 29.41, 29.37 (2C), 29.33, 29.23, 29.09, 29.08, 28.56, 26.92, 22.93, 22.35, 13.06. LCMS (ESI) calcd. for $[M+H]^+$ 563.36, observed 563.32.

REFERENCES

(1) Haigis, M. C.; Sinclair, D. A. Mammalian Sirtuins: Biological Insights and Disease Relevance. *Annu Rev Pathol* **2010,** *5*, 253.

(2) Jing, H.; Hu, J.; He, B.; Negron Abril, Y. L.; Stupinski, J.; Weiser, K.; Carbonaro, M.; Chiang, Y. L.; Southard, T.; Giannakakou, P.et al. A SIRT2-Selective Inhibitor Promotes c-Myc Oncoprotein Degradation and Exhibits Broad Anticancer Activity. *Cancer Cell* **2016,** *29* (5), 767.

(3) Zhao, D.; Zou, S. W.; Liu, Y.; Zhou, X.; Mo, Y.; Wang, P.; Xu, Y. H.; Dong, B.; Xiong, Y.; Lei, Q. Y.et al. Lysine-5 acetylation negatively regulates lactate dehydrogenase A and is decreased in pancreatic cancer. *Cancer Cell* **2013,** *23* (4), 464.

(4) Serrano, L.; Martinez-Redondo, P.; Marazuela-Duque, A.; Vazquez, B. N.; Dooley, S. J.; Voigt, P.; Beck, D. B.; Kane-Goldsmith, N.; Tong, Q.; Rabanal, R. M.et al. The tumor suppressor SirT2 regulates cell cycle progression and genome stability by modulating the mitotic deposition of H4K20 methylation. *Genes Dev* **2013,** *27* (6), 639.

(5) Liu, P. Y.; Xu, N.; Malyukova, A.; Scarlett, C. J.; Sun, Y. T.; Zhang, X. D.; Ling, D.; Su, S. P.; Nelson, C.; Chang, D. K.et al. The histone deacetylase SIRT2 stabilizes Myc oncoproteins. *Cell Death Differ* **2013,** *20* (3), 503.

(6) Kim, H. S.; Vassilopoulos, A.; Wang, R. H.; Lahusen, T.; Xiao, Z.; Xu, X.; Li, C.; Veenstra, T. D.; Li, B.; Yu, H.et al. SIRT2 maintains genome integrity and suppresses tumorigenesis through regulating APC/C activity. *Cancer Cell* **2011,** *20* (4), 487.

(7) North, B. J.; Marshall, B. L.; Borra, M. T.; Denu, J. M.; Verdin, E. The human Sir2 ortholog, SIRT2, is an NAD+-dependent tubulin deacetylase. *Mol Cell* **2003,** *11* (2), 437.

(8) Teng, Y. B.; Jing, H.; Aramsangtienchai, P.; He, B.; Khan, S.; Hu, J.; Lin, H.; Hao, Q. Efficient demyristoylase activity of SIRT2 revealed by kinetic and structural studies. *Sci Rep* **2015,** *5*, 8529.

(9) Jin, J.; He, B.; Zhang, X.; Lin, H.; Wang, Y. SIRT2 Reverses 4-Oxononanoyl Lysine Modification on Histones. *J Am Chem Soc* **2016,** *138* (38), 12304.

(10) Cui, Y.; Li, X.; Lin, J.; Hao, Q.; Li, X. D. Histone Ketoamide Adduction by 4-Oxo-2-nonenal Is a Reversible Posttranslational Modification Regulated by Sirt2. *ACS Chem Biol* **2017,** *12* (1), 47.

(11) Cha, Y.; Han, M. J.; Cha, H. J.; Zoldan, J.; Burkart, A.; Jung, J. H.; Jang, Y.; Kim, C. H.; Jeong, H. C.; Kim, B. G.et al. Metabolic control of primed human pluripotent stem cell fate and function by the miR-200c-SIRT2 axis. *Nat Cell Biol* **2017,** *19* (5), 445.

(12) Seo, K. S.; Park, J. H.; Heo, J. Y.; Jing, K.; Han, J.; Min, K. N.; Kim, C.; Koh, G. Y.; Lim, K.; Kang, G. Y.et al. SIRT2 regulates tumour hypoxia response by promoting HIF-1alpha hydroxylation. *Oncogene* **2015,** *34* (11), 1354.

(13) Jing, H.; Zhang, X.; Wisner, S. A.; Chen, X.; Spiegelman, N. A.; Linder, M. E.; Lin, H. SIRT2 and lysine fatty acylation regulate the transforming activity of K-Ras4a. *Elife* **2017,** *6*.

(14) Tiago Fleming Outeiro, E. K., Stephen M. Altmann, Irina Kufareva, Katherine E. Strathearn, Allison M. Amore, Catherine B. Volk, Michele M. Maxwell, Jean-Christophe Rochet, Pamela J. McLean, Anne B. Young, Ruben Abagyan,; Mel B. Feany, B. T. H., Aleksey G. Kazantsev. Sirtuin 2 Inhibitors Rescue a-Synuclein–Mediated Toxicity in Models of Parkinson's Disease. *Science* **2007,** *317* (5837), 516.

(15) Rumpf, T.; Schiedel, M.; Karaman, B.; Roessler, C.; North, B. J.; Lehotzky, A.; Olah, J.; Ladwein, K. I.; Schmidtkunz, K.; Gajer, M.et al. Selective Sirt2 inhibition by ligand-induced rearrangement of the active site. *Nat Commun* **2015,** *6*, 6263.

(16) Lain, S.; Hollick, J. J.; Campbell, J.; Staples, O. D.; Higgins, M.; Aoubala, M.; McCarthy, A.; Appleyard, V.; Murray, K. E.; Baker, L.et al. Discovery, in vivo activity, and mechanism of action of a small-molecule p53 activator. *Cancer Cell* **2008,** *13* (5), 454.

(17) Mellini, P.; Itoh, Y.; Tsumoto, H.; Li, Y.; Suzuki, M.; Tokuda, N.; Kakizawa, T.; Miura, Y.; Takeuchi, J.; Lahtela-Kakkonen, M.et al. Potent mechanism-based sirtuin-2-selective inhibition by an in situ-generated occupant of the substrate-binding site, "selectivity pocket" and NAD(+)-binding site. *Chem Sci* **2017,** *8* (9), 6400.

(18) Schiedel, M.; Rumpf, T.; Karaman, B.; Lehotzky, A.; Olah, J.; Gerhardt, S.; Ovadi, J.; Sippl, W.; Einsle, O.; Jung, M. Aminothiazoles as Potent and Selective Sirt2 Inhibitors: A Structure-Activity Relationship Study. *J Med Chem* **2016,** *59* (4), 1599.

(19) Yang, L. L.; Wang, H. L.; Zhong, L.; Yuan, C.; Liu, S. Y.; Yu, Z. J.; Liu, S.; Yan, Y. H.; Wu, C.; Wang, Y.et al. X-ray crystal structure guided discovery of new selective, substrate-mimicking sirtuin 2 inhibitors that exhibit activities against non-small cell lung cancer cells. *Eur J Med Chem* **2018,** *155*, 806.

(20) Wang, C.; Wang, F.; Chen, X.; Zou, Y.; Zhu, H.; Zhao, Q.; Shen, J.; Li, Y.; Li, Y.; He, B. The mimics of N(epsilon)-acyl-lysine derived from cysteine as sirtuin inhibitors. *Bioorg Med Chem Lett* **2018,** *28* (14), 2375.

(21) Yang, L.; Ma, X.; Yuan, C.; He, Y.; Li, L.; Fang, S.; Xia, W.; He, T.; Qian, S.; Xu, Z.et al. Discovery of 2-((4,6-dimethylpyrimidin-2-yl)thio)-N-phenylacetamide derivatives as new potent and selective human sirtuin 2 inhibitors. *Eur J Med Chem* **2017,** *134*, 230.

(22) Tatum, P. R.; Sawada, H.; Ota, Y.; Itoh, Y.; Zhan, P.; Ieda, N.; Nakagawa, H.; Miyata, N.; Suzuki, T. Identification of novel SIRT2-selective inhibitors using a click chemistry approach. *Bioorg Med Chem Lett* **2014,** *24* (8), 1871.

(23) Spiegelman, N. A.; Price, I. R.; Jing, H.; Wang, M.; Yang, M.; Cao, J.; Hong, J. Y.; Zhang, X.; Aramsangtienchai, P.; Sadhukhan, S.et al. Direct Comparison of SIRT2 Inhibitors: Potency, Specificity, Activity-Dependent Inhibition, and On-target Anticancer Activities. *ChemMedChem* **2018**, DOI:10.1002/cmdc.201800391 10.1002/cmdc.201800391.

(24) Kudo, N.; Ito, A.; Arata, M.; Nakata, A.; Yoshida, M. Identification of a novel small molecule that inhibits deacetylase but not defatty-acylase reaction catalysed by SIRT2. *Philos Trans R Soc Lond B Biol Sci* **2018,** *373* (1748).

(25) Hu, J.; Jing, H.; Lin, H. Sirtuin inhibitors as anticancer agents. *Future Med Chem* **2014,** *6* (8), 945.

(26) Vaziri, H.; Dessain, S. K.; Ng Eaton, E.; Imai, S. I.; Frye, R. A.; Pandita, T. K.; Guarente, L.; Weinberg, R. A. hSIR2(SIRT1) functions as an NAD-dependent p53 deacetylase. *Cell* **2001,** *107* (2), 149.

(27) Zhang, X.; Spiegelman, N. A.; Nelson, O. D.; Jing, H.; Lin, H. SIRT6 regulates Ras-related protein R-Ras2 by lysine defatty-acylation. *Elife* **2017,** *6*.

(28) Zhou, Y.; Huang, C.; Yin, L.; Wan, M.; Wang, X.; Li, L.; Liu, Y.; Wang, Z.; Fu, P.; Zhang, N.et al. N(epsilon)-Fatty acylation of Rho GTPases by a MARTX toxin effector. *Science* **2017,** *358* (6362), 528.

(29) Zhang, X.; Khan, S.; Jiang, H.; Antonyak, M. A.; Chen, X.; Spiegelman, N. A.; Shrimp, J. H.; Cerione, R. A.; Lin, H. Identifying the functional contribution of the defatty-acylase activity of SIRT6. *Nat Chem Biol* **2016,** *12* (8), 614.

(30) Schindelin, J.; Arganda-Carreras, I.; Frise, E.; Kaynig, V.; Longair, M.; Pietzsch, T.; Preibisch, S.; Rueden, C.; Saalfeld, S.; Schmid, B.et al. Fiji: an open-source platform for biological-image analysis. *Nat Methods* **2012,** *9* (7), 676.

(31) Aramsangtienchai, P.; Spiegelman, N. A.; He, B.; Miller, S. P.; Dai, L.; Zhao, Y.; Lin, H. HDAC8 Catalyzes the Hydrolysis of Long Chain Fatty Acyl Lysine. *ACS Chem Biol* **2016,** *11* (10), 2685.

CHAPTER 6

S-PALMITOYLATION OF JUNCTIONAL ADHESION MOLECULE C REGULATES ITS TIGHT JUNCTION LOCALIZATION AND CELL MIGRATION[5]

Abstract

Junctional Adhesion Molecule C (JAM-C) is an immunoglobulin superfamily protein expressed in epithelial cells, endothelial cells, and leukocytes. JAM-C has been implicated in leukocyte transendothelial migration, angiogenesis, cell-adhesion, cell polarity, spermatogenesis and metastasis. Here, we show that JAM-C undergoes S-palmitoylation on two juxtamembrane cysteine residues, Cys264 and Cys265. We have identified DHHC7 as a JAM-C palmitoylating enzyme by screening all known palmitoyltransferases (PATs or DHHCs). Ectopic expression of DHHC7, but not a DHHC7 catalytic mutant, enhances JAM-C S-palmitoylation. Moreover, DHHC7 knockdown decreases the S-palmitoylation level of JAM-C. Palmitoylation of JAM-C promotes its localization to tight junctions and inhibits transwell migration of A549 lung cancer cells. These results suggest that S-palmitoylation of JAM-C can be potentially targeted to control cancer metastasis.

1. Introduction

JAM-C is a member of the junctional adhesion molecule (JAM) family, and is localized at the cell-cell contact sites, in particular the tight-junction (TJ) region of endothelial and

[5] This is a revised version of the published paper: Aramsangtienchai, P., Spiegelman, N.A., Cao, J., Lin, H. S-Palmitoylation of Junctional Adhesion Molecule C Regulates Its Tight Junction Localization and Cell Migration. *Journal of Biological Chemistry* 292(13), 5325-5334 (2017).
For this paper, I (NAS) preformed the experiments presented in Figures 6.3, 6.4, 6.5, 6.6, and 6.7C, synthesized Alk14 and revised the manuscript. P.A. and H.L. designed the experiments and wrote the manuscript. P.A. preformed all of the other biochemical assays except for the experiments shown in Figure 6.10 which were preformed by J.C.. All authors reviewed and approved the final version of the manuscript.

epithelial cells. JAM-C is a type I transmembrane protein with two conserved immunoglobulin-like domains in the extracellular amino (N)-terminal region (Fig 1A). At its intracellular carboxyl (C)-terminal region, JAM-C contains a PDZ binding domain motif, which allows JAM-C to interact with other PDZ motif-containing proteins at the TJ including ZO-1 and PAR-3 [1-3].

JAM-C has been found to regulate leukocyte adhesion and transmigration across endothelial cells through a heterophillic interaction between endothelial JAM-C and leukocyte integrin MAC-1 ($\alpha M\beta 2$) [4]. JAM-C is essential for polarized round spermatids, and JAM-C deficient mice have defective spermatid differentiation [5]. JAM-C deletion in mice leads to neuropathy, and some Jam-C mutations affect the integrity of the vascular system and the brain [6,7].

Recently, JAM-C has been shown to play a role in metastasis and development of certain cancer cells [8-11]. In melanoma cells, the homophillic JAM-C/JAM-C trans-interaction between melanoma cells and endothelial cells promotes metastasis [12]. Additionally, the JAM-C expression level in fibrosarcoma and lung cancer cells is reported to be positively correlated to metastasis. Knocking down JAM-C in highly metastatic lung cancer cells leads to a decrease in cell migration [8,13]. JAM-C, therefore, could be a therapeutic target for certain cancers.

Cys-palmitoylation (S-palmitoylation), a reversible lipid posttranslational modification, is the addition of a 16-carbon palmitoyl group onto cysteine residues of proteins via a labile thioester bond. S-palmitoylation plays a crucial role in cell signaling, localization and protein-protein interactions [14,15]. Palmitoyltransferases (PATs or DHHCs) catalyze S-palmitoylation. To date 23 mammalian DHHCs have been identified [16,17]. Here we showed that JAM-C undergoes S-palmitoylation on two membrane-proximal cysteine residues (Cys264 and Cys265) and this modification can be catalyzed by DHHC7. We found that S-palmitoylation of JAM-C promotes its localization to the cell-cell contact region and regulates cell migration.

2. Results

2.1 JAM-C is S-palmitoylated on two conserved juxtamembrane cysteine residues, Cys264 and Cys265

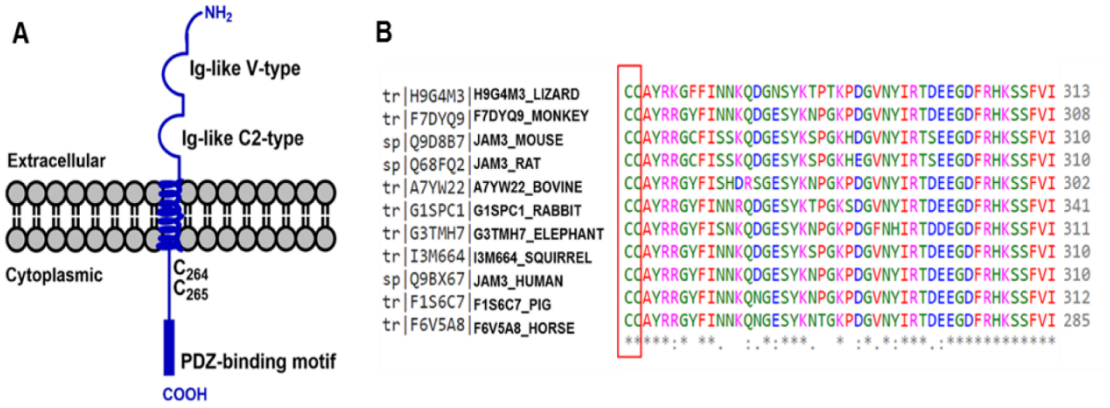

Figure 6.1. JAM-C is an immunoglobulin superfamily protein containing two conserved cysteine residues (Cys264 and Cys265, human sequence) in different species. **(A)** schematic structure of JAM-C transmembrane protein with two Ig-like domains in the extracellular region and one PDZ-binding motif in the cytoplasmic region. **(B)** Multiple sequence alignment by Clustal Omega showing the two cytoplasmic cysteine residues that are conserved across multiple species.

In addition to a PDZ-binding domain, the JAM-C intracellular C-terminus contains two transmembrane proximal cysteine residues (Figure 6.1A). These two cysteine residues are conserved across multiple mammalian species, suggesting these residues may have an important role (Figure 6.1B). Moreover, JAM-C has been identified in palmitoyl-protein proteomics studies as a protein that potentially has Cys-palmitoylation; yet, it had not been previously validated [18]. To test whether S-palmitoylation occurs on JAM-C, we employed a metabolic labeling strategy using an alkyne-tagged palmitic acid analogue (Alk14) [19,20]. Human T lymphocyte Jurkat cells and human umbilical vein endothelial cells (HUVEC) were cultured in the presence of Alk14, and endogenous JAM-C was immunoprecipitated and conjugated to BODIPY-azide (B-N_3) via click chemistry (Figure 6.2A). JAM-C had fluorescent labeling suggesting that it contains fatty acylation (Figure 6.2B). Similar results were obtained from ectopically expressed FLAG-tagged JAM-C in Human Embryonic Kidney 293T (HEK-293T) cells (Figure 6.2C and Figure 6.3).

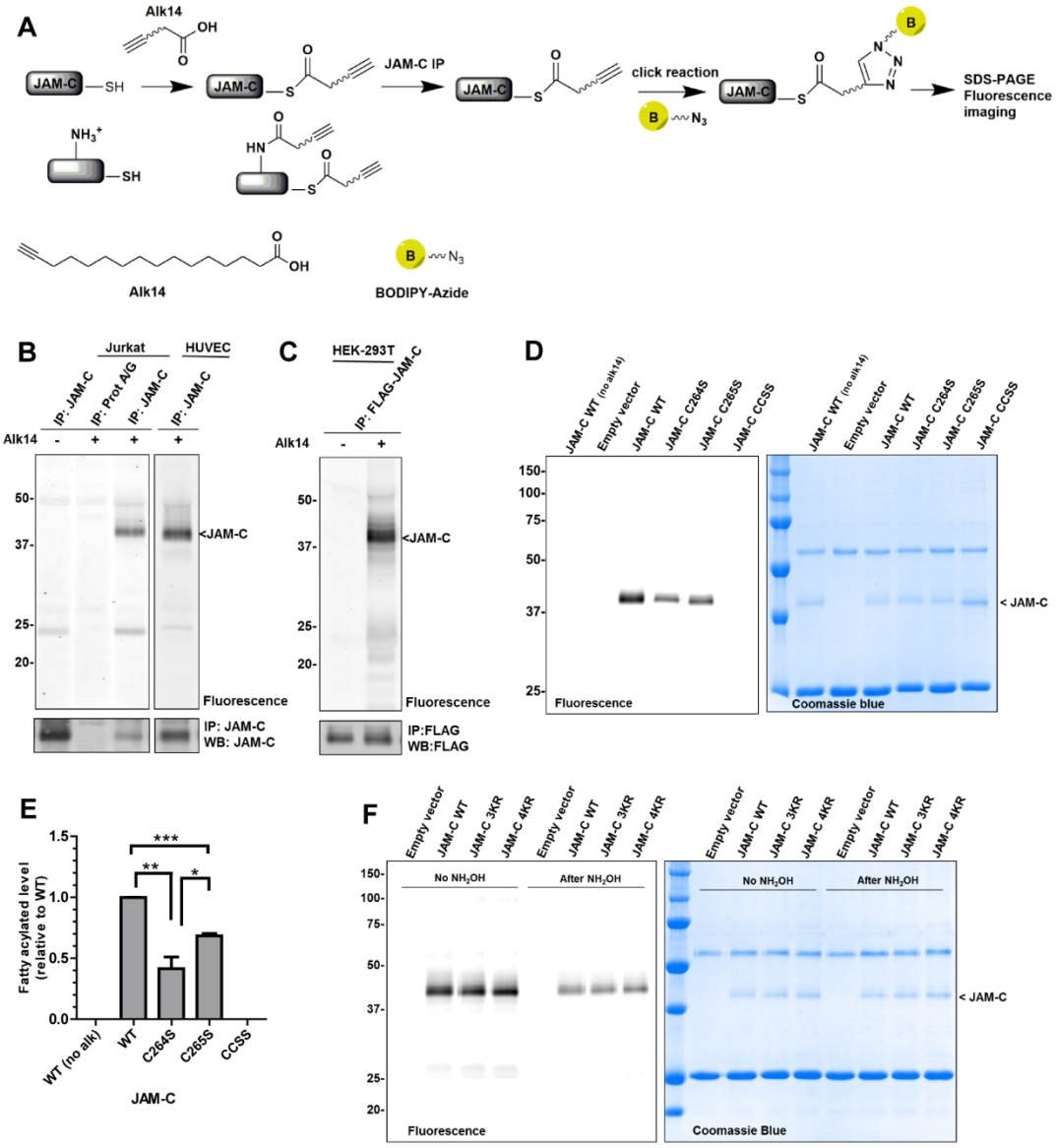

Figure 6.2. S-palmitoylation of JAM-C depends on Cys264 and Cys265. (A) Method for the detection of S-palmitoylation in JAM-C with Alk14. Cells were cultured with the palmitic acid analogue (Alk14) for metabolic labeling. JAM-C was immunoprecipitated from total lysate, and BODIPY-azide was then conjugated to the alkyne group using click chemistry. The fluorescence signal was imaged after SDS-PAGE. **(B)** Endogenous JAM-C in both Jurkat and HUVEC cells was fatty acylated by Alk14. **(C)** Overexpressed FLAG-tagged JAM-C in HEK-293T cells also contained fatty acylation. **(D)** The C264S and C265S mutations of JAM-C decreased the Alk14 labeling signal. Compared to the wild type JAM-C, palmitoylation in the single cysteine mutants (C264S and C265S) was reduced whereas it was abolished in the double cysteine mutant (CCSS). **(E)** Quantified fatty acylation level of the JAM-C mutants relative to WT (mean ± SD, n =3). The palmitoylation signal was quantified and normalized by the protein level on the Coomassie blue gel using Quantity One software (Bio-Rad). *, $P < 0.05$; **, $P < 0.01$; ***, $P < 0.001$. **(F)** The cytosolic lysine to arginine mutants, 3KR (K276R, K283R and K287R) and 4KR (K276R, K283R, K287R, and K305R) of JAM-C did not significantly reduce the Alk14 labeling signal. Representative results from two independent experiments are shown.

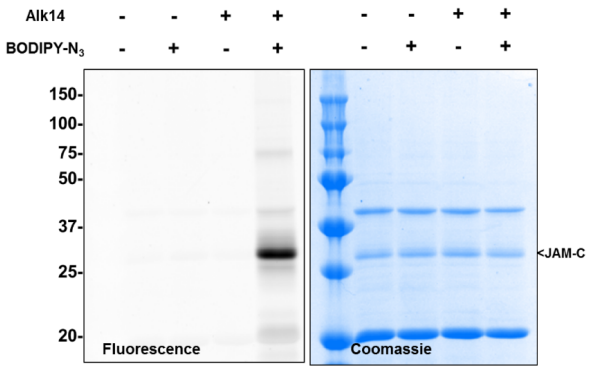

Figure 6.3. JAM-C undergoes S-palmitoylation detected by Alk14 labeling method. Overexpressed FLAG-tagged JAM-C in HEK-293T cells was labeled with Alk14. BODIPY-azide was then conjugated to the alkyne group using click chemistry and the fluorescent signal was imaged after SDS-PAGE.

To further confirm that this modification occurs on cysteine residues, we mutated these residues to serine. We observed a significant decrease in the fluorescence signal of the single cysteine mutants, C264S and C265S. However, the C264S mutation had a more profound effect on the fluorescence signal. Furthermore, we observed no fluorescence signal for the double cysteine mutant (CC264-265SS). These results indicated that S-palmitoylation on JAM-C depends on both Cys264 and Cys265 (Figure 6.2D,E). After the samples were treated with 0.5 M of hydroxylamine (pH 10.0), most of the fluorescence signal of FLAG-JAM-C was removed (Figure 6.2F) further confirming JAM-C has cysteine palmitoylation. However, there was some hydroxylamine resistant signal, similar to what was observed with TNF-α, a protein with lysine myristoylation [21].

To ensure that the hydroxylamine treatment was sufficient, we compared the labeling of FLAG-JAM-C before and after hydroxylamine treatment, with the labeling of the FLAG-TNFα mutant (KK19-20RR or KR mutant), a protein that has only cysteine palmitoylation [21], as well as other membrane proteins reported to have S-palmitoylation such as Transferrin Receptor 1 (TfR1) [22] and Syntaxin6 (STX6) [18]. After hydroxylamine treatment, the majority, if not all, of the labeling on the other proteins was removed, however some FLAG-JAM-C fluorescence signal remained (Figure 6.4). However, since there was a noticeable decrease in

fluorescence signal after hydroxylamine treatment, this supports that JAM-C has cysteine palmitoylation.

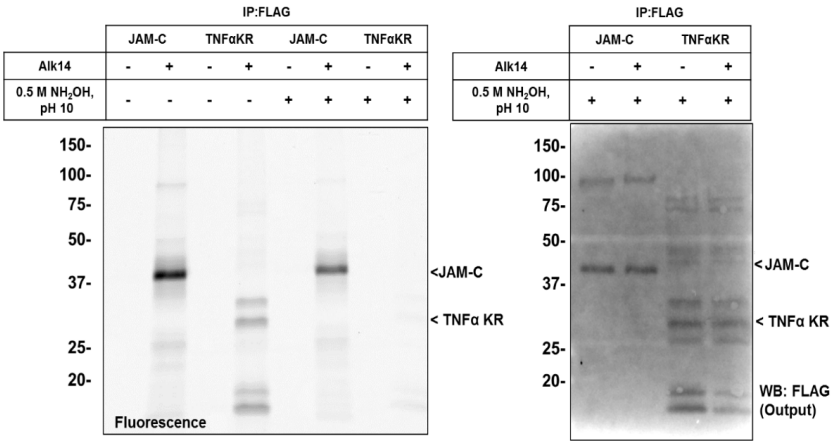

Figure 6.4. The S-palmitoylation of JAM-C is resistant to hydroxylamine treatment. The fluorescence gel of FLAG-JAM-C and FLAG-TNFα KR mutant before and after treatment with 0.5 M NH_2OH solution (pH 10.0) is shown. All the signal on FLAG-TNFα KR mutant was removed after 0.5 M NH_2OH solution treatment while that on FLAG-JAM-C still remained. TNFα has multiple bands due to different glycosylation and proteolysis.

To determine if JAM-C has lysine fatty acylation, we mutated all the cytosolic lysine residues to arginine (K276R, K283R, and K287R or 3KR; K276R, K283R, K287R and K305R or 4KR) and examined the fatty acylation signal. There was no significant change in the fluorescence signal with the 3KR and 4KR mutants compared to WT JAM-C suggesting that JAM-C does not have lysine fatty acylation (Figure 6.2F).

2.2 JAM-C is a DHHC7 Target

We next wanted to identify palmitoyltransferases that can control JAM-C S-palmitoylation. In mammals, there are 23 DHHC enzymes known to act as palmitoyltransferases. We co-overexpressed HA-tagged DHHC1-23 with FLAG-tagged JAM-C in HEK-293T cells and examined the fatty acylation level using the Alk14 metabolic labeling approach. From the initial DHHC-screening, and subsequent comparison of JAM-C palmitoylation levels with DHHC7 and 15 overexpressed (Figure 6.5 and Figure 6.6A, B), we decided to further validate DHHC7 as a palmitoyltransferase of JAM-C. Notably, it is possible

that JAM-C is a target of other palmitoyltransferases although co-overexpression of JAM-C with HA-tagged DHHC7 resulted in the most increase in JAM-C fatty acylation signal.

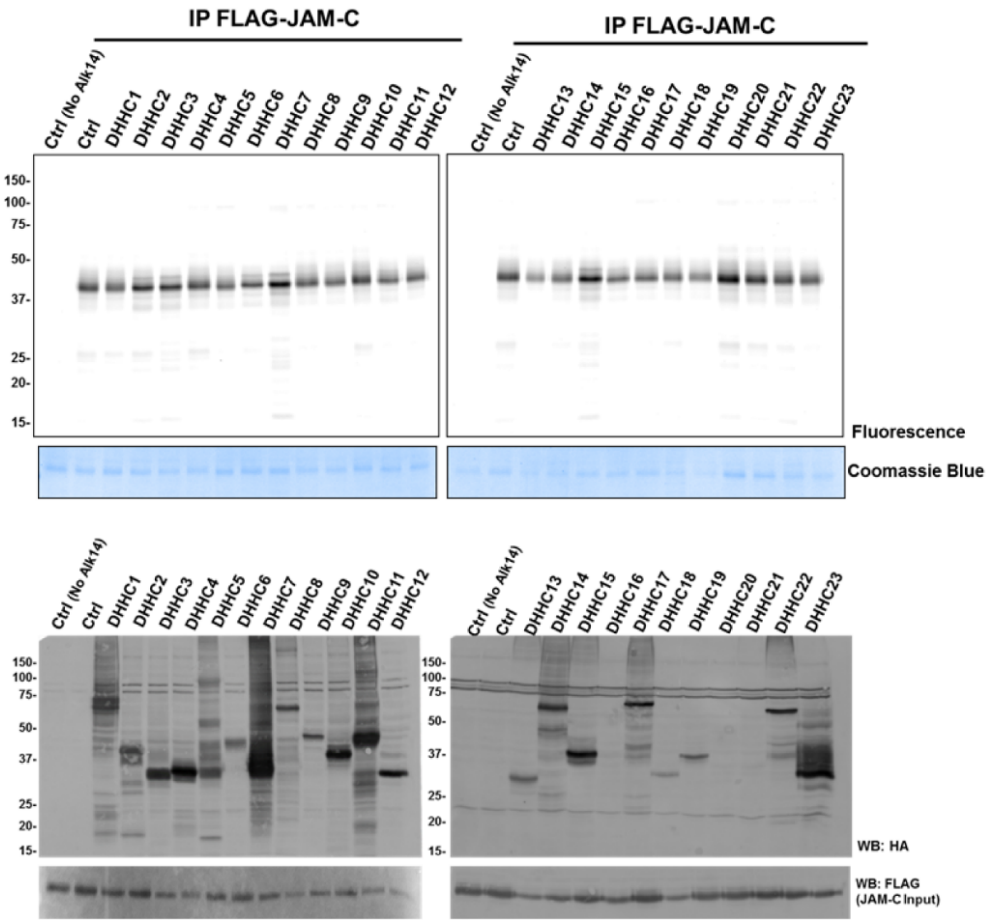

Figure 6.5. Screening different DHHCs for JAM-C palmitoyltransferase. Top panels show the fatty acylation level (Alk14 labeling signal) of immunoprecipated FLAG-tagged JAM-C. The bottom panels show the expression of HA-tagged DHHCs by Western blots.

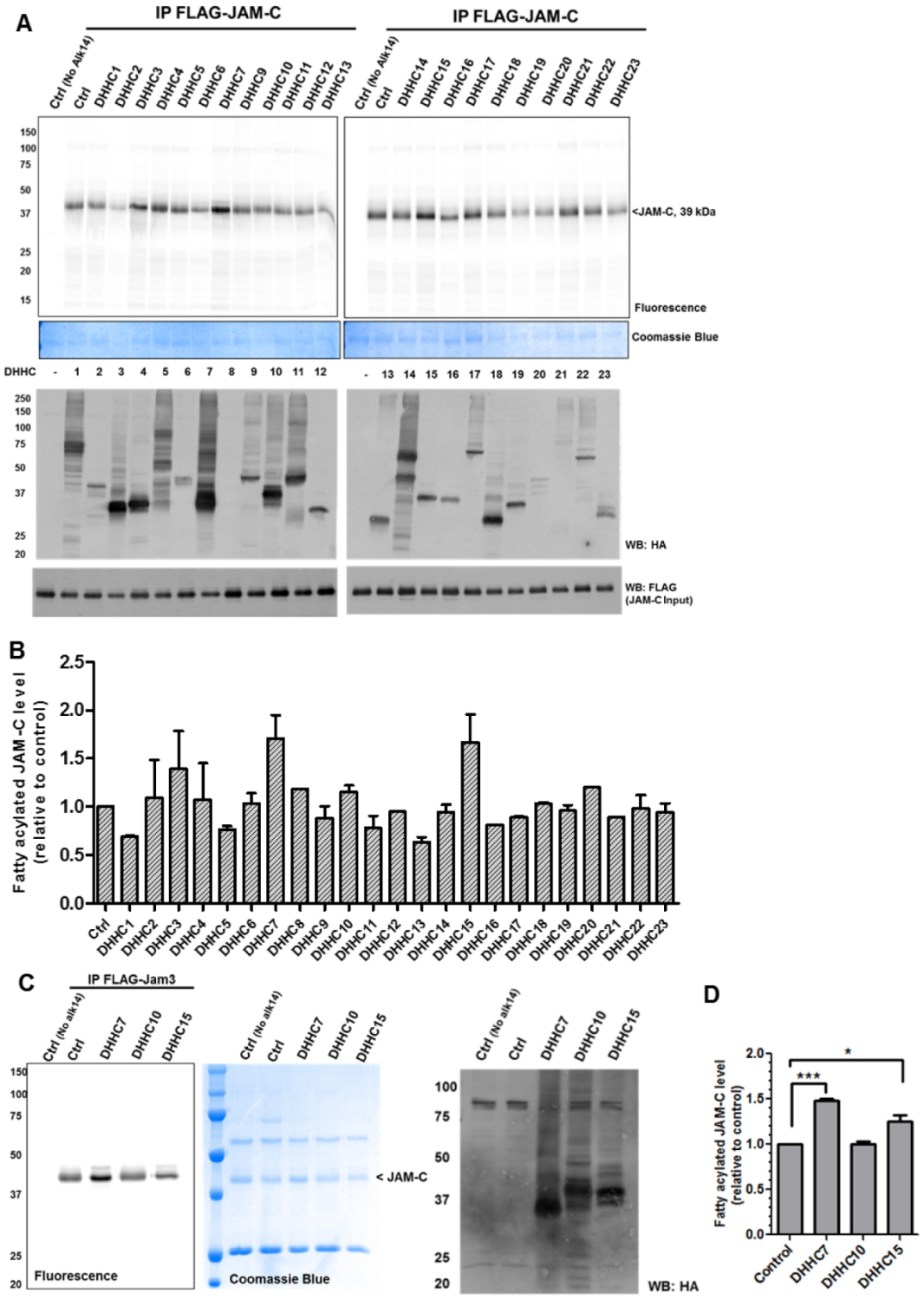

Figure 6.6. DHHC7 overexpression enhances the palmitoylation of JAM-C. (A) The palmitoylation levels of FLAG-tagged JAM-C co-overexpressed with different HA-tagged DHHC1-23 in HEK-293T cells. **(B)** Quantification of the results shown in A, mean ± SD, n =2. The palmitoylation signal was quantified and normalized with the protein levels on Coomassie blue gel using Quantity One software

(Bio-Rad). The signal in control cells without DHHC overexpression was set to 1.00 and served as the reference point for all other samples. **(C)** DHHC7 overexpression most significantly increased JAM-C palmitoylation. A representative result from two independent experiments was shown. **(D)** The quantified fatty acylation level of JAM-C co-overexpressed with DHHC 7, 10 or 15 relative to control (mean ± SD, n=2). *, $P < 0.05$; **, $P < 0.01$; ***, $P < 0.001$.

To confirm that DHHC7 can directly catalyze the palmitoylation of JAM-C, we examined the S-palmitoylation of JAM-C with co-expression of wild type DHHC7 and a catalytic dead mutant, DHHS7, in which the conserved catalytic cysteine residue is mutated to serine. As expected, only overexpression of DHHC7, but not DHHS7, augmented the JAM-C fatty acylation level in HEK293T cells (Figure 6.7A). Similar results were also obtained in U87 cells (Figure 6.7B). These results suggest that the catalytic activity of DHHC7 is required for the S-palmitoylation of JAM-C.

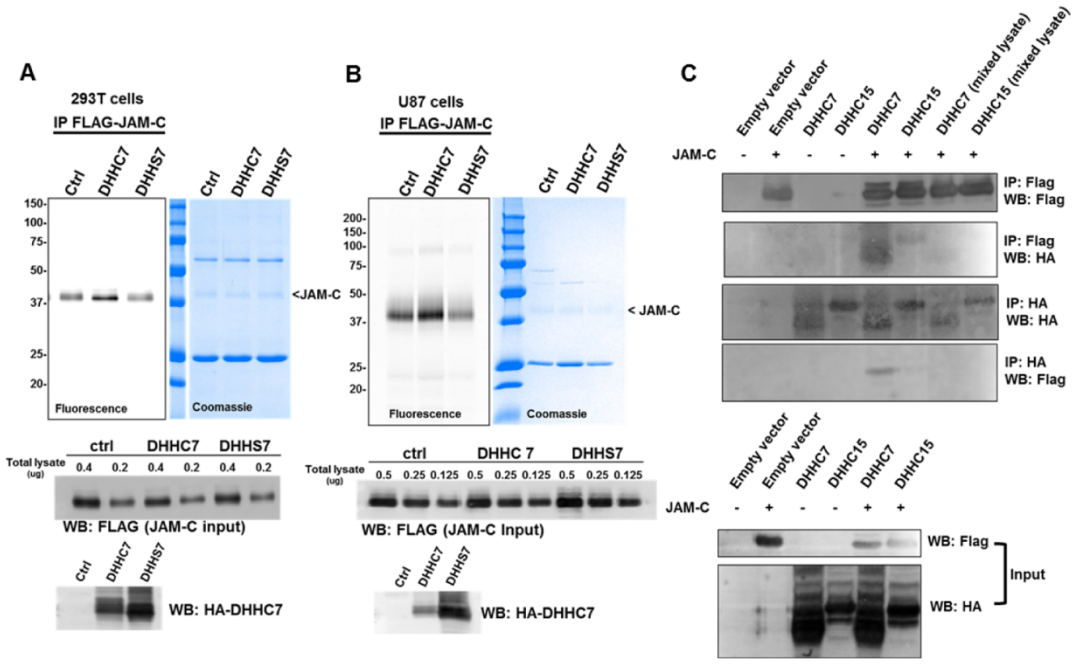

Figure 6.7 DHHC7 interacts with JAM-C and its catalytic activity is required for JAM-C S-palmitoylation. **(A)** Overexpression of DHHC7, but not DHHS7, increased JAM-C S-palmitoylation in HEK-293T cells. HA-tagged DHHC7 or HA-tagged DHHS7 were co-overexpressed with FLAG-tagged JAM-C. FLAG-tagged JAM-C was pulled down for palmitoylation detection. **(B)** The same experiment as in *A* was performed in U87 cells. **(C)** DHHC7 interacts with JAM-C. HA-tagged DHHC7 was co-overexpressed with FLAG-tagged JAM-C in HEK-293T cells. HA-tagged DHHC7 was pulled down and FLAG-tagged JAM-C was detected by western blot, and vice versa. A representative result from two independent experiments is shown.

Additionally, we investigated whether DHHC7 could interact with JAM-C. HA-tagged DHHC7 was co-overexpressed with FLAG-tagged JAM-C in HEK-293T cells. We carried out HA- and FLAG-pull down experiments. Indeed, HA-tagged DHHC7 was able to pull down FLAG-tagged JAM-C and vice versa, suggesting that JAM-C physically interacts with DHHC7 (Figure 6.7C). In contrast, FLAG-JAM-C and HA-DHHC15 did not exhibit a strong interaction, as the signal is only slightly above the background on the Western blots (Figure 6.7C).

2.3 Knockdown of DHHC7 decreases JAM-C S-palmitoylation

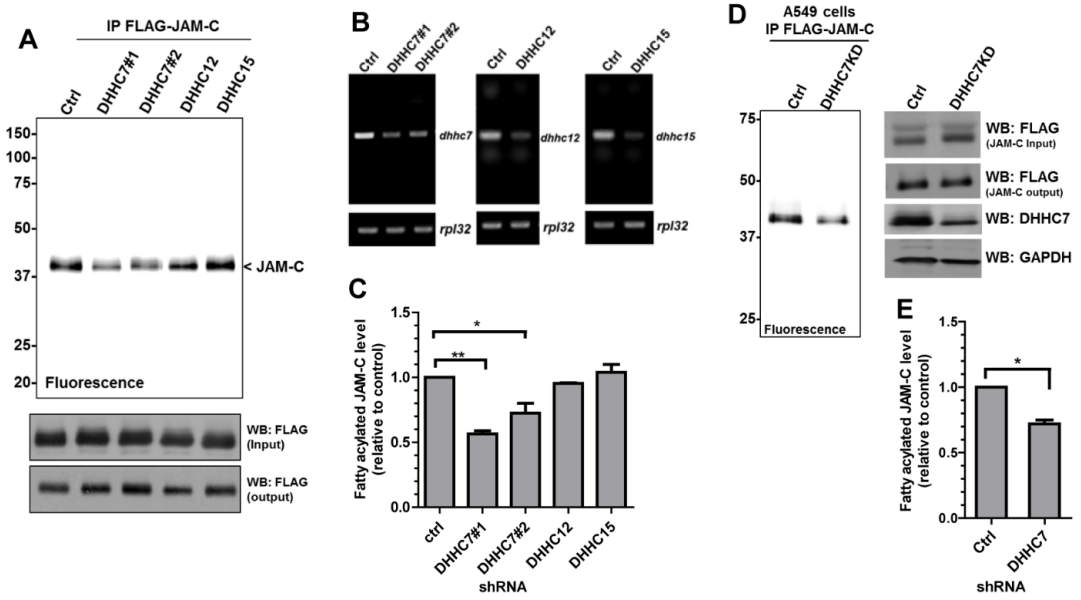

Figure 6.8. JAM-C palmitoylation level decreases in DHHC7 knockdown cells. (A) HEK-293T cells were infected with lentiviruses containing scramble shRNA (control), DHHC7, 12 or 15 shRNAs. Puromycin resistant cells were selected for stable DHHC knockdown cells and used for FLAG-tagged JAM-C overexpression. The FLAG-tagged JAM-C in the DHHC7, 12 and 15 knockdown cells was then immunoprecipitated and detected for the palmitoylation level by fluorescence labeling. **(B)** Semi-quantitative RT-PCR showing the mRNA expression levels of *Dhhc7, 12* and *15* in DHHC7, 12 and 15 stable knockdown HEK-293T cells, respectively. **(C)** Quantified fatty acylation levels of FLAG-tagged JAM-C expressed in DHHC7, 12 and 15 knockdown HEK-293T cells relative to control (mean ± SD, n=2). The palmitoylation level from each group was quantified and normalized with the corresponding protein level on the Coomassie blue gel using Quantity One software (Bio-Rad). The signal from FLAG-tagged JAM-C in the control knockdown cells was set to 1.00 and served as the reference point for the other samples. *D,* DHHC7 knockdown in A549 cells also decreases the palmitoylation of JAM-C. The experiments were carried out similar to that described in A. *E,* Quantified fatty acylation levels of JAM-C in A549 cells (mean ± SD, n = 2). *, $P < 0.05$; **, $P < 0.01$; ***, $P < 0.001$.

Ectopic expression of the DHHCs might affect the selectivity of the enzyme and possibly lead to an increase in S-palmitoylation of non-specific targets [23]. To verify that JAM-C is a palmitoylation target of endogenous DHHC7, we generated DHHC7, DHHC12 and DHHC15 stable knockdown HEK-293T cells using shRNAs targeting DHHC7, DHHC12 and DHHC15 mRNA, respectively. We then examined the JAM-C palmitoylation level (Figure 6.8A-C). Knockdown of DHHC7 led to a decrease in the JAM-C palmitoylation level, compared to the control with scrambled shRNA, while no significant difference in JAM-C palmitoylation was observed in DHHC12 and DHHC15 knockdown cells. These results demonstrate that JAM-C is a palmitoylation target of endogenous DHHC7. Based on BioGPS gene database (http://biogps.org/), DHHC7 gene expression level in lung tissue is relatively high when compared to other tissues. Thus, we also looked at JAM-C palmitoylation in A549 lung cancer cells. In stable DHHC7 knockdown A549 cells JAM-C palmitoylation also decreased (Figure 6.8 D,E).

2.4 S-palmitoylation promotes JAM-C localization to the tight junction (TJ)

To further understand the physiological function of JAM-C S-palmitoylation, we investigated whether this modification is required for the TJ localization of JAM-C. FLAG-tagged JAM-C WT and the palmitoylation deficient CCSS mutant were ectopically expressed in A549 lung cancer cells. The cells were stained with an anti-FLAG and anti-ZO-1 antibodies to visualize JAM-C and the TJ, respectively. Images were viewed and analyzed using ZEN 2012 imaging software (Zeiss). Both WT and the CCSS mutants were localized on plasma membrane in intracellular organelles. However, JAM-C WT was more concentrated at the TJ (white arrow) as indicated by

the co-localization with ZO-1, while the CCSS mutant had very little co-localization with ZO-1 (Figure 6.9). The co-localization between JAM-C and ZO-1 was quantified using the Coloc2 plugin in Fiji software, and are presented as the mean of Manders coefficient (M1 and M2) ± SEM. Thus, it appears that S-palmitoylation of JAM-C facilitates its localization to the TJ.

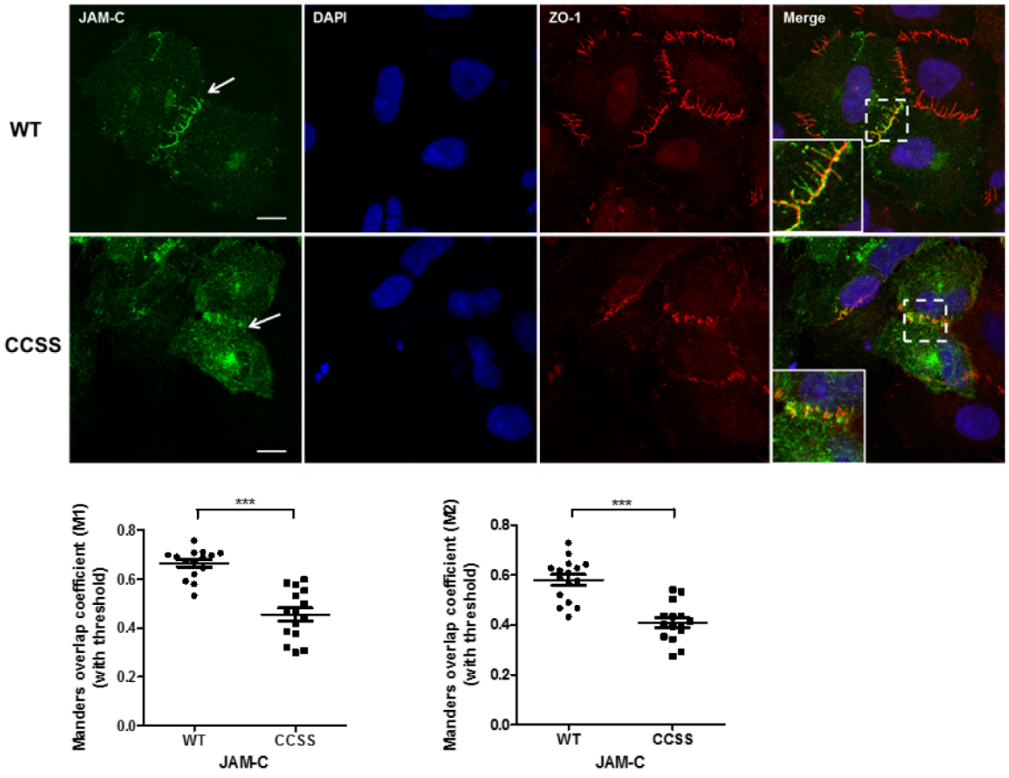

Figure 6.9. S-palmitoylation promotes JAM-C localization to the tight junction region. (A) FLAG-tagged JAM-C WT and the CCSS mutant were ectopically expressed in A549 cells. The cells were immunofluorescently stained with anti-FLAG and anti-ZO1 antibodies after fixation. JAM-C WT was more co-localized with ZO-1 at the tight junction (a white arrow), while the CCSS mutant had much less co-localization with ZO-1. The cells were visualized at the room temperature with a Zeiss LSM 710 confocal microscope with a 63×/1.4 oil immersion objective. Images were viewed and analyzed using ZEN 2012 imaging software (Zeiss). These representative images were from three independent experiments with at least 15 FLAG-JAM-C-containing cells analyzed in each experiment. Scale bar, 10 μm. *B*, The co-localization between JAM-C and ZO-1 was analyzed by the coloc2 plugin in Fiji software and was presented as the mean of Mander's coefficient (M1 and M2) ± SEM, n = 15. *** $p \leq 0.0001$, Student's t-test.

2.5 JAM-C S-palmitoylation affects cell migration

Since JAM-C S-palmitoylation affects its localization to the cell-cell contact TJ regions,

we wondered if it would also affect cell-cell adhesion. We therefore decided to check if JAM-C S-palmitoylation could affect cell migration, which is influenced by cell-cell adhesion. A549 cells were transfected with FLAG-tagged JAM-C WT or the CCSS mutant for 24 hrs. We used a transwell migration assay, which was performed in a 24-well transwell plate with 8 mm polycarbonate sterile membranes. Overexpression of JAM-C WT dramatically decreased cell migration compared to control cells that were transfected with an empty vector. In contrast, overexpression of the non-palmitoylable CCSS mutant only slightly decreased the cell migration compared to control cells that was transfected with an empty vector (Figure 6.10). The difference in cell migration was not due to the variation of cell proliferation as there was no significant difference in cell proliferation when JAM-C WT and the CCSS mutant were overexpressed (data not shown). Thus, S-palmitoylation of JAM-C affects cell migration.

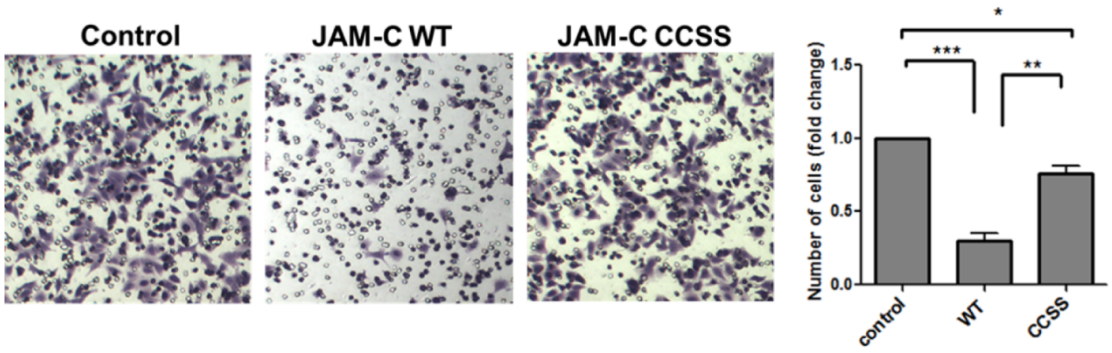

Figure 6.10. JAM-C S-palmitoylation affects cell migration. A549 cells were transfected with FLAG-tagged JAM-C WT or the CCSS mutant for 24 hr and then cultured in RPMI serum-free medium for 14 hr. The cell migration assay was then performed in a 24-well transwell plate with 8 mm polycarbonate sterile membranes. A total of 3.5 x 10^4 cells in 200 μl of RPMI serum-free medium were plated into each upper chamber and placed in wells containing 600 μl of RPMI medium supplemented with 10% FBS. After 24 hr, cells on the upper surface were detached with a cotton swab. The chambers were fixed and cells in the lower filter were stained with 0.1% crystal violet for 15 minutes and counted. The quantified results were calculated by counting three random fields of migrated cells. The control cells were transfected with an empty pCMV4a vector. Representative images of migrated cells from three independent experiments are shown. The number of migrated cells per field was quantified and normalized by the value of the control. Bars, mean ± S.D. (n = 3). *, $P < 0.05$; **, $P < 0.01$; ***, $P < 0.001$.

3. Discussion

Protein lipidation has become a more widely identified class of protein post-translational

modifications, and has been found to be involved in numerous biological pathways [15,24]. Here, using a bio-orthogonal palmitic acid probe [19,20], we demonstrated that both endogenous and ectopically expressed JAM-C contain S-palmitoylation. S-palmitoylation occurs on Cys264 and Cys265 of JAM-C. Why JAM-C has hydroxylamine resistant signal of JAM-C remains unclear. Since the hydroxylamine cleavage depends on the environment around protein structures [25], one plausible explanation to our case is the S-palmitoylation in the membrane proximal region of JAM-C may be shielded from hydroxylamine attack. Further experiment is required to prove this assumption. However, the decrease in labeling after hydroxylamine treatment supports that JAM-C has S-palmitoylation.

The palmitoyl acyltransferase (PAT) family members share a conserved Asp-His-His-Cys (DHHC)-cysteine rich domain (CRD) as a catalytic domain of the enzyme [26,27]. DHHCs have broad substrate specificity, and how substrate specificity is determined remains unclear. By screening the 23 DHHCs, we have found that overexpression of DHHC7 can substantially increase the JAM-C palmitoylation level. Moreover, we showed that knockdown of DHHC7 decreased the S-palmitoyl level of JAM-C, supporting that JAM-C is a direct palmitoylation target of endogenous DHHC7. Nevertheless, other DHHCs may also be able to regulate JAM-C palmitoylation as some DHHCs have redundant functions and act on the same targets [28].

JAM-C has previously been shown to be phosphorylated at Ser281, and JAM-C localization at the cell-cell contact region is negatively regulated by Ser281 phosphorylation [29,30]. The JAM-C S281A mutant led to the mis-localization and diffusion from the cell-cell contact region. In our case, we observed that JAM-C WT was concentrated at the cell-cell contact region, while the CCSS mutant was distributed more evenly on the cell membrane and the cytosol, which is similar to the effect of S281A. It is therefore possible that there is cross-talk between the phosphorylation and S-palmitoylation of JAM-C. However, we found that the non-phosphorylable JAM-C mutant (S281A) and the phosphomimetic JAM-C mutants (S281D

or S281E) had no significant effect on the S-palmitoylation of JAM-C (Figure 6.11). We could not determine whether CCSS JAM-C mutant can affect the phosphorylation on JAM-C due to the lack of proper antibodies to detect S281 phosphorylation.

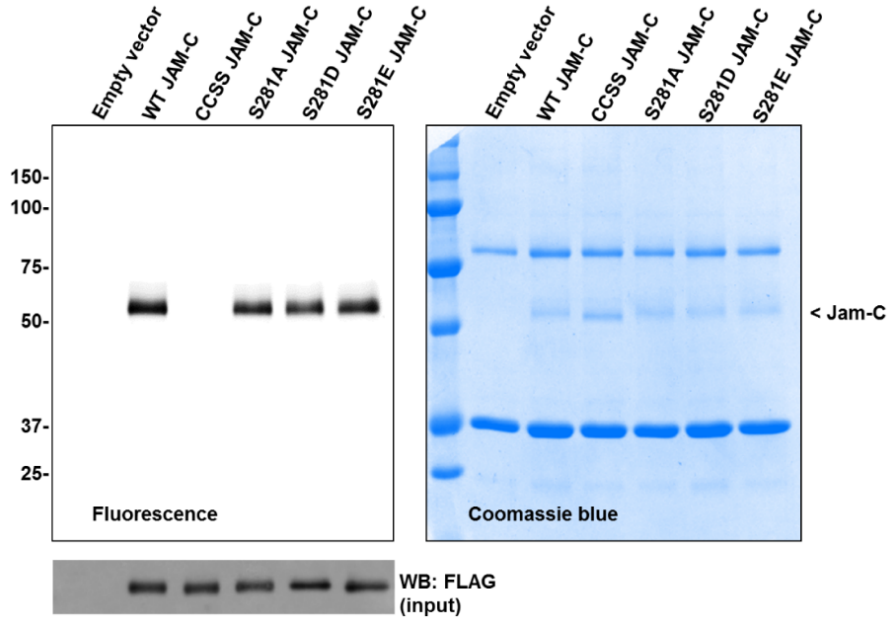

Figure 6.11. S-palmitoylation of JAM-C is independent of JAM-C phosphorylation on Ser281. The non-phosphorylable JAM-C (S281A) mutant and the phosphomimetic JAM-C (S281D and S281E) mutants exhibited comparable S- palmitoylation to WT-JAM-C.

JAM-C has been reported to have homophilic interactions with JAM-C, and heterophilic interactions with other PDZ-containing domain proteins such as ZO-1 and PAR3 at the cell tight junction. A possible explanation for the effect of palmitoylation on JAM-C localization is that S-palmitoylation facilitates the interaction of JAM-C with its interacting partners leading to the enrichment of JAM-C WT at the cell-cell contact regions.

We demonstrated for the first time that JAM-C palmitoylation can affect cell migration. Overexpression of WT JAM-C decreased migration of A549 cells, but overexpression of the non-palmitoylatable JAM-C mutant did not affect the migration much. S-palmitoylation of CD44, an adhesion protein, has previously been found to decrease the migration of breast cancer cells, and the invasiveness of cancer is negatively correlated with palmitoylation status of CD44

[31]. This is similar to our finding that WT JAM-C decreases the cell migration of A549 cells but the non-palmitoylatable mutant did not. The effect of JAM-C palmitoylation on cell migration is likely connected to its effect on the cell-cell contact localization of JAM-C and cell tight junction integrity. However, exactly how JAM-C palmitoylation regulates cell migration remains elusive.

Currently, only a few substrate proteins for DHHC7 are known, including Fas [32], sex steroid receptors [33], phosphatidylinositol 4-kinase IIα [34], Gα [35], stress-regulated exon (STREX) [28] and Scribble (SCRIB) [36]. Our findings expand the substrate scope of DHHC7, which eventually will help to understand the substrate specificity and function of different DHHCs.

Interestingly, a decrease in DHHC7 levels has been related to tumorigenesis [37], suggesting that DHHC7 may play a role in preventing tumorigenesis. Our finding that JAM-C palmitoylation affects cancer cell migration and that DHHC7 directly controls the palmitoylation level of JAM-C suggests that pharmacologically controlling DHHC7 could be a useful strategy to control cancer cell migration, and possibly cancer metastasis. However, to fully take advantage of this, a more detailed understanding of the function of DHHC7 is needed.

4. Methods

JAM-C cloning and expression -Human JAM-C cDNA was purchased from Transomic (clone ID BC012147). The full length cDNA was PCR-amplified by Platinum® Pfx DNA Polymerase (ThermoFisher) and subcloned into the pCMV-tag 4a vector using the BamHI and EcoRV restriction sites using the following primers:

Sense: 5'**-**AGTCAGGGATCCATGGCGCTG AGGCGGCCA-3'**;**

antisense: 5'-AGTCAGGATATCGATCACAA ACGATGACTTGTGTCT-3'

JAM-C mutants (C264S, C265S and CCSS) were generated by quick change mutagenesis. The JAM-C in pCMV-tag 4a vector was PCR-amplified using Phusion® High-Fidelity DNA polymerase and the following mutagenic primers:

C264S sense: 5'-CCCTGATCACGTTGGGCATC AGCTGTGCATACAGACGTGGCTA-3',

antisense: 5'-GATGCCCAACGTGATCAGGG-3';

C265S sense: 5'-TGATCACGTTGGGCATCTGC AGTGCATACAGACGTGGCTACTT-3',

antisense: 5'-GCAGATGCCCAACGTGATCA-3'.

CCSS sense: 5'-CCCTGATCACGTTGGGCATC

AGCAGTGCATACAGACGTGGCTACTT-3',

antisense: 5'-GATGCCCAACGTGATCAGGG-3';

The plasmids of DHHC 1-23 in pEF-BOS-HA vector for screening were generously provided by Prof. Maurine Linder and Prof. Masaki Fukata.

Cell Culture and Transfection–Human Embryonic Kidney 293T (HEK-293T) cells were cultured in Dulbecco's Modified Eagle Medium (DMEM) supplemented with 10% Fetal Bovine Serum (Invitrogen), and Jurkat and A549 cells in Roswell Park Memorial Institute (RPMI) 1640 Media (Invitrogen) supplemented with 10% Fetal Bovine Serum (Invitrogen). All cells were incubated in a humidified incubator at 37 °C with 5% CO_2. FuGENE® 6 Transfection Reagent (Promega) was used for cell transfection according to the manufacturer's instruction.

Antibodies - Anti-FLAG® M2-Peroxidase (HRP) antibody (mouse monoclonal IgG) for western blotting and anti-FLAG® M2 Affinity Gel for immunoprecipitation were purchased from Sigma (catalog #A8592 and #A2220, respectively). Anti-FLAG antibody (mouse monoclonal IgG1) for immunofluorescence was purchased from Cell Signaling (catalog #8146). Secondary Antibody- Alexa Fluor® 488 conjugate (Mouse polyclonal IgG) was purchased from ThermoFisher (catalog #A-11001). Anti-HA-Peroxidase (rat IgG1) was purchased from Roche (catalog #12013819001). The anti-human JAM-C antibody (mouse monoclonal IgG) was purchased from Enzo Life Sciences (catalog #ALX-803-306), and anti-DHHC7 (rabbit IgG) antibody was purchased from AssayBiotech (catalog #R12-3691). All other peroxidase conjugated secondary antibodies were from Santa Cruz Biotechnology.

Western Blot – Cells were collected and lysed with 1% NP40 lysis buffer (50 mM Tris-HCl pH 7.4, 150 mM NaCl and 1% v/v NP40 (Igepal) containing Protease Inhibitor Cocktails (Sigma). Protein concentration was determined by Bradford assay (Pierce™ Coomassie Protein Assay Kit). Protein samples were separated by 12% SDS-PAGE and transferred to PVDF membrane (Bio-Rad) for 90 min. The membrane was blocked with 5% bovine serum albumin (BSA, Santa Cruz) in TBST (25 mM Tris-HCl pH 7.4, 150 mM NaCl, and 0.1% Tween-20) and incubated with the primary antibody for 3 hrs at room temperature, or overnight at 4 °C. After washing 5 times with TBST, the membrane was incubated with the secondary antibody for 1 hr at room temperature. The membrane was washed five more times with TBST before it was developed in ECL-Plus western blotting detection reagent (GE Healthcare). The signal was visualized using a Typhoon 9400 Variable Mode Imager (GE Healthcare) with 457 nm excitation and 526 nm detection filters, using a PMT of 600 V (normal sensitivity). The signal was analyzed by Image Quant TL v2005 and Quantity One (Bio-Rad).

Metabolic labeling of palmitoylation on FLAG-tagged JAM-C - Cells were transfected with FLAG-tagged JAM-C pCMV4a. After 24 hrs, the cells were incubated with 50 μM Alk14 in media supplemented with 10% FBS for 6 hrs. Cells were collected and washed with 1x phosphate saline buffer (PBS) three times. The cell pellets were lysed with 1% NP40 lysis buffer (50 mM Tris-HCl pH 7.4, 150 mM NaCl, and 1% v/v NP40) containing Protease Inhibitor Cocktails (Sigma). The protein concentration was determined by Bradford assay (Pierce™ Coomassie Protein Assay Kit). The expression of FLAG-JAM-C level was confirmed by western blot. For FLAG-JAM-C immunoprecipitation, 25 μl of Anti-FLAG M2 affinity gel (Sigma) was added into 600 μg of total cell lysate with the final volume of 1 ml in an eppendorf tube. The samples were gently agitated at 4 °C for 2 hrs. The samples were then centrifuged at 1,000 xg for 2 min at 4 °C to remove the supernatant. The beads were washed three times with 0.1% NP40 lysis buffer. After the last wash, all the buffer was removed. The beads were re-

suspended in 15 µl of 0.1% NP40 buffer. To perform the click reaction, 5.6 µl of the reaction master mix was added to each sample (click reaction master mix: 3 µl of 1 mM BODIPY Azide in DMF, 1 µl of 50 mM tris(2-carboxyethyl) phosphine hydrochloride (TCEP.HCl, Calbiochem) in water, 0.6 µl of 10 mM tris [(1-benzyl-1H-1,2,3-triazol-4-yl)methyl] amine (TBTA, Sigma or Anal Tech) in DMF, 1 µl of 50 mM $CuSO_4$ in water). After 1 hr at room temperature, 20 µl of 3x protein loading buffer (187 mM Tris-HCl pH 6.8, 6% SDS, 150 mM DTT, 30% v/v glycerol, 0.006% bromphenol blue) was added to each sample, and the samples were boiled at 95 °C for 5 min and centrifuged at 17,000x g for 2 min. The supernatants were transferred into new eppendorf tubes and loaded on 12% SDS-PAGE gels. The fluorescence signal was visualized with a Typhoon 9400 Variable Mode Imager (GE Healthcare Life Sciences) using 488 nm excitation and 520 nm detection filters, and a PMT setting of 550 V (normal sensitivity). The signal was analyzed by Image Quant TL v2005, and quantified by Quantity One (Bio-Rad) within a linear range of exposure.

Generation of DHHC7, DHHC12 and DHHC15 stable knockdown in HEK-293T cell line - Different DHHC shRNA lentiviral plasmids in pLKO.1-puro vector were purchased from Sigma (catalogue# DHHC7-SHCLNG-NM_017740, shRNA#1-TRC N0000143647, shRNA#2-TRCN0000275633; DHHC12-SHCLNG-NM_025428; DHHC15-SHCLNG-NM_144969). To generate the lentiviruses, low passage number of HEK-293T cells in a 10 cm^3 plate were transfected with 6 µg of each DHHC shRNA, 4 µg of pCMV-dR8.2, and 2 µg of pM2D.G mixed with 36 µl of FuGENE6 (promega). The cell media containing the lentiviruses were collected after 48 hrs by centrifugation, and filtered through 0.45 µm syringe filter to remove cell debris. The day before infection, $3x10^5$ cells of low passage number HEK-293T cells were split into each well of a 6-well plate and grown overnight in 2 ml of DMEM with 10% FBS. The media were then removed and replaced with a mixture of 1.5 ml of the lentiviruses media collected above, 0.5 ml of fresh DMEM with 10% FBS, and 6 µg/µl

polybrene (Sigma). After 6 hrs, 3 ml of DMEM with 10% FBS was added to each well, and after 48 hrs, 1.5 μg/μl of puromycin dihydrochloride (Santa Cruz) was added into the cells to select for stable DHHC knockdown cells.

Cell migration assay -A549 cells were transfected with FLAG-tagged JAM-C WT in pCMV4a, the FLAG-tagged CCSS mutant in pCMV4a, or empty pCMV4a vector (control) for 24 hrs, and then cultured in RPMI serum-free medium for an additional 14 hrs. The cell migration assay was performed in a 24-well transwell plate with 8 mm polycarbonate sterile membrane (Corning Incorporated). A total of $3.5x10^4$ cells, in 200 μl of RPMI serum-free medium, were plated in each upper chamber and then placed in wells containing 600 μl of RPMI medium supplemented with 10% FBS. After 24 hrs, the cells on the upper surface were detached with a cotton swab, and the upper chambers were fixed. The cells in the lower filter were stained with 0.1% crystal violet for 15 minutes and then counted. The quantified results represent three random fields of migrated cells.

Immunofluorescence Microscopy - A total of $2x10^5$ A549 cells were split into each glass bottom culture dishes (MatTek) and cultured overnight. The cells were then transfected with either the FLAG-JAM-C WT in pCMV4a vector or the CCSS mutant. After 24 hrs, cells were washed twice with 2 ml of 1x phosphate-buffered saline (PBS, ThermoFisher), fixed with 4% paraformaldehyde in PBS on ice for 15 min, and then kept at room temperature for 5 min. Then cells were subsequently washed three times with 2 ml of 1x PBS and incubated with 0.1% Saponin (TCI-America) with 3% BSA in 1x PBS at room temperature. After 1 hr, the blocking solution was removed and the anti-FLAG antibody (rabbit monoclonal IgG1, 1:1,000, Cell Signaling) and the anti-ZO1 antibody (mouse monoclonal IgG1, 1: 800, BD Biosciences) in a Saponin-BSA solution was added to the cells and incubated at 4 ^oC overnight. The cells were washed with 1 ml of Saponin-BSA solution five times and then incubated with the secondary

antibodies, Alexa Fluor® 488 conjugate (Goat anti-Rabbit IgG polyclonal antibody, ThermoFisher, 1:1,000) and Texas Red® conjugate (Goat anti-Mouse IgG polyclonal antibody, ThermoFisher, 1:1,000) in the Saponin-BSA solution at room temperature for 1 hr. The cells were washed with 1 ml of Saponin-BSA solution five times, then mounted with 200 µl of DAPI Fluoromount-G (Southern Biotech) and covered with a cover glass. After 24 hrs, the cells were visualized with a Zeiss LSM 710 confocal microscope with a 63×/1.4 oil immersion objective. Images were viewed and analyzed using ZEN 2012 imaging software (Zeiss). For JAM-C and ZO-1 co-localization analysis, the Manders overlap coefficient with automatic thresholds (M1 and M2) were calculated using the Coloc2 plugin in Fiji (background subtraction, rolling ball radius 50 pixels) [38].

Statistical analysis – Data were shown as mean ± S.D. (Standard Deviation) or mean ± SEM (standard error of the mean). Differences were analyzed by two-tailed Student's t- test between two groups. *, $P < 0.05$; **, $P < 0.01$; ***, $P < 0.001$.

REFERENCES

(1) Ebnet, K.; Suzuki, A.; Ohno, S.; Vestweber, D. Junctional adhesion molecules (JAMs): more molecules with dual functions? *Journal of cell science* **2004,** *117* (Pt 1), 19.

(2) Keiper, T.; Santoso, S.; Nawroth, P. P.; Orlova, V.; Chavakis, T. The role of junctional adhesion molecules in cell-cell interactions. *Histology and histopathology* **2005,** *20* (1), 197.

(3) Bazzoni, G. The JAM family of junctional adhesion molecules. *Current opinion in cell biology* **2003,** *15* (5), 525.

(4) Weber, C.; Fraemohs, L.; Dejana, E. The role of junctional adhesion molecules in vascular inflammation. *Nature reviews. Immunology* **2007,** *7* (6), 467.

(5) Gliki, G.; Ebnet, K.; Aurrand-Lions, M.; Imhof, B. A.; Adams, R. H. Spermatid differentiation requires the assembly of a cell polarity complex downstream of junctional adhesion molecule-C. *Nature* **2004,** *431* (7006), 320.

(6) Guo, J.; Wang, L.; Zhang, Y.; Wu, J.; Arpag, S.; Hu, B.; Imhof, B. A.; Tian, X.; Carter, B. D.; Suter, U.et al. Abnormal junctions and permeability of myelin in PMP22-deficient nerves. *Annals of neurology* **2014,** *75* (2), 255.

(7) Akawi, N. A.; Canpolat, F. E.; White, S. M.; Quilis-Esquerra, J.; Morales Sanchez, M.; Gamundi, M. J.; Mochida, G. H.; Walsh, C. A.; Ali, B. R.; Al-Gazali, L. Delineation of the clinical, molecular and cellular aspects of novel JAM3 mutations underlying the autosomal recessive hemorrhagic destruction of the brain, subependymal calcification, and congenital cataracts. *Human mutation* **2013,** *34* (3), 498.

(8) Hao, S.; Yang, Y.; Liu, Y.; Yang, S.; Wang, G.; Xiao, J.; Liu, H. JAM-C promotes lymphangiogenesis and nodal metastasis in non-small cell lung cancer. *Tumour biology : the journal of the International Society for Oncodevelopmental Biology and Medicine* **2014,** *35* (6), 5675.

(9) Leinster, D. A.; Colom, B.; Whiteford, J. R.; Ennis, D. P.; Lockley, M.; McNeish, I. A.; Aurrand-Lions, M.; Chavakis, T.; Imhof, B. A.; Balkwill, F. R.et al. Endothelial cell junctional adhesion molecule C plays a key role in the development of tumors in a murine model of ovarian cancer. *FASEB journal : official publication of the Federation of American Societies for Experimental Biology* **2013,** *27* (10), 4244.

(10) Arcangeli, M. L.; Frontera, V.; Bardin, F.; Thomassin, J.; Chetaille, B.; Adams, S.; Adams, R. H.; Aurrand-Lions, M. The Junctional Adhesion Molecule-B regulates JAM-C-dependent melanoma cell metastasis. *FEBS letters* **2012,** *586* (22), 4046.

(11) Tenan, M.; Aurrand-Lions, M.; Widmer, V.; Alimenti, A.; Burkhardt, K.; Lazeyras, F.; Belkouch, M. C.; Hammel, P.; Walker, P. R.; Duchosal, M. A.et al. Cooperative expression of junctional adhesion molecule-C and -B supports growth and invasion of glioma. *Glia* **2010,** *58* (5), 524.

(12) Langer, H. F.; Orlova, V. V.; Xie, C.; Kaul, S.; Schneider, D.; Lonsdorf, A. S.; Fahrleitner, M.; Choi, E. Y.; Dutoit, V.; Pellegrini, M.et al. A novel function of junctional adhesion molecule-C in mediating melanoma cell metastasis. *Cancer research* **2011,** *71* (12), 4096.

(13) Fuse, C.; Ishida, Y.; Hikita, T.; Asai, T.; Oku, N. Junctional adhesion molecule-C promotes metastatic potential of HT1080 human fibrosarcoma. *The Journal of biological chemistry* **2007,** *282* (11), 8276.

(14) Smotrys, J. E.; Linder, M. E. Palmitoylation of intracellular signaling proteins: regulation and function. *Annual review of biochemistry* **2004,** *73*, 559.

(15) Resh, M. D. Fatty acylation of proteins: new insights into membrane targeting of myristoylated and palmitoylated proteins. *Biochimica et biophysica acta* **1999,** *1451* (1), 1.

(16) Fukata, M.; Fukata, Y.; Adesnik, H.; Nicoll, R. A.; Bredt, D. S. Identification of PSD-95 palmitoylating enzymes. *Neuron* **2004,** *44* (6), 987.
(17) Linder, M. E.; Jennings, B. C. Mechanism and function of DHHC S-acyltransferases. *Biochemical Society transactions* **2013,** *41* (1), 29.
(18) Kang, R.; Wan, J.; Arstikaitis, P.; Takahashi, H.; Huang, K.; Bailey, A. O.; Thompson, J. X.; Roth, A. F.; Drisdel, R. C.; Mastro, R.et al. Neural palmitoyl-proteomics reveals dynamic synaptic palmitoylation. *Nature* **2008,** *456* (7224), 904.
(19) Yount, J. S.; Zhang, M. M.; Hang, H. C. Visualization and Identification of Fatty Acylated Proteins Using Chemical Reporters. *Current protocols in chemical biology* **2011,** *3* (2), 65.
(20) Wilson, J. P.; Raghavan, A. S.; Yang, Y. Y.; Charron, G.; Hang, H. C. Proteomic analysis of fatty-acylated proteins in mammalian cells with chemical reporters reveals S-acylation of histone H3 variants. *Molecular & cellular proteomics : MCP* **2011,** *10* (3), M110 001198.
(21) Jiang, H.; Khan, S.; Wang, Y.; Charron, G.; He, B.; Sebastian, C.; Du, J.; Kim, R.; Ge, E.; Mostoslavsky, R.et al. SIRT6 regulates TNF-alpha secretion through hydrolysis of long-chain fatty acyl lysine. *Nature* **2013,** *496* (7443), 110.
(22) Jing, S. Q.; Trowbridge, I. S. Identification of the intermolecular disulfide bonds of the human transferrin receptor and its lipid-attachment site. *EMBO J* **1987,** *6* (2), 327.
(23) Dietrich, L. E.; Ungermann, C. On the mechanism of protein palmitoylation. *EMBO reports* **2004,** *5* (11), 1053.
(24) Resh, M. D. Targeting protein lipidation in disease. *Trends in molecular medicine* **2012,** *18* (4), 206.
(25) Iwamoto, M.; Sudo, Y.; Shimono, K.; Kamo, N. Selective reaction of hydroxylamine with chromophore during the photocycle of pharaonis phoborhodopsin. *Biochimica et biophysica acta* **2001,** *1514* (1), 152.
(26) Roth, A. F.; Feng, Y.; Chen, L.; Davis, N. G. The yeast DHHC cysteine-rich domain protein Akr1p is a palmitoyl transferase. *The Journal of cell biology* **2002,** *159* (1), 23.
(27) Lobo, S.; Greentree, W. K.; Linder, M. E.; Deschenes, R. J. Identification of a Ras palmitoyltransferase in Saccharomyces cerevisiae. *The Journal of biological chemistry* **2002,** *277* (43), 41268.
(28) Tian, L.; McClafferty, H.; Jeffries, O.; Shipston, M. J. Multiple palmitoyltransferases are required for palmitoylation-dependent regulation of large conductance calcium- and voltage-activated potassium channels. *J Biol Chem* **2010,** *285* (31), 23954.
(29) Mandicourt, G.; Iden, S.; Ebnet, K.; Aurrand-Lions, M.; Imhof, B. A. JAM-C regulates tight junctions and integrin-mediated cell adhesion and migration. *The Journal of biological chemistry* **2007,** *282* (3), 1830.
(30) Ebnet, K.; Aurrand-Lions, M.; Kuhn, A.; Kiefer, F.; Butz, S.; Zander, K.; Meyer zu Brickwedde, M. K.; Suzuki, A.; Imhof, B. A.; Vestweber, D. The junctional adhesion molecule (JAM) family members JAM-2 and JAM-3 associate with the cell polarity protein PAR-3: a possible role for JAMs in endothelial cell polarity. *Journal of cell science* **2003,** *116* (Pt 19), 3879.
(31) Babina, I. S.; McSherry, E. A.; Donatello, S.; Hill, A. D.; Hopkins, A. M. A novel mechanism of regulating breast cancer cell migration via palmitoylation-dependent alterations in the lipid raft affiliation of CD44. *Breast cancer research : BCR* **2014,** *16* (1), R19.
(32) Rossin, A.; Durivault, J.; Chakhtoura-Feghali, T.; Lounnas, N.; Gagnoux-Palacios, L.; Hueber, A. O. Fas palmitoylation by the palmitoyl acyltransferase DHHC7 regulates Fas stability. *Cell Death Differ* **2015,** *22* (4), 643.
(33) Pedram, A.; Razandi, M.; Deschenes, R. J.; Levin, E. R. DHHC-7 and -21 are

palmitoylacyltransferases for sex steroid receptors. *Mol Biol Cell* **2012,** *23* (1), 188.
(34) Lu, D.; Sun, H. Q.; Wang, H.; Barylko, B.; Fukata, Y.; Fukata, M.; Albanesi, J. P.; Yin, H. L. Phosphatidylinositol 4-kinase IIalpha is palmitoylated by Golgi-localized palmitoyltransferases in cholesterol-dependent manner. *J Biol Chem* **2012,** *287* (26), 21856.
(35) Tsutsumi, R.; Fukata, Y.; Noritake, J.; Iwanaga, T.; Perez, F.; Fukata, M. Identification of G protein alpha subunit-palmitoylating enzyme. *Mol Cell Biol* **2009,** *29* (2), 435.
(36) Chen, B.; Zheng, B.; DeRan, M.; Jarugumilli, G. K.; Fu, J.; Brooks, Y. S.; Wu, X. ZDHHC7-mediated S-palmitoylation of Scribble regulates cell polarity. *Nat Chem Biol* **2016**, DOI:10.1038/nchembio.2119 10.1038/nchembio.2119.
(37) Gaspar, C.; Cardoso, J.; Franken, P.; Molenaar, L.; Morreau, H.; Moslein, G.; Sampson, J.; Boer, J. M.; de Menezes, R. X.; Fodde, R. Cross-species comparison of human and mouse intestinal polyps reveals conserved mechanisms in adenomatous polyposis coli (APC)-driven tumorigenesis. *The American journal of pathology* **2008,** *172* (5), 1363.
(38) Schindelin, J.; Arganda-Carreras, I.; Frise, E.; Kaynig, V.; Longair, M.; Pietzsch, T.; Preibisch, S.; Rueden, C.; Saalfeld, S.; Schmid, B.et al. Fiji: an open-source platform for biological-image analysis. *Nat Methods* **2012,** *9* (7), 676.

CHAPTER 7

PROGRESS TOWARDS THE DVELOPMENT OF A CHEMICAL PROTEOMIC PLATFORM FOR IDENTIFICATION OF PROTEIN LYSINE FATTY ACYLATION[6]

Abstract:

Protein lysine fatty acylation is increasingly recognized as an abundant and important protein post translational modification (PTM) with the recent identification of several proteins with myristoyl or palmitoyl modifications on lysine residues. However, there is still no robust method to directly identify proteins with lysine fatty acylation from proteomics experiments. Here, we aim to use a cleavable biotin-diazo-azide probe to identify proteins containing lysine fatty acylation. We successfully improved the synthetic method used to obtain this class of probes by modifying the conditions used to form the diazo bond. Biochemical validation shows that protein lysine fatty acylation can be successfully enriched using a biotin-diazo-azide linker. Furthermore, initial proteomics studies show that protein fatty acylation can be detected on endogenous proteins. However, optimization is necessary to generate confident and complete lysine fatty acylation proteomes. Successfully accomplishing this will help to better elucidate the physiological function of protein lysine fatty acylation.

---

[6] This is unpublished work. For this study, I (NAS) designed and performed all the biochemical studies except those noted below, and synthesized the cleavable biotin-diazo-azide linker and the Alk14 probe. Xiaoyu Zhang, Ji Cao, Xiao Chen, and Zhen Tong assisted with method optimization. Hui Jing helped generate the stable K-Ras4a overexpressing cell line. Professor Yingming Zhao (University of Chicago) and He Huang and Okwang Zhang from his lab assisted with the mass spectrometry experiments and the method optimization. and HL directed and supervised the study.

1. Introduction

Protein posttranslational modifications (PTMs) affect a wide range of biological functions including transcription, cell signaling, metabolism, cell survival, and life span. Protein lipidation, including N-terminal glycine myristoylation, cysteine palmitoylation (*S*-palmitoylation), cysteine prenylation, and modifications by GPI anchors, occur on important signaling proteins and play important roles in biology.[1,2] Lysine fatty acylation was initially identified in the 1990s. However, until 2017 only TNFα, IL-1α and lens integral membrane protein aquaporin-0 were reported to have this modification.[3-5] In the past year, we have shown that several other proteins including KRAS4a, H-Ras, and RRas2 also have lysine fatty acylation.[6,7] These findings suggest that lysine fatty acylation is likely an abundant and important PTM that regulate many proteins. However, compared to N-terminal glycine myristoylation, S-palmitoylation, cysteine-prenylation, and modifications by GPI anchors, lysine-fatty acylation has been understudied.

One difficulty associated with studying lysine fatty acylation is that no existing method can predict the site of lysine fatty-acylation and current proteomic method cannot easily identify the modified cysteine and lysine residues. Direct detection of cysteine and lysine fatty-acylation by mass spectrometry has been challenging due to the hydrophobic nature of the modification, the instability of the thioester bond (cysteine-palmitoylation) and the low abundance of the modification or the modified protein.[8] While there have been some advances in detecting cysteine fatty-acylation by mass spectrometry, a robust proteomic methods that allows direct detection of the modification is still lacking. The same can also be said about direct detection of N-terminal glycine myristoylation. To fully understand protein lysine fatty acylation and other protein lipidation, a method to directly identify proteins fatty acylation sites is needed.

Protein lipidation, particularly lysine fatty-acylation, is often found in low stoichiometry, requiring enrichment prior to detection. Others have made use of cleavable

biotin-azide probes to enrich and release the modified peptides or proteins after streptavidin enrichment.[9-11] This method was previously used in proteomic studies to identify proteins with cysteine palmitoylation.[10,12] However, the modification site itself was not detected. We therefore set out to use this established method as a foundation to develop a method to directly detect the modification site.

2. Results

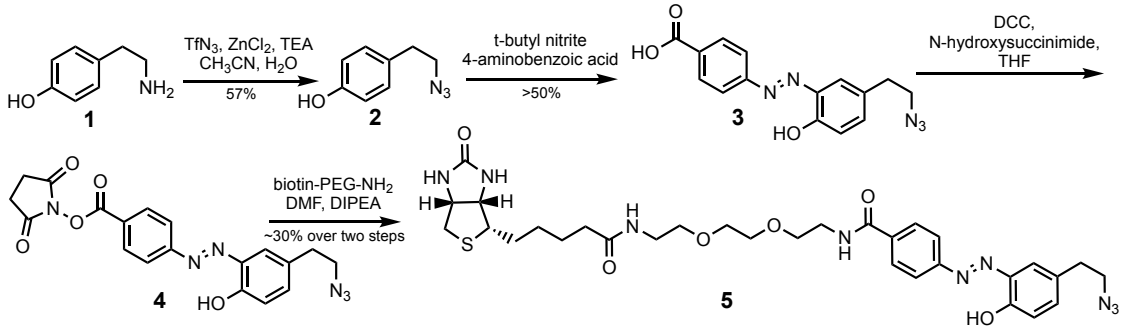

Figure 7.1. Synthesis of the cleavable biotin-diazo-azide probe

As cleavable biotin probes are useful for many applications, we first sought out to improve the synthesis of these probes.[10] In literature, the formation of the diazo bond is often accomplished using sodium nitrite. However, this reaction often affords low yields for the synthesis of this class of linkers, and using the established method we were unsuccessful in obtaining the desired product. We therefore aimed to improve this step as we synthesized our variation of the cleavable biotin-diazo-azide linker, compound **5** (Figure 7.1). To form the diazo bond, we found that we were able to consistently get a yield > 50% using t-butyl nitrite. This is a great improvement from current methods. Standard methods were followed to obtain linker **5**.

As the linker we synthesized differs from those previously reported. We first validated that the probe could be cleaved in the presence of sodium dithionite (Figure 7.2A-C). We also confirmed that the probe could undergo click chemistry reactions in whole cell lysate from cells treated with the biorthogonal myristic and palmitic acid analogues, Alkyne 12 (Alk12) and Alkyne 14 (Alk14) (Figure 7.2D and 7.2E).

To verify that the cleavable linker allows us to affinity purify and subsequently cleave fatty acylated proteins labeled with Alk12 and 14, we used two proteins that are known to have fatty acylation: FYN and RALA. FYN is a protein kinase with N-terminal glycine myristoylation[13], while RALA is a RAS family GTPase with cysteine palmitoylation.[14,15] Using the biotin-azo-azide probe, we demonstrated that overexpressed fatty acylated FYN and RALA can be captured on streptavidin beads and subsequently eluted using the reducing reagent

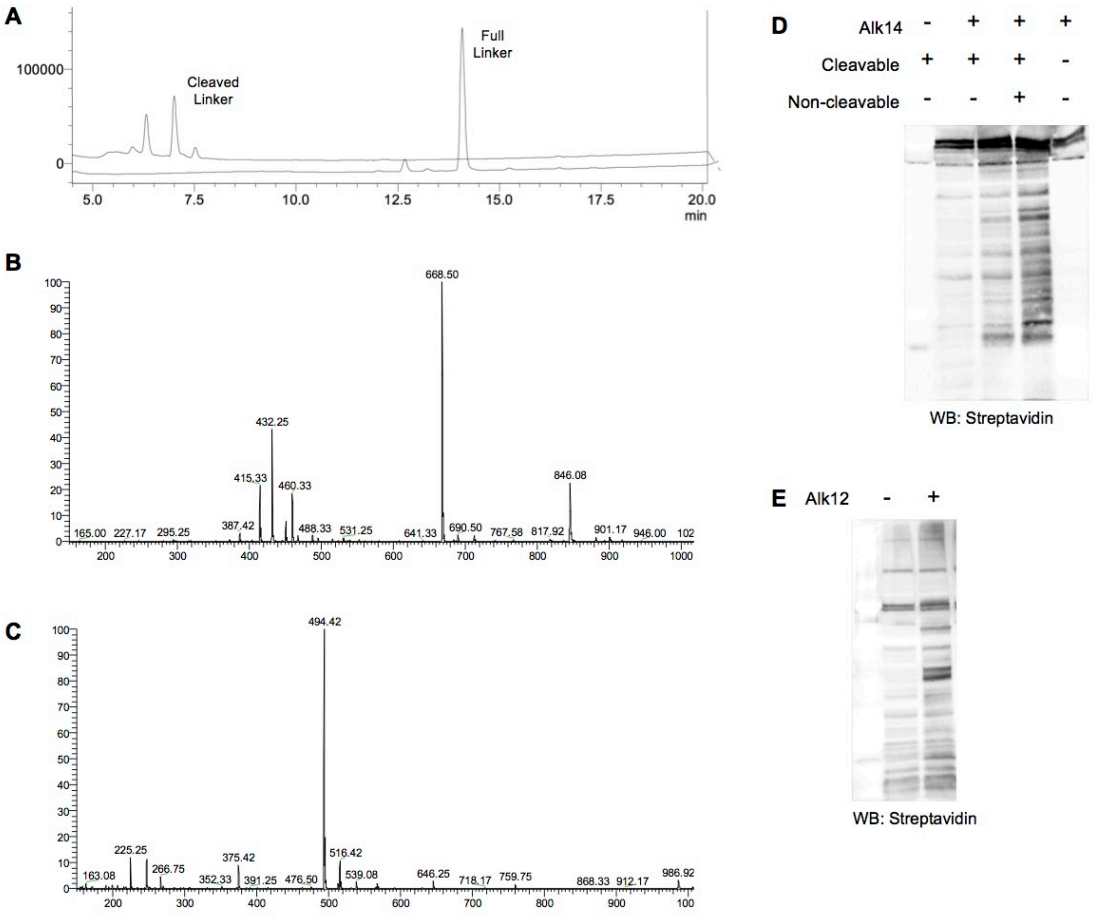

Figure 7.2. Validation of the Cleavable Probe. (**A**) In vitro assay showing the probe is cleaved after sodium dithionite treatment. (**B** and **C**) The LCMS spectra of the full linker (**B**) and cleaved linker(**C**). (**D and E**) The probe can be incorporated to fatty acylated proteins by click chemistry with Alk14 (**D**) treated cells and Alk12 (**E**) treated cells.

dithionite (Figure 7.3, A-C). To further confirm that we are able to cleave lysine fatty acylated proteins using this method, we investigated if we could capture and release the K-RAS4a. We

were able to release this protein from the streptavidin beads in a sodium dithionite dependent manner (Figure 7.3D). Further, the non S-palmitoylated K-RAS4a CS mutant could also be cleaved from the streptavidin beads suggesting that lysine fatty acylated proteins could be enriched and subsequently isolated (Figure 7.3E). We also confirmed that lysine fatty acylated R-Ras2 could be cleaved from streptavidin breads (Figure 7.3F)

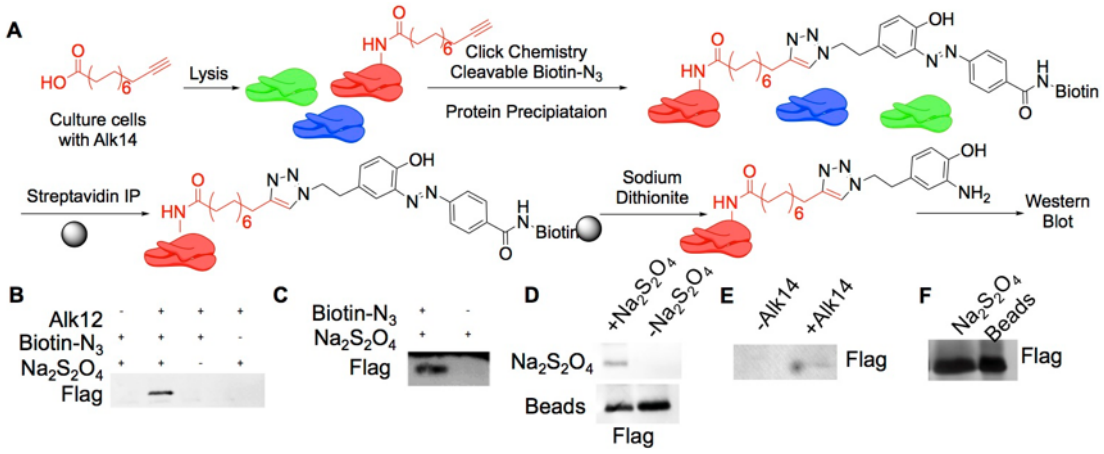

Figure 7.3. The probe can be used to enrich proteins with lipidation. (**A**) The method used to validate the ability of the probe to affinity purify proteins with lipidation. Cells overexpressing the denoted proteins were culture with Alk14. Cells were harvested and the cleavable biotin linker (Biotin-N_3) was attached to labeled proteins using click chemistry. The labeled protein was then pulled down using streptavidin beads and eluted with dithionite. (**B**) Flag-Fyn (**C**) Flag-RalA (**D**) Flag- K-Ras4a (**E**) the non s-palmitoylated Flag-K-Ras4a cysteine to serine mutant and (**F**) Flag-R-Ras2 were eluted from streptavidin beads in a sodium dithionite dependent manner.

Since we are interested in using the linker as a proteomic tool, we next confirmed that endogenous proteins with cysteine palmitoylation or lysine fatty acylation can be captured and subsequently released from the streptavidin beads in a sodium dithionite dependent manner. We blotted for endogenous Jam3, a protein reported to have *S*-palmitoylation, transferrin receptor 1 (TfR1), which has *S*-palmitoylation, and total Ras proteins, which have both *S*-palmitoylation and lysine fatty acylation.[6,7,16-18] Only when the cells were treated with Alk14 could Jam3, Ras, and TfR1 proteins be released from streptavidin beads (Figure 7.4, A & B). Silver staining and blue staining SDS PAGE gels suggested that a wide range of endogenous proteins were being cleaved from the streptavidin beads after sodium dithionite treatment, suggesting the method is

efficient enough for proteomic studies (Figure 7.4, C & D).

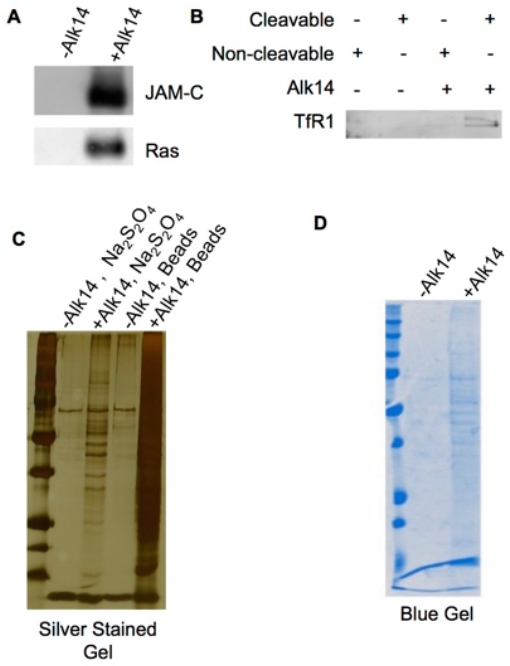

Figure 7.4. Endogenous fatty acylated protiens can be enriched and cleaved from streptavidin beads. (**A**) JAM-C and Ras proteins can be enriched using Alk14 labeling and streptavidin IP, and eluted with sodium dithionite. (**B**) Transferrin receptor can be enriched and cleaved with sodium dithionite with the cleavable biotin-diazo-azide linker but not with non-cleavable biotin-azide linker. (**C**) Silver staining and (**D**) blue staining showing all the endogenous proteins that are eluted from the streptavidin beads using Alk14 and biotin-diazo-azide linker.

It is well known that lipid modifications such as myristoylation and palmitoylation are challenging to detect by mass spectrometry due to the hydrophobicity of the modification as well as the low abundance. To test the ability to use the linker for mass spectrometry, we first tried to detect the fatty acylated site on R-Ras2. We recently reported that R-Ras2 was fatty acylated on lysine 194.[6] After isolation of Flag-R-Ras2, streptavidin enrichment, and sodium dithionite cleavage, we could detect the parent mass for the modified peptide (Figure 7.5, A & B).

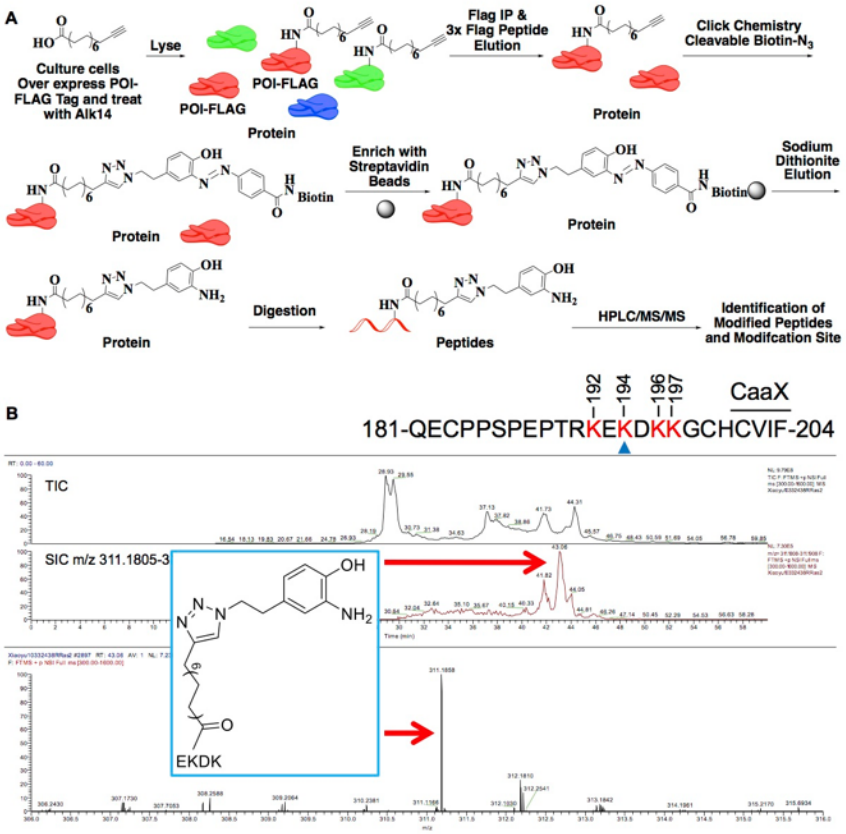

Figure 7.5. Direct detection of the fatty acylated K194 peptide on R-Ras2. (**A**) The method used to detect lysine fatty acylation on R-Ras2. (**B**) The mass spectra showing the parent mass of the peptide where lysine 194 is modified.

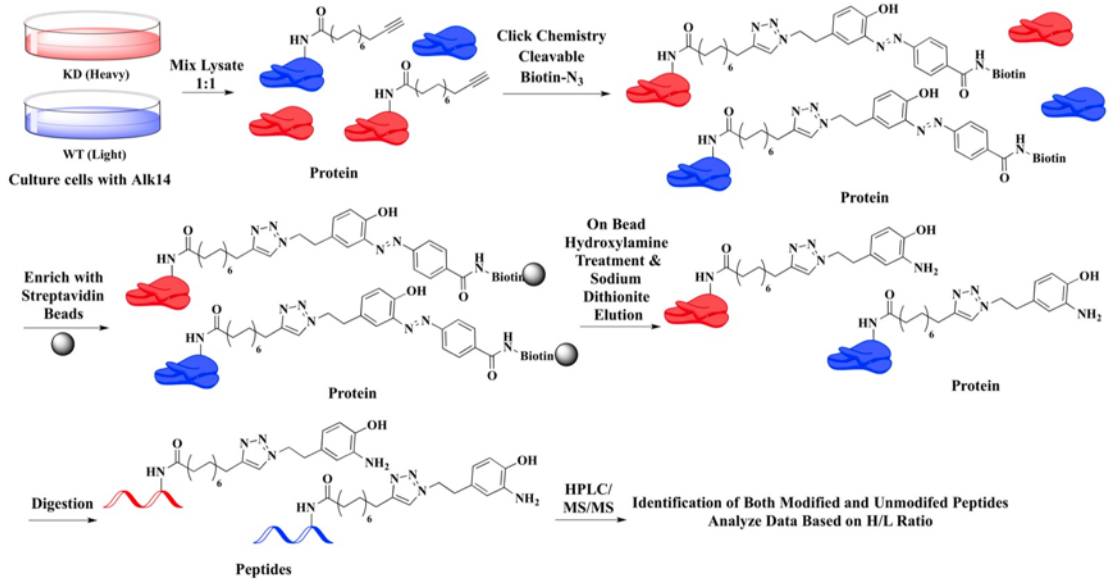

Figure 7. 6. Method to detect SIRT6 defatty-acylation substrates.

With these results, we next wanted to see if we can use this method on a proteomic scale to identify protein modified by fatty acylation sites. We slightly modified the method to detect SIRT6 substrates. Using stable isotope labeling of amino acids in cell culture (SILAC), we cultured SIRT6 WT and KO MEF cells in heavy and light lysine and arginine supplemented media respectively. The cells were treated with the Alk14 probe, and subsequently collected. All fatty acylated proteins were enriched by streptavidin immunoprecipitation after click chemistry to attach the cleavable-biotin-N_3 probe. Subsequently, the fatty acylated proteins were eluted from the streptavidin beads by sodium dithionite, digested with trypsin, and analyzed by HPLC-MS/MS analysis (Figure 7.6). As some proteins exhibit hydroxylamine resistant *S*-palmitoylation, such as Jam-3, we searched for *S*-palmitoylation and lysine fatty acylation with an appropriate mass shift to account for the addition of the cleaved probe.[16] We detected twenty-five proteins that had either *S*-pamitoylation or lysine fatty acylation with the addition of either the full cleavable biotin probe, or the expected mass shift (Table 7.1).

Table 7.1. Lysine and cysteine palmitoylatted peptides that were detected from the SIRT6 WT/ KO MEF SILAC experiment. (alc) means the cysteine or lysine residue is modified with Alk14 conjugated to the cleaved biotin diazo linker and (alcb) means the cysteinie or lysine residue is modified with Alk14 conjugated to the full biotin-diazo linker

	Gene Names	K or C	Sequence of Modified Peptide	H/L Ratio
Cleaved Linker	zDHHC2	C	_PDRC(ca)HHCSVC(alc)DK_	
	Abca5	C	_ELM(ox)GC(alc)QC(ca)C(ca)EEK_	
	Golga1	K	_DQEWSEK(alc)M(ox)EQLEK_	
	Gab2	C	_INHTFNSSSSQYC(alc)R_	3.1511
	Gpc3	C	_M(ox)WYC(alc)SYCQGLM(ox)MVK_	
	Rprd1a	C	_ESGERLSKM(ox)VEDAC(alc)M(ox)LLADYNGR_	
	Ccdc158	K	_NTLK(alc)TMEGSDGHAM(ox)K_	
	Fam81a	K	_DVEKK(alc)LSQM(ox)SAR_	.1729
	Ank2	C	_LRC(ca)FC(alc)MTDDK_	
	Dlg5	K	_EQM(ox)ECQLEK(alc)EARFR_	0.0304
	Tex14	C	_ELHCFC(alc)EEDK_	
		C	_CNECGKLFTC(alc)SSSLK_	
	Lrp2	K	_LMSDK(alc)RTCVDIDEC(ca)K_	
	Kif18a	C	_QIEMMC(alc)SEDK_	0.0592
	Gm6526	C	_SSQNC(alc)NITNHMK_	
		C	_GFTLIC(alc)LFCILAAEC(al)QK_	7.7323
Non-cleaved Linker	Cnp	C	_LDEDLAGYC(alcb)R_	2.0106
	zDHHC1	K	_MNICNK(alcb)PSNK_	
	Dab2ip	K	_SK(alcb)EELSQAEK_	
	Adam30	K	_K(alcb)DLC(ca)C(ca)GPDCK_	
	Pla2g4d	K	_LQLK(alcb)TDCCPK_	
	Crim1	C	_CVCDPAGC(alcb)LRK_	0.059882
	Mt1	C	_C(alcb)AQGCVCKGAADK_	
	PdxK	K	_C(ca)AK(alcb)AEAGEGQK_	
	Znf410	C	_SFIC(alcb)PAEGC(ca)GK_	0.061424

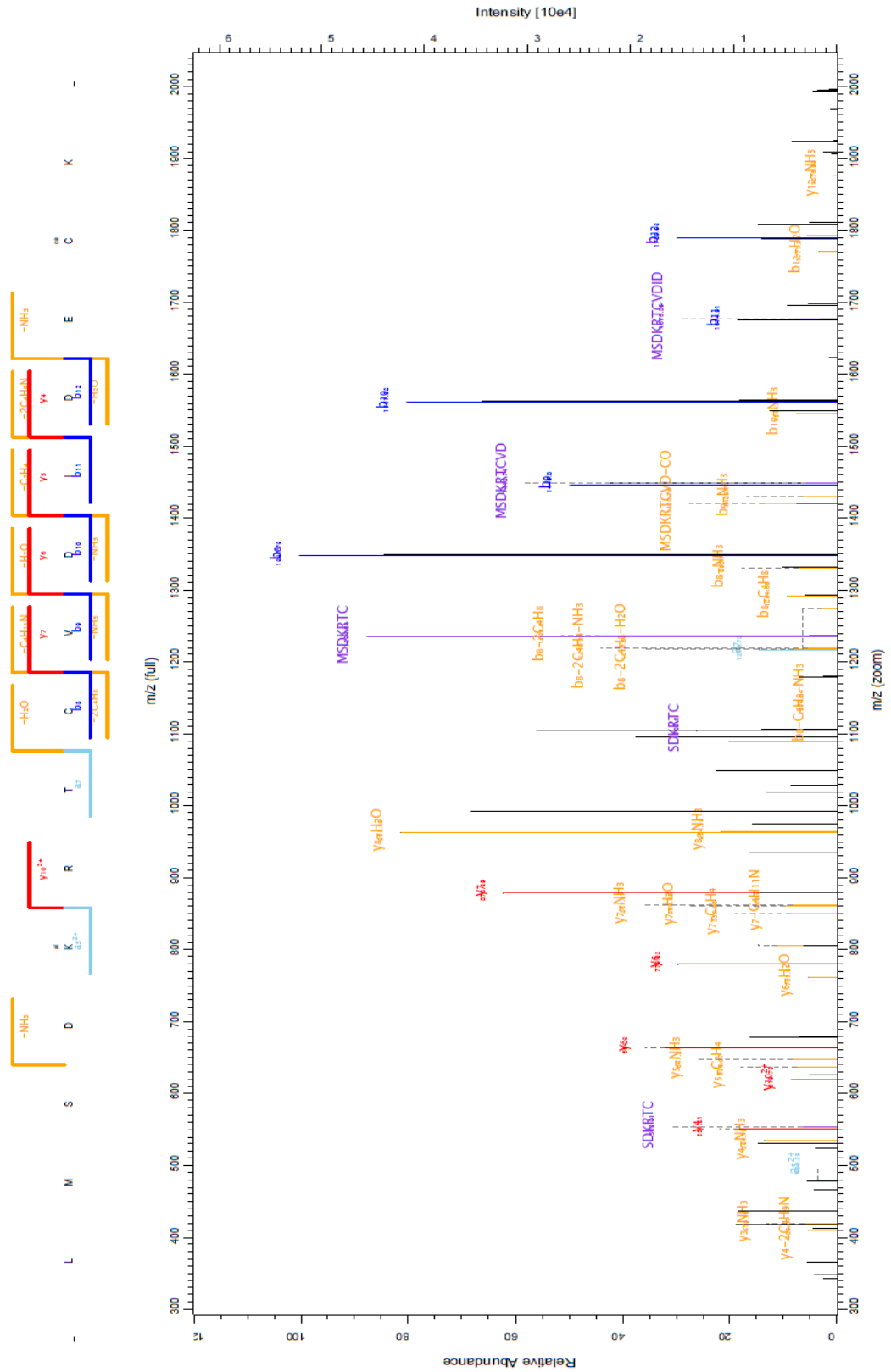

Figure 7.7. MS/MS spectra of Low-density lipoprotein receptor-related protein 2

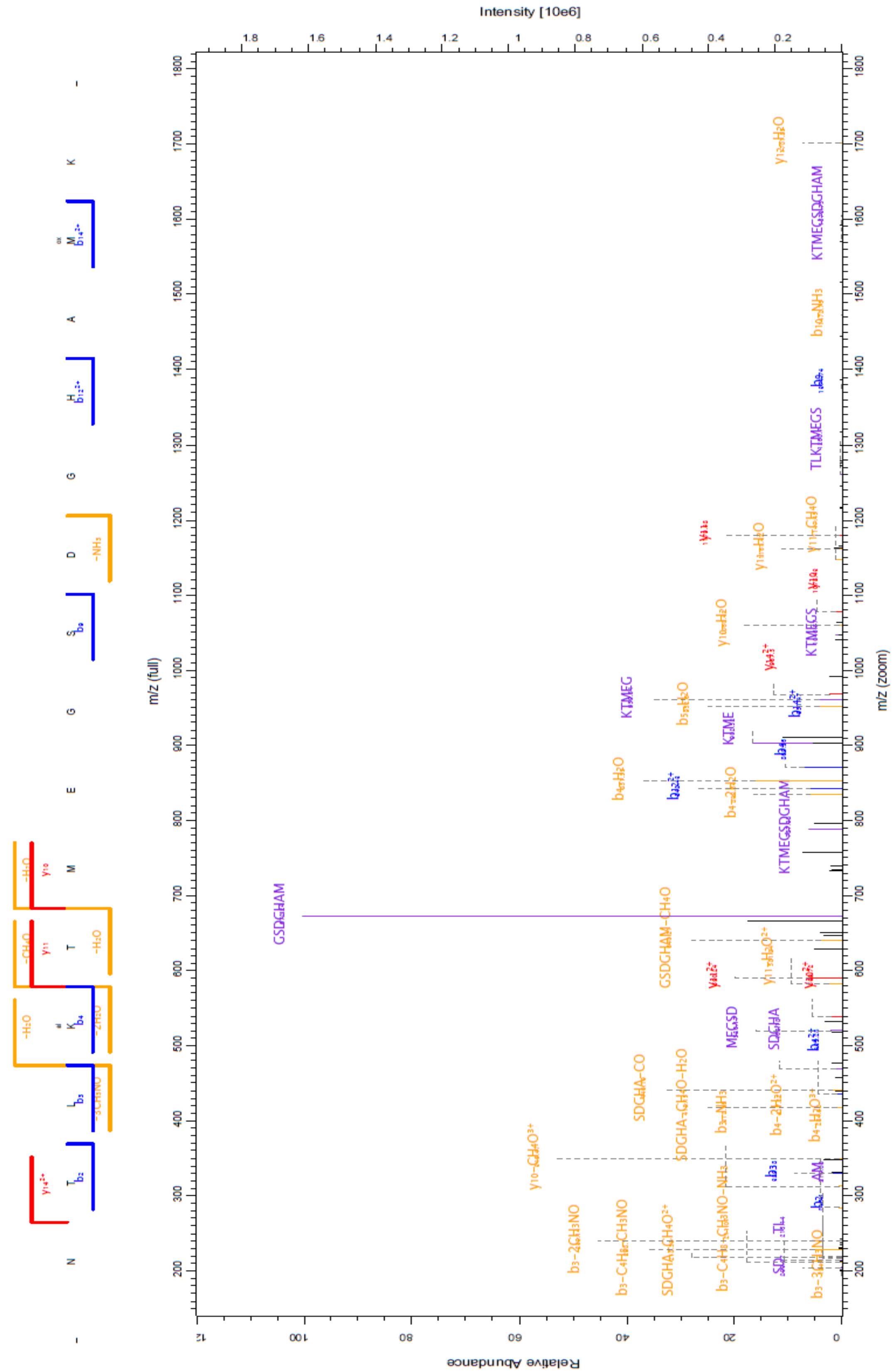

Figure 7.8. MS/MS spectra of Coiled-coil domain-containing protein 158

From this list, we were confident in the MS/MS spectra of two of the proteins Low-density lipoprotein receptor-related protein 2 and coiled coiled domain containing protein 158 (Figure 7.6, Figure 7.7). However, based on the heavy to light rations, these proteins were likely not SIRT6 substrates.

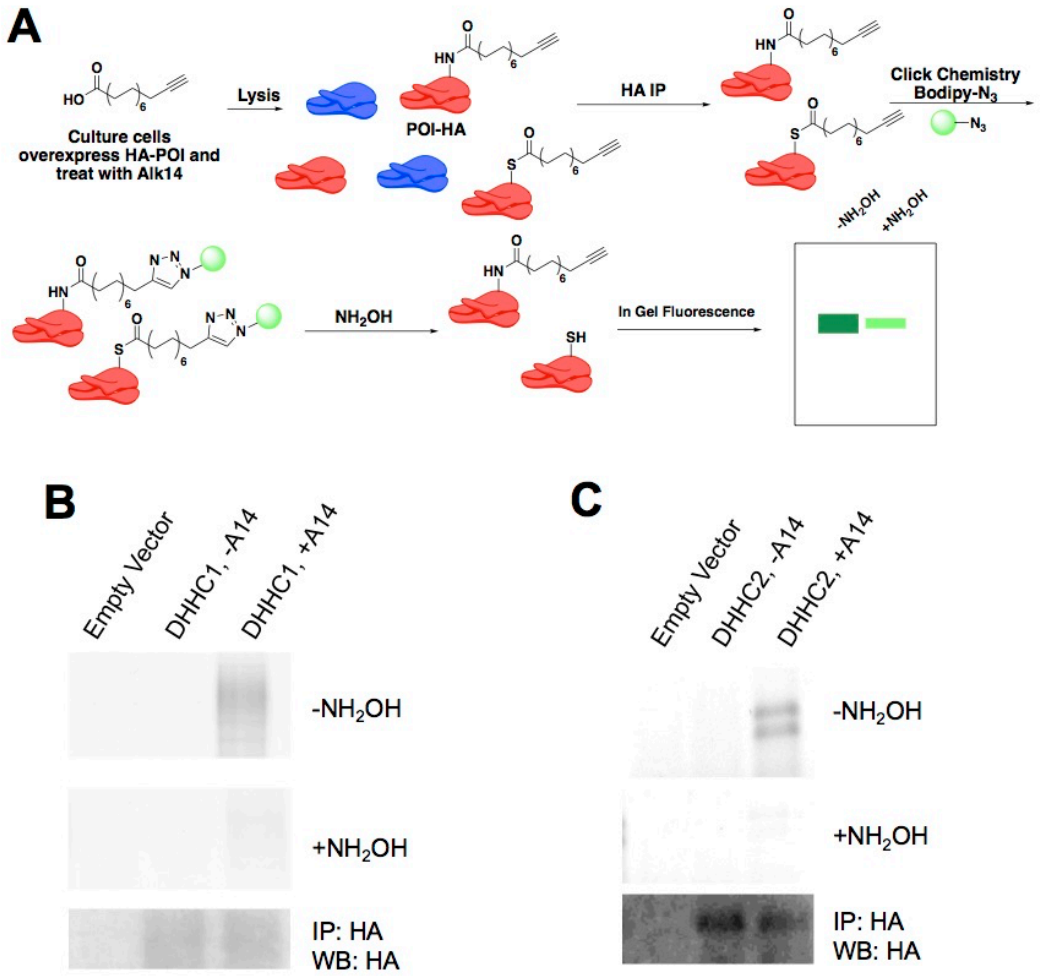

Figure 7.9. Validation of DHHC1 and 2 as fatty acylated proteins (**A**) the method used to detect lysine and s-palmitoylation by in gel fluorescence. Fluorescence gels showing the fatty acylation levels of (**B**) DHHC1 and (**C**) DHHC2 before and after hydroxylamine treatment.

Interestingly, the experiment also suggested that DHHC1 may have lysine fatty acylation, and DHHC2 may have *S*-palmitoylation. We decided to further investigation the fatty acylation level of these two-established cysteine palmitoyl transferases. To evaluate the fatty

acylation level of both proteins, we again made use of the bio-orthogonal Alk14 probe. However, instead of attaching the cleavable biotin-N_3 probe, we attached a fluorophore through click chemistry and evaluated the fatty acylation levels by in-gel fluorescence (Figure 7.9A). DHHC1 did exhibit hydroxylamine resistant fatty acylation, suggesting it may have lysine fatty acylation (Figure 7.9B). Furthermore, DHHC2 exhibited a significant amount of hydroxylamine sensitive fatty acylation, suggesting that it has *S*-palmitoylation (Figure 7.9C).

3. Discussion

These initial proteomics studies suggest that direct detection of fatty acylation sites is possible, however since we were not able to consistently detect these fatty acylation sites in repeat experiments additional work still needs to be done to optimize the mass spectrometry portion, as well as the sample preparation.

Fatty acylation is a hydrophobic modification, and the modified peptides can be easily lost throughout the sample preparation process. Identifying optimal conditions for the mass spectrometry could help improve and enhance the number of fatty acylated proteins that can be identified. To help improve the enrichment and cleavage efficiency, peptide enrichment and cleavage can be tried.

To aid in the optimization of the mass spectrometry, a standard peptide with the cleaved biotin-N_3 probe could be synthesized and used as an internal standard for sample quality control as well as form mass spectrometry optimization. Additionally, other probes that would contain a signature ion could be synthesized. Incorporation of a bromine or other halide could lead to a unique signature isotope peak pattern. Alternatively, a probe with a MS signature ion that differs from the mass of an amino acid could be developed. This could readily allow for a more targeted MS approach and help to obtain high-quality MS/MS spectra. The progress made so far suggest that it is plausible to achieve the goal of direct identification of lipid modifications of endogenous proteins, but a lot of optimization is still required.

Once direct identification of the lipid modification is robust, this probe and method would be useful to identify substrates for enzymes that regulate lysine fatty acylation or other lipid modifications, such as the deacylase enzymes (HDACs, Sirtuins), and the fatty acyl transferases (DHHCs, NMTs). There are still a lot of questions regarding the function, selectivity, and substrate specificity of these enzymes. Robust identification of substrates could help shed light on these questions.

4. Methods

Reagents: All chemicals were purchased at the highest purity available from Sigma Aldrich unless otherwise notes. Tryamine was purchased from TCI (A0302). Alk14 and Alk12 were synthesized as previously described.[19] Bodipy-N_3 (520) was purchased from Lumiprobe. Biotin-PEG-N_3 (non-cleavable biotin) (762024), Tris[(1-benzyl-1H-1,2,3-triazol-4-yl)methyl]amine (TBTA) (678937), Tris(2-carboxyethyl)phosphine (TCEP) (75259), hydroxylamine (159417), and anti-Flag M2 antibody conjugated with horseradish peroxidase (A8592), the anti-HA, and the anti-Flag M2 affinity gel (A2220) were purchased from Sigma-Aldrich. FuGENE6 transfection reagent and sequencing grade modified trypsin (V5117) were purchased from Promega. Enzyme-linked chemiluminescence (ECL) plus (32132) western blotting detection reagent, Thermo Silver Staining Kit, and the high capacity Streptavidin agarose (20357) were purchased from Thermo Fisher Scientific. The anti- rabbit HRP(7074) antibody were purchased from cell signaling technologies. The pan-Ras antibody (05-516) was purchased from Millipore. The antibody to detect TfR1 was purchased from Abcam. pCMV5-Flag-RalA was a kind gift from Dr. Maurine Linder (Cornell University). pCMV5-Flag-K-Ras4a and the cys to ser mutant, as well as pCMV5-Flag-R-Ras2 were cloned as previously described.[6,7]

Synthesis of the Cleavable Biotin-N_3 Linker (5):

Synthesis of Compound (**2**): This procedure was adapted from literature. Briefly, 316.3 mg of

NaN_3 was placed in 6.25 mL of anhydrous acetonitrile on ice. To the ice-cold suspension, 0.75 mL of Tf_2O was added dropwise. The solution was allowed to stir at 0°C for 2 hours. Then 523.8 mg of tyramine (**1**) and 52.3 mg of $ZnCl_2$ was dissolved in a solution of 7:3 acetonitrile: water and the resulting solution was added dropwise to the Tf-N_3 solution. After that, 1.5 mL of triethyl amine (TEA) was added dropwise. The reaction turned orange. The reaction was allowed to stir overnight at room temperature. The solution was concentration and resuspended in ethyl acetate. Subsequently, the organic layer was washed with water twice, and dried with sodium sulfate. The crude mixture was a brown oil that was purified by silica gel chromatogaph (3:1 hexanes:ethyl acetate). The isolated pure product was a clear oil (70% yield). All characterization matched the published values.

Synthesis of Compound (**3**): In a round bottom flask 157.6mg of compound **2** and 145mg of 4-amino benzoic acid were dissolved in 1.15mL of dichloromethane and placed under nitrogen. The reaction was placed on ice, and 115µL of t-butyl nitrite was slowly added. The reaction was allowed to warm up to room temperature and stir overnight. The crude reaction mixture was acidified and with 1M HCl, and subsequently washed with ethyl acetate three times. The organic layers were dried with sodium sulfate and purified by silica gel chromatography with gradient solvent concentrations starting at 3:7 Hex:EtOAc, to 1:19 MeOH:DCM, 1:9 MeOH:DCM and 2:8 MeOH:DCM. Characterization matched published data. All of the crude was not purified.

Synthesis of Compound (**5**): To activate compound **3**, 25mg of compound **3** was dissolved in 5mL of THF. To the homogenous solution, 29mg of dicyclohexylcarbodiimide (DCC) and 19.3mg of N-hydroxysuccinimide (NHS) was added. After 4 hours, the reaction was concentrated the resulting Urea was filtered off. The crude reaction mixture was in anhydrous DMF (~1mL) and was added to Biotin-PEG in DMF. The total reaction volume was 7mL. To the reaction 50µL of diisopropylamine (DIPEA). The reaction was allowed to stir overnight. The reaction was extracted with water and ethyl acetate. The organic layer was dried with ethyl

acetate and purified by silica gel chromatography with a solvent gradient from 1:20 MeOH: DCM to 2:8 MeOH:DCM. The product was characterized by LCMS (M^+ = 669) and ^{1}HNMR (300 MHz, CD_3OD) δ8.05 (m, 4), δ7.8(s, 1), δ7.3(d, 1), δ7.0(d,1), δ4.5(m, 1), δ4.3(m,1), δ4.0(d,2), δ3.7(m,2), δ2.25(m), δ2.0(m), δ1.5(m), δ1.0(m). (the compound was not 100% pure, so integration values are not entirely accurate) The ^{1}HNMR pattern matched what was expected based on literature precedence for very similar linkers)

In Vitro Sodium Dithionite Cleavage Assay. The cleavable biotin-N_3 linker (1 mM in DMF) was diluted to 0.1 mM in 100 μL of PBS (pH 7.4). Then 100 μL of freshly made 100 mM sodium dithionite in PBS was added to the linker. After 1 minute of incubating at room temperature, the sample was filtered and run on the HPLC. The peaks were collected and detected by LC-MS. The same concentration of the linker mixed with only PBS was also run as a control.

Whole Cell Lysate Click Chemistry. 1 10cm dish of WT HEK-293T Cells at 70% confluency were treated with Alk12, Alk14, or DMSO (vehicle control) at a final concentration of 50 μM for 6 hours. After 6 hours, the cells were collected and washed with ice cold PBS (pH 7.4) twice. The cells were subsequently lysed in 350μL of 4% SDS lysis buffer (50mM triethanolamine pH=7.4, 150mM NaCl, 4% SDS (w/v)) supplemented with protease inhibitor cocktail (1:100) and universal cell nuclease (1:1000). Protein concentration was determined by BCA assay (Thermo) following the manufacture's protocol. After normalization, the 60μg of whole cell lysate was diluted to 42 μL with additional 4% SDS lysis buffer. For the click reaction 5 μL of 1 mM cleavable-biotin linker, 1 μL of 10 mM TBTA, 1 μL of 40 mM $CuSO_4$, and 1 μL of 40mM TCEP was added to the lysate. After 30 minutes, the reaction was quenched by precipitating the protein by adding 200 μL of methanol, 75 μL of chloroform, and 150 μL of water to the sample. After vortexing, the samples were spin down at 17,000 g for 20 minutes.

The supernatant was removed and the protein pellet was washed with 1 mL of methanol twice. The protein pellet was resuspended in 2x loading dye and analyzed by SDS-PAGE. Western blot with streptavidin HRP antibody was used to evaluate if the click chemistry worked after transferring the proteins from the SDS-PAGE gel to a PVDF membrane.

Cleavable Biotin Azide Enrichment and Sodium Dithionite Elution. WT-HEK-293T cells were treated with 50 μM Alk14 for 6 hours. The cells were collected, and washed with PBS twice. The cells were lysed with 1% NP40 lysis buffer supplemented with PIC (100x). Protein concentration was quantified using a standard Bradford assay. The total amount of lysate used dependened on the fatty acylation level of each protein, but ranged between 2mg of whole cell lysate to 10mg of whole cell lysate. Lysate was diluted to a concentration of 2 mg/mL of lysis buffer. For a 5 mL click chemistry reaction (10 mg of whole cell lysate), 150 μL of 5 mM biotin-diazo-azide linker in DMF, 100 μL of 10 mM TBTA in DMF, 100 μL of 50 mM TCEP in H_2O, and 100 μL of 50 mM $CuSO_4$ in H_2O were added. The reaction was mixed and allowed to incubate for 1 hour at room temperature. To quench the click chemistry reaction, 13.3 mL of ice cold methanol, 5 mL of ice cold chloroform and 10 mL of ice cold water were added to precipitate the proteins. The reaction mixtures were vortexed and centrifuged at 4˚C for 40 minutes (4,500 g). After removing the supernatant, the protein pellet was washed with 20 mL of ice-cold methanol twice. Each wash was followed by centrifugation at 4˚C for 25 minutes (4,500 g) after adding methanol and vortexing to pellet the protein. After the second wash, the methanol was removed as much as possible and the pellet was air dried at room temperature for 10 minutes. The protein pellet was resupspended in 1 mL of 4% SDS buffer with PIC (100x) and 20 μL of 0.5 M EDTA. The SDS concentration was diluted to below 1.5% (compatible for biotin/streptavidin binding) by adding 2 mL of 1% Brij97 buffer with EDTA-free protease inhibitors. Then 200μL of high efficiency streptavidin beads were washed three times with 1

mL of PBS and resuspended in 100 μL of 1% Brij97 buffer with EDTA-free protease inhibitors. The beads were then added to the protein solution obtained above and incubated on a rocker at room temperature for 1.5 hours. The beads were spin down at 4000 g and room temperature. The supernatant was removed and the beads were washed 4 times with 5-7 mL of 0.2% SDS in PBS. After the last wash transfer beads to a 1.5 mL eppendorf tube. To the beads, 150μL of freshly prepared sodium dithionite solution was added. After placing on a rocker for 30 minutes at room temperature, the beads were spin down at 4000 g for 2 minutes at room temperature and the supernatant was collected. For western blot detection, the sample was boiled with 2x loading dye, resolved on a 12% SDS-PAGE gel, and transfer to PVDF membrane. Alternatively, instead of transferring to PVDF, the protein gel was stained using a thermos silver staining kit or coomassie blue stain.

For mass spectrometry analysis, 0.5 M dithiothreitol was added to a final concentration of 5 mM and incubated for 30 min at 50 °C. Then, 0.5 M iodoacetamide was added to a final concentration of 10 mM and incubated in the dark for 30 min. Finally, 0.5 M of cysteine to a final concentration of 15 mM and incubated for another 30 min. The proteins were precipitated out using methanol, chloroform and water as described above and redissovled in 6 M urea. The resulting protein solution was diluted with 100mM NH_4HCO_3 (pH = 8.0) so that the urea concentration was less than 1 M. Trypsin was added to the sample (1:50 ratio w/w) based on BCA assay quantification. The digestion proceeded at 37˚C for 16 hours. More trypsin was added to the sample (1:100 ratio w/w) and the digestion continued at 37˚C for an additional 6 hours. The digestion was quenched adding trifluoroacetic acid to 1%. The resulting peptides were cleaned up using a C4 cartridge following the maunfactures protocol and detected by LC-MS/MS.

Detection of RRas2 Lysine Fatty Acylation by Mass Spectrometry. Flag-RRas2 was expressed in SIRT6 KD 293T cells. The cells were treated with 50 μM of Alk14 for 6 hours.

The cells were collected and washed two times with 1x PBS. The cells were lysed in 1% NP40 lysis buffer supplemented with PIC. After 30 minutes at 4˚C, the lysate was cleared by centrifugation at 17000 g for 20 minutes. Flag-RRas2 was isolated using flag immunoprecipitation. The flag agarose was pre-washed three times with 0.2% NP40 wash buffer (0.2% NP40, 150 mM Tris pH 8.0, 50 mM NaCl). After incubating the lysate with the flag resin for two hours, the flag resin was washed three times with the 0.2% NP40 wash buffer. Flag-RRas2 was then eluted using triple flag peptide. The volume of flag peptide used was twice that of the flag resin used. The flag resin was incubated with the flag peptides for 20 minutes on ice and then the supernatant was collected. The elution was repeated three times and the supernatant was combined. Flag-RRas2 was precipitated using water, methanol, and chloroform. The precipitated protein was resolubilized in 4% SDS lysis buffer, and standard click chemistry with the cleavable biotin probe was carried out as describe above. After click chemistry, the protein was again precipitated using water, methanol, and chloroform. The protein was resolubilized in 4% SDS lysis buffer supplemented with 50 μM of EDTA, and diluted with 1% Brij97 buffer to decreases the SDS concentration to less than 1%. To enrich fatty acylated RRas2, high capacity streptavidin beads were washed three times with Brij97 buffer, and then added to the RRas2 sample. After two hours at room temperature, the beads were washed three times with 1% SDS in PBS, and then treated with 1 M hydroxylamine in 1% SDS in PBS (pH 7.4) for 1 hour at room. The streptavidin beads were washed again three times with 1% SDS in PBS. After the last wash, the beads were dried using a gel loading tip. To the beads, 50 μL of 50 mM sodium dithionite in 1% SDS in PBS was added. After 30 minute incubation, the dithionite supernatant was collected, and the beads were treated with sodium dithionite for two more times. After the third dithionite treatment, the combined supernatant was then alkylated and digested with trypsin following the procedure described above. LC-MS/MS analysis was performed with the digested peptides dissolved in 20% acetonitrile.

Validation of Fatty Acylation on Overexpressed Proteins: HA-DHHC1 or HA-DHHC2 were overexpressed in HEK-239T cells. After 24 hours, the cells were treated with 50μM of Alk14 or DMSO for 6 hours. After 6 hours, the cells were collected and lysed with 1% NP40 lysis buffer supplemented with protease inhibitor cocktail. After clearing the lysate, the protein concentrations were determined by Bradford assay. The DHHCs were isolated using HA-immunoprecipitation. HA affinity agarose was prewashed three times with 0.2% NP40 wash buffer. The beads were subsequently added to the lysate that was diluted to a protein concentration of 1 mg/mL. The samples were placed on a rocker at 4˚C for 2 hours. After two hours, the samples were washed three times with 1 mL of 0.2% NP40 lysis buffer. After the third wash, the affinity gel was dried and resuspended in 20μL of 0.2% NP40 lysis buffer. To attach a fluorophore to visualize fatty acylation levels by in gel fluorescence, 1 μL of 1 mM TAMRA-N_3 (in DMF), 1 μL of 10 mM TBTA (in DMF), 1 μL of 40 mM $CuSO_4$ (in water) and 1 μL of 40 mM TCEP (in water) were added. The samples were agitated in the dark for 30 minutes. After 30 minutes, 10 μL of 6x protein loading dye was added and the samples were boiled at 95˚C for 7 minutes. The sample was split in half. One half was treated with 330 μM of hydroxylamine (pH 7.6) for 7 minutes at 95˚C, while the half was not treated (water was added to make up the volume). Fatty acylation levels were visualized by in gel fluorescence on a Typhoon 9400 variable mode imager (GE Healthcare Life Sciences, Piscataway, NJ) after resolving the samples by 12% SDS PAGE.

REFERENCES

(1) Yeste-Velasco, M.; Linder, M. E.; Lu, Y. J. Protein S-palmitoylation and cancer. *Biochim Biophys Acta* **2015,** *1856* (1), 107.

(2) Jiang, H.; Zhang, X.; Chen, X.; Aramsangtienchai, P.; Tong, Z.; Lin, H. Protein Lipidation: Occurrence, Mechanisms, Biological Functions, and Enabling Technologies. *Chem Rev* **2018,** *118* (3), 919.

(3) Stevenson, F. T.; Bursten, S. L.; Locksley, R. M.; Lovett, D. H. Myristyl acylation of the tumor necrosis factor alpha precursor on specific lysine residues. *J Exp Med* **1992,** *176* (4), 1053.

(4) Stevenson, F. T.; Bursten, S. L.; Fanton, C.; Locksley, R. M.; Lovett, D. H. The 31-kDa precursor of interleukin 1 alpha is myristoylated on specific lysines within the 16-kDa N-terminal propiece. *Proc Natl Acad Sci U S A* **1993,** *90* (15), 7245.

(5) Schey, K. L.; Gutierrez, D. B.; Wang, Z.; Wei, J.; Grey, A. C. Novel fatty acid acylation of lens integral membrane protein aquaporin-0. *Biochemistry* **2010,** *49* (45), 9858.

(6) Zhang, X.; Spiegelman, N. A.; Nelson, O. D.; Jing, H.; Lin, H. SIRT6 regulates Ras-related protein R-Ras2 by lysine defatty-acylation. *Elife* **2017,** *6*.

(7) Jing, H.; Zhang, X.; Wisner, S. A.; Chen, X.; Spiegelman, N. A.; Linder, M. E.; Lin, H. SIRT2 and lysine fatty acylation regulate the transforming activity of K-Ras4a. *Elife* **2017,** *6*.

(8) Ji, Y.; Leymarie, N.; Haeussler, D. J.; Bachschmid, M. M.; Costello, C. E.; Lin, C. Direct detection of S-palmitoylation by mass spectrometry. *Anal Chem* **2013,** *85* (24), 11952.

(9) Raghavan, A.; Charron, G.; Flexner, J.; Hang, H. C. Chemical probes for profiling fatty acid-associated proteins in living cells. *Bioorganic & medicinal chemistry letters* **2008,** *18* (22), 5982.

(10) Yang, Y. Y.; Grammel, M.; Raghavan, A. S.; Charron, G.; Hang, H. C. Comparative analysis of cleavable azobenzene-based affinity tags for bioorthogonal chemical proteomics. *Chem Biol* **2010,** *17* (11), 1212.

(11) Leriche, G.; Chisholm, L.; Wagner, A. Cleavable linkers in chemical biology. *Bioorganic & medicinal chemistry* **2012,** *20* (2), 571.

(12) Grammel, M.; Hang, H. C. Identification of lysine acetyltransferase substrates using bioorthogonal chemical proteomics. *Methods in molecular biology* **2013,** *981*, 201.

(13) Resh, M. D. Fatty acylation of proteins: new insights into membrane targeting of myristoylated and palmitoylated proteins. *Biochimica et biophysica acta* **1999,** *1451* (1), 1.

(14) Roberts, P. J.; Mitin, N.; Keller, P. J.; Chenette, E. J.; Madigan, J. P.; Currin, R. O.; Cox, A. D.; Wilson, O.; Kirschmeier, P.; Der, C. J. Rho Family GTPase Modification and Dependence on CAAX Motif-signaled Posttranslational Modification. *The Journal of biological chemistry* **2008,** *283* (37), 25150.

(15) Nishimura, A.; Linder, M. E. Identification of a novel prenyl and palmitoyl modification at the CaaX motif of Cdc42 that regulates RhoGDI binding. *Mol Cell Biol* **2013,** *33* (7), 1417.

(16) Aramsangtienchai, P.; Spiegelman, N. A.; Cao, J.; Lin, H. S-Palmitoylation of Junctional Adhesion Molecule C Regulates Its Tight Junction Localization and Cell Migration. *J Biol Chem* **2017,** *292* (13), 5325.
(17) Jing, S. Q.; Trowbridge, I. S. Identification of the intermolecular disulfide bonds of the human transferrin receptor and its lipid-attachment site. *EMBO J* **1987,** *6* (2), 327.
(18) Aicart-Ramos, C.; Valero, R. A.; Rodriguez-Crespo, I. Protein palmitoylation and subcellular trafficking. *Biochim Biophys Acta* **2011,** *1808* (12), 2981.
(19) Charron, G.; Zhang, M. M.; Yount, J. S.; Wilson, J.; Raghavan, A. S.; Shamir, E.; Hang, H. C. Robust fluorescent detection of protein fatty-acylation with chemical reporters. *J Am Chem Soc* **2009,** *131* (13), 4967.

CHAPTER 8

CONCLUSION AND FUTURE DIRECTIONS

With the recent findings that K-Ras4a is a SIRT2 defatty acylation substrate, and R-Ras2 is a SIRT6 defatty acylation substrate, we decided to investigate if other small GTPases are also regulated by lysine fatty acylation.[1,2] We were excited to find that several other small GTPases also exhibited a fair amount of hydroxylamine resistant fatty acylation—which may be lysine fatty acylation. What was more interesting was that only one of the two highly related Ral isoforms, RalB, exhibited hydroxylamine resistant fatty acylation. This was an intriguing finding as the two Ral GTPases, RalA and RalB, exhibit 85% sequence identify, yet both have multiple lysine residues in their C-terminal hyper variable region.

After we further confirmed only RalB had lysine fatty acylation, we hypothesized that lysine fatty acylation could explain some of the functional differences between these two related GTPases. Hence, we decided to further study the physiological function of RalB lysine fatty acylation. We found that RalB is a SIRT2 defatty acylation substrate, and that lysine fatty acylation can promote RalB-GTP binding. The enhanced GTP binding is evident by the enhanced co-localization of RalB and Sec5 when SIRT2 levels are lowered (knocked down). Furthermore, we found that RalB lysine fatty acylation can promote A549 cancer cell migration.

From this study, there are still several questions that remain. The first one being how lysine fatty acylation promotes RalB-GTP binding, or its interaction with its known effector Sec5. Furthermore, we still do not know which enzymes are lysine fatty acyl transferases. Future studies should focus on identifying these enzymes. The finding that RalB, and not RalA, has lysine fatty acylation could help us better understand sequence requirements for acyl transferases once they are identified. As RalB lysine fatty acylation can promote lung cancer cell migration, inhibiting the lysine fatty acyl transferase could serve as a promising therapeutic method for lung cancer.

Our study suggested that several other small GTPases have lysine fatty acylation but we did not have further validate them. It would be interesting to further confirm these finding and study the functional significance. Recently, it was also reported that the small GTPase Rac1 has lysine fatty acylation which can modulate its GTP binding.[3] It is possible that lysine fatty acylation serves as a regulatory mechanism for GTP binding of several other small GTPases.

Another intriguing question is what the stoichiometry of lysine fatty acylation is. The level of RalB lysine fatty acylation appears to be weak compared to that of other GTPases such as E-Ras or R-Ras, based on comparing the fluorescence signal/ protein level. However, the relative amount of hydroxylamine resistant fatty acylation on RalB is much higher than that on other small GTPases. It would also be worthwhile to investigate if both S-palmitoylation and lysine fatty acylation occur concurrently, and what the relative abundance of the two modifications are. As the level of RalB lysine fatty acylation is relatively low, it is worth investigating if RalB is a substrate for other enzymes that are lysine deacylases. While we did test most of the known lysine deacylases, it is possible that there are other enzymes that catalyze the removal of fatty acyl groups from lysine residues. To better understand when lysine fatty acylation on RalB is important, or when cell migration might want to be promoted, it would be worthwhile to study if there are certain stress conditions that promote lysine fatty acylation.

The fact that lysine fatty acylation on RalB promotes A549 cancer cell migration was a bit surprising since SIRT2 is a promising cancer target, and lysine fatty acylation inhibited the transforming activity of K-Ras4a. It is possible that the tumor suppressor, or tumor promoting role of SIRT2 in cancer specific. Exploring when SIRT2 promotes or inhibits cancer phenotypes could help us better understand the physiological function of SIRT2, and help us better understand how to target SIRT2. As highlighted by this study, there is still much to learn about the role of SIRT2, especially its defatty acylation activity.

Initially, we were very surprised by the finding that RalB, but not RalA, had lysine fatty acylation. These two small GTPases have approximately 85% sequence identity so the fact that

only one isoform had protein lysine fatty acylation made us wonder what other differences there are between these two proteins. It is well known that despite their similarities, the Ral GTPases exhibit different, and even opposing roles in several cancers. To further explore the differences between RalA and RalB, we decided to use an affinity purification mass spectrometry based interactome. We decided to compare the interactomes for constitutively active and inactive Ral mutants as we believed this would provide useful insight into the function of these two proteins. Consistent with our hypothesis, the interactome did provide a lot of useful information.

We found that inactive Ral (RalAS28N, RalBS28N) associates with Transferrin Receptor 1 (TfR1), and overexpression of Ral can prevent transferrin receptor forming puncta in the cytosol. However, the physiological significance is not entirely clear. We hypothesized that this might be related to ability of active Ral to inhibit receptor mediated endocytosis but more work needs to be done to prove this. In line with this hypothesis, it is possible that Ral serves to balance intracellular iron concentrations.

Ral GTPases have previously been established to regulate exocytosis, studying the balance between the GTP/GDP cycle and its role in endocytosis and exocytosis could help elucidate the cellular functions of the GTPases. One way to study the GTP/GDP cycle, would be develop a robust FRET based Ral probe that could allow detection of the activity of Ral through imaging. If this is achieved co-localization studies with TfR1, transferrin or other factors important for endocytosis and exocytosis could help answer if the Ral GTP/GDP cycle is important for modulating a balance between endocytosis and exocytosis. It would be interesting to investigate if serum depletion can alone activate Ral, or if TfR1 is actually a Ral GEF.

We also found that Ral could associate with GCN1, and lead to a slight increase in GCN2 activity as determined by ATF4 levels. It is possible that the activation of GCN1 by Ral is related to their reported roles in regulating mTORC activity. Due to the important role of mTORC in regulating cell growth, among other things, it would be interesting to further study

this connection.

Finally, we showed that RalB selectively interacts with ERK2. We were initially very surprised to find ERK2 as a potential RalB interacting protein. It has previously been shown, and we further validated, that RalB does not affect ERK1/2 phosphorylation status. We believe that ERK2 selectively interacts with RalB because of its C-terminal hyper variable region. Overexpression of RalB lead to a decrease in ERK2 nuclear localization. The physiological significance of this change in localization remains unknown. It is possible that preventing ERK2 nuclear localization can prevent it from activating a specific transcription factor, or can increase its kinase activity on membrane or cytosolic substrates. The RalB-ERK2 interaction could also help explain the difference the role the Ral GTPases play in anchorage independent growth. Both the finding that only RalB has protein lysine fatty acylation, and the results from the interactome highlight there is still much to understand about the Ral GTPases.

As highlighted by the finding that SIRT2 regulated lysine fatty acylation promotes cancer cell migration, there is still much to learn about the defatty acylation activity of SIRT2. Small molecule inhibitors are a powerful tool to study an enzymes function. An advantage to using small molecule inhibitors is you can modulate the activity of a protein without changing its protein level. When proteins are knocked down, or knocked out, protein-protein interactions are disrupted and this can lead to numerous cellular effects. Therefore, selective small molecule inhibitors make it easier to study the enzymatic activity of certain proteins.

Several SIRT2 inhibitors have been developed and used to study the function of SIRT2. However, most reporting studies have only reported *in vitro* IC_{50} values for SIRT2 deacetylation activity, or have shown the compound has an anticancer effect but not shown that the effect is through SIRT2 inhibition. As we and others want to use these inhibitors to study SIRT2 we decided to do an in-depth comparison. We found that TM is the most potent and selective SIRT2 inhibitor. TM was also the only compound that could inhibit the defatty acylation activity of SIRT2 *in vitro*, albeit weakly. The other interesting property about TM was it did not exhibit

cytotoxicity in normal mammary epithelial cells. An interesting question to address is why TM is cancer cell specific. It could be attributed to its enhanced SIRT2 selectivity. But what also made TM interesting is that some cell lines are more sensitive to its treatment than others. As we are interested in developing more potent SIRT2 inhibitors, that retain the selectivity of TM it could be interesting to investigate what makes cell lines more, or less sensitive to TM treatment. The difference in selectivity could be studied in a couple of different ways. First, RNAseq could be used to see if TM treatment caused changes in gene expression. Alternatively, the interacting partners of SIRT2 could be investigated in different cell lines with and without TM treatment to see if there are any changes.

SirReal2 exhibited a decent fold of selectivity towards SIRT2 inhibition, but was unable to inhibit its defatty acylation activity. As we are interested in better understanding the role SIRT2 lysine defatty acylation and the role it plays in cancer, SirReal2 could be used as a tool to differentiate the enzymatic activity of SIRT2. Previously, a SIRT6 G60A mutant was established that allowed for identification of physiological functions that can be attributed to SIRT6 defatty acylation activity. SirReal2 could allow us, and others, to differentiate between the role of SIRT2 deacetylation and defatty acylation in cells.

One other finding from the inhibitor comparison was that AGK2 was not particularly potent in cell viability assays, but was much more potent in inhibiting anchorage independent growth. The opposite was true for SirReal2, which was not particularly potent at inhibiting anchorage independent growth but was exhibited decent cytotoxicity in the cell viability assays. It might be interesting to evaluate why this was the case. One common problem for all of the current SIRT2 inhibitors was their poor solubility. As our data suggests SIRT2 is a promising therapeutic target, better SIRT2 inhibitors are needed. Enhancing solubility should be a priority as we and other work on developing more potent and selective SIRT2 inhibitors.

Despite its ability to inhibit SIRT2 defatty acylation activity *in vitro*, we found that TM was not able to inhibit SIRT2 defatty acylation activity robustly on either K-Ras4a or RalB

(*data not shown*) the only known SIRT2 defatty acylation substrates. However, we were interested in seeing if we could find an inhibitor that could inhibit SIRT2 defatty acylation on K-Ras4a.

In our efforts to develop better SIRT2 inhibitors, our lab synthesized a TM analogue JH-T4. This compound was more potent than TM in cell studies, but was not as selective at inhibiting SIRT2. However, JH-T4 was able to more efficiently inhibit SIRT2 defatty acylation activity *in vitro* when the inhibitor and enzyme were not pre-incubated. We hypothesized that in cells, JH-T4 should be able to compete with a fatty acylated substrate more effectively. Our hypothesis was true, as we found that JH-T4 can promote K-Ras4a lysine fatty acylation in cells. We think this can be attributed to the ability of JH-T4 to bind more tightly to amino acid backbone of SIRT2, which was further supported by the *in vitro* studies with another inhibitor NH-TM. This suggested that inhibition of SIRT2 defatty acylation activity in cells is possible. It would be advantageous to be able to develop SIRT2 selective inhibitors that are also potent against its defatty acylation activity. However, as JH-T4 can efficiently inhibit defatty acylation activity in cells, it could be used as a tool to study Sirtuin regulated lysine fatty acylation.

Our study also showed that JH-T4 was more potent than TM in all of the cell studies evaluated. It is possible that pan-Sirtuin inhibition could be a promising therapeutic strategy. To evaluate this, the effect of knocking down or inhibiting multiple Sirtuins at the same time should be investigated. However, JH-T4 also exhibited toxicity against the normal mammary epithelial cells that we tested suggesting that pan-Sirtuin inhibition could have other challenges.

In addition to identifying small molecule inhibitors that can be used as tools to study Sirtuin regulated lysine fatty acylation, we also decided to use proteomics based methods to identify proteins with lysine fatty acylation. In our attempts to identify lysine fatty acylated proteins that are HDAC targets, we found that JAM-C has S-palmitoylation that inhibited A549 cell migration. We were intrigued to further study this modification, and found that DHHC7 could regulate Jam-C S-palmitoylation. This study highlighted, once again, that S-

palmitoylation is important for regulating cancer. Furthermore, we identified an additional DHHC7 substrate. There are still a few remaining questions from this study. The first being a detailed mechanism for the change in tight junction localization and migration. The second being if this physiologically relevant, or true in animal models.

As highlighted by the DHHC screening of Jam-C, often proteins are substrates of multiple DHHCs enzymes. Despite the identification of several DHHC substrates, we still don't have a good understanding of substrate specificity. To better understand substrate specificity profiling, either by an array analysis or proteomics, should be done. However, we are currently limited by our ability to directly detect lipidation through proteomics experiments due to the low abundance, labile state and hydrophobicity of the modifications.

Our Jam-C finding highlighted that proteomics without direct site identification would yield false positive results, as many proteins exhibit N-terminal glycine myristoylation or hydroxylamine resistant S-palmitoylation. We tried to address these problems by developing a chemical-proteomic approach to directly detect fatty acylation from proteomic samples. We showed that the probe we made could achieve our goals through biochemical proof on concept studies. However, direct detection of the lipid modification proved to be challenging by mass spectrometry. To fully achieve the goal, it would be advantageous to redesign the probe to incorporate a mass signature ion, or ion pattern. This could allow for directed searched. However, the preliminary results we got suggested that it would be possible to detect protein lipidation from the proteomics level. Furthermore, this study highlighted that there are likely many more proteins that have lysine fatty acylation.

We are only beginning to understand protein lysine fatty acylation. There are still many questions that remain about its function, abundance and significance. To fully understand this modification, we need to use the enzymes that regulate it, such as SIRT2, as a tool to identify more proteins that are modified. What I have worked on throughout my time in graduate school has shown that there is a complex interplay between lysine fatty acylation and cancer. SIRT2 is

an important regulator of cancer, and one of its substrates is RalB. Despite identifying this connection, several questions still remain about the function of SIRT2 regulated lysine fatty acylation on RalB. My studies also highlight that there is still much to learn about the Ral GTPases and what regulates them.

REFERENCES

(1) Jing, H.; Zhang, X.; Wisner, S. A.; Chen, X.; Spiegelman, N. A.; Linder, M. E.; Lin, H. SIRT2 and lysine fatty acylation regulate the transforming activity of K-Ras4a. *Elife* **2017,** *6*.

(2) Zhang, X.; Spiegelman, N. A.; Nelson, O. D.; Jing, H.; Lin, H. SIRT6 regulates Ras-related protein R-Ras2 by lysine defatty-acylation. *Elife* **2017,** *6*.

(3) Zhou, Y.; Huang, C.; Yin, L.; Wan, M.; Wang, X.; Li, L.; Liu, Y.; Wang, Z.; Fu, P.; Zhang, N.et al. N(epsilon)-Fatty acylation of Rho GTPases by a MARTX toxin effector. *Science* **2017,** *358* (6362), 528.